LIPOSOMES
FOR
DRUG DELIVERY

Surface modifications &
screening for compositions at the edge of stability

Dissertation zur Erlangung des Grades

"Doktor der Naturwissenschaften" (Dr. rer. nat.)

am Fachbereich 09 - Chemie, Pharmazie und Geowissenschaften

der Johannes Gutenberg-Universität in Mainz

Diplom-Chemiker Matthias Voigt

geboren am 24.06.1988 in Suhl

Mainz, den 11.11.2019

JG|U
JOHANNES GUTENBERG
UNIVERSITÄT MAINZ

Dekan: Prof. Dr. Dirk Schneider

1. Berichterstatter: Prof. Dr. Mark Helm

2. Berichterstatter: Prof. Dr. Holger Frey

Datum der mündlichen Prüfung: 17. Dezember 2019

Prüfungskommission der mündlichen Prüfung:

1. Prüfer   Prof. Dr. Mark Helm
2. Prüfer   Prof. Dr. Holger Frey
3. Prüfer   Prof. Dr. Andrea Tüttenberg

The present dissertation was composed at the Institute of Pharmacy and Biochemistry at the Johannes Gutenberg-University Mainz under supervision of Prof. Dr. Mark Helm in the time between the 1st March 2015 and the 11th November 2019.

Supervisor

Prof. Dr. Mark Helm

Faculty of Chemistry, Pharmaceutical Science and Geoscience

Institute of Pharmacy and Biochemistry

Johannes Gutenberg-University Mainz

I hereby declare that I wrote the dissertation submitted without any unauthorized external assistance and used only sources acknowledged in the work. All textual passages, which are appropriated verbatim or paraphrased from published and unpublished texts, as well as all information obtained from oral sources are duly indicated and listed in accordance with bibliographical rules. In carrying out this research, I complied with the rules of standard scientific practice as formulated in the statutes of Johannes Gutenberg-University Mainz to ensure standard scientific practice.

Place, Date	Matthias Voigt

FÜR MEINE FAMILIE

„Man merkt nie, was schon getan wurde, man sieht immer nur, was noch zu tun bleibt."

Marie Curie

„Ohne Spekulation gibt es keine neue Beobachtung."

Charles Darwin

DANKSAGUNG

CONTENTS

ABSTRACT

Liposomes as most important nanoparticular drug delivery vehicles already in clinical application were prepared by dual centrifugation with increasing amounts and molecular weights of different surface modifications like classic 'stealth' polymer poly-(ethylene) glycol (PEG) or novel hyperbranched polyglycerol (*hb*PG). Incorporation of high amounts of large polymers resulted in an overall decrease of liposome diameters as assessed by dynamic light scattering and nanoparticle tracking analysis, and a qualitative increase in blood circulation within zebrafish embryos, a potential advantage for passive targeting of tumors *via* the EPR effect. The cellular uptake of *hb*PG modified liposomes by macrophages was considerably higher *in vitro* and *in vivo* than for PEGylated liposomes independently from the protein corona, resulting in lower circulation times. While modification of liposomes with *hb*PG seems to offer the unique possibility of effectively 'targeting' macrophages and therefore possesses a great potential for the treatment of macrophage associated diseases, *hb*PG itself surprisingly provided a less efficient stealth effect when compared to conventional PEG.

To enhance pharmacokinetics of liposomes as drug delivery vehicles, their design ideally combines storage and circulation stability while also providing triggered fragility for effective release of encapsulated drugs at the target tissue or within the target cells. Therefore, liposomes 'at the edge' of stability were desired and systematically screened for, amongst others, by membrane-incorporation of the solvatochromic fluorescent probe laurdan, ultimately leading to a few defined lipid compositions that were considered 'at the edge' of stability. The identified candidate liposomes were modified with small amounts of pH-sensitive lipid cholesteryl hemisuccinate and complied a moderately high cargo release under late endosomal/lysosomal conditions while for the most part retaining their cargo upon storage, as evaluated by a semi-automated size exclusion chromatography for fluorescent model cargos sulforhodamine b and calcein. Physicochemical characterization of candidate liposomes confirmed pharmaceutical quality comparable to conventional liposomes used in the clinic. *In vitro* cell experiments revealed that candidate liposomes were non-toxic and released considerably more encapsulated anti-cancer drug doxorubicin in comparison to conventional liposomes, which was measured by flow cytometry, confocal laser scanning microscopy and imaging flow cytometry (ImageStream®). While candidate liposomes with encapsulated antibiotic ceftriaxone did not surpass the therapeutic efficacy of free ceftriaxone for the *in vivo* treatment of salmonella infected zebrafish embryos, they were nevertheless able to considerably increase zebrafish embryo survival when compared to the treatment with conventional liposomes. Finally, modification of candidate liposomes with pH-sensitive ketal- or vinylether-PEG resulted in higher cargo release capabilities when compared to conventional PEG or *hb*PG.

ZUSAMMENFASSUNG

Liposomen, die das wichtigste nanopartikuläre Wirkstoffträgersystem in klinischer Anwendung darstellen, wurden über duale Zentrifugation mit steigenden Mengen und Molekulargewichten von unterschiedlichen Oberflächenmodifikationen hergestellt, wie dem klassischen „Stealth" Polymer Poly(-ethylen)glycol (PEG) oder dem neuartigen hyperverzweigten Polyglycerol (*hb*PG). Inkorporierung von hohen Mengen großer Polymere resultierte insgesamt in einer Verringerung des Liposomendurchmessers, gemessen über dynamische Lichtstreuung und Nanopartikel Tracking Analyse, wie auch in einer qualitativen Zunahme der Blutzirkulation in Zebrafisch Embryonen, was einen potentiellen Vorteil für passives Ansteuern von Tumoren über den EPR Effekt darstellt. Die Zellaufnahme von *hb*PG modifizierten Liposomen durch Makrophagen war unabhängig von der Proteinkorona *in vitro* und *in vivo* wesentlich höher als für PEGylierte Liposomen, was auch zu einer geringeren Zirkulationszeit führte. Während die Modifizierung von Liposomen mit *hb*PG die einzigartige Möglichkeit bietet, Makrophagen effektiv anzusteuern und dadurch ein sehr großes Potential besitzt, mit Makrophagen assoziierte Krankheiten potentiell besser behandeln zu können, führte *hb*PG selbst überraschenderweise zu einem weniger effizienten „Stealth" Effekt verglichen mit konventionellem PEG.

Um die Pharmakokinetik von Liposomen als Wirkstoffträgersystem zu verbessern, muss deren Design sowohl die Lagerungs- und Zirkulationsstabilität als auch die gesteuerte Instabilität zur effektiven Freisetzung verkapselten Wirkstoffs im Zielgewebe oder in der Zielzelle berücksichtigen. Deshalb wurden Liposomen „am Rande" der Stabilität über systematisches Screening gesucht, unter anderem durch Membran-Inkorporation der solvatochromen Fluoreszenzsonde Laurdan, was letztendlich zu wenigen definierten Lipidkompositionen „am Rande" der Stabilität führte. Die identifizierten Liposomenkandidaten wurden mit kleinen Mengen des pH-sensitiven Lipids Cholesterolhemisuccinat modifiziert und zeigten eine moderat hohe Wirkstofffreisetzung unter späten endosomalen/lysosomalen Bedingungen, während der Wirkstoff bei Lagerung größtenteils im Liposom verblieb. Dies wurde über eine halbautomatische Größenausschlusschromatographie für fluoreszierende Modelsubstanzen Sulforhodamin b und Calcein evaluiert. Die physikochemische Charakterisierung der Liposomenkandidaten bestätigte deren pharmazeutische Qualität, die vergleichbar mit (selbst hergestellten) konventionellen Liposomen aus klinischen Anwendungen war. *In vitro* Zellexperimente zeigten auf, dass die Liposomenkandidaten selbst nicht toxisch waren und wesentlich mehr verkapseltes Antikrebsmittel Doxorubizin freisetzten als konventionelle Liposomen, was über Durchflusszytometrie, konfokale Laserscanningmikroskopie und bildgebende Durchflusszytometrie (ImageStream®) gemessen wurde. Obwohl Liposomenkandidaten mit verkapseltem Antibiotikum Ceftriaxon die therapeutische Effizienz von freiem Ceftriaxon bei der Behandlung von mit Salmonellen infizierten Zebrafisch-Embryos nicht übertrafen, zeigten sie dennoch eine stark erhöhte Überlebensrate im Vergleich zur Behandlung mit konventionellen Liposomen. Schließlich wurden Liposomenkandidaten mit pH-sensitivem Ketal- oder Vinylether-PEG modifiziert, was zu einer erhöhten Wirkstofffreisetzungfähigkeit im Vergleich zu konventionellem PEG oder *hb*PG führte.

GRAPHICAL ABSTRACT

Section 3.1: Hyperbranched polyglycerol shielded liposomes: Control of physical behavior and biological performance
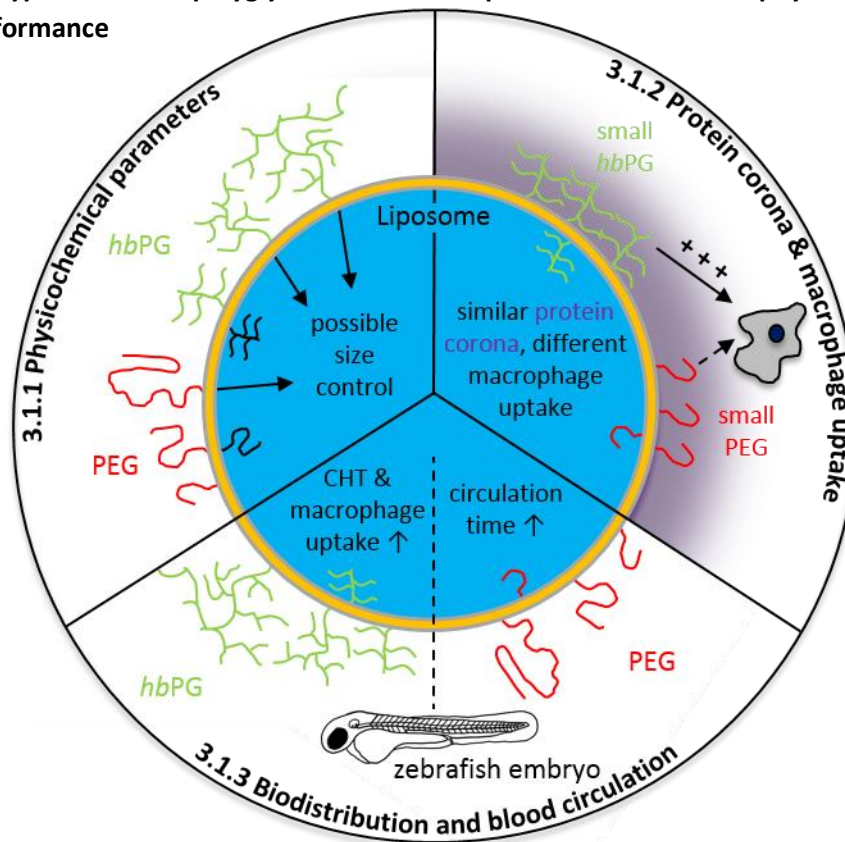
**Section 3.2: Screening for lipid compositions at the edge of stability**
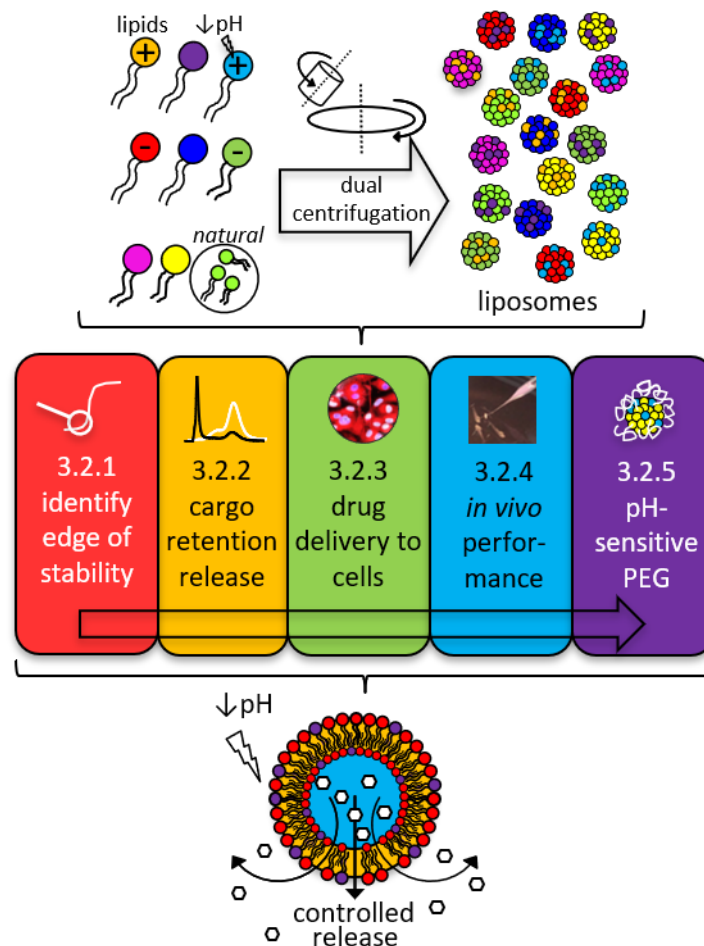
1. INTRODUCTION

1.1 LIPOSOMES FOR DRUG DELIVERY

Liposomes are well-investigated nano vesicles for drug delivery consisting of a large aqueous core surrounded by one or multiple double lipid membranes. Liposomes represent the first and most successful nanoparticular drug delivery system that made it into the clinic, although recent progress for clinical applications has decreased incrementally, due to several challenges as detailed later.[1] Besides drug delivery, liposomes are of interest in other scientific fields such as cosmetics, biological model membranes or investigations on the origin of life.[2][3] Their success is based on their ability for self-assembly [4][5], entrapment of a high variety of lipo- and hydrophilic compounds in their membrane or core [6]–[8], respectively, high intrinsic biocompatibility [9] with potential biodegradability [10] and therefore low toxicity while also being amenable to modification of their physicochemical [11] and biophysical [1] properties, for example by surface modifications [12] or changes in lipid composition [6]. They were originally discovered by English hematologist Alec Bangham *et al.* in the 1960s [13][14], and their impact in biomedical areas has expanded ever since, especially due to the fact that drug delivery plays an increasingly important role in modern nanomedicine. There is a great need for protection of certain therapeutic compounds, e.g. RNA or DNA, from degradation, inactivation or dilution inside the blood stream [6], and to transport the compound to a target location while decreasing systemic side effects. All of these can be achieved by using liposomes as drug delivery vehicle.[15] Liposomes can be classified based on their lamellarity and size as small, large or giant uni-, oligo-, multilamellar or multivesicular vesicles.[11] They can alternatively be classified based on their lipid composition including surface modifications as conventional [16], stimuli-sensitive [17], sterically stabilized (stealth) [12], ligand-targeted [18] or cationic [19] liposomes (Figure 1).[20] While conventional liposomes consist of neutral and/or negatively charged phospholipids and cholesterol [21], stimuli-sensitive liposomes require lipids or other amphiphilic membrane compounds amenable to ionization or changes e.g. in conformation or lipid phase. Stimuli-sensitive liposomes are developed to improve a controlled release of encapsulated therapeutic compounds upon stimuli, such as pH, temperature, light, redox-potential, ultrasound, enzymes or magnetic fields. Steric stabilization of liposomes aims to increase the liposomal half-life upon storage and in circulation. Liposomes are typically modified with poly-(ethylene) glycol (PEG) for steric stabilization, which can be crosslinked to lipids and integrated into the liposomal membrane during liposome formulation.[12] Ligand-targeted liposomes aim to achieve active targeting of specific cells and therefore respective ligands are either covalently attached to their surface or attached to PEG, such as antibodies, small molecules, proteins, carbohydrates or peptides (sometimes also

combined with an imaging agent for theranostics).[1][22] Cationic liposomes are (partly) composed of cationic lipids to enhance encapsulation of negatively charged compounds like RNA or DNA.[23]
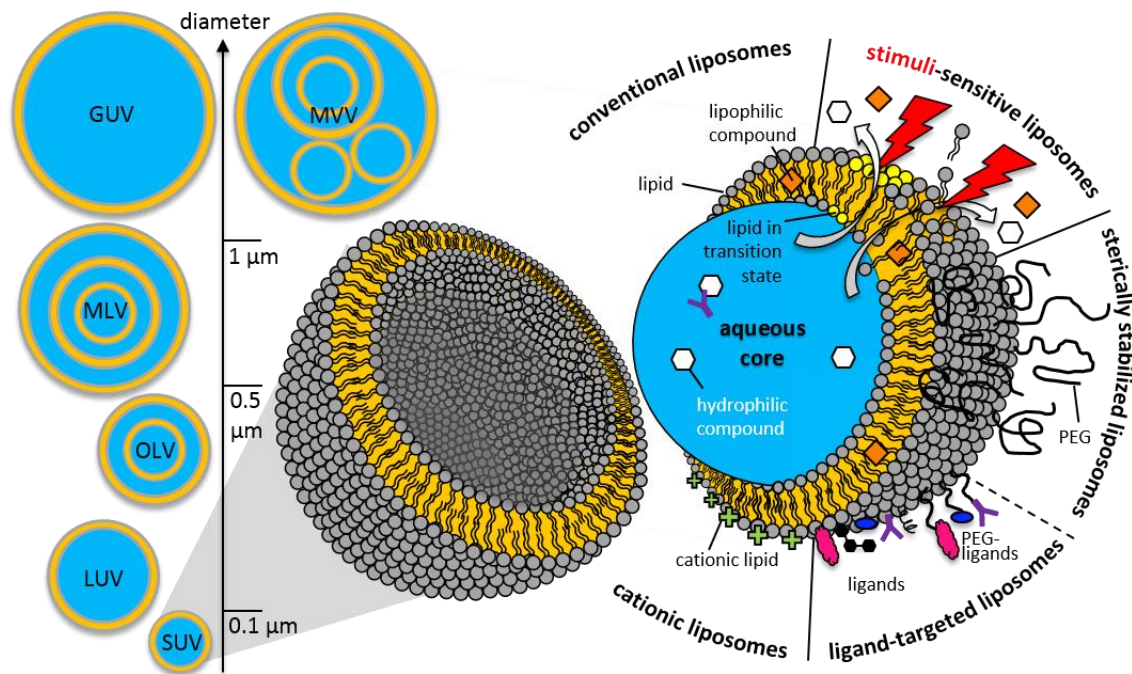
FIGURE 1: 2D CROSSECTIONS OF LIPOSOMES CLASSIFIED ACCORDING TO THEIR SIZE AND LAMELLARITY AS SMALL UNILAMELLAR VESICLES (SUV), LARGE UNILAMELLAR VESICLES (LUV), OLIGOLAMELLAR VESICLES (OLV), MULTILAMELLAR VESICLES (MLV), GIANT UNILAMELLAR VESICLES (GUV) OR MULTIVESICULAR VESICLES (MVV) AND A 3D SCHEME OF A LIPOSOME CLASSIFIED BASED ON ITS LIPID COMPOSITION AS CONVENTIONAL, STIMULI-SENSITIVE, STERICALLY STABILIZED (PEG = POLY-(ETHYLENE) GLYCOL), LIGAND-TARGETED OR CATIONIC LIPOSOME.

Liposomal membranes as simple mimics of natural cellular membranes can be composed of extracted and purified naturally occurring lipids and/or synthetic amphiphiles that can form a stable bilayer. Conventional liposomes typically consist of natural phospholipids extensively present within mammalian cells as egg or soy phosphatidylcholine in combination with cholesterol.[20] These phospholipids consist of an nonpolar fatty acid chain and a polar headgroup and are therefore amphiphilic by nature. Due to the hydrophobic effect, these lipids organize themselves into lipid bilayers to separate their hydrophobic tails from the hydrophilic surroundings, which leads to formation of liposomes in aqueous media.[3][24] The stability of a liposomal membrane consisting of one lipid mainly derives from electrostatic interactions and hydrogen bonds between the headgroups as well as Van der Waals forces between the tails.[25]

1.2 LIPIDS AND THE LIPOSOMAL MEMBRANE

Depending on their chemical structure, hydration and environmental conditions, such as temperature, pressure, ionic strength or pH, lipids within liposomal membranes can exist in different phases (Figure 2 A).[26]–[28] One of the three naturally most relevant lamellar phases is the liquid disordered phase L_α, a phase in which the often unsaturated lipid molecules are irregularly packed at an environmental temperature above the phase transition temperature (Tm) of the respective lipids, causing them to laterally move across the membrane surface. Below the Tm of the respective lipids, the membrane is in the gel phase L_β, a solid-like state induced by tighter lipid packing due to stronger Van der Waals interactions and therefore more prominent for saturated lipids. Membranes in gel phase are less fluid and less permeable than membranes in liquid disordered phase, therefore retaining encapsulated hydrophilic cargo more effectively. Upon membrane incorporation of sufficient amounts (typically 33 — 45 mol-% [29]) of the rigid sterol cholesterol, a lipid that is also present in mammalian membranes, the organization of the other lipids present within the liposomal membrane is modified. If the lipids within the liposomal membrane are in liquid disordered phase, incorporation of cholesterol leads to a permeability and fluidity decrease and an overall increase of stability.[30]
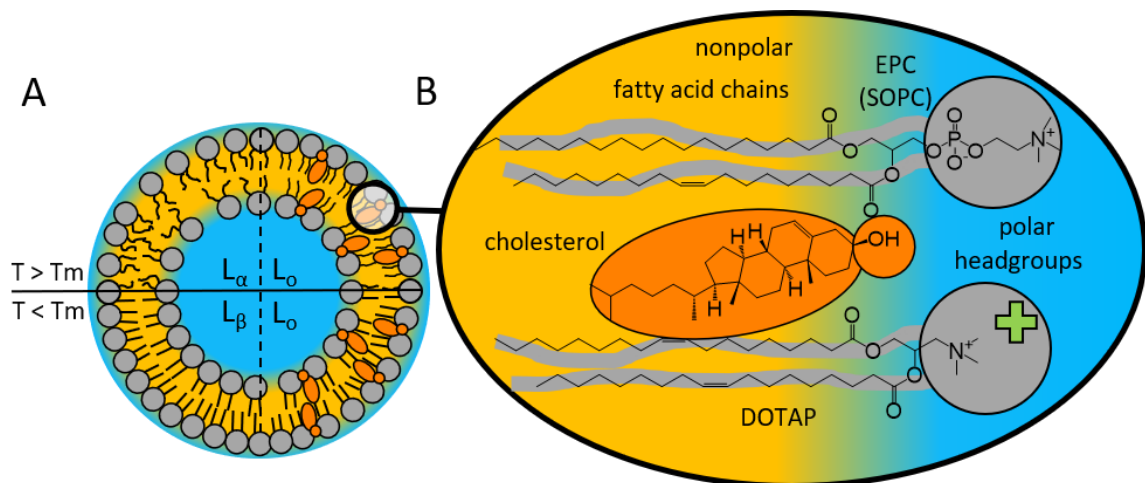
FIGURE 2: (A) LAMELLAR PHASES OF A CONVENTIONAL LIPOSOME DEPENDING ON ITS PHASE TRANSITION TEMPERATURE (Tm). AT AN AMBIENT TEMPERATURE T ABOVE THE Tm, LIPIDS ARE IN THE LIQUID DISORDERED PHASE L_α, WHILE BELOW THE Tm, THEY ARE IN THE GEL PHASE L_β. UPON INCORPORATION OF SUFFICIENT AMOUNTS OF CHOLESTEROL, THE LIPID PHASES CHANGE TO THE LIQUID ORDERED PHASE L_o. **(B)** ALIGNMENT OF NEUTRAL PHOSPHOLIPID SOPC (1-STEAROYL-2-OLEOYL-*SN*-GLYCERO-3-PHOSPHOCHOLINE) DERIVING FROM EGG PHOSPHATIDYLCHOLINE (EPC), SYNTHETIC CATIONIC LIPID DOTAP (1,2-DIOLEOYL-3-TRIMETHYLAMMONIUM-PROPANE) AND CHOLESTEROL ALONG THE LIPOSOMAL MEMBRANE.

This membrane tightening effect is caused by cholesterol aligning its long axis parallel to the phospholipid fatty acid chains, with the hydroxyl group in close proximity to the carbonyl groups of the phospholipids (Figure 2 B).[31]–[33] Due to this alignment, the cholesterol squeezes the fatty acid alkyl chains of surrounding phospholipids so that they become more rigid, leading to a lipid phase change from liquid disordered to liquid ordered (L_o) phase, an effect that is also achievable by incorporation of sphingomyelin.[33] If the lipids within the liposomal membrane are in gel phase L_β, incorporation of cholesterol leads to a separation of the gel phase phospholipids, rendering the membrane more fluid and leading to a liquid ordered phase L_o. Therefore, the liquid ordered phase represents a hybrid between the liquid disordered and gel phase. There is also the possibility of a nonuniform membrane organization that can lead to the formation of micro domains called lipid rafts, which are often enriched with cholesterol and reside in the liquid-ordered phase L_o while being immiscible with the liquid disordered phase L_α.[27][34]

Besides the amount of incorporated cholesterol, the headgroup, charge, chain length, chain saturation and Tm of the lipid have a major influence on liposomal physicochemical properties and biological behavior. Sufficient amounts of positively charged lipids like DOTAP with a trimethylammonium headgroup (Figure 2 B) can lead to an overall positive surface charge of the liposome, which was shown to increase accumulation in vascular endothelium and to decrease extravasation.[35] Longer fatty acid chains lead to stronger Van der Waals interactions and an increased number of degrees of freedom, generally resulting in a higher Tm.[28] Saturated lipids within the bilayer lead to kinks and therefore to a reduction of the accessible fatty acid chain area, reducing Van der Waals interactions while also lowering the Tm.[36] The steric demand of the fatty acid chain and the headgroup determine whether a lipid would form liposomes on its own or other formations like micelles or inverted structures.[27][37] Moreover, the steric demand can be changed by protonation, temperatures higher than physiologic temperatures, treatment with divalent cations or dehydration, making the liposomal membrane stability amenable to manipulation.[38][39]

If a liposome is composed of more than one lipid, the parameters that affect liposomal physicochemical and biological properties are additionally dependent on lipid composition, ratio, miscibility and interactions between different lipids, for example ionic interactions, Van der Waals forces or hydrogen bonds. Of note, lipid phases can be co-existing when liposomes are composed of multiple lipids, which opens an *n*-dimensional parameter space which is difficult to capture.[40][41] When increasing or decreasing the environmental temperature of a liposome composed of two lipids with different Tms, one lipid reaches the phase transition prior to the other, which can lead to packing defects. A lipid that transitioned from liquid disordered to gel

phase is straightened, leading to gaps to lipids in close proximity still in liquid disordered phase, potentially allowing encapsulated cargo to be released from the liposome. Therefore, the lipid composition and ratio determine the physicochemical and biological properties of the resulting liposomes, enabling their manifold application.

1.3 LIPOSOME FORMULATION AND CHARACTERIZATION

Lipids possess the ability for self-assembly to liposomes upon an energy input due to the hydrophobic effect, so the challenge in liposome preparation is not to assemble the membranes, but to achieve liposomes of the right size and lamellarity, which is strongly dependent on the method used for liposome preparation.[11] Liposome preparation methods can be categorized into mechanical dispersion methods, solvent dispersion methods and detergent removal methods, which are all passive cargo-loading techniques, meaning the cargo is encapsulated during liposome formation. In general, hydrophilic cargo is encapsulated by dissolving it in an aqueous solution that serves as lipid hydrating fluid, whereas lipophilic cargo is dissolved in the respective organic solution and added to the dissolved liposome-forming lipids, which are both then dried under vacuum prior to (re-)hydration. In contrast to that, active or remote loading is also possible after liposome formation, but typically requires a pH gradient and certain compounds with ionizable groups, as for example doxorubicin in clinically relevant Doxil®.[42] Besides the numerous lab-scale liposome preparation methods, there are only a few large-scale preparation methods. The most commonly used methods including dual centrifugation, the liposome preparation method used in this work, their classification, advantages and limitations are presented in the following.

LIPID FILM HYDRATION AND SIZING

For preparation of liposomes with the lipid film hydration method, a mechanical dispersion method already used by Bangham *et al.* [14], the respective lipids and hydrophobic cargo are first dissolved in an appropriate solvent (typically chloroform or ethanol) and combined in a round bottom flask (Figure 3). The solvent is subsequently evaporated, for example by a rotary evaporator with subsequent lyophilization, resulting in a thoroughly dry thin lipid film on the bottom glass wall of the flask. The lipid film is subsequently hydrated by adding a suitable hydration medium to the flask, such as phosphate buffered saline, 5% dextrose or 10% sucrose solution, which contains the designated hydrophilic cargo.[11] Subsequent agitation at a temperature above the Tm of the lipid or several freeze-thaw cycles [43] lead to the formation of liposomes. However, depending on the lipids, liposome complex formation, lipid self-aggregation as reported

for phosphatidylethanolamine (PE) [11], or viscous gel formation can occur during hydration and agitation. The resulting liposomes can be classified as multilamellar large vesicles (MLV) with low encapsulation efficiencies (5-15%) [15], which need subsequent downsizing by sonication, extrusion or high pressure homogenization to be applicable. Bath sonicaters are mostly used for sonication of liposomes and typically yield small unilamellar vesicles (SUVs), depending on the temperature, sonication time and power, lipid composition and concentration.[24] However, different size distributions between different liposome batches can occur, since it is almost impossible to reproduce sonication conditions, while degradation of cargo or lipids is also not uncommon due to the high energy input.[44] Additionally, resulting SUVs are relatively unstable due to their high degree of membrane curvature, resulting in the formation of larger vesicles especially upon storage below the T_m of the respective lipids. Sonication also lacks the possibility of receiving liposomes in another size-range. However, this is achievable by extrusion of the MLVs through a polycarbonate membrane with defined pore sizes (Figure 3).[45]
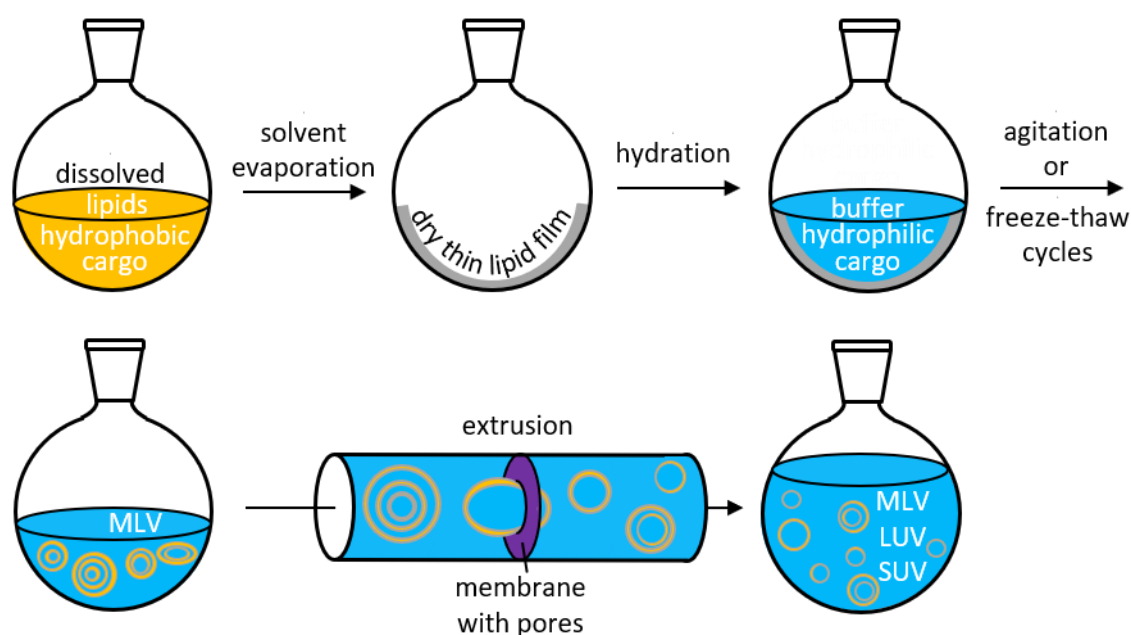
FIGURE 3: PREPARATION OF LIPOSOMES BY THE THIN FILM HYDRATION METHOD FOLLOWED BY EXTRUSION TO YIELD MAINLY LARGE (LUV) OR SMALL UNILAMELLAR VESICLES (SUV) DEPENDING ON THE MEMBRANE PORE SIZE, BESIDES SOME MULTILAMELLAR VESICLES (MLV). INSPIRED BY [46].

During extrusion, the liposome sample is pressed through a polycarbonate membrane containing pores with defined diameters smaller than the liposomes, potentially leading to deformation and ultimately to rupture of the liposomal membrane. It is thought that the ruptured membranes assemble afterwards to form liposomes smaller than or as large as the pore. Of note, extrusion of

liposomes at a temperature below the respective Tm, which renders the liposomal membrane relatively rigid and inflexible, is difficult and can result in disruption of the polycarbonate membrane. Extrusion generally leads to a well-characterized size distribution of liposomes close to the size of the respective pores, but sequential extrusion through several membranes is often necessary, especially if smaller sized liposomes are wanted.[47] In addition, the liposome sample is overall diluted, and the encapsulation efficiency of the designated cargo decreases if the extrusion is not carried out in a solution containing cargo in the respective concentration as present within the hydrophilic core of the liposomes. Maintenance of higher encapsulation efficiencies for hydrophilic cargo can be achieved by high pressure homogenization, a technique in which the liposome dispersion is pumped into a so-called interaction chamber with microchannels that separate it into two streams.[48][49] The interaction of the resulting streams at high velocities under high pressure around 150 bar leads to the formation of SUVs.[50] While this process is scalable to several liters for industrial purposes, it lacks the possibility of downscaling for laboratory purposes, with 10 — 20 mL of liposome dispersion volumes as lower limit.[51]

OTHER PREPARATION METHODS

During the so-called solvent dispersion methods, the dissolved lipids are injected into an aqueous buffer containing the hydrophilic cargo and subsequently the solvent is removed by heating under vacuum. Depending on the solvent used in this method, typically diethyl-, isopropyl-ether or ethanol, it is also referred to as ether or ethanol injection method, respectively.[52] While ether can be removed under vacuum, the removal of ethanol is difficult due to formation of an azeotrope with water. This is a major drawback of this method, since even traces of ethanol can affect liposomal stability and could represent a possible health risk for *in vivo* applications.[53] Other disadvantages are the typically broad size distributions between SUVs and LUVs of the resulting liposomes, the cargo exposure to higher temperatures and to organic solvent, and the low encapsulation efficiency for hydrophilic molecules, although typically higher than for the lipid film hydration method.[15] The ethanol injection method can be improved to be scalable for industrial production of several liters of liposome dispersions by using a cross-flow injection module.[54][55] With this module, it is also possible to control the size of the formed liposomes to a certain extent, which depends on the dissolved lipid concentration, the injection tube diameter, the injection pressure and the flow rate of the aqueous buffer.[56] It is also possible to form an emulsion by sonication or mechanical agitation upon injection of the dissolved lipids in aqueous buffer before removal of residual solvent, which is referred to as reverse phase evaporation method.[57]

Encapsulation efficiencies for hydrophilic cargo of up to 65% can be achieved, but the rather harsh conditions caused by sonication or agitation as well as the cargo exposure to organic solvents could lead to conformational changes of therapeutic RNA, DNA strand breaks or denaturation of proteins. The detergent removal technique represents another possibility for liposome formation.[52] In this technique, detergents like Triton-X 100 ™ at or above their critical micelle concentration are used to solubilize the lipids.[58] Removal of the detergents, e.g. by dialysis [59], gel filtration [60] or adsorption to polystyrene beads [61] leads to the formation of LUVs. Liposomes prepared this way are highly reproducible and show narrow size distributions. However, traces of detergent could remain within the liposomes.

Besides passively loading therapeutic compounds into the liposomes during preparation, a transmembrane pH gradient enables the active loading of suitable amine drugs after liposome formulation, including the anti-cancer drug doxorubicin.[62][63] The gradient can be achieved by adjustment of the buffer pH during lipid hydration and increase of the exterior buffer pH after liposome formation, for example by addition of alkaline buffer or complete buffer exchange *via* dialysis. However, the acidic pH within the liposomes can affect their characteristics and stability.

DUAL CENTRIFUGATION

Dual centrifugation (DC), first described by Massing *et al.* in 2008 [64], is a passive cargo loading mechanical dispersion technique for liposome preparation. As in the thin film hydration method, dissolved lipids and hydrophobic cargo are combined in a reaction tube and pre-dried thoroughly by lyophilization. Reaction tubes are available in a broad range from small PCR tubes with volumes of 200 μL to polypropylene tubes with volumes of up to 50 mL, enabling up- and downscaling of liposome batches for laboratory use or even pre-clinical *in vivo* trials. The dried lipids are subsequently hydrated with an appropriate aqueous buffer containing the designated hydrophilic cargo. The amount of added water is chosen to be just enough to hydrate the polar headgroups of the respective lipids. If hydrophilic polymers like PEG are part of the lipid composition, more water for hydration is needed. Furthermore, glass or ceramic beads are added to the reaction tube for a higher energy input and a better homogenization during DC. The dual centrifuge is constructed like a conventional centrifuge but has a second rotary axis with an offset of 40° to the main rotary axis. This spins the sample holder containing the reaction tubes (which are aligned horizontally) in the opposite direction as compared to the main rotary axis while in operation (Figure 4 A).
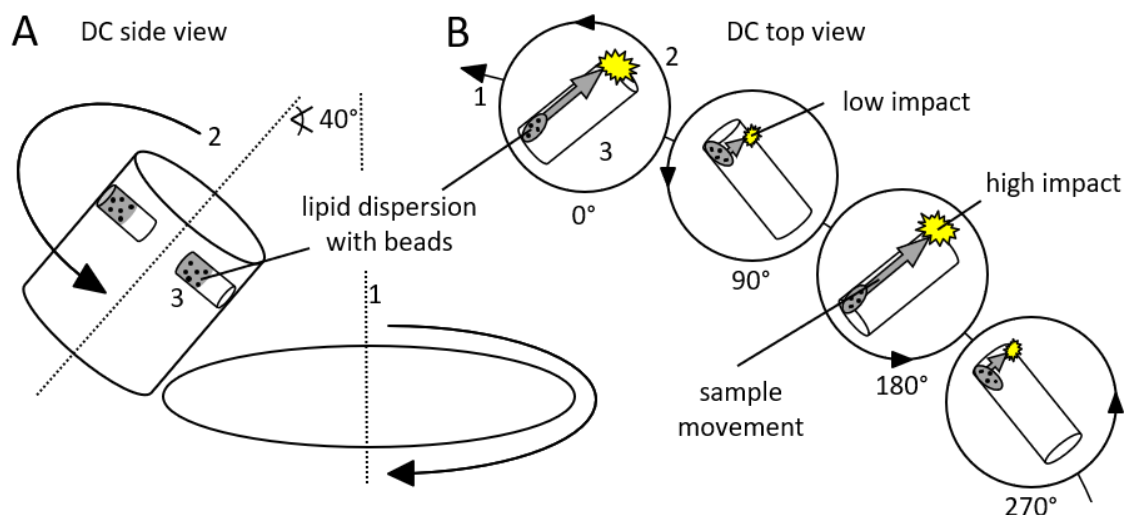
FIGURE 4: (A) PRINICPAL OF DUAL CENTRIFUGATION (DC) AS SIDE VIEW. A MAIN AXIS (1) AND A SECONDARY AXIS (2) DISPLACED BY 40° TURN CONTRARY AND LEAD TO AN EFFECTIVE HOMOGENIZATION OF THE LIPID DISPERSION WITHIN THE SAMPLE HOLDER (3), WHICH IS FURTHER INCREASED BY THE ADDITION OF BEADS TO THE LIPID DISPERSION. **(B)** SAMPLE MOVEMENT (GREY ARROWS) WITHIN THE REACTION TUBE RELATIVE TO THE MAIN AXIS (1) DURING DC DEPENDING ON THE ROTATION OF THE SECONDARY AXIS (2) WITH 0°, 90°, 180° AND 270° AS EXAMPLE FOR SAMPLE HOLDER PLACEMENT (3), LEADING TO LOW AND HIGH IMPACTS ON THE TUBE WALL. INSPIRED BY [65].

During DC, the viscous lipid dispersion gets pressed to the tube wall by the main rotation, while the second rotation simultaneously skids it within the reaction tube with up to 1000 x g, leading to a strong homogenization (Figure 4 B). Vertical sample orientation is also possible but leads to less effective homogenization when small amounts of sample material are used. As a result, a vesicular phospholipid gel (VPG) is created.[66] This VPG is reported to be stable upon storage [65] but can also be used directly to form liposomes by addition of aqueous buffer to the reaction tube and another short subsequent DC run. The resulting liposome dispersion can be separated from the ceramic beads by filtration or by pipetting the dispersion and then rinsing remaining beads with small amounts of buffer in order to retain the whole sample. This preparation method has several advantages over aforementioned methods, mainly the high encapsulation efficiencies (EE) for hydrophilic cargo of around 50% or even higher as reported for siRNA by Hirsch *et al.* [67]. The scalability from several grams down to milligrams of total lipid enables a broad applicability range and makes the use of cost intensive materials economically feasible. The simultaneous preparation of up to 80 individual liposome batches within 30 minutes also qualifies this method suitable for screening purposes. By using aseptic tubes for liposome preparation and by placing the DC under a flow bench, it is possible to prepare liposomes in a sterile manner. DC typically does not require subsequent work-up as extrusion, and with just one instrument needed, it is quite feasible and easy to learn. Resulting liposomes can mostly be classified as LUVs of diameters in the range of

100 – 500 nm. The resulting liposome size and cargo encapsulation efficiencies are mainly dependent on the lipid composition and the volume ratio between cargo, lipids, buffer and ceramic beads. The DC device can also control the temperature during liposome formulation, which prevents overheating and therefore enables protection of temperature sensitive material within the sample, for example proteins from degradation, as already shown by Parmentier *et al.* [68] and Pohlit *et al.* [69]. In addition to numerous reports in the literature with DC as liposome formulation technique [70]–[76], other nanovesicles like polymersomes only composed of synthetic amphiphilic polymers were also shown to be producible by DC [77]–[79]. While this technique combines excellent features for laboratory or pre-clinical scale formulation of liposomes, it has not been scaled for industrial purposes yet.

LIPOSOME CHARACTERIZATION

In order to be applicable for pharmaceutical use, liposomes need to be thoroughly characterized in terms of their size, size distribution, polydispersity, shape and lamellarity, zeta potential, cargo encapsulation efficiency and cargo release, which all depend on the lipid composition, cargo properties and liposome formulation method.[11] Aforementioned liposomal properties can determine liposome aggregation [80], stability [81], fate and transport [82], circulation time [83], toxicity [84], biological uptake [35] and therapeutic efficiency [85]. The liposomal size and size distribution is mostly measured by dynamic light scattering (DLS), a photon correlation spectroscopy method.[86] It is a common tool for measuring the liposomal hydrodynamic radii given that the liposomes are (near-)spherical, the distribution is monomodal and relatively monodisperse and the sample is measured in a suitable dispersant.[87] The hydrodynamic radius R_H is calculated from the liposomes' diffusion coefficient D, the absolute measurement temperature T, the Boltzmann constant κ_B, and the solvent viscosity h by using the Stokes-Einstein equation (formula 1).

$$R_H = \frac{\kappa_B\, T}{6\pi h D} \tag{1}$$

Diffusion coefficients derive from autocorrelated temporal intensity fluctuations of the scattered photons, which depend on the Brownian motion that increases with decreasing liposomal size. The size distribution or sample polydispersity index (PDI) is a dimensionless parameter that can be received from a cumulants fit of the obtained DLS data [88], with indices below 0.3 indicating narrow distributions desirable in pharmaceutical applications [83], and indices above 0.7 indicating broad size distributions not suitable for DLS measurements. However, such polydisperse samples can be more effectively addressed by the rather new technique called Nanoparticle Tracking

Analysis (NTA).[89]–[91] NTA also utilizes the Brownian motion of the liposomes and their scattered light in order to obtain their hydrodynamic radii *via* the Stokes-Einstein equation, but in this case, only a small frame of the total sample is analyzed by a x20 magnification microscope objective with a mounted charged coupled device (CCD) camera (Figure 5 A).
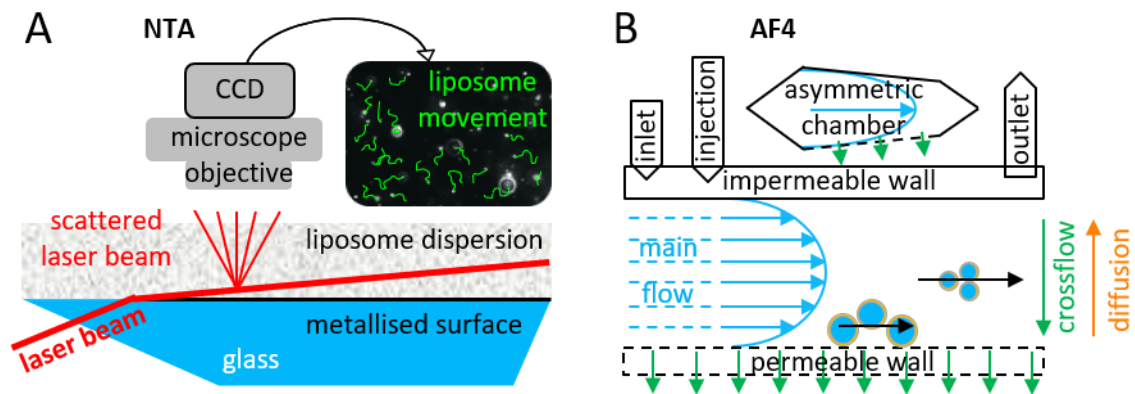
FIGURE 5: **(A)** PRINCIPLE OF NANOPARTICLE TRACKING ANALYSIS (NTA) INSPIRED BY [91]. A LASERBEAM GETS DIRECTED THROUGH GLASS INTO THE LIPOSOME DISPERSION. LIPOSOMES SCATTER THE LASER BEAM, AND THE SCATTERED LASER BEAM IS RECORDED BY A CHARGED COUPLED DEVICE (CCD) CAMERA ATTACHED TO A MICROSCOPE. A PROGRAM ANALYZES THE LIPOSOME MOVEMENT AND YIELDS A SIZE DISTRIBUTION. **(B)** PRINCIPLE OF ASYMMETRIC FLOW FIELD FLOW FRACTIONATION (AF4) INSPIRED BY [92]. THE SAMPLE IS INJECTED INTO THE ASYMMETRIC CHAMBER CONTAINING THE MAIN FLOW WITH A PARABOLIC FLOW PATTERN. A PERMEABLE WALL ON THE BOTTOM LEADS TO A CROSSFLOW. SMALL LIPOSOMES CAN DIFFUSE BACK TO THE FAST FLOWING CENTER OF THE MAIN FLOW DUE TO HIGHER BROWNIAN MOTION COMPARED TO LARGER LIPOSOMES, WHICH REMAIN CLOSER TO THE PERMEABLE WALL AND THEREFORE FLOWING SLOWER AND ELUTING LATER. THIS ENABLES THE SEPARATION OF LIPOSOMES BASED ON THEIR HYDRODYNAMIC RADII.

The camera records a video of the laser scattered light from the liposomes within the frame, with approximately 100 µm x 80 µm x 10 µm as typical dimensions of the frame covering only hundreds of liposomes, and a program tracks the movement of each particle individually. The distance moved can then be converted into particle sizes, and accumulated results of all particles measured yield a size distribution profile. In comparison to DLS, around 10 times less lipid material is necessary for measurement, particle concentrations can be obtained, and small amounts of large particles or aggregates do not comprise the accuracy of the measurement. However, the total number of measured liposomes is several orders of magnitude lower than in DLS. All in all, NTA is a valuable complementary technique to DLS.

Another method for liposome size determination is size exclusion chromatography (SEC), even enabling the separation of liposomes with different hydrodynamic radii, for example by using Sephacryl-S100 to separate liposomes between 30-300 nm in size.[11] *Via* retrieved retention

times, diffusion coefficients can be obtained and based on that information the R_H can be calculated. Although less popular than SEC in the past, but now increasingly being used in a wide range of research areas [93][94], asymmetric flow field flow fractionation (AF4) can be used for liposome size determination.[95] In this chromatography-like technique, the liposome containing sample flows within an asymmetric ribbon-like channel, while a second flow perpendicular to the main flow (crossflow) moves the liposomes towards a permeable wall (Figure 17 B).[96] These two flows allow for the separation of liposomes according to their diffusion coefficients, while their hydrodynamic radii can again be obtained from the Stokes-Einstein equation. Since the main flow travels with a parabolic pattern, the speed at which the liposomes move is higher at the center, and lower at the bottom of the channel. The crossflow guides the liposomes to the bottom, but their natural Brownian motion allows them to diffuse back into the channel, with larger particles remaining lower and smaller particles diffusing back to the center of the main flow, therefore eluting first. The gentleness of this method is its main advantage and enables the purification of liposomes with a protein corona or other loosely attached substances from free and unbound compounds. The limitations of AF4 comprise the small amounts of sample that are applicable, the irreproducibility of results with another solvent, and the necessity of development and optimization of different instrument settings and running methods for more complex samples.[92] AF4 can even be coupled to transmission electron microscopy (TEM), which provides more information about the liposomal shape and lamellarity.[97] In TEM, the liposome dispersion is placed on a carbon grid and a beam of electrons is transmitted through them. Due to differential electron scattering depending on the mass-thickness difference between the liposomes and the surrounding solution containing trehalose (α-D-glucopyranosyl-α-D-glucopyranoside) as preservative [98], an electron image is generated. To increase the overall mass density and therefore the contrast of the image, the sample is negatively stained with uranyl acetate.[99] The image is magnified by a microscope and recorded by a CCD camera.[100] In Cryo-TEM, the sample gets vitrified in liquid nitrogen or ethane without crystallizing, omitting dehydration and staining while preserving the liposomal structure.[101]–[103]

The zeta potential of liposomes is the electric potential on their surface, reflecting the potential difference between the liposomal electric double layer and the dispersant layer around it at a slipping plane.[104] The electric double layer is formed when liposomes are dispersed inside a solution. It consists of the inner, strongly adhered Stern layer containing molecules or ions with an opposite charge to that of the liposome. The outer layer consists of negative and positive charges and is more diffuse.[105] Upon electrophoresis, the liposomes move towards the opposite electrode depending on their charge. The potential at a hypothetical slipping plane between the diffuse outer electric layer of the liposomes and the dispersant is referred to as zeta potential ζ. It

can be calculated from the dispersant viscosity η, the relative permittivity/dielectric constant ε_r, the permittivity of vacuum ε_0 and the electrophoretic mobility of the particle μ_e by using the Helmholtz-Smoluchowski equation (formula 2).

$$\zeta = \frac{\varepsilon_r \varepsilon_0 \mu_e}{\eta} \qquad\qquad (2)$$

The electrophoretic mobility μ_e can be calculated by dividing the particle velocity V by the electric field strength E, which are both known quantities. The actual surface potential on the liposomes also referred to as Nernst potential can however not be measured.[106]

Cargo encapsulation efficiencies (EE), meaning the percentage of encapsulated cargo of total cargo added, can be determined by separation of the cargo-containing liposomes from free cargo present on the outside. It can be achieved either by dialysis [107], centrifugation [108] or size exclusion chromatography [109]. Cargo release can be measured by the same methods, after respective incubation of the liposomes with appropriate buffer or plasma.[110]

1.4 LIPOSOME SURFACE MODIFICATIONS AND 'STEALTH' EFFECT

Liposomes can get surface modified, typically in order to improve their drug delivery efficacy or storage stability. After liposome discovery, initial enthusiasm cooled down since first *in vivo* experiments revealed certain disadvantages, such as low circulation times, low stability, and high uptake into the kidney, spleen, reticuloendothelial system (RES) and liver.[111][112] This behavior can be explained by binding of opsonins to the liposomal surface that form the so-called protein corona, which is comprised of selected serum proteins, for example certain immunoglobulins [113] or beta 2-glycoprotein [114], mediating the recognition of liposomes by macrophages. The complement component system [115] is also able to enhance liposomal uptake by the RES as well as initiating liposome lysis and subsequent cargo release. However, serum proteins like serum albumin or immunoglobulin A have shown dysopsonic properties and therefore inhibit liposome phagocytosis.[116] Therefore, the composition of the protein corona and the ratio between bound opsonic and dysopsonic proteins on the liposomal surface determines the rate of liposomal clearance. The low stability of conventional liposomes *in vivo* can be explained by their interaction and lipid exchange with high (HDL) and low density lipoproteins (LDL). Incorporation of cholesterol and using saturated instead of unsaturated lipids for liposomal membrane formation was shown to lead to an increased stability and a reduction in lipid transfer to HDL. However, this strategy was not enough to fully overcome the binding and exchange with serum components, which is why a liposomal surface coating using rather inert molecules that can form a spatial barrier around the

liposome was needed. This so-called steric stabilization [117][118] can be realized by a variety of hydrophilic glycolipids and polymers [119]–[121], with brain-tissue-derived monosialoganglioside (GM1) and poly-(ethylene)glycol (PEG) coated liposomes as the best studied systems (Figure 6 A).

GM1, a sialic acid-containing glycosphingolipid, is exclusively present on plasma membrane surfaces and increases the circulation half-life of native red blood cells.[122] GM1 as natural and PEG as synthetic material both possess flexible chains that occupy the liposomal surface and therefore reduce binding of opsonins, leading to a diminished liposome recognition by the RES (Figure 6 B). For this reason, liposomes that possess such a steric barrier are also referred to as 'stealth' liposomes, meaning they evade detection by the RES. The surface of the liposomes can be modified with such molecules either by incorporation during liposome formulation, physical adsorption or covalent binding to reactive surface moieties.[123] PEG is often modified with cholesterol or dialkyl-moieties, for example with 1,2-disteaoryl-sn-glycero-3-phospho-ethanolamine (DSPE), that render the molecule amphiphilic and suitable for liposome incorporation during formulation.

It was shown that incorporation of 10 mol-% GM1 into liposomes reduced their uptake by the RES in mice by 90%, therefore also leading to increased blood circulation times.[124] However, this effect was only observable in mice and not observable upon removal of the sialic acid moiety, indicating that this part of the molecule is essential to avoid macrophage uptake.[125] Therefore, two possible mechanisms or their combination might contribute to the reduced recognition and uptake of GM1 liposomes by the RES: (i) reduced opsonization and/or (ii) binding of dysopsonins. GM1 liposomes have been investigated by Taira *et al.* [126] for oral administration, with results suggesting that GM1 liposomes have a higher possibility of surviving the gastrointestinal tract than conventional liposomes. Also, Mora *et al.* [127] observed crossing of the blood-brain-barrier (BBB) by GM1 liposomes in rats, and subsequent quantification of an encapsulated brain-tracer revealed a higher uptake in the rat brain compared to conventional liposomes.
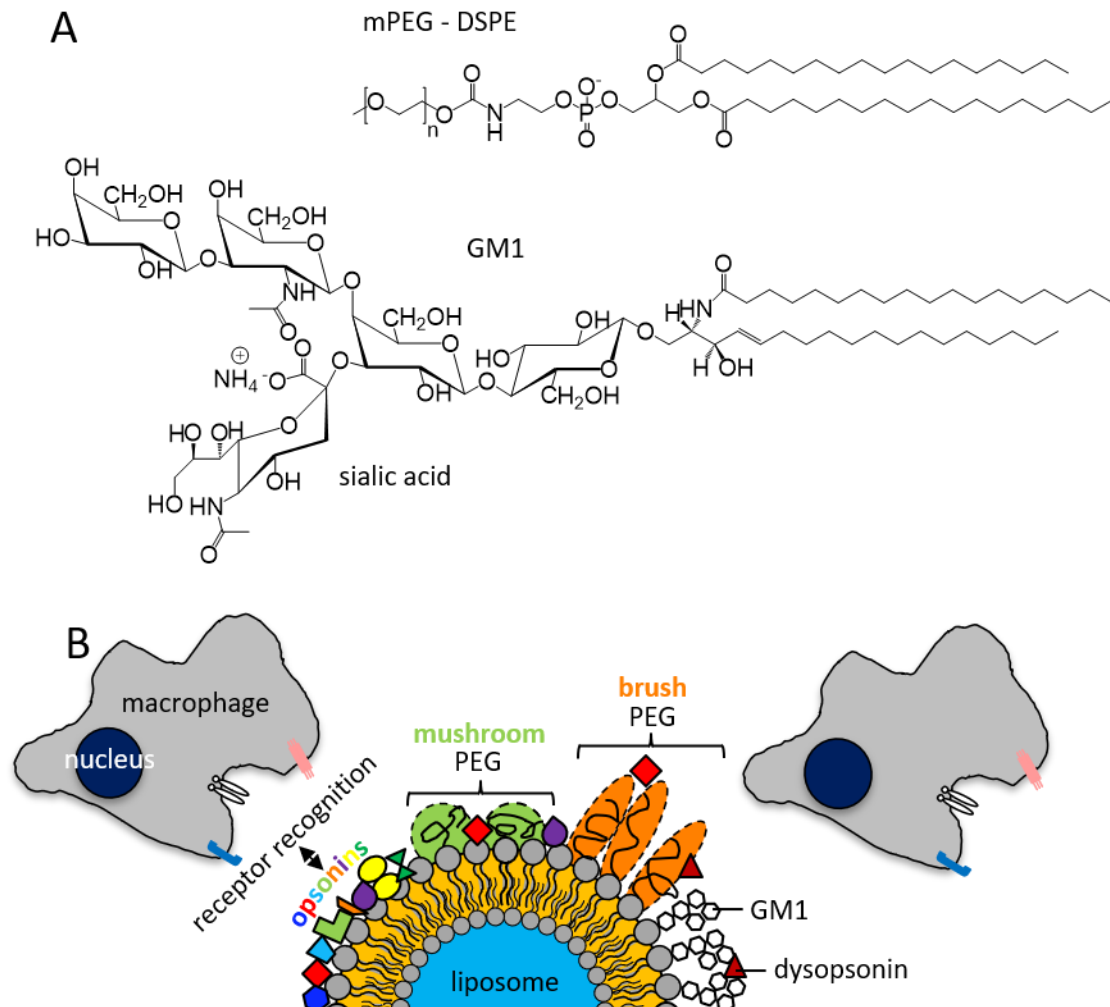
FIGURE 6: **(A)** MOLECULAR STRUCTURES OF METHOXYPOLY-(ETHYLENE) GLYCOL (MPEG) ATTACHED TO 1,2-DISTEAORYL-SN-GLYCERO-3-PHOSPHOETHANOLAMINE (DSPE) AND GLYCOLIPID GM1. **(B)** LIPOSOME RECOGNITION BY MACROPHAGES DEPENDS ON OPSONIN BINDING TO THE LIPOSOMAL SURFACE, WHICH IS THOUGHT TO BE INHIBITED BY PEG AND GM1 AND IS REFERRED TO AS 'STEALTH EFFECT'. PEG CAN UNDERGO CONFORMATIONAL CHANGES FROM MUSHROOM REGIMEN (GREEN) TO BRUSH REGIMEN (ORANGE) UPON INCREASING GRAFTING DENSITY OR PEG CHAIN LENGTH.

PEG and the EPR-effect

The linear polyether diol PEG is the gold standard among different polymers investigated for steric stabilization of liposomes due to its biocompatibility [128], solubility, low toxicity [129] and immunogenicity [130] and good excretion kinetics [131]. PEG is typically incorporated into liposomes by cross-linking it to a lipid like 1,2-disteaoryl-sn-glycero-3-phosphoethanolamine (DSPE) as shown in Figure 6 A.[132][133] Besides modification of liposomes with PEG, several other therapeutic compounds such as proteins and peptides can be derivatized with PEG to increase their stability, solubility and half-life while decreasing toxicity, clearance and immunogenicity.[134]

The main advantage of modifying liposomes with PEG (PEGylation) is the strongly reduced uptake by the RES, therefore prolonging blood circulation times due to a reduced interaction with cell-surfaces and plasma proteins because of the steric hindrance effect.[135][136] It is also possible that dysopsonins bind to PEGylated liposomes, further reducing uptake by the RES.[137][138] Additionally, liposome aggregation is avoided by PEGylation due to a stronger interbilayer repulsion.[139] The stealth effect of polymers like PEG depends on their properties like size (molecular weight / length), uniformity, flexibility or grafting density on the liposomal surface.[132][140] Fortunately, the molecular weight of PEG can be tuned during synthesis depending on the intended purpose. As proposed by de Gennes *et al.*, PEG can undergo conformational changes depending on the available distance between each polymer.[141] At low grafting densities or by using short PEG chains, the flexible PEG is in the so-called mushroom conformation, meaning it possesses a rather diffused globular structure. When the steric repulsion between single chains increases at higher grafting densities or by using long PEG chains, they extend in a rather elongated conformation called brush (Figure 6 B). To reduce the probability of opsonins binding to the liposomal surface and therefore to increase the stealth effect, it was shown that PEG grafting densities need to exceed the minimum for brush conformation.[142][143] As a result of increased circulation times, PEGylated liposomes are capable of accumulating in tumors and infracted areas *via* the enhanced permeability and retention (EPR) effect (Figure 7).[144]–[147] Due to the fact that most solid tumors rapidly grow, newly built blood vessels (angiogenesis) exhibit an enhanced permeability to ensure sufficient nutrient and oxygen supply. Long-circulating liposomes therefore accumulate passively within tumor tissue, which is also referred to as passive targeting, while barely passing healthy vasculature.[148][149]
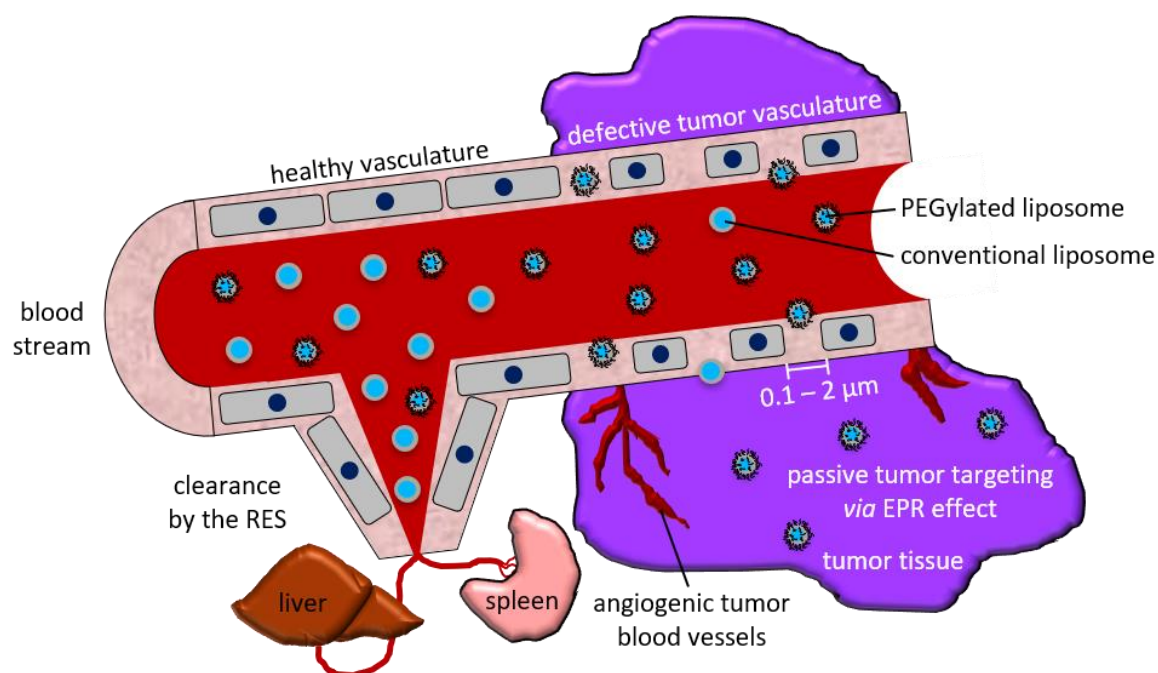
FIGURE 7: CROSS SECTION OF A BLOOD VESSEL WITH CIRCULATING CONVENTIONAL AND PEGYLATED LIPOSOMES. WHILE CONVENTIONAL LIPOSOMES GET RAPIDLY CLEARED BY THE RETICULENDOTHELIAL SYSTEM (RES), ENDING UP MAINLY IN THE LIVER AND SPLEEN, PEGYLATED LONG CIRCULATING LIPOSOMES CAN PASS DEFECTIVE TUMOR VASCULATURE AND THEREFORE ACCUMULATE WITHIN TUMOR TISSUE, WHICH IS ALSO REFERRED TO AS ENHANCED PERMEABILITY AND RETENTION (EPR) EFFECT. INSPIRED BY [150].

Besides mentioned advantages, it has to be pointed out that PEGylated liposomes, like PEGylated liposomal doxorubicin (Doxil®), are not biologically inert and can induce activation of the human complement system.[151][152] The so-called accelerated blood clearance (ABC) phenomenon leads to a fast clearance of PEGylated liposomes that are administered after the first injection, due to antibody production against PEG.[153][154] It has also been reported that PEGylation inhibits cellular uptake of liposomes and subsequent endosomal escape of encapsulated therapeutic compounds, also referred to as PEG-dilemma [155][156], a problem further discussed in section 1.5. Coupling PEG to cell targeting ligands, also referred to as active targeting, is one way to overcome the inhibited cellular uptake of PEGylated liposomes.[155]

Active targeting

Aside from passive targeting, it is also possible to modify PEG with targeting ligands like proteins, peptides, antibodies, aptamers or small molecules to achieve active targeting of cells overexpressing a receptor as docking-site (Figure 8).[157]
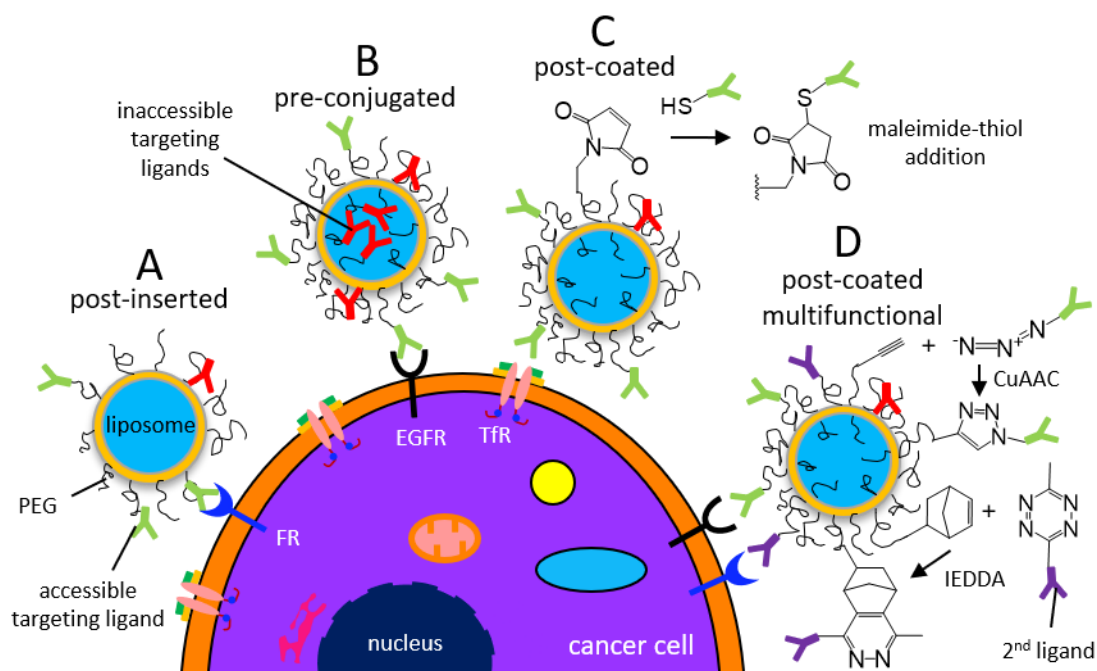
FIGURE 8: ACTIVE TARGETING OF LIPOSOMES TO CELLULAR RECEPTORS LIKE ENDOTHELIAL GROWTH FACTOR RECEPTORS (EGFR), FOLATE RECEPTORS (FR) OR TRANSFERRIN RECEPTORS (TfR). **(A)** TARGETING LIPID-PEG-LIGAND CONJUGATES POST-INSERTED INTO THE LIPOSOMAL MEMBRANE AFTER LIPOSOME FORMULATION. **(B)** PRE-CONJUGATED LIPID-PEG-LIGANDS INCOPORATED DURING LIPOSOME FORMULATION, WITH INACCESSIBLE TARGETING LIGANDS ON THE INSIDE OF THE LIPOSOMAL MEMBRANE. **(C)** POST-COATED LIPOSOMES CONTAINING MALEIMIDE-PEG MOIETIES, COUPLED TO THIOL BEARING TARGETING LIGANDS *VIA* THE MALEIMIDE-THIOL ADDITION. **(D)** POST-COATED MULTIFUNCTIONAL LIPOSOMES CONTAINING PEG WITH TERMINAL ALKYNE-MOIETIES FOR THE COPPER CATALYZED AZIDE-ALKYNE CYCLOADDITION (CuAAC) WITH RESPECTIVE TETRAZINE-FUNCTIONALIZED LIGANDS, WHILE ALSO CONTAINING PEG WITH TERMINAL NORBORNENE MOIETIES FOR THE INVERSE ELECTRON DEMAND DIELS-ALDER CYCLOADDITION (IEDDA) WITH RESPECTIVE TETRAZINE FUNCTIONALIZED TARGETING LIGANDS (PURPLE).

Such ligand-targeted liposomes have been shown to reduce side effects in healthy tissue while enhancing cellular uptake to target cells.[158] Lipid-PEG-ligand conjugates can be post-inserted into preformed liposomes, resulting in liposomes with targeting ligands on their surface (Figure 8 A).[159] However, cargo leakage can occur during this post-insertion, and subsequent removal of free lipid-PEG-ligand conjugates is necessary. Additionally, an effective insertion is hindered at higher PEG grafting densities, which makes a reproducible insertion challenging.[160] Another possibility is to incorporate the lipid-PEG-ligand conjugates during the liposome formulation step (pre-conjugation, Figure 8 B).[161][162] This leads to a statistically even distribution of lipid-PEG-ligand conjugates on the inner and outer surface of the liposomal membrane. However, this approach has the disadvantage that the ligands on the inner liposomal membrane are inaccessible for targeting, while liposomal characteristics such as stability or drug

encapsulation efficiency are more dependent on the respective ligand. To overcome mentioned limitations, the liposomal surface could be modified with targeting ligands after formulation with the so-called post-coating method.[163] To achieve this, the hydroxyl group at the end of the lipid-PEG chain is chemically modified to be reactive for mild ligand coupling with respectively modified ligands. For example, exposed maleimide moieties would be suitable for thiol-coupling in a Michael addition with thiolated antibodies or proteins containing accessible cysteines [164] (Figure 8 C). Another possibility are the so-called click-reactions [165] with e.g. norbornene moieties for the inverse electron demand Diels-Alder cycloaddition (IEDDA) with a tetrazine-modified ligand, or azide/alkyne moieties for the copper catalyzed azide-alkyne cycloaddition (CuAAC) [166], or a combination to achieve multifunctional liposomes as reported by our group [167] (Figure 8 D). Such multifunctional liposomes could potentially be of advantage for the treatment of multidrug resistant cancer.[77] Attractive targets in cancer-cell therapy for active targeting (Figure 8) are, amongst others (i) endothelial growth factor receptors (EGFRs) [168], whose targeting led to a better internalization of anti-cancer drug doxorubicin containing liposomes bearing PEG-DSPE maleimide-thiol coupled with an appropriate antibody (FabV fragments of cetuximab, a monoclonal immunoglobulin G antibody) [169]. Additionally, an efficient transfection of small interfering siRNA from cationic EGFR-targeted liposomes to lung cancer cells in mice was reported.[170] (ii) Folate receptors (FR), which are overexpressed in cancer cells since folate is essential for cell proliferation after reduction to tetrahydrofolate. FR targeting was shown to increase the internalization of PEG-folate containing liposomes loaded with doxorubicin.[171] (iii) Transferrin receptors (TfR), which are overexpressed in cancers due to a higher cellular iron demand. Targeting TfR with lipid-PEG-transferrin containing liposomes was shown to enhance therapeutic efficiency against liver cancer when compared to non-targeted liposomes.[172] Unfortunately, the receptor presence and density on cancer cells varies between cancer types, patients and possibly also within one patient, which is why ligand-targeted liposomes were not able to surpass passively targeted liposomes in therapeutic efficiency yet.[173] Additionally, coupling of targeting ligands like antibodies to liposomes is cost-intensive and leads to a more complex drug delivery system. Therefore it is more difficult to achieve pharmaceutical quality, explaining the slow progress of such systems in clinical development.[174]

PEG alternatives

Besides the gold-standard PEG, there is an ongoing research for other hydrophilic, soluble and biocompatible polymers that can be used for steric stabilization of liposomes.[175] Some examples from the literature are poly(acryl amide) (PAA) [176] , poly(vinyl pyrrolidone) (PVP) [177][178],

poly(vinyl alcohol) (PVA) [179], poly(2-methyl-2-oxazoline) [180], phosphatidyl polyglycerol [181] and poly[*N*-(2-hydroxypropyl)methacrylamide] (poly(HPMA)) [182] (Figure 9). All the mentioned polymers possess a highly flexible main chain and have been shown to decrease liposomal clearance and therefore increase circulation times in a comparable manner to PEG, influenced by grafting density and polymer size.
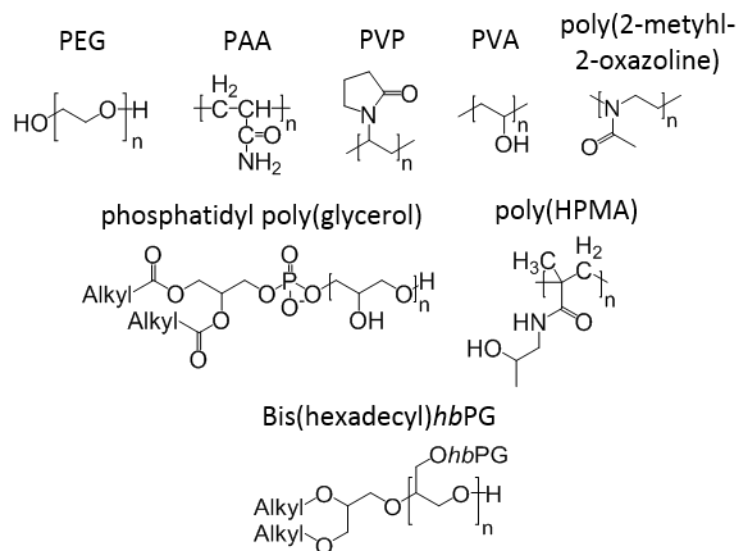
FIGURE 9: MOLECULAR FORMULAS OF POLYMERS USED FOR STERIC STABILIZATION OF LIPOSOMES. SHOWN ARE POLY(ETHYLENE)GLYCOL (PEG), POLY(ACRYL AMIDE) (PAA), POLY(VINYL PYRROLIDONE) (PVP), POLY(VINYL ALCOHOL) (PVA), POLY(2-METHYL-2-OXAZOLINE), PHOSPHATIDYL POLYGLYCEROL, POLY[*N*-(2-HYDROXYPROPYL)METHACRYLAMIDE] (POLY(HPMA)) AND BIS(HEXADECYL) HYPERBRANCHED POLYGLYCEROL (*hb*PG).

In 2010, Hofmann *et al.* from the group of Prof. Frey published the controlled synthesis of hyperbranched polyglycerols (*hb*PG) *via* anionic ring-opening polymerization (AROP) [183] linked to lipid structures like cholesterol or aliphatic glyceryl ethers as initiators [184], making subsequent lipid-polymer conjugation reactions obsolete. Such amphiphilic *hb*PGs, as for example bis(hexadecyl)*hb*PG shown in Figure 9, are readily incorporable into liposomes, possess a flexible aliphatic polyether backbone, are biocompatible and bear multiple hydroxyl end groups for functionalization. Due to more potentially available ligand coupling sites per polymer in comparison to PEG, *hb*PG is a promising candidate for active targeting of liposomes. Incorporation of *hb*PG-lipids into liposomes resulted in lower aggregation in human blood serum when compared to PEGylated liposomes [185], and biodistribution studies in mouse model showed comparable behaviors [186]. Repetitive administration of polyglycerol containing liposomes were also shown to not cause the ABC-phenomenon as reported for PEGylated liposomes [187].

1.5 STIMULI SENSITIVE LIPOSOMES

After the liposomes reached their target site *via* passive and/or active targeting, encapsulated therapeutics only become bioavailable upon a release from the liposomes. Therefore, stimuli-sensitive liposomes, meaning liposomes that destabilize and release their encapsulated cargo upon a stimulus, were developed to increase the therapeutic potential of liposomal drug delivery. In cancer therapy, the tumor microenvironment as well as intracellular stimuli, such as pH, redox potential and enzymes, can serve as triggers for cargo release. External stimuli such as light, heat, magnetic field or ultrasound can also cause the liposomal membrane to destabilize and lead to subsequent cargo release.

pH-sensitive liposomes undergo an acid-triggered change in membrane permeability or stability that causes the rapid release of encapsulated cargo. They are typically composed of one or more lipids such as cholesterolhemisuccinat (CHEMS) or phosphoethanolamines (PE), such as 1,2-dioleoyl-*sn*-glycero-3-phospho-ethanolamine (DOPE) (Figure 10 A). These lipids are widely used for pH-sensitive liposomes that are capable of releasing encapsulated cargo in acidic environment as present at inflammatory or infectious sites, in tumor microenvironment or after cellular uptake in endosomes and lysosomes.[188][189] While CHEMS is negatively charged at neutral pH, it gets protonated at acidic pH, which alters its interaction to neighbouring phospholipids and consequently liposomal membrane acyl chain fluidity, motion, surface charge and therefore also stability and permeability.[190][191] Sudimack *et al.* reported that no membrane fusion upon destabilization of liposomes containing only CHEMS as pH-sensitive lipid was found.[192] Other lipids as fusogenic DOPE (and other unsaturated species of phosphoethanolamines) undergo a lipid phase change upon acidification, for example from liquid disordered phase L_α to inverted hexagonal phase II (H_{II}), leading to destabilization of the liposomal membrane and/or to its fusion with the endosomal membrane (Figure 10 B).[193][194] While DOPE is zwitterionic, the positively charged amine of its PE headgroup can form an ion pair to phosphate groups of neighbouring phospholipids, greatly reducing its polar character. At lower pH, the therefore relatively hydrophobic surface facilitates the formation of non-bilayer phases.[195] Additionally, pH-sensitive PEG on the liposomal surface could increase their passive accumulation to the tumor site, while being cleaved off within the tumor tissue to enhance cellular uptake, release cargo, expose targeting ligands or positive charges, or after cellular uptake to enhance endosomal escape of encapsulated therapeutics (Figure 10 C).
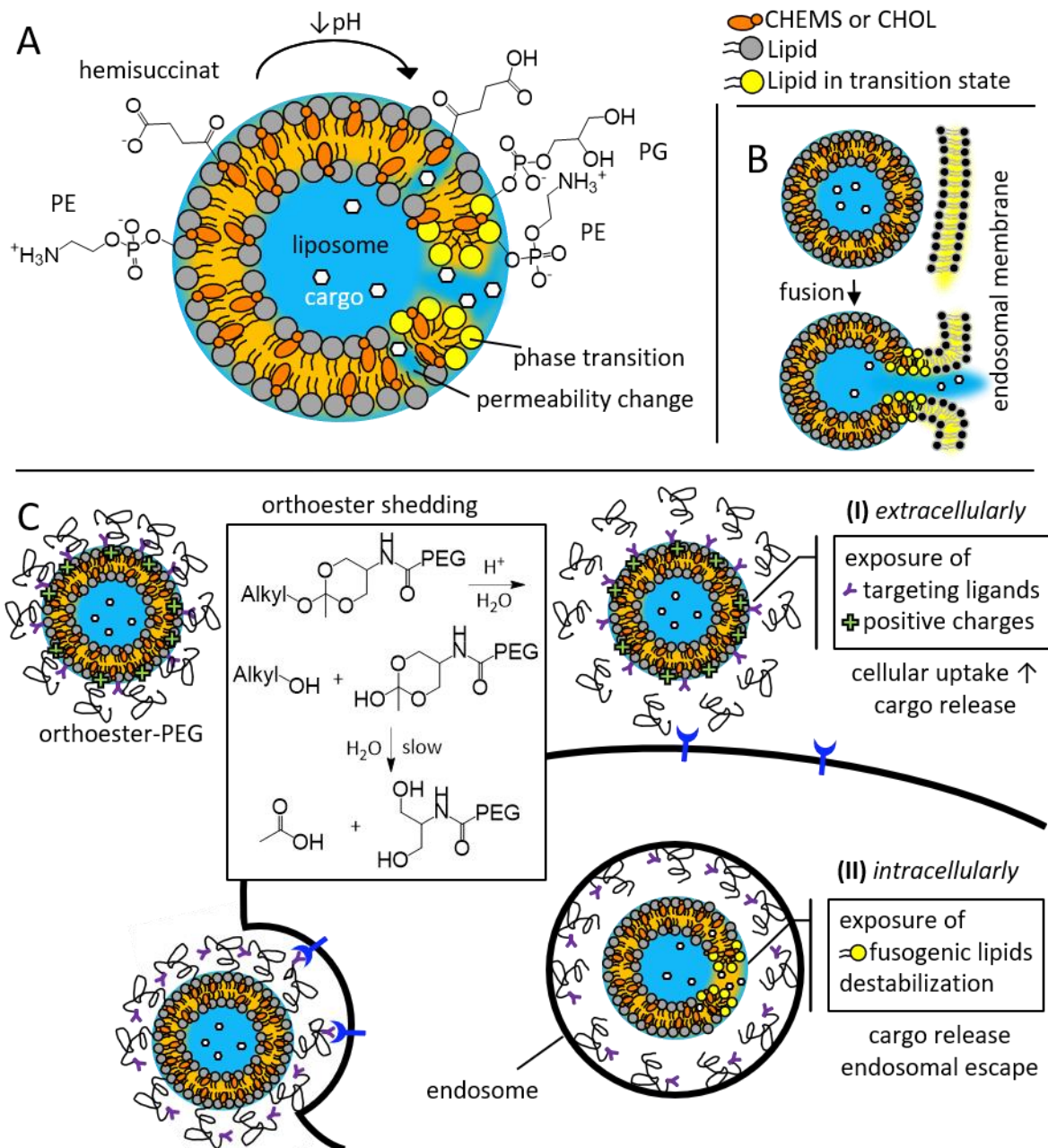
FIGURE 10: (A) pH-SENSITIVE LIPOSOME WITH PHOSPHOETHANOLAMINE (PE) LIPIDS AND SUCCINAT RESIDUES DERIVING FROM CHOLESTERHOLHEMISUCCINAT (CHEMS). UPON ACIDIFICATION, THE AMINE GROUPS OF THE PE INTERACT STRONGLY WITH NEIGHBOURING PHOSPHATE GROUPS, RENDERING THE LIPID MORE HYDROPHOBIC AND POTENTIALLY FACILITATING LIPID PHASE TRANSITION. PROTONATION OF THE HEMISUCCINAT LEADS TO A MEMBRANE PERMEABILITY CHANGE AND CARGO RELEASE. **(B)** FUSION OF LIPOSOMAL AND ENDOSOMAL MEMBRANE ALLOWS FOR ENDOSOMAL ESCAPE OF CARGO. **(C)** pH-DEPENDENT CLEAVAGE OF LIPID-ORTHOESTER-PEG SHIELDING ({N-(2-METHYL-2-ALKOXY-[1,3]DIOXAN-5-YL)-AMIDO}-POLY-(ETHYLENEGLYCOL) [196] **(I)** EXTRACELLULARLY, FOR EXAMPLE DUE TO LOW pH IN TUMOR MICROENVIRONMENT, TO POTENTIALLY EXPOSE TARGETING LIGANDS OR POSITIVE CHARGES THAT CAN INCREASE CELLULAR UPTAKE. RESULTING DESTABILIZATION CAN ALSO LEAD TO EXTRACELLULAR CARGO RELEASE. **(II)** INTRACELLULARLY, FOR EXAMPLE DUE TO LOW pH IN ENDOSOMES, TO POTENTIALLY EXPOSE FUSOGENIC LIPIDS OR LEAD TO AN OVERALL MEMBRANE DESTABILIZATION, RESULTING IN CARGO RELEASE AND/OR ENDOSOMAL ESCAPE.

Typical pH-sensitive PEGs contain orthoester- [197], acetal- [69][198], ketal- [77] or vinylether-linkages [199][200] amenable to pH dependent cleavage. By modifying the ratio of the pH-sensitive linkages to other liposomal components, either during PEG synthesis or liposome formulation, the liposome stability can be tuned. However, *in vivo* validation of pH-cleavable PEGylated liposomes is just recently beginning to be explored.[201]

Thermosensitive liposomes (TLs) are typically composed of lipids with a gel to liquid phase transition temperature around the target temperature, for example 1,2-dipalmitoyl-sn-glycero-3-phosphatidylcholine (DPPC) with a Tm of 41 °C close to body temperature (Figure 11 A). Such liposomes are reported to effectively release encapsulated cargo under controlled hyperthermia conditions, which are typically achieved by the use of external heat-generating medical systems, such as magnetic resonance guided high intensity focused ultrasound.[202] Kim *et al.* reported a hyperthermia approach using DPPC liposomes in combination with active-targeting to effectively deliver and release DXR to tumor cells.[203]

A rather rapid 'burst' release of cargo from liposomes can be achieved by low intensity ultrasound (20 kHz to several MHz) in combination with ultrasound responsive perfluorocarbon (PFC) gas. Liposomes or other vesicular structures containing PFC gas (or comparable) are also referred to as microbubbles.[204][205] The applied acoustic pressure causes the microbubbles to oscillate, causing convection microstreams up to the point at which the microbubbles reach resonance and collapse. The resulting shockwaves lead to disruption of the liposomal membrane (Figure 11 B).[206] It was shown by Lin *et al*. that liposomes with encapsulated DXR and perfluoropentane nanodroplets release DXR to the cytosol after cellular uptake in response to ultrasound.[207]

Another strategy for triggered cargo release is the incorporation of amphiphiles containing disulphide linkages or cross-links that can be disrupted by thiolytic reducing agents as dithiothreitol (DTT), or by changes in the reductive potential at tumor sites caused by glutathione (GSH), leading to a lipid phase change and/or membrane destabilization (Figure 11 C).[150] Fu *et al.* prepared liposomes with disulphide-linked PEG and cell-penetrating peptides (CPPs) on the liposomal surface. Upon diffusion to the tumor site, the PEG was cleaved by GSH and the now accessible CPPs facilitated cellular uptake, leading to an enhanced therapeutic efficiency for cancer treatment.[208]
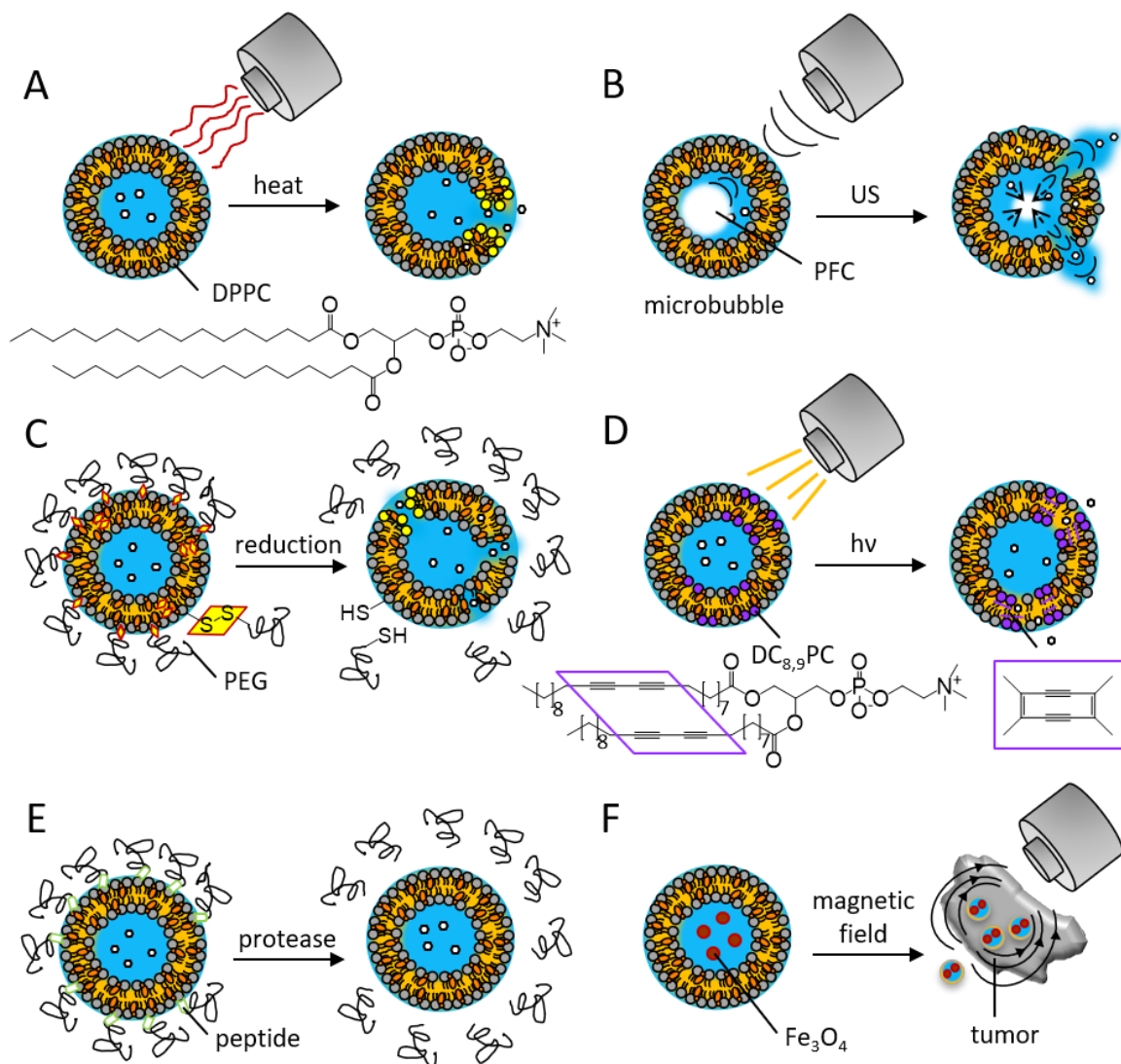
FIGURE 11: (A) THERMOSENSITIVE LIPOSOMES CONTAINING DPPC (1,2-DIPALMITOYL-SN-GLYCERO-3-PHOSPHATIDYLCHOLINE). UPON HEATING ABOVE THE Tm OF THE RESPECTIVE LIPID, CARGO IS RELEASED DUE TO PHASE TRANSITION AND/OR MEMBRANE PACKING DEFECTS. **(B)** LIPOSOME WITH ENCAPSULATED PERFLUORCARBON (PFC) GAS ALSO TERMED MICROBUBBLE. UPON LOW INTENSITY ULTRASOUND, THE MICROBUBBLE COLLAPSES AND CAUSES MICROSTREAMS AND SHOCKWAVES THAT DISRUPT THE LIPOSOMAL MEMBRANE LEADING TO CARGO RELEASE. **(C)** DISULPHIDE LINKAGES BETWEEN PEG AND LIPIDS OR BETWEEN LIPIDS CAN CAUSE DESTABILIZATION OF THE LIPOSOMAL MEMBRANE UPON REDUCTION, FOR EXAMPLE WITH DITHIOTHREITOL. **(D)** LIPOSOME CONTAINING 1,2-BIS(TRICOSA-10,12-DIYNOYL)-SN-GLYCERO-3-PHOSPHOCHOLINE ($DC_{8,9}PC$) THAT POLYMERIZES UPON UV IRRADIATION CAUSING LIPOSOMAL MEMBRANE DEFECTS AND CARGO RELEASE. **(E)** LIPID-PROTEIN-PEG CONTAINING LIPOSOME LOSES ITS PEG SHIELD UPON CONTACT WITH PROTEASES. **(F)** LIPOSOMES CONTAINING SUPER MAGNETIC IRONOXIDE ACCUMULATE WITHIN TUMOR TISSUE UPON APPLICATION OF A MAGNETIC FORCE TO THE TUMOR AREA.

Light able to transmit deep into biological tissues, typically with a wavelength in the range of 600 — 900 nm, can also trigger liposomal cargo release during photodynamic therapy.[209] The

liposome has to contain a photosensitizing agent, typically hydrophobic and therefore located within the liposomal membrane, that is amenable to photocleavage, polymerization or conformational changes.[210][211] Yavlovich *et al.* prepared DPPC liposomes containing 20 mol-% 1,2-bis(tricosa-10,12-diynoyl)-sn-glycero-3-phosphocholine (DC$_{8,9}$PC) [212] (Figure 11 D), a lipid that can polymerize upon UV irradiation, leading to defects within the liposomal membrane [213]. Although UV irradiation is not able to transmit deep into biological tissues, it led to a complete release of calcein from liposomes within 40 min of irradiation.[214] Liposomes with encapsulated photosensitive sulphonated dye aluminium phthalocyanine [215] showed high phototoxicity when irradiated with red light (wavelength 600 — 700 nm) due to the formation of reactive oxygen species (ROS) as investigated by Morgan *et al.* [216].

Two further possibilities for triggered cargo release are incorporation of enzyme- or magneto-sensitive components. Zhu *et al.* formulated liposomes bearing matrix metalloproteinase (MMP) sensitive PEG-lipids containing a respective peptide which was cleaved within the tumor area due to highly expressed extracellular MMPs [217], resulting in tumor-specific PEG removal and subsequently in enhanced cellular uptake (Figure 11 E).[218] Encapsulation of super magnetic iron oxide (Fe$_3$O$_4$) into liposomes and application of a magnetic force to the tumor area was shown to result in a higher liposome accumulation (Figure 11 F).[219]

Of note, stimuli-sensitive liposomes can be combined with active targeting moieties to achieve a more complex, but potentially also more potent drug delivery system. Barbosa *et al.* formulated pH-sensitive CHEMS:DOPE liposomes containing lipid-PEG-folate for active targeting of cancer cells, that showed increased cytotoxicity over non-targeted pH-sensitive liposomes.[220] On the other hand, Sudimack *et al.* reported that folate receptor(FR)-targeted pH-sensitive liposomes showed increased cancer cell cytotoxicity over FR-targeted non-pH-sensitive liposomes, indicating that a combination of targeting and triggered release is a promising approach for drug delivery.[192]

1.6 LIPOSOMES AND MACROPHAGES

Besides evading the reticuloendothelial system (RES) by stealth liposomes, numerous studies also focused on developing liposomes that specifically target macrophages and monocytes, since they are involved in many diseases like cancer, asthma or atherosclerosis and play an important role for infectious and inflammatory diseases.[221] Therefore, RES-targeted liposomal drug delivery is a

promising approach for treating aforementioned diseases. Hematopoietic stem cells can differentiate to monocytes and enter the circulation. While monocytes are immune effector cells themselves, they can differentiate depending on microenvironmental conditions into dendritic cells or macrophages.[222][223] Macrophages themselves are polarized into the mainly inflammation associated M1 phenotype after activation by lipopolysaccharides or inflammatory cytokines, or into the tissue repair and regeneration related M2 phenotype after activation by certain interleukins, glucocorticoids or pathogen-associated molecular patterns (PAMPs). M2-like tumor associated macrophages (TAMs) promote tumor growth by increasing angiogenesis through releasing matrix metalloproteases and endothelial growth factors.[224] M2 and TAMs contain toll-like receptors (TLRs), which can recognize conserved PAMPs. Therefore, attachment of TLR ligands to liposomes is an efficient strategy for targeting M2 and TAMs in order to enhance cellular uptake, while other receptors are also possible targets, such as scavenger (SR) and mannose receptors (MR) (Figure 12).[225] Liposomes containing mannose or trimannose as targeting vectors, for example coupled to 1,2-dipalmitoyl-sn-glycero-3-phosphoethanolamine (DPPE) (Figure 12) [226][227] and incorporated during liposome formulation, were shown enhanced *in vitro* and *in vivo* uptake to macrophages, which was MR-mediated as revealed by inhibition studies.[228]–[231] Various other reports investigated the influence of the liposomal charge and size on macrophage recognition and uptake.[232]–[234] It was found that the uptake does rather not depend on the size, but on the charge and other specific properties of the liposomes, with negatively charged liposomes containing phosphatidylgylcerol (PG) or phosphatidylserine (PS) (Figure 12) showing the best internalization into macrophages [235], while omitting association with monocytes and dendritic cells [236]. The enhanced internalization of PS containing liposomes likely originates from the apoptosis or necrosis of a cell, during which PS flips from the inner to the outer side of the cell membrane and gets recognized by SRs on macrophages for subsequent phagocytosis and clearance.[237]

Macrophage-targeted liposomes with encapsulated bisphosphonate Clodronate (Figure 12), a drug normally used to treat osteoporosis [238], were shown to induce macrophage apoptosis, therefore reducing TAM promoted tumor growth [239] or arthritis [240]. In arthritic regions, macrophages scavenge oxidised low-density lipoproteins (LDLs) and become foam cells that act as core for atherosclerotic plagues. Targeting of these scavenger receptors using liposomes would decrease scavenging of LDL and simultaneously enable the effective delivery of encapsulated therapeutics [241][242], while encapsulated contrast agents could reveal atherosclerotic lesions.[221][243][244] Metformin (1,1-Dimethylbiguanid, Figure 12), another small molecule normally used to treat diabetes type 2 [245], was found to suppress M2 polarization of macrophages in tumor environment, which resulted in a suppressed tumor growth [246][247].

Although the underlying mechanism remains unclear, Metformin seems to be an interesting cargo for macrophage-targeted liposomal delivery.
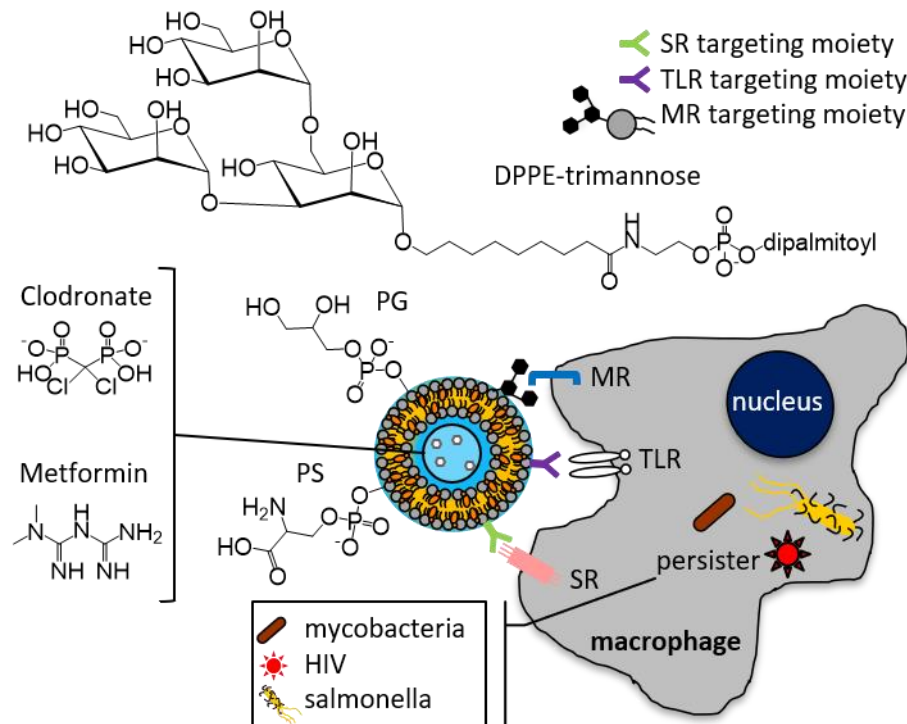
FIGURE 12: CONCEPT FOR MACROPHAGE-TARGETING OF LIPOSOMES WITH ENCAPSULATED SMALL MOLECULES. LIPOSOMES CONTAINING LIPIDS WITH PHOSPHATIDYLGLYCEROL (PG) OR PHOSPHATIDYLSERINE (PS) HEADGROUPS ARE REPORTED TO ENHANCE PHAGOCYTOSIS. SCAVENGER RECEPTORS (SR), TOLL-LIKE RECEPTORS (TLR) AND MANNOSE RECEPTORS (MR) ARE POTENTIAL TARGETS FOR ACTIVE TARGETING MOIETIES PRESENT ON THE LIPOSOMAL SURFACE, FOR EXAMPLE TRIMANNOSE COUPLED TO 1,2-DIPALMITOYL-SN-GLYCERO-3-PHOSPHOETHANOLAMINE (DPPE) TO TARGET THE MR. AS HYDROPHILIC CARGO, SMALL MOLECULES LIKE CLODRONATE OR METFORMIN KILL OR POLARIZE M2 MACROPHAGES UPON INTRACELLULAR RELEASE, RESPECTIVELY. CERTAIN PATHOGENS AS MYCOBACTERIA, HUMAN IMMUNODEFICIENCY VIRUS (HIV) AND SALMONELLA CAN RESIDE AND PERSIST IN MACROPHAGES AS RESERVOIR, A CIRCUMSTANCE THAT COULD BE HANDLED BY TARGETING THERAPEUTIC LIPOSOMES TO MACROPHAGES.

Some bacteria and viruses, as mycobacteria (e.g. tuberculosis) [248], human immunodeficiency virus (HIV) [249] or salmonella [250][251], can survive macrophage phagocytosis and therefore persist within for proliferation and re-infection. This is especially dangerous since macrophages can cross the blood brain barrier (BBB) and spread engulfed pathogens.[252] It is therefore of great importance to design liposomes that contain antiretroviral drugs and efficiently target potentially pathogen-infected macrophages.[253][254] Several studies reported on macrophage targeting strategies using PEGylated antibody or (tri)mannose containing 1,2-dipalmitoyl-sn-glycero-3-

phospho-(1'-rac-glycerol) (DPPG) liposomes, that resulted in an enhanced efficiency of encapsulated anti-infective agents.[255]–[257] However, the fact that macrophages can cross the BBB could also be exploited by using macrophage-targeted liposomes to deliver therapeutics to the brain which are normally not able to cross the BBB. To increase the transmigration of macrophages across the BBB, a combined approach by Saiyed *et al.* [258] using liposomes with encapsulated supermagnetic Fe_3O_4 and therapeutics led to magnetic-sensitive macrophages after uptake of the Fe_3O_4 containing liposomes. An applied magnetic field was then guiding the magnetic macrophages to the brain.

1.7 ZEBRAFISH EMBRYOS AS MODEL SYSTEM FOR *IN VIVO* EVALUATION OF LIPOSOMES

Liposomal therapeutics in preclinical development are typically evaluated first by physicochemical characterization, then by *in vitro* cell culture experiments and after that by *in vivo* studies using mammalians like dogs, pigs, rats or mice.[259] Due to evolutionary proximity, these organisms possess a striking homology to the human genome and a relatively similar anatomy, cell biology and physiology.[260] However, in addition to ethical issues, the usage of mammalians as animal models is quite laborious, cost- and time-intensive.[261] Furthermore, imaging possibilities within these animals are restricted to mainly nuclear imaging, near-infrared emitting dyes or magnetic resonance imaging.[262] Already in the 1930s, zebrafishes (*Danio rerio*) were used as embryological and developmental model, while in the 1980s, genetic techniques (e.g. cloning) allowed further investigations on vertebrate development.[263] The zebrafish was finally established as a mainstream model in developmental biology after the identification of early developmental zebrafish mutants by genetic screening in the 1990s.[264]–[266] Since then, an increasing number of publications report on the use of zebrafish embryos (ZFEs) for *in vivo* evaluation of nanoparticular therapeutics, closing the huge gap between cell culture and mammalian *in vivo* studies.[260][267] In contrast to invertebrate models such as Drosophila melanogaster[268], the ZFE model possesses a high level of genetic homology to humans [269], although zebrafish diverged from humans around 450 million years ago [270]. The ZFE model offers several advantages over classical mammalian models, despite the obvious differences between fish and human physiology, with a comparison of certain characteristics to the mouse model shown in table 1.[271]

TABLE 1: COMPARISON OF IMPORTANT ATTRIBUTES OF ZEBRAFISH EMBRYO AND MOUSE MODEL SYSTEMS ADAPTED FROM [260]. $ AND + DESCRIBE THE RELATIVE COST AND STRENGTH OF THE MODEL, RESPECTIVELY.

model system attributes		
husbandry infrastructure	$	$$$
cost per day	1 cent	1 dollar
genetic similarity	++	+++
anatomical similarity	+	++
transient *in vivo* assays	++++	+
feasibility for HTS	+++	+
sequencing progress	++	+++
cell lines and tissue culture	+	++++
antibody reagents	+	++++

A successful adult mating yields between 200 and 300 ZFEs per day per adult pair, with the embryogenesis being completed 72 hours post fertilization (hpf). ZFE husbandry and experimental costs are low and their small size renders them suitable to arraying into multiwell plates for high throughput screening (HTS). The embryos are optically transparent and robust, which enables the use of a broad variety of fluorescent-based (live) imaging, a unique feature for a vertebrate research animal (Figure 13).[272] Spaink *et al.* reported the use of robotic injection of DNA, microbes and human cancer cells into ZFEs at a speed of up to 2000 ZFEs per hour and subsequent screening *via* fluorescence analysis.[273] This *in vivo* HTS enables determination of circulation, clearance, tissue targeting and side effects not accessible *via in vitro* HTS in cell culture.[274] Additional advantageous treats of ZFEs are their high reproducibility, ethical considerations and the availability of transgenic lines, for example with green fluorescent protein (GFP) expressing vasculature or macrophages.[275] In contrast to adult zebrafish [276], ZFEs lack an adaptive immune system within the first month [277] and therefore support growth of human cancer cells, since an active immune suppression is not necessary upon cancer cell injection. However, several mammalian organs as breast, lung or the prostrate are not present and can therefore not be addressed in zebrafish embryos, while in addition some metabolizing liver enzymes are not fully characterized yet.[278]
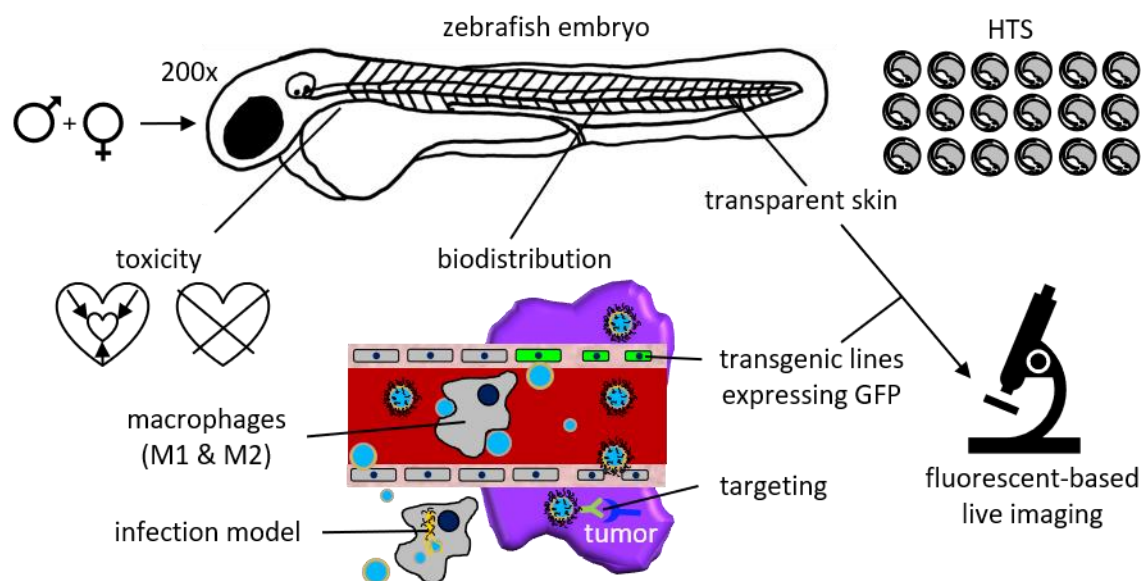
FIGURE 13: SPECIAL TRAITS OF THE ZEBRAFISCH EMBRYO (ZFE) MODEL FOR HIGH THROUGHPUT SCREENING (HTS) OF LIPOSOMES. AROUND 200 ZFES ARE OBTAINED FROM THE MATING OF ONE ADULT PAIR. TOXICITY ASSAYS TYPICALLY RELY ON THE HEARTBEAT OR MORPHOLOGICAL CHANGES. LIPOSOME BIODISTRIBUTION AND TARGETING CAN BE ASSASSED BY FLUORESCENT-BASED LIVE IMAGING USING FLUORESCENT PROBES SINCE THE FISH HAS A TRANSPARENT SKIN. TRANSGENIC ZFE LINES CAN EXPRESS THE GREEN FLUORESCENT PROTEIN (GFP) E.G. IN THE VASCULATURE, FURTHER ENHANCING IMAGING POSSIBILITIES. ZFES POSSESS M1 AND M2 MACROPHAGES 30 HOURS POST FERTILIZATION, MAKING THEM AMENABLE TO INVESTIGATIONS ON INFLAMMATORY DISEASES AND CANCER. SEVERAL INFECTION MODELS, FOR EXAMPLE SALMONELLA, ARE AVAILABLE FOR STUDIES. ADAPTED FROM [267].

ZFEs are already used by various companies for *in vivo* evaluation of new drugs, including toxicity, absorption, metabolism and half-life, to early identify complications which lowers the probability of failing in subsequent cost-intensive *in vivo* mammalian or even clinical trials.[272] The complex systemic circulation behavior of liposomes, taking the serum proteins, blood flow and shear stress into account, could be assessed recently in a time-effective manner by various groups using the ZFE model.[279]–[281] Since ZFEs already possess M1 and M2 macrophages 30 hours post fertilization, it is also possible to evaluate liposomes designed for the treatment of cancer or inflammatory disorders.[282]–[284] Several infection models are available, for example salmonella or tuberculosis, with the latter showing features of human pathology [285][286] that are often absent in the mouse model [287]. Increasingly new compounds are developed for liposome formation and surface modification, and the seemingly endless probabilities of combining them could render the ZFE model beneficial for *in vivo* screening of future nanomedicines prior application to higher vertebrate model systems.

1.8 LIPOSOMES IN CLINICAL APPLICATION AND DEVELOPMENT

Often, the bottleneck for translation of newly identified and thoroughly characterized liposomal drug-carriers are issues in pharmaceutical manufacturing, government regulations and intellectual property.[1] For pharmaceutical manufacturing, the manufacturing process should be scalable, reliable and reproducible, while not affecting encapsulated therapeutics. Resulting liposomes should have pharmaceutical quality and possess long-term stability.[288] The complexity of liposomal drug delivery vehicles increases with more components, like surface modifications and targeting ligands, which makes such evaluations of scalability and stability difficult and cost intensive. The intellectual property of a liposomal drug depends on various factors, as the encapsulated drug, liposome composition, or targeting vectors, with likely multiple patents associated with any of these, probably reducing the commercial attractiveness of the liposome. Clinical trials of liposomal drugs are more complex compared to conventional drugs since the control groups have to account for different aspects not only of the drug, but also of the liposome. A cost-benefit analysis of the liposomal drug with its approved counterparts or other therapies can even lead to a fail at clinical phase III. Nevertheless, 15 liposome-based products made it to the market, with three of the most important briefly described in the following.

Doxil® was the first PEGylated liposomal drug delivery system approved by the united states food and drug administration (FDA) in 1995. The liposomes were remote loaded with the anti-cancer drug doxorubicin hydrochloride (DXR) (efficiency 90%) *via* a transmembrane gradient of ammonium sulfate for intravenous injection against advanced ovarian cancer and HIV-associated Kaposi's sarcoma [289]. The liposomal composition contains hydrogenated soy phosphatidylcholine (HSPC), cholesterol and mPEG-DSPE in a molar ratio of 65:38:5.[290] In comparison to free DXR, Doxil® showed up to 16 times higher tumoral DXR concentrations [291], reduced cardiotoxicity and slower clearance (0.1 *vs.* 45 L/h) [292].

Moycet® is the non-PEGylated liposomal DXR consisting of egg phosphatidylcholine (EPC) and cholesterol in a molar ratio of 55:45. DXR is actively loaded *via* a transmembrane pH gradient, with pH 4 within the liposomes and pH 7.4 on the outside, leading to the formation of ion-pairs between the negatively charged EPC lipids on the liposomal surface and the positively charged DXR [293], resulting in DXR crossing the lipid bilayer and being subsequently protonated and entrapped within the acidic liposomal core with efficiencies of up to 99%.[294] Myocet® showed 2-10 times higher levels of DXR in tumor tissue compared to free DXR, while also reducing clearance (5 *vs.* 45 L/h), cardiotoxicity and gastrointestinal adverse effects.[295] Myocet® in combination with the

chemotherapeutic compound cyclophosphamide is approved for the use in Europe and Canada (2000), but was not approved by the FDA so far.

Ambisome® was FDA-approved in 1997 due to the higher therapeutic index in comparison to free Amphotericin B (AmB), a compound used for treatment of severe fungal infections like leishmaniasis or aspergillosis. It is composed of HSPC, cholesterol, 1,2-disteaoryl-sn-glycero-3-phosphatidylglycerol (DSPG) and AmB in a molar ratio of 2:1:0.8:0.4.[296] Ambisome® showed a higher therapeutic index, prolonged circulation times and higher dose toleration in comparison to free AmB.[297][298]

Other examples for approved liposomal drug delivery systems are Visudyne® (2000), the first light-activated system used to treat choroidal neovascularization [299], or Inflexal® V (1998), a liposome composed of lecithins and phospholipids 1,2-diolyeol-sn-glyocero-3-phosphatidylcholine (DOPC) and DOPE coated with a haemagglutinin surface from influenca A and B viruses, therefore also referred to as virosome.[300] These virosomes are almost non-immunogenic in comparison to conventional influenza vaccines and showed statistically significant improved therapeutic efficiency.[301]

Besides the approved liposome-based products, about 30 are already in clinical trials, including liposomes for inhalation against bacterial infections (Afrikace™ [302]) and liposomes for topical application for DNA repair in Xeroderma pigmentosum patients (T4N5 [303]). ThermoDox® is a temperature-sensitive formulation for DXR delivery to tumors [304], while liposomal Cisplatin is used for the treatment of pancreatic cancer (Lipoplatin™) and lung cancer (Nanoplatin™).[305] The cationic liposome Endotag-I composed of DOTAP and DOPC with encapsulated anti-cancer drug Paclitaxel is used for the treatment of breast and pancreatic cancer by reducing tumor angiogenesis.[306]

Recently conducted *in vivo* studies furthermore investigated the encapsulation of insulin in biotinylated liposomes as oral treatment of diabetes [307], primaquine containing heparin-targeted cationic liposomes for intravenous injection against malaria [308], pro-liposomal dry (liposomal) powder for inhalation containing pyrazinamide or antibiotic levofloxacin to treat tuberculosis [309][310] and many more.[311]

2. MOTIVATION AND OBJECTIVES

Hyperbranched polyglycerol shielded liposomes: Control of physical behavior and biological performance

Passive targeting, cellular uptake, biodistribution and blood circulation time of liposomes are influenced by their physicochemical properties and biological identity, which are both amenable to alteration by liposome surface modifications.[221][155] The gold standard of surface modifications is poly(ethylene glycol) (PEG), due to its biocompatibility and low immunogenicity.[155][312][313] Although PEGylation of liposomes leads to enhanced blood circulation times, increased stability and decreased recognition by the reticuloendothelial system [132][135][314][315], it comprises certain drawbacks also known as PEG dilemma, as reduced cellular uptake to target cells, decreased drug release and side effects like the accelerated blood clearance (ABC) phenomenon caused by repetitive administration of PEGylated liposomes.[198] [316]–[319] Recently developed polymeric amphiphile hyperbranched polyglycerol (*hb*PG) represents a promising alternative to PEG, since it is also biocompatible and possesses multiple hydroxyl-groups for functionalization with targeting moieties, potentially increasing the liposome's active targeting ability upon chemical modification with targeting vectors.[183][184][186][320]– [322] Prior active targeting however, it is advantageous when the liposomes already accumulated within the target tissue, which is usually accomplished by liposomes that are small enough to penetrate the target tissue.[83] The different architectures of *hb*PG and PEG suggest a disparate influence on aforementioned physicochemical properties and accordingly also on the biological identity of liposomes. Therefore, the impact of *hb*PG-based lipids in various sizes and amounts on physicochemical properties of liposomes was investigated and compared to PEG based lipids in section 3.1.1, with the aim to achieve small liposomes with potentially enhanced passive targeting ability. Another objective was to compare the effect of PEG- and *hb*PG-based lipids on the liposomes' protein corona, which is formed within the blood stream and is proposed to be important for the liposomes' biological identity and recognition by macrophages.[323]–[327] Therefore, liposomes containing either *hb*PG, PEG or no polymer were investigated in terms of their protein corona composition and their uptake by macrophages in section 3.1.2. Since the physicochemical properties and biological identity have a huge impact on the liposomal biodistribution and blood circulation time, the latter were analyzed in zebrafish embryo model in section 3.1.3 for liposomes containing *hb*PG and PEG in various sizes and amounts in comparison to conventional unmodified liposomes.

**Screening for lipid compositions at the edge of stability**

The prospect of enhancing the therapeutic potential of liposomes as drug delivery vehicles depends on an effective and fast release of cargo after uptake to target cells, which is contradictory to desired stability during circulation inside the blood stream and upon storage.[21] PEGylation of liposomes was a huge step towards increasing blood circulation time to intensify the enhanced permeability and retention (EPR) effect (see Introduction section 1.4) and to enhance liposome stability, but consequently, cargo release efficiency suffered.[8][12][13][26]–[28] This contradictory problem was addressed in part 3.2 by developing a systematic screening approach to identify non-PEGylated liposomes at the 'edge of stability' using the fluorescent membrane stability indicator 6-dodecanoyl-2-dimethylaminonaphthalene (laurdan) [40][41][328] in combination with dual centrifugation [32][33]. To cover a high variety of commercially available lipids in terms of their charge, fatty acid chain length and saturation, pH sensitivity and headgroup, 168 individual liposome compositions consisting of varying amounts of stabilizing and modifying lipids served as starting point for screening of their membrane stability using laurdan in section 3.2.1. The aim was to identify liposomes that would destabilize and subsequently release encapsulated cargo upon decreased pH and elevated temperature as present in tumor environment or in lysosomes/endosomes after liposome endocytosis by macrophages.[329] To quantify the desired cargo release under aforementioned conditions as well as the cargo retention upon storage of identified liposomes at the 'edge of stability' in comparison to conventional liposomes, a semi-automated method had to be developed to accomplish an easy readout and to handle the large amounts of samples necessary for screening (section 3.2.2). Since the liposomes at the 'edge of stability' were potentially fragile, helper lipids known from literature as cholesterol [15] or pH-sensitive cholesterylhemisuccinate [150][330][331] were prepositioned for liposome modification, in order to potentially increase liposomal cargo retention while not decreasing the desired cargo release to an insufficient level. To ensure that candidate liposomes achieved pharmaceutical quality, they had to be physicochemically characterized by dynamic light scattering. With the aim to confirm applicability of candidate liposomes *in vitro*, cell experiments using macrophages and melanoma cells as potential targets [21][332][333] had to be performed, while a method for a simple read out of cargo release after internalization of liposomes had to be conducted (section 3.2.3). *In vivo* experiments in section 3.2.4 using zebrafish embryos (ZFE) as model system, as recently reported by the lab of Prof. Dr. Huwyler [267][280][284], would be the last step to evaluate performance of identified liposomes at the 'edge of stability'. Finally, PEG-based lipids containing pH-sensitive ketal [38] or novel vinyl-ether [37] cleavage sites were incorporated into liposomes, with the aim to achieve even more stable liposomes capable of still releasing cargo at decreased pH (section 3.2.5).

3. Results and discussion

3.1 Hyperbranched polyglycerol shielded liposomes: Control of physical behavior and biological performance

Abstract

Hyperbranched polyglycerol (*hb*PG) and PEG based lipids in different sizes from 3000 to 8000 g/mol were incorporated in amounts ranging from 1 to 10 mol-% into liposomes during formulation by dual centrifugation. Physicochemical characterization revealed the possibility of a decrease in liposome diameter using high amounts of large polymers, potentially increasing the liposomes' passive targeting / tumor penetration ability. Analysis of the protein corona after incubation of *hb*PG and PEG containing liposomes with blood and subsequent purification revealed a comparable protein composition, albeit differences in macrophage uptake *in vitro*, which was higher for *hb*PG liposomes. Biodistribution studies in zebrafish embryos displayed enhanced liposome circulation times with increasing molecular weight and amount of large polymers on the liposomal surface. PEG liposomes overall circulated better than *hb*PG liposomes, which were mainly taken up in circulating and tissue resident macrophages. The latter might offer the possibility of passively "targeting" macrophages by application of *hb*PG-shielded liposomes as drug delivery vehicle.
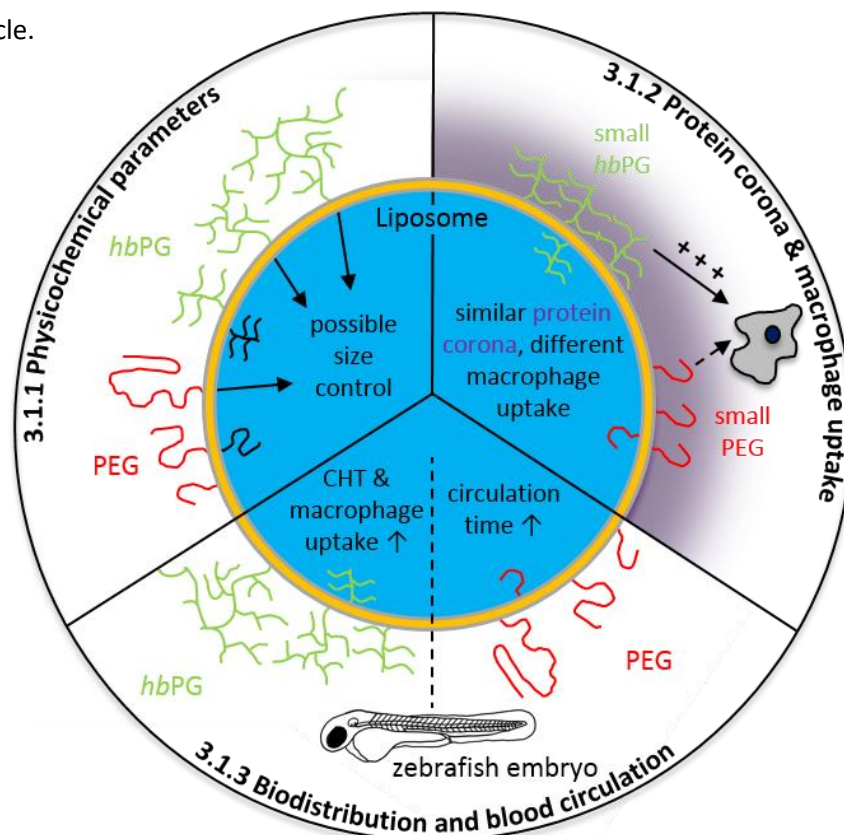
FIGURE 14: SECTION OVERVIEW. PHYSICOCHEMICAL PARAMETERS OF LIPOSOMES CONTAINING DIFFERENT AMOUNTS AND SIZES OF HBPG- OR PEG-BASED LIPIDS WERE ANALYZED IN THE FIRST SUBSECTION 3.1.1. THE PROTEIN CORONA OF LIPOSOMES CONTAINING SMALL HBPG OR PEG WAS INVESTIGATED IN SUBSECTION 3.1.2. THE BIODISTRIBUTION OF LIPOSOMES CONTAINING HBPG- AND PEG-BASED LIPIDS IN DIFFERENT SIZES WAS STUDIED USING THE ZEBRAFISH EMBRYO MODEL IN SUBSECTION 3.1.3.

INTRODUCTION

Hyperbranched polyglycerol (*hb*PG) based lipids were synthesized by the group of Prof. Dr. Frey (Mainz, Germany).[184] These amphiphilic polymers are anchored *via* bis-(hexadecyl)glycerol to the liposomal membrane, extend blood circulation time and bear multiple terminal hydroxyl-groups for functionalization with targeting moieties (Figure 15).[18][39][40] The latter was one of the initial reasons for picking *hb*PG as alternative to PEG, which is typically used in formulation of long-circulating "stealth" liposomes.[12] Terminal PEG molecules can also be synthetically modified to achieve active targeting, but multi-functionalization of *hb*PG could possibly lead to an increased targeting efficiency.[335]–[337] Commercially available PEG is typically anchored *via* di-stearoyl or cholesterol to the liposomal membrane, whereas the latter was previously reported by our group to be less stable as anchorage.[167] Because of that, the group of Prof. Dr. Frey synthesized PEG with bis-(hexadecyl)glycerol as membrane anchor, which was used in the following sections. The focus was set on the influence of *hb*PG- and PEG-based lipids with various molecular weights (MW) and amounts on the liposomes' physicochemical parameters, protein corona, macrophage uptake and biodistribution (Figure 14). The conventional non-shielded liposome (CL) served as control and consisted of egg phosphatidylcholine (EPC) and cholesterol (55:45 mol-%, same lipid composition as clinically relevant liposome Myocet®), whereas for the surface modified liposomes, EPC was substituted with the respective mol-% of *hb*PG or PEG based lipids.

TABLE 2: HYPERBRANCHED POLYGLYCEROL (HBPG) AND POLY-(ETHYLENE GLYCOL) (PEG) BASED LIPIDS SYNTHESIZED BY THE GROUP OF PROF. DR. FREY. MOLECULAR WEIGHTS (MW) AND MOLECULAR WEIGHT DISTRIBUTION (Đ, DEFINED AS M_W/M_N, WITH M_W AS WEIGHT AVERAGE AND M_N AS NUMBER AVERAGE MOLECULAR WEIGHT)[338][339] ARE INDICATED.

amphiphilic polymer	polymer size	N	MW in g/mol [a]	$Đ$ [b]	formula
*hb*PG	Small (S)	35	3084	1.20	
	Medium (M)	67	5420	1.19	
	Large (L)	106	8270	1.29	
PEG	Small (S)	61	3191	1.09	
	Medium (M)	113	5470	1.08	
	Large (L)	160	7560	1.08	
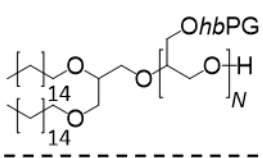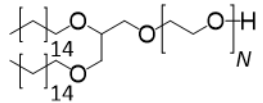
[a]determined using ^{1}H-NMR spectroscopy
[b]determined by SEC

A   B
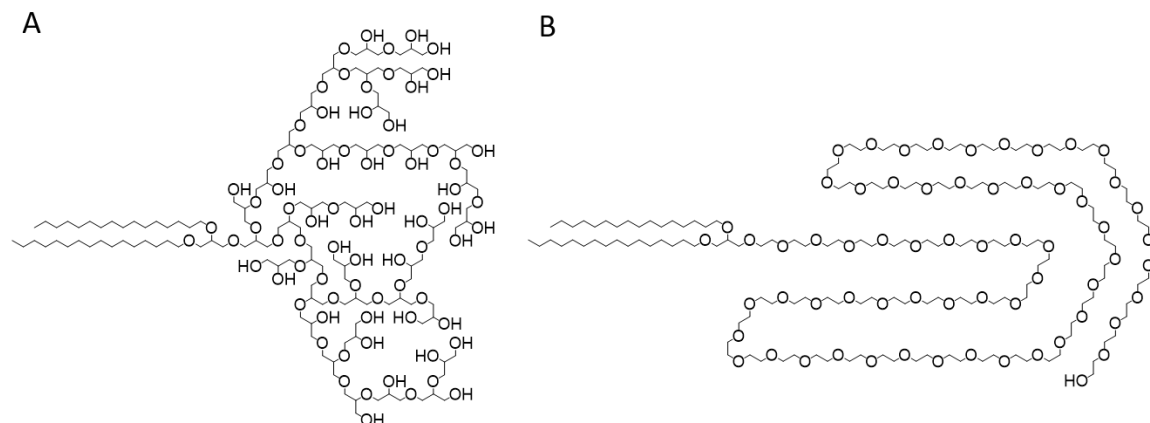
**FIGURE 15:** POSSIBLE STRUCUTRES OF POLYMERIC AMPHIPHILES. **(A)** HBPG-S AND **(B)** PEG-S.

3.1.1 PHYSICOCHEMICAL PARAMETERS

All polymeric amphiphiles were synthesized by ███████████████████████████ and ████████████
from the research group of Prof. Dr. Frey (Johannes Gutenberg-University, Duesbergweg 10-14, Mainz, Germany). TEM images shown in this section were recorded by Dr. Claudia Weber from the research group of Prof. Dr. Landfester (Max Planck Institute for Polymer Research, Ackermannweg 10, 5518 Mainz, Germany).

Prior actively targeting liposomes to specific cells by modification of the respective polymer with a targeting ligand, which was previously reported by our group with a model ligand for *hb*PG [322], it is of advantage when the liposomes already accumulated in the target tissue, which is also referred to as passive targeting. It is achieved by nanoparticles that are small enough (typically ≤ 150 nm) to penetrate the target tissue to reach the side of action (see also Introduction section 1.4).[83] In most tumor environments, active targeting occurs primarily after the passive targeting process.[340]–[343] This is why the effect of *hb*PG in comparison to PEG on the liposomal diameter was addressed in this section, with the aim to achieve small liposomes with potentially increased passive targeting / tumor penetration ability.

To investigate the effect of PEG and *hb*PG in different sizes and amounts on the physicochemical parameters of liposomes, all polymer permutations shown in table 2 were incorporated into liposomes with increasing mole percentages ranging from 1 to 8 during liposome preparation. A conventional, non-shielded liposome (CL) with the same lipid composition besides the amphiphilic polymers served as control. Commercially available methoxypoly(ethyleneglycol) 1,2-distearoyl-sn-glycero-3-phosphoethanolamine (mPEG-DSPE) with a molecular weight of 3000 g/mol was also incorporated as comparison to small PEG-based lipids. Sulforhodamine B (SRb) was used as hydrophilic model cargo for encapsulation. Liposome stocks directly obtained after dual centrifugation were purified by size exclusion chromatography (SEC) to determine encapsulation efficiencies (%EE) as described in the methods section. Purified liposomes were then subjected to

dynamic light scattering (DLS) for size, PDI and zeta potential analysis. Nanoparticle tracking analysis (NTA) for determination of liposome size and concentration was also performed, and transmission electron microscopy (TEM) images were recorded.[344] Liposome sizes obtained from DLS, NTA and TEM are depicted in Figure 16 A, B and C, respectively.
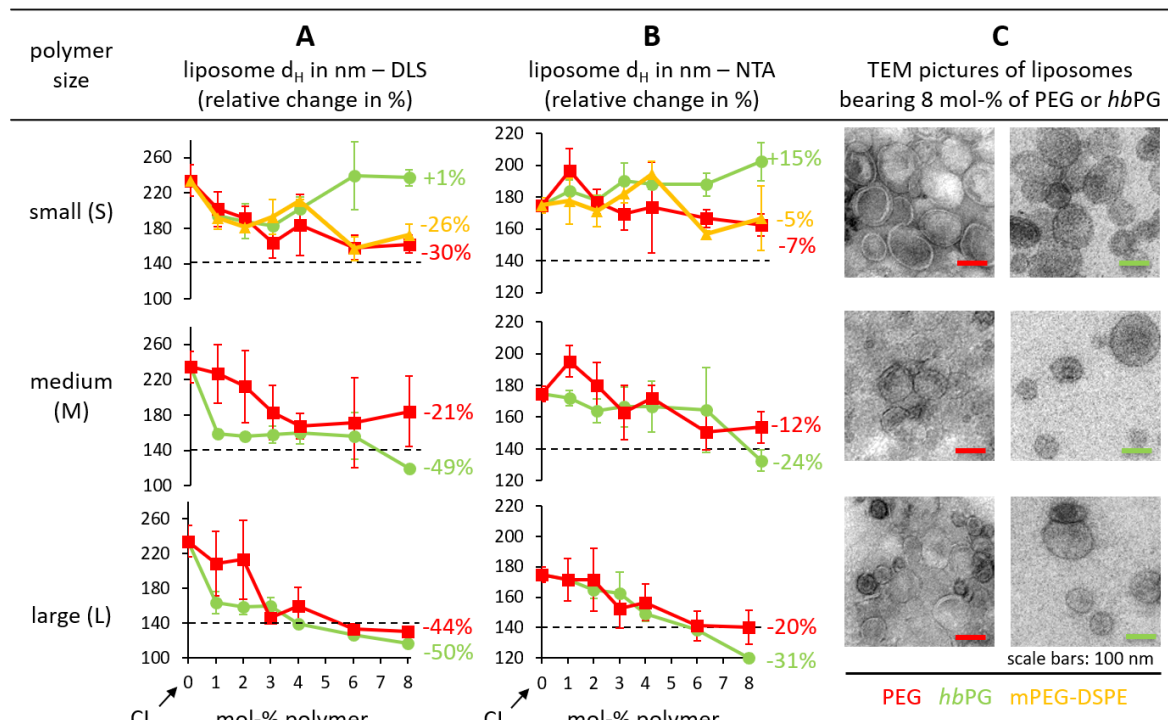
FIGURE 16: EFFECT OF SMALL, MEDIUM AND LARGE HBPG (GREEN) AND PEG (RED, FREY GROUP; YELLOW, COMMERCIAL) IN INCREASING MOLE PERCENTAGES ON THE HYDRODYNAMIC DIAMETER (d_H) OF LIPOSOMES, MEASURED *VIA* **(A)** DLS AND **(B)** NTA. DOTTED LINES ARE PROVIDED TO SIMPLIFY COMPARISON BETWEEN ROWS. CONVENTIONAL NON-SHIELDED LIPOSOMES (CL) SERVED AS STARTING POINT. ERROR BARS INDICATE 3 INDIVIDUAL LIPOSOME PREPARATIONS, EACH CONTAINING THREE TECHNICAL REPLICATES. **(C)** TEM IMAGES OF LIPOSOMES CONTAINING 8 MOL-% PEG OR HBPG IN THE RESPECTIVE SIZE.

DLS results (Figure 16 A) show a relative decrease in liposome diameter of around 50% for liposomes containing 8 mol-% *hb*PG-M, *hb*PG-L or PEG-L when compared to CL without polymer. A general trend that an increase of polymer amount results in a decrease of liposome diameter is visible for all medium and large polymers. This has been reported for PEG before [345] and is also visible for *hb*PG liposomes. A second trend generally shows a decrease in liposome diameter with bigger polymers (higher molecular weights), which is most prominent when comparing small and large polymers. It is difficult to explain the origin of the observed trends without minor speculations. Taking into account that high amounts of these large polymers themselves should increase liposome membrane thickness and therefore should lead to an overall size increase, the likely induced steric repulsion between single polymer units on the liposomal surface, which

should increase with polymer amount and size, could to be a decisive factor for the overall decrease in liposome diameter. With higher steric demand of the polymers, a higher curvature of the liposomal surface could be promoted. Conclusively, the incorporation of high amounts of large polymers resulted in the formation of more (Figure 17 B) smaller liposomes, leading to an enhanced maximum available surface and therefore probably to an attenuation of steric hindrance. Calculations on this are addressed later (table 3).

Yet, the decrease in liposome diameter is not linear, which could be explained by the so-called mushroom-brush transition (Figure 18 B).[346] At low polymer density on the liposomal surface, PEG and *hb*PG behave like isolated units in solution, which leads to a hemisphere (mushroom) conformation. However, as soon as the density increases, polymers start to laterally repulse, which linear polymers like PEG appease by extending in the brush conformation.[347] This phenomenon occurs at lower mol-% with increasing polymer size, prior complete saturation of the liposomal surface, which is reported for PEG_{2000} (roughly PEG-S) and PEG_{5000} (PEG-M) at around 5 and 2 mol-%, respectively.[143][348] Considering the rather compact architecture of *hb*PG in comparison to PEG as described in literature [320], this transition is probably reached at even lower mol-% for *hb*PG, and overcoming steric repulsion by formation of smaller liposomes could occur even earlier. That could be one explanation of DLS results for 1 and 2 mol-% of *hb*PG-M and -L containing liposomes, that resulted in a stronger decrease in liposome diameters when compared to the same amounts of PEG-M and -L, respectively (Figure 16 A). Calculations addressed later indicate that PEG-M and -L at 1 and 2 mol-% can be considered in mushroom conformation (see Figure 18 C). The observed phenomenon could be of advantage, since less material would be needed to initially form smaller liposomes with *hb*PG-M and -L in comparison to PEG with the respective molecular weights. The difference is equalized at 3 mol-% of polymer (Figure 16 A, rows 2 & 3), where PEG-M and -L should have reached the brush conformation according to Lee *et al.* [143], which is in line with subsequent calculations, and steric repulsion is probably only constricted by the formation of smaller liposomes.

Of note, when more than 8 mol-% of large polymers were introduced during liposome preparation, a second species could be observed with diameters around 20 — 30 nm during DLS measurements (Sup Figure 1). It presumably arose from the formation of micelles, as the liposomal surface was assumed to be completely saturated with polymer already, which would be in line with the literature.[143]

Surprisingly, for small polymers (Figure 16 A, row 1) above 3 mol-%, a liposome diameter decrease of up to 30% was only observable for PEGylated liposomes, both with commercially available mPEG-DSPE and PEG synthesized by the Frey group. Small *hb*PG containing liposomes showed an increase in size again after 3 mol-%, resulting in no significant diameter change at 8 mol-%.

In comparison to liposome size changes obtained from DLS measurements, NTA results were more moderate (Figure 16 B). Related to the conventional liposome with no surface modification (at 0 mol-%), which was initially measured 175 nm in diameter compared to 234 nm measured *via* DLS, size decreases were less distinct. The only pronounced relative size decreases with 20, 24 and 31% were obtained for 8 mol-% PEG-L, *hb*PG-M and *hb*PG-L containing liposomes, respectively. Overall, although diminished, data trends were similar when compared to DLS results. The difference in liposome diameters between the two used methods DLS and NTA most likely derived from the measurements themselves. Whereas in DLS, millions of liposomes were measured in triplicate measurements and the overall average was calculated, in NTA, only around 100 liposomes were recorded in one measurement.[104] In addition, aggregates, which likely occur in non-shielded liposomes, are mostly ignored during NTA measurements, which could be another explanation of the differences to DLS results. Obtained TEM images show vesicular, unilamellar liposomes with 8 mol-% of the respective polymer (Figure 16 C). There were no micelles visible, indicating that the liposome surface was not oversaturated with polymer.

While the total liposome number measured by NTA increased with decreasing liposome size, the encapsulation efficiency (%EE) of SRb decreased accordingly (Figure 17 A), as expected. More small than large liposomes can get formed with a constant available lipid amount (calculations follow). However, the available intra liposomal volume decreases with the liposome size for constant lamellarity, resulting in a decreased encapsulation efficiency for hydrophilic substances.[349] Notably, even though *hb*PG polymers showed a higher molecular weight distribution Đ compared to PEG (table 2), *hb*PG liposomes were better reproducible overall than PEG liposomes by dual centrifugation, indicated by the overall smaller error bars in Figure 16 A and liposome PDIs recorded by DLS (Figure 17 C).
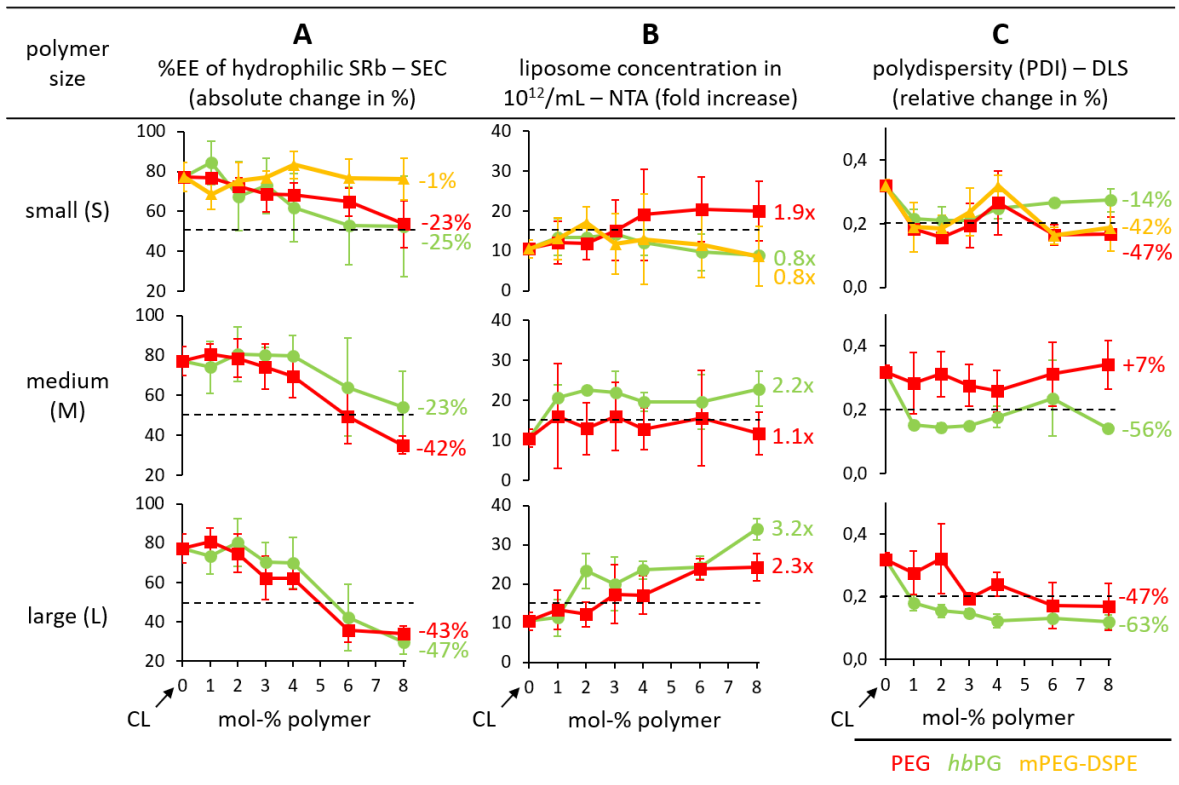
FIGURE 17: EFFECT OF SMALL, MEDIUM AND LARGE HBPG (GREEN) AND PEG (RED, FREY GROUP; YELLOW, COMMERCIAL) IN INCREASING MOLE PERCENTAGES ON LIPOSOME **(A)** SULFORHODAMINE B ENCAPSULATION EFFICIENCY (%EE), **(B)** CONCENTRATION MEASURED *VIA* NTA AND **(C)** POLYDISPERSITY (PDI) MEASURED *VIA* DLS. DOTTED LINES ARE PROVIDED TO SIMPLIFY COMPARISON BETWEEN ROWS. CONVENTIONAL NON-SHIELDED LIPOSOMES (CL) SERVED AS STARTING POINT. ERROR BARS INDICATE 3 INDIVIDUAL LIPOSOME PREPARATIONS, EACH CONTAINING THREE TECHNICAL REPLICATES.

Zeta potentials of 8-mol% *hb*PG containing liposomes showed comparable values to the non-shielded conventional liposomes with around −10 mV, whereas PEGylated liposomes showed slightly higher zeta potentials (Sup. Fig. 3). Exceptions for *hb*PG-S or mPEG-DSPE were observed, for whom the zeta potential decreased to −20 or −40 mV, respectively. The latter can be explained by the negatively charged phosphate of the phospho-ethanolamine (PE) group that likely induced the decrease in zeta potential, whereas for *hb*PG-S, the decrease could derive from other factors like sample ion strength, particle concentration or pH, which is however highly speculative.

The obtained experimental data is majorly in line with calculations done (table 3). Assuming that a liposome is a globular sphere, it's volume V can be calculated by formula 3 with d as the diameter of the liposome

$$V = \frac{1}{6}\pi d^3 \tag{3}$$

If the liposome diameter d now decreased by a factor x (around 0.5 in the case of hbPG-M, -L and PEG-L) the surface area O (formula 4) also decreases.

$$O=\pi(xd)^2 \tag{4}$$

However, it has to be calculated how many of these smaller liposomes could theoretically be formed out of a larger liposome with a constant amount of lipids, and their overall resulting surface area. Considering that egg phosphatidyl choline (EPC), the major component of all tested liposomes, mainly consists of 1-steaoryl-2-oleoyl-glycero-3-phosphocholine (SOPC), which has an estimated length of 4 nm, a maximum lamellar thickness l of 8 nm is assumed, which would also be in line with obtained TEM images (Figure 18 A). The inner volume V_i of the liposome can then be calculated using formula 5.

$$V_i=\frac{1}{6}\pi(d-2l)^3 \tag{5}$$

The resulting lipid volume V_l can be calculated as shown in formula 6.

$$V_l=V-V_i \tag{6}$$

If the diameter d gets multiplied by the diameter decrease factor x, the percentage of lipid needed for one liposome with its respective diameter can be calculated with formula 7, with V_l corresponding to the lipid volume of the conventional non-shielded liposome CL.

$$\%lipid=\frac{V_{l(xd)}}{V_l}\cdot100\% \tag{7}$$

Values for *%lipid* were obtained for 8 mol-% polymer containing liposomes (table 3). Results show that for hbPG-M, -L and PEG-L containing liposomes, around 4 liposomes (#lipos) with l = 8 nm could be formed with the available lipid volume from the conventional liposomes. Comparing the theoretical data with the liposome number measured by NTA (#lipos NTA) normalized to CL, the overall increase differs, since the measured liposome diameter decrease between NTA and DLS also differs, but trends are similar. The overall percentage of surface area increase *%O↑* can finally be calculated with formula 8.

$$\%O_\uparrow=\left(\#lipos\cdot\frac{\pi(xd)^2}{\pi d^2}-1\right)\cdot100\% \tag{8}$$

Results in table 3 show that there is an increase in surface area by formation of smaller liposomes, albeit it is relatively low with around 7% for hbPG-M and -L liposomes half the size of CL. Figure 18 A depicts TEM images of CL and liposomes with 8 mol-% hbPG-L, which fit the overlaid circles representing sizes obtained from DLS and calculated membrane thickness.

TABLE 3: EXPERIMENTAL DATA AND CALCULATIONS FOR CONVENTIONAL LIPOSOME CL AND LIPOSOMES WITH 8 MOL-% HBPG OR PEG -S, -M AND -L. EXPERIMENTAL DATA INCLUDES THE LIPOSOME HYDRODYNAMIC DIAMETERS (d_H) OBTAINED FROM DLS AND THE NUMBER OF LIPOSOMES (LIPOSOME CONCENTRATION) OBTAINED FROM NTA NORMALIZED TO CL (#LIPOS NTA). CALCULATED DATA INCLUDES THE SIZE DECREASE FACTOR X, THE PERCENTAGE OF LIPID NEEDED TO FORM A LIPOSOME NORMALIZED TO CL (%LIPID), THE MAXIMUM NUMBER OF LIPOSOMES THAT CAN BE FORMED WITH THE SAME LIPID MATERIAL AVAILABLE FOR CL (#LIPOS), THE OVERALL INCREASE IN SURFACE AREA %O↑, THE POLYMER CONTOUR LENGTH C (ESTIMATED FOR HBPG), THE FLORY DIMENSION R_F AND THE RATIO OF R_F TO THE DISTANCE D BETWEEN TWO POLYMERS AT 8 MOL-%.

Sample ID (8 mol-% polymer)	d_H in nm	x	%lipid	#lipos	#lipos NTA	%O↑	C in nm (est.)	R_f in nm	R_f / D at 8 mol-%
CL	234	1	100	1.0	1.0	-	-	-	-
*hb*PG-S	237	1	103	1.0	0.8	0	(7)	-	-
*hb*PG-M	119	0.5	24	4.1	2.2	7.0	(13)	-	-
*hb*PG-L	116	0.5	23	4.4	3.2	7.4	(20)	-	-
PEG-S	162	0.7	46	2.2	1.9	3.2	17	3.3	1.1
PEG-M	184	0.8	61	1.7	1.1	1.9	31	4.8	1.6
PEG-L	130	0.6	29	3.4	2.3	5.8	45	5.9	2.0

For calculations on PEG, the Flory dimension (R_f) is needed. It describes the coil size or spatial configuration of macromolecular chains, which is illustrated in Figure 18 B. It is calculated *via* formula 9, where N is the total number of monomers (see table 2), a is the length of a single monomer unit in water (ethylene glycol: 0.28 nm), and v is the Flory exponent, a dimensionless measure of flexibility, which is ≈3/5 for good solvent (here: aqueous buffer).[350][351]

$$R_f = a \cdot N^v \tag{9}$$

The average distance between two adjacent polymers D can be calculated using formula 10, with A as PEG area per lipid molecule in the bilayer (0.67 nm^2 [352]) and M as mole fraction of PEG lipid.[353]

$$D = \left(\frac{A}{M}\right)^{1/2} \tag{10}$$

The ratio of the Flory dimension R_f to the distance D can be used to determine the conformation of PEG, with a ratio of $\frac{R_f}{D} < 1$ indicating a mushroom conformation where PEG forms a loose coil as in water.[352] At higher PEG density on the liposomal surface, in the case of $\frac{R_f}{D} > 1$, chains expand in rather elongated conformations (brush), as soon as the steric repulsion overcomes the conformational entropy cost of stretching the chain. Theoretical conformations $\left(\frac{R_f}{D}\right)$ of PEG lipids depending on mol-% and respective molecular weights are shown in Figure 18 C. At

8 mol-%, regardless of the polymer size, all PEG based lipids can be considered in brush conformation with $\frac{R_f}{D}>1$ (table 3), which is in line with the literature.[143][352] The length of a polymer chain in a maximally elongated conformation can be described by the contour length C calculated *via* formulas 11 and 12, with a as the length of a single monomer unit in water, P as the overall molecular weight of the polymer, R as the molecular weight of the bis(hexadecyl)-glycerol anchor (500 g/mol) and *mono* as the monomer weight.

$$C = a \cdot N \qquad\qquad (11)$$

$$N = \frac{P\text{-}R}{mono} \qquad\qquad (12)$$
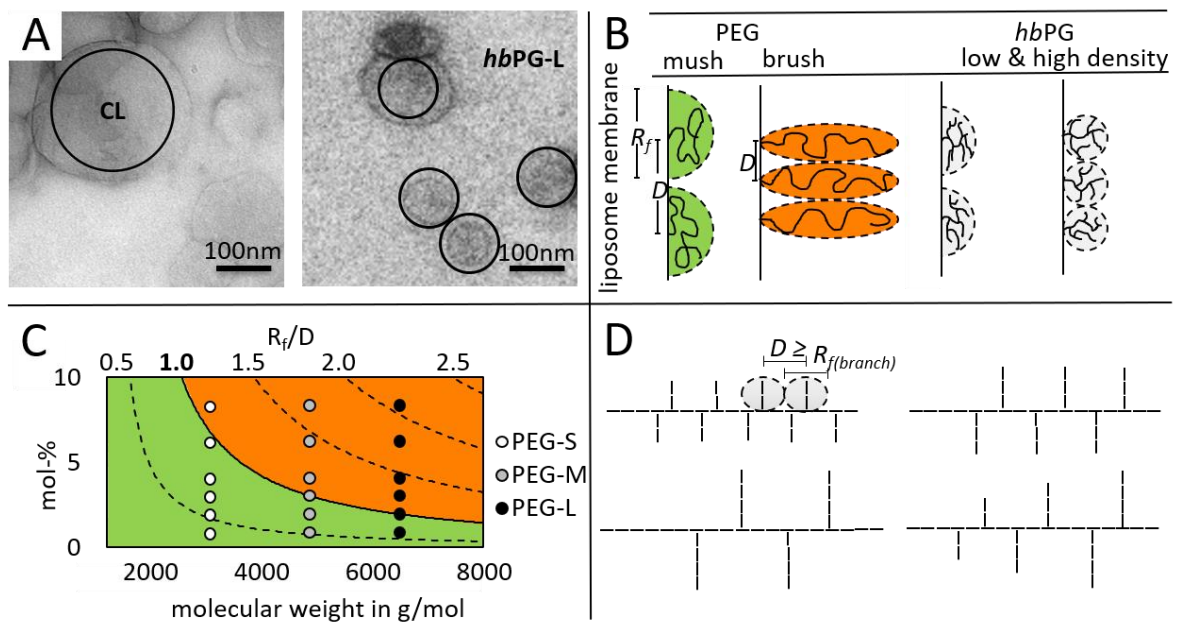
FIGURE 18: **(A)** TEM IMAGES OF CONVENTIONAL LIPOSOME CL (LEFT) AND LIPOSOMES CONTAINING 8 MOL-% HBPG-L (RIGHT) OVERLAID BY CIRCLES REPRESENTING SIZES OBTAINED BY DLS AND CALCULATED MEMBRANE THICKNESS. **(B)** POSSIBLE STRUCTURAL CHANGES OF PEG IN MUSHROOM (MUSH) OR BRUSH CONFORMATION AND HBPG AT LOW OR HIGH SURFACE DENSITY, WITH ILLUSTRATION OF THE FLORY DIMENSION (R_F) AND THE DISTANCE D BETWEEN TWO POLYMERS. **(C)** THEORETICAL CONFORMATIONS $\left(\frac{R_f}{D}\right)$ OF PEG LIPIDS DEPENDING ON MOL-% AND RESPECTIVE MOLECULAR WEIGHTS. $\frac{R_f}{D}>1$ INDICATES BRUSH (ORANGE), $\frac{R_f}{D}<1$ MUSHROOM CONFORMATION (GREEN). **(D)** POSSIBLE STRUCTURES OF HBPG-S (35 MONOMERS) BASED ON ASSUMPTIONS MENTIONED IN THE TEXT, WITH ILLUSTRATION OF THE FLORY DIMENSION (R_F) OF A BRANCH AND THE DISTANCE D BETWEEN TWO BRANCHES.

Calculations on the size of a hyperbranched polymer like *hb*PG would have to take all sidechains (branches) into account, which are all flexible and can be hyperbranched unevenly, leading to a

much higher complexity compared to a linear PEG chain. To illustrate possible simplified structures of *hb*PG, only the main PG backbone was assumed to build atactic branches. The latter is likely the case, since racemic glycidol was used for polymerization, and no stereoselective catalysator was applied. The minimum distance D of each branch was assumed to be $D \geq R_{f(branch)}$, with $R_{f(branch)}$ as the Flory dimension of one linear branch calculated as above, so that branches have maximum flexibility and no steric repulsion. For *hb*PG-S, the 35 PG subunits were then arranged as an even grid or tree-like, with a minimum branch length of 2 monomers (Figure 18 D). The estimated length of the PG backbone between 17 and 19 PG monomers derived from the number of branches and their distance D and is in line with ^{1}HNMR measurements of the PG backbone before hyperbranching.[354] For the contour length C of *hb*PG, mainly PGs within the backbone were assumed to contribute, which resulted in relatively short contour lengths (table 3). Possible structures for *hb*PG-M (Sup Figure 3) and *hb*PG-L were also drawn and resulted in increased structural possibilities with increased molecular weight. As mentioned above, *hb*PG is described as more compact than PEG in literature [320] (illustrated in Figure 18 B) and it is therefore tentatively suggested that these polymers begin to sterically repulse another even earlier than linear PEG chains, leading to fully covered liposomes already at lower mole percentages.

Since liposomes were prepared in aqueous media, a brief comment on hydrodynamic volumes V_H is also necessary. V_H is approximately proportional to the intrinsic viscosity η of a polymer and its molecular weight M_w.[355]–[357] So V_H tends to increase with increasing molecular weight, which could explain the tendency that larger polymers lead to a stronger decrease in liposome size due to more spatial demand. The intrinsic viscosity of hyperbranched PG is lower than for linear PEG, and therefore the hydrodynamic volume of *hb*PG should also be lower than for PEG.[320] [321][183] Obtained results indicate however that the situation is more complex due to different structural conformations of the polymers (mushroom *vs.* brush and branched *vs.* linear), which have a high impact on their spatial demand and also influence polymer hydration levels as it is reported in literature.[347][358][359] Of note, when the ratio of total lipids to aqueous buffer was increased by the factor 2 (according to previous protocols [322]) during preparation of liposomes containing more than 5 mol-% of PEG-L, resulting liposomes showed increased diameters, probably due to a worse mixing inside the dual centrifuge caused by a higher sample viscosity, which was not observable for liposomes with corresponding amounts and sizes of *hb*PG (Sup Figure 4).

To briefly conclude this first part, shielding of liposomes with 8 mol-% of *hb*PG-M, -L or PEG-L led to a decrease in liposome diameter measured by DLS and NTA, which could be of importance for
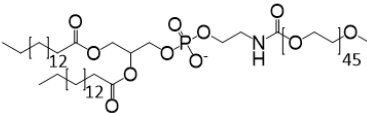
potentially enhancing liposomal passive targeting / tumor penetration ability. PDIs (0.13±0.02), reproducibility and sizes (117±6 nm) of these liposomes achieved pharmaceutical quality.[83]

### 3.1.2 PROTEIN CORONA & MACROPHAGE UPTAKE

In this section, recent findings obtained in a collaboration with the research group of Prof. Dr. Landfester (Max Planck Institute for Polymer Research, Ackermannweg 10, 5518 Mainz, Germany) are briefly illustrated. Protein corona and cell experiments were performed by Dr. Claudia Weber and Johanna Simon. Most parts of this chapter are published in [360].

In a complex biological system, many influences on nanoparticles such as liposomes have to be considered. Amongst others, proteins are adsorbed onto the liposomal surface, forming a so-called protein corona upon injection into the blood stream and therefore changing the liposomes' biological identity.[361]–[365] The latter can influence cellular uptake, body distribution and clearance.[366] It is known from the literature that PEG minimizes unspecific protein adsorption onto the liposomal surface, due to its hydrophilicity, excluded volume and its ability to act as a steric barrier.[367] However, so-called 'stealth' proteins (dysopsonins) are adsorbed onto the PEGylated liposomal surface, which could explain the minimized unspecific cell uptake of PEGylated liposomes.[324][368]–[370] The conventional liposome used in this section consisted of 55 mol-% EPC and 45 mol-% cholesterol as before (composition of clinically relevant Myocet®), whereas for shielded liposomes, 5 mol-% of EPC was replaced by mPEG-DSPE^{3000} (composition comparable to clinically relevant Doxil®) or *hb*PG-S2, respectively (table 4). To compare conventional, PEGylated and *hb*PG-bearing liposomes in terms of their protein corona composition, they were incubated with human plasma, purified by asymmetric flow field flow fractionation (AF4) or centrifugation and subjected to liquid chromatography/mass spectrometry (LC-MS).[371]–[373] In AF4 as chromatography like technique without a stationary phase, only minimal shear stress is applied to the liposome sample, enabling access of loosely bound proteins, whereas after purification by centrifugation, this so-called soft corona cannot be analyzed.[374] Purified fluorescently labeled liposomes (0.1 mol-% lipophilic carbocyanine dye DiD, see section 5.1 Materials) were subsequently incubated with murine macrophages (RAW 264.7 cells) to investigate cellular uptake by flow cytometry and confocal laser scanning microscopy (CLSM).

TABLE 4: SAMPLES USED IN PROTEIN CORONA AND MACROPHAGE UPTAKE STUDIES. SHOWN ARE THE RESPECTIVE LIPID COMPOSITIONS, POLYMERS WITH MOLECULAR WEIGHT AND FORMULA, AND LIPOSOME DIAMETER, PDI AND ZETA POTENTIAL MEASURED BY DLS. ERRORS INDICATE THREE INDIVIDUAL LIPOSOME PREPARATIONS, EACH CONTAINING THREE TECHNICAL REPLICATES.

liposome ID	composition EPC:CHOL: polymer in mol-%	amphiphilic polymer	polymer MW in g/mol	d_H in nm	PDI	zeta potential in mV	amphiphilic polymer formula
CL	55:45:0	-	-	172 ±17	0.16 ±0.04	-20±1	
L-PEG	50:45:5	mPEG-DSPE	3000	125 ±14	0.15 ±0.03	-28±1	
L-*hb*PG	50:45:5	*hb*PG-S2	2750	196 ±21	0.29 ±0.06	-21±1	
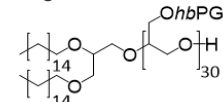
It was found that the composition and amounts of loosely bound proteins of the soft protein corona assessed *via* AF4 were rather similar for CL, PEGylated and *hb*PG liposomes, with the latter showing a slightly increased amount of apolipoporotein AI (Figure 19 A). For the hard corona analyzed after liposome centrifugation, changes were only visible for *hb*PG liposomes when compared to CL, but surprisingly not for PEGylated liposomes. The amount of albumin was decreased within the hard corona of L-*hb*PG, while tissue leakage proteins, histidine-rich glycoprotein and coagulation factor XII were enriched. Overall, the liposomal surface modifications seemed to not strongly alter the composition of the adsorbed proteins, albeit slight differences of protein amounts observed for the hard corona of L-*hb*PG. Regarding the total amount of adsorbed proteins, it was rather low (< 0.7 mg/m^2) when compared to more hydrophobic polystyrene based nanoparticles, but in range of other hydrophilic hydroxyethyl starch based nanoparticles.[371][372]
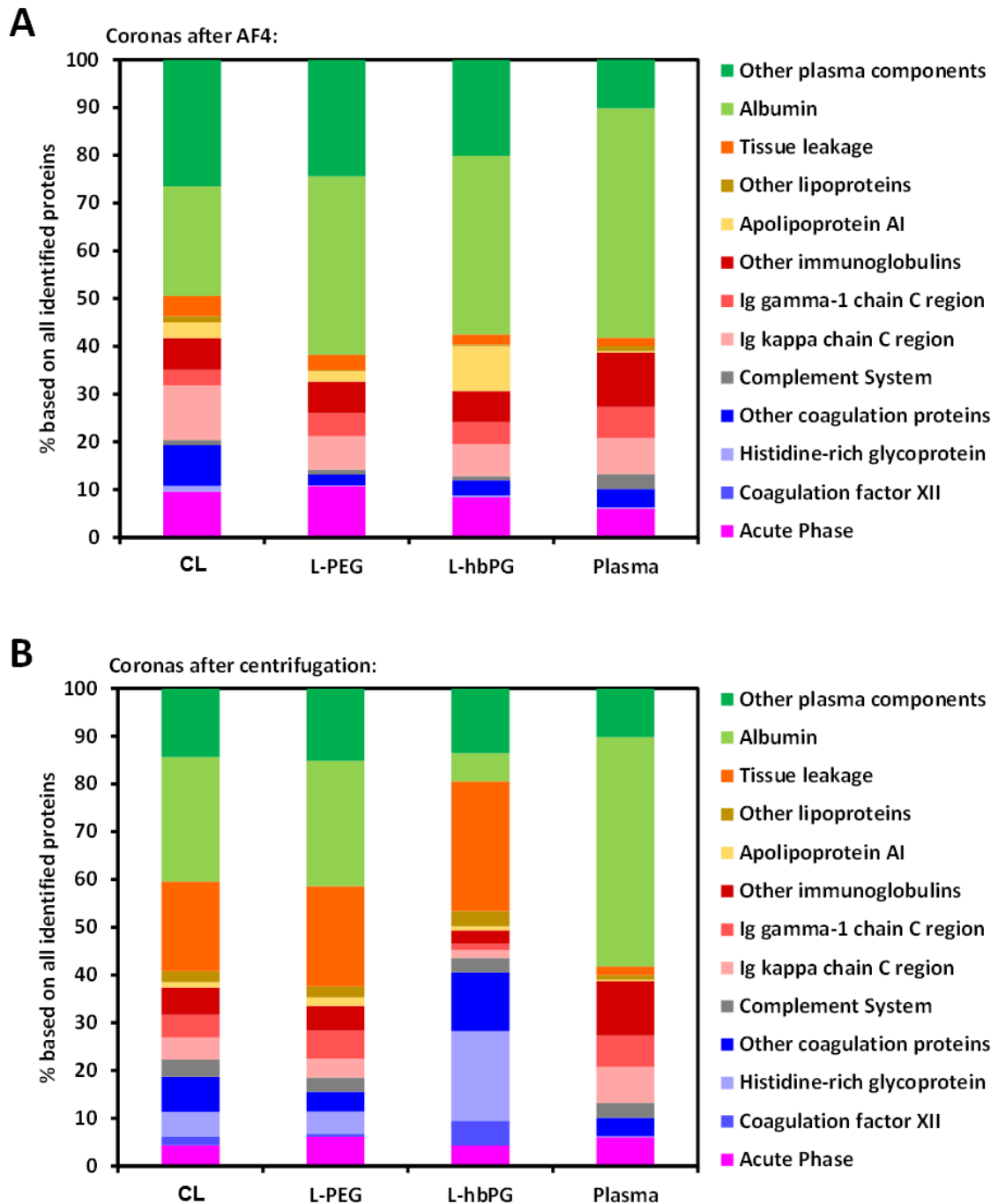
FIGURE 19: PROTEIN CORONA COMPOSITION OF CONVENTIONAL LIPOSOME (CL) AND PEG OR HBPG LIPOSOMES IN COMPARISON WITH PURE BLOOD PLASMA AS AQUIRED FROM LIQUID CHROMATOGRAPHY/MASS SPECTROMETRY (LC-MS) OF TWO BIOLOGICAL REPLICATES. **(A)** CORONA COMPOSITION AFTER AF4. **(B)** CORONA COMPOSITION AFTER CENTRIFUGATION.

Strikingly, flow cytometry results indicate that cellular uptake by macrophages differed strongly between the three investigated formulations (Figure 20), despite similar protein corona compositions.
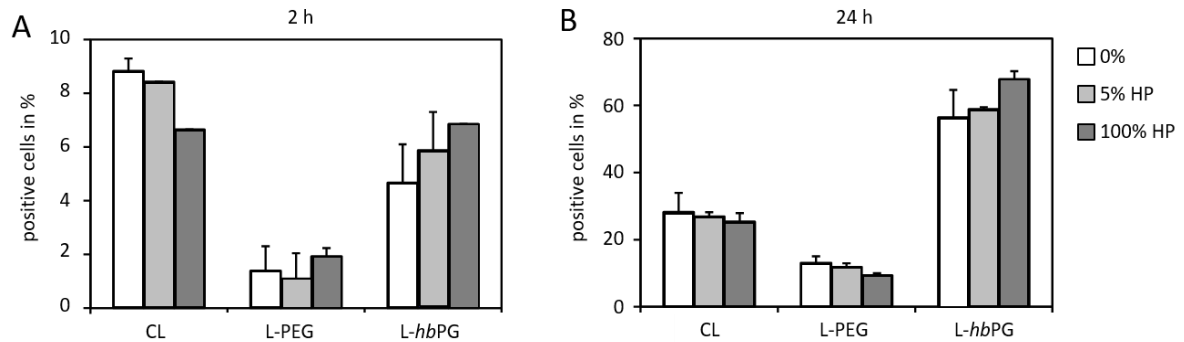
FIGURE 20: INFLUENCE OF LIPOSOME SURFACE MODIFICATION AND PROTEIN CORONA ON MACROPHAGE UPTAKE ASSESSED BY FLOW CYTOMETRY. FLUORESCENTLY LABELED (DID) CONVENTIONAL LIPOSOME (CL) AND LIPOSOMES CONTAINING PEG (L-PEG) OR *HB*PG (L-*HB*PG) WERE INCUBATED FOR 2 AND 24 H WITH RAW264.7 CELLS AT A CONCENTRATION OF 7.5 µg/mL PRIOR (REFERRED TO AS 0%) OR AFTER INCUBATION WITH 5 OR 100% HUMAN PLASMA (HP). THE PERCENTAGE OF CELLS SHOWING A POSITIVE FLUORESCENCE SIGNAL IS SHOWN. **(A)** AFTER 2 H INCUBATION TIME, CELLS INCUBATED WITH PEGYLATED LIPOSOMES L-PEG SHOWED A LOWER FLUORESCENCE IN COMPARISON WITH CL AND L-*HB*PG. **(B)** AFTER 24 H INCUBATION TIME, L-PEG AND L-*HB*PG SHOWED THE LOWEST AND HIGHEST CELLULAR FLUORESCENCE SIGNALS, RESPECTIVELY. OVERALL, CELLULAR UPTAKE SEEMED TO BE INDEPENDENT FROM PLASMA INCUBATION. ERROR BARS INDICATE TWO BIOLOGICAL REPLICATES.

Regardless of liposomal pre-incubation with human plasma (0, 5 and 100%), the uptake of liposomes by macrophages did barely alter, indicating that not the protein corona, but the liposomal properties themselves have a higher influence on macrophage uptake. First of all, the size of the respective liposomes could be one important factor for recognition and uptake by macrophages.[221] That is why at least a part of the difference in macrophage uptake could derive from the fact that L-*hb*PG is 1.5 times larger than L-PEG. However, regarding the comparable sizes of CL and L-*hb*PG, the liposome sizes were suggested to be non-decisive for observed differences. All tested liposomes had diameters in the range of 100 – 200 nm, which is reported to not lead to a distinct difference in macrophage uptake.[375] Zeta potentials of all three tested liposomes were negative and comparable and should therefore only have a minor influence on cell uptake (table 4). Notably, negatively charged liposomes were previously reported to lead to an enhanced macrophage internalization.[376] CLSM images (Figure 21) indicated qualitatively that all tested liposomes were successfully internalized, with differences roughly corresponding to flow cytometry results.
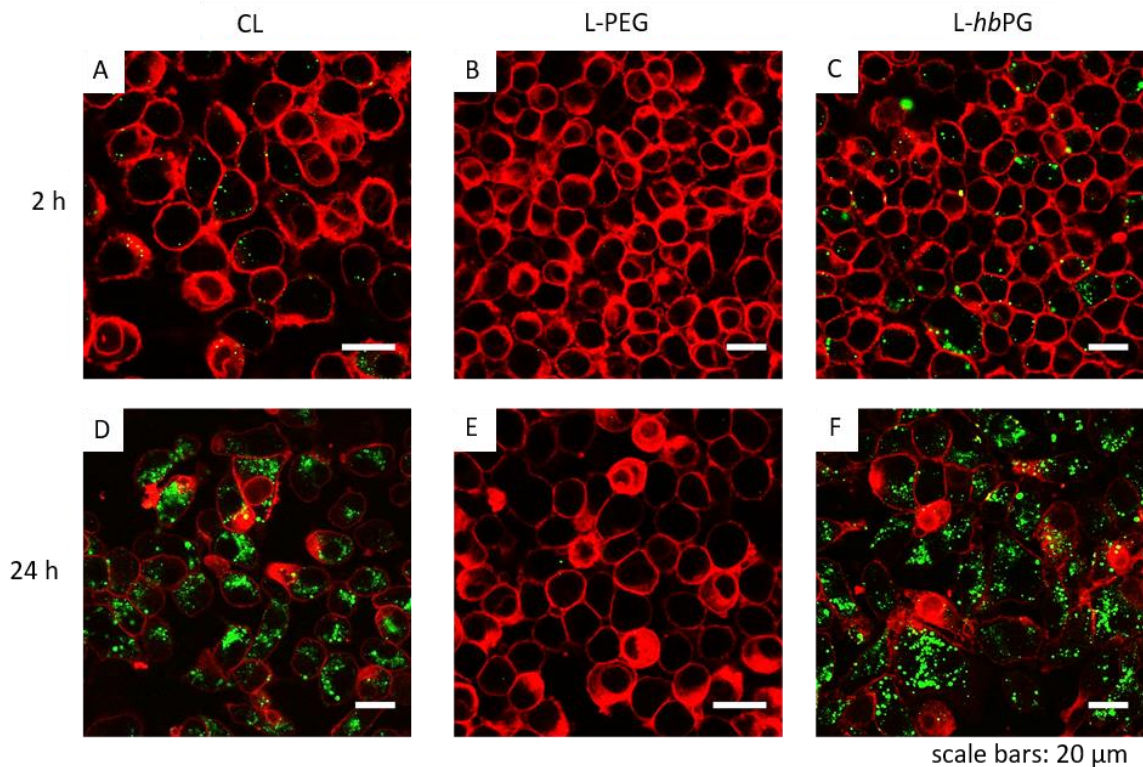
FIGURE 21: CONFOCAL LASER SCANNING MICROSCOPY (CLSM) IMAGES OF CONVENTIONAL LIPOSOME (CL), PEGYLATED LIPOSOME (L-PEG) AND HBPG CONTAINING LIPOSOME (L-HBPG) INCUBATED WITH MACROPHAGES (RAW264.7 CELLS) FOR 2 H (TOP) AND 24 H (BOTTOM) AT A CONCENTRATION OF 75 µg/ml. LIPOSOMES WERE FLUORESCENTLY LABELED WITH MEMBRANE DYE DID AND ARE DEPICTED IN GREEN, CELL MEMBRANES WERE STAINED WITH CELLMASK™ DEEP RED AND ARE DEPICTED IN RED.

PEGylated liposomes L-PEG showed the lowest uptake after 2 and 24 h, which was expected, since PEG is reported to reduce unspecific uptake by macrophages.[12] Scavenger receptors present on the macrophage surface are reported to recognize PEG, in particular in combination with albumin, which was the main part of the L-PEG protein corona (Figure 19). These PEG-albumin complexes could potentially lead to a block of the scavenger receptor mediated cell uptake of L-PEG.[377][378] Remarkably, liposomes L-*hb*PG showed a strong increase in cellular uptake from 2 to 24 hours incubation time, even surpassing CL at 24 h. Since CL, L-PEG and L-*hb*PG only differ in their composition by their polymer shielding, the latter is thought to be mainly responsible for observed differences.

Besides other dissimilar intrinsic properties like viscosity or hydrodynamic radii, multiple hydroxyl groups are exposed in *hb*PG, while mPEG-DSPE possesses one methoxy group at the end of the PEG chain. Unfortunately, it is not clear to what extent the investigated liposomes are taken up by macrophages receptor mediated or non-receptor mediated, and the role of the hydroxyl groups

of *hb*PG in liposome recognition and internalization. Microscopy images (Figure 21) indicate that liposomes were taken up mainly by endocytosis rather than membrane fusion, since liposomal membrane dye was exclusively present in liposomes even after cell uptake, which is in line with the literature.[379] However, more than a single uptake mechanism can occur simultaneously, which is why the explanation of observed differences is fairly ambiguous.[329]

A study from Wagener *et al.* found comparable biodistribution of PEG and *hb*PG liposomes in mice *via* positron emission tomography imaging.[186] However, splenic uptake for *hb*PG liposomes was found to be higher than for PEGylated liposomes. Besides the more complex *in vivo* situation, this phenomenon could possibly be attributed to a higher monocyte uptake, since the red pulp as the main part of the spleen is a center of activity of the reticuloendothelial system and contains more than half of the bodies' monocytes.[380] Monocytes can differentiate into macrophages after recruitment to inflammatory sites, but are also immune effector cells themselves with a very similar nature.[381][223] These observations could therefore be in line with abovementioned findings.

To conclude this part, although PEG and *hb*PG are both very hydrophilic, other intrinsic properties of *hb*PG presumably affect not only the liposomal physicochemical parameters as shown in the first section, but also the biological identity and can therefore have a strong impact on liposome recognition and uptake by macrophages, independently from the protein corona. This could lead to a unique opportunity of 'targeting' liposomes to mononuclear phagocytes like monocytes and macrophages, to potentially stimulate macrophage-mediated host defense mechanisms.[329][333] Additionally, the overall low protein adsorption of tested liposomes could be advantageous for *in vivo* application, since individual deviations deriving from divergent plasma compositions between patients are likely reduced.[23][97][98]

3.1.3 BIODISTRIBUTION & BLOOD CIRCULATION

In this section, findings obtained in a collaboration with the research group of Prof. Dr. Huwyler (Pharmaceutical Technology Uni Basel, Klingelbergstrasse 50, 4056 Basel, Switzerland) are illustrated. Zebrafish experiments were performed by Dr. Dominik Witzigmann and Dr. Sandro Sieber.

The situation *in vivo* is far more complex than *in vitro* due to various parameters that can affect the pharmacokinetic profile of the administered liposomes, like their abovementioned interaction with proteins inside the blood stream, their surface modification or their lipid composition.[173][201][311] Therefore, obtaining *in vivo* data as basis for optimization of

biodistribution and pharmacokinetics is a pre-requisite for clinical development of all nanoparticular drug delivery vehicles. It is in general accomplished by a systemic injection of candidate liposomes into rodents and subsequent organ extraction for analysis of biodistribution *via* microscopic, magnetic resonance, radioactive or fluorescent tracers.[201] However, these *in vivo* studies are quite laborious and cost intensive. Zebrafish embryos (ZFE*)* were recently proposed as simple vertebrate screening model to investigate biodistribution and blood circulation behavior for nanoparticles like liposomes.[280][281][287][384] Main advantages of using ZFEs as *in vivo* model are low experimental costs, high reproducibility, husbandry conditions, high level of genetic homology to humans, available transgenic lines, ethical considerations and the transparent skin, enabling direct non-invasive fluorescence measurements of the whole fish.[272][260] It has been shown by Sieber *et al.* that certain data obtained from *in vivo* studies in mice could be reproduced using ZFEs, and *vice versa* that results obtained from ZFE studies could predict behavior in mice.[280][279] In this section, the focus was set on the influence of amount and size of PEG or *hb*PG on liposome circulation and biodistribution using the ZFE model, by comparing low and high amounts of small, medium and large PEG to respective *hb*PG containing liposomes (physicochemical parameters in sup. table 1), which were already introduced in section 3.1.1. Liposomes were loaded with hydrophilic model cargo SRb and additionally fluorescently membrane labeled with DiD as in section 3.1.2. Biodistribution and blood circulation was analyzed by CLSM qualitatively and semi-quantitatively in the whole fish or tail region 24 hours post injection using image analysis as stated in the methods section.

The workflow from fertilization to CLSM is depicted in Figure 22 A. Fertilized zebrafish eggs were kept for 2 days at 28 °C, then the emerged hatchlings were fixated on warm agarose gel for liposome injection. Around 1 nL of liposome sample was injected into the bloodstream in front of the heart (duct of Cuvier) and ZFEs were kept from now on at 37 °C. After 72 hours post fertilization, embryogenesis was completed and CLSM was performed.[272]
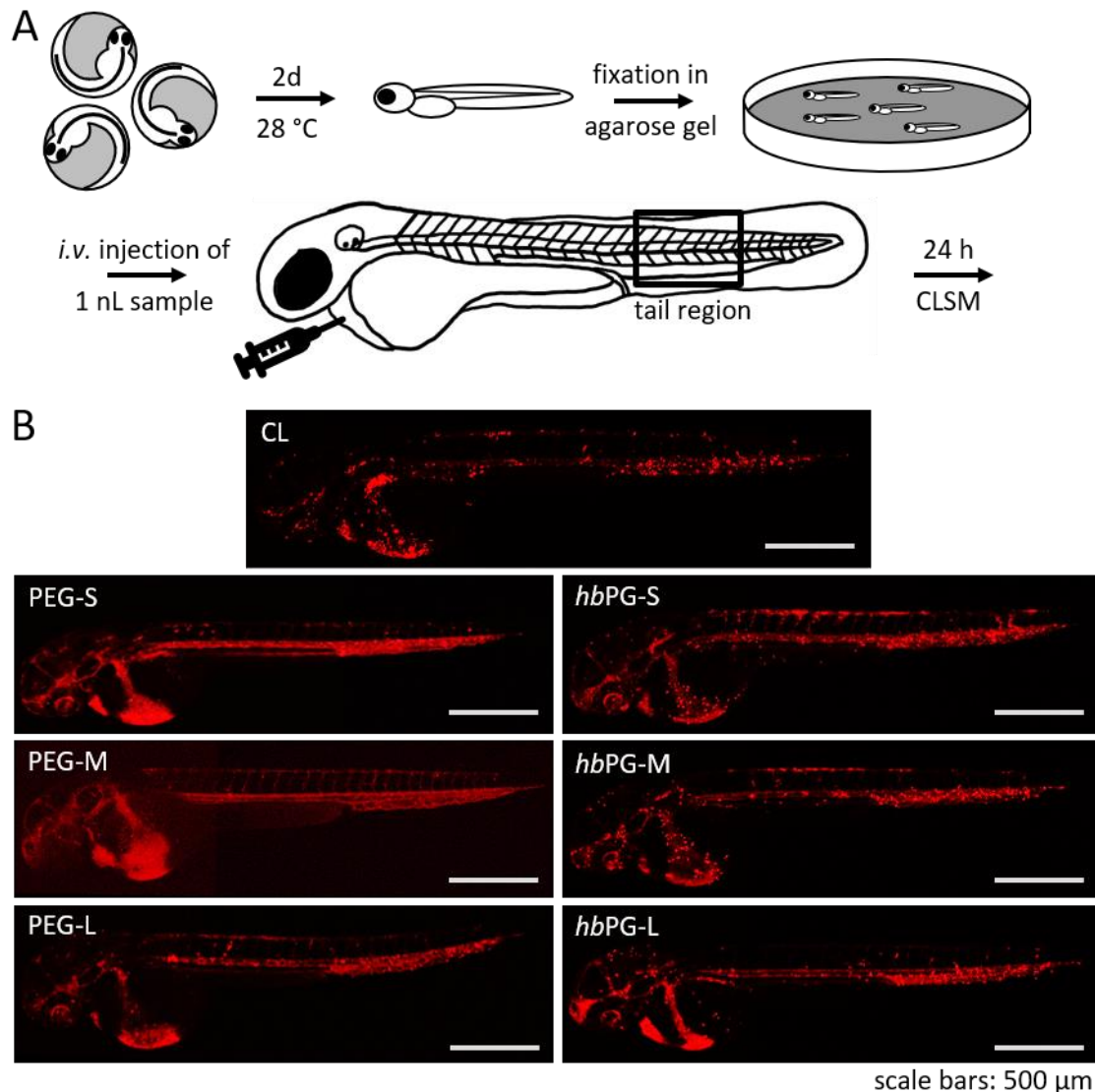
FIGURE 22: (A) EXPERIMENTAL SETUP FOR INJECTION OF LIPOSOME SAMPLES INTO ZEBRAFISH EMBRYOS (ZFE). INSPIRED BY [279]. **(B)** INFLUENCE OF POLYMER SIZE AND TYPE ON LIPOSOME CIRCULATION AND BIODISTRIBUTION. CONFOCAL LASER SCANNING MICROSCOPY (CLSM) IMAGES OF MEMBRANE-LABELED (DID, RED) CONVENTIONAL LIPOSOME (CL, TOP), PEGYLATED (LEFT) AND *HB*PG LIPOSOMES (RIGHT) WITH 5 MOL-% OF POLYMER WITH INCREASING MOLECULAR WEIGHT FROM SMALL (S) OVER MEDIUM (M) TO LARGE (L) 24 HOURS POST INJECTION.

First, the effect of polymer sizes on liposome biodistribution and circulation was addressed. Figure 22 B shows the biodistribution and circulation of fluorescently membrane labeled liposomes (red) within the whole ZFE 24 hours post injection. Beginning with the conventional liposomes CL, their red fluorescence staining pattern was mainly arranged in dotted clusters, indicating a bound non-circulating state possibly caused from binding to the vasculature or for example from uptake by macrophages.[280] Besides, hardly any circulating liposomes could be observed, which would result in a more diffuse fluorescence along the blood vessels. This indicates a low half-life in

circulation and a rather fast clearance, which would be in line with the literature.[16] Regarding PEGylated liposomes (5 mol-%), their fluorescence was evenly distributed across the ZFEs blood vessel structure. This is an indication for a better circulation [280], mainly due to a slower clearance by macrophages according to literature [16], as no dotted fluorescence pattern could be observed. In contrast to PEGylated liposomes, *hb*PG (5 mol-%) containing liposomes showed cluster formation in all permutations, indicating a decreased circulation probably caused by an increased recognition and uptake by macrophages. Also, increasing liposome surface polymer size of PEG and *hb*PG probably led to a better circulation in blood, indicated by a more diffuse distribution pattern. Also, shielded liposomes seemed to circulate better than conventional liposomes, with PEGylated liposomes circulating better than *hb*PG liposomes. Of note, biodistribution and circulation of liposomes is also dependent on their physicochemical parameters like diameter, which generally decreased with increasing molecular weight of the polymer as already discussed in section 3.1.1, so the better circulation could also derive from the fact that liposomes with bigger polymers were smaller in general. Zeta potentials were slightly negative for all tested liposomes, and PDIs were between 0.1 and 0.3, which is why these parameters were assumed to have no major impact on differences in circulation behavior (sup. table 1).

To identify whether the observed dotted distribution patterns arose from macrophage uptake, the transgenic zebrafish cell line expressing green fluorescent protein (GFP) in its macrophages Tg(mpeg1:Gal4;UAS:KAEDE) was used for injection with 1 nL of DiD-labeled liposomes prepared with 10 mol-% hbPG-L as surface modification and sulforhodamine b (SRb) as cargo. Images obtained from CLSM after 24 hours incubation can be seen in Figure 23.

As visible in Figure 23, liposomal hydrophilic cargo SRb (Figure 23 D) and lipophilic membrane dye DiD (Figure 23 C) mainly co-localized, indicating that most liposomes were still intact after 24 hours incubation. This can also be seen in the merged images (Figure 23 B, F), resulting in a rather pink color. Most importantly, liposomes seemed to strongly colocalize with macrophages (Figure 23 C-F), both circulating macrophages within the blood vessels, and tissue resident macrophages. Still, most of the liposomes were in circulation. This qualitatively confirmed previous assumptions, that dotted distribution patterns indicate an increased uptake by macrophages.

scale bars: 500 μm

scale bars: 100 μm
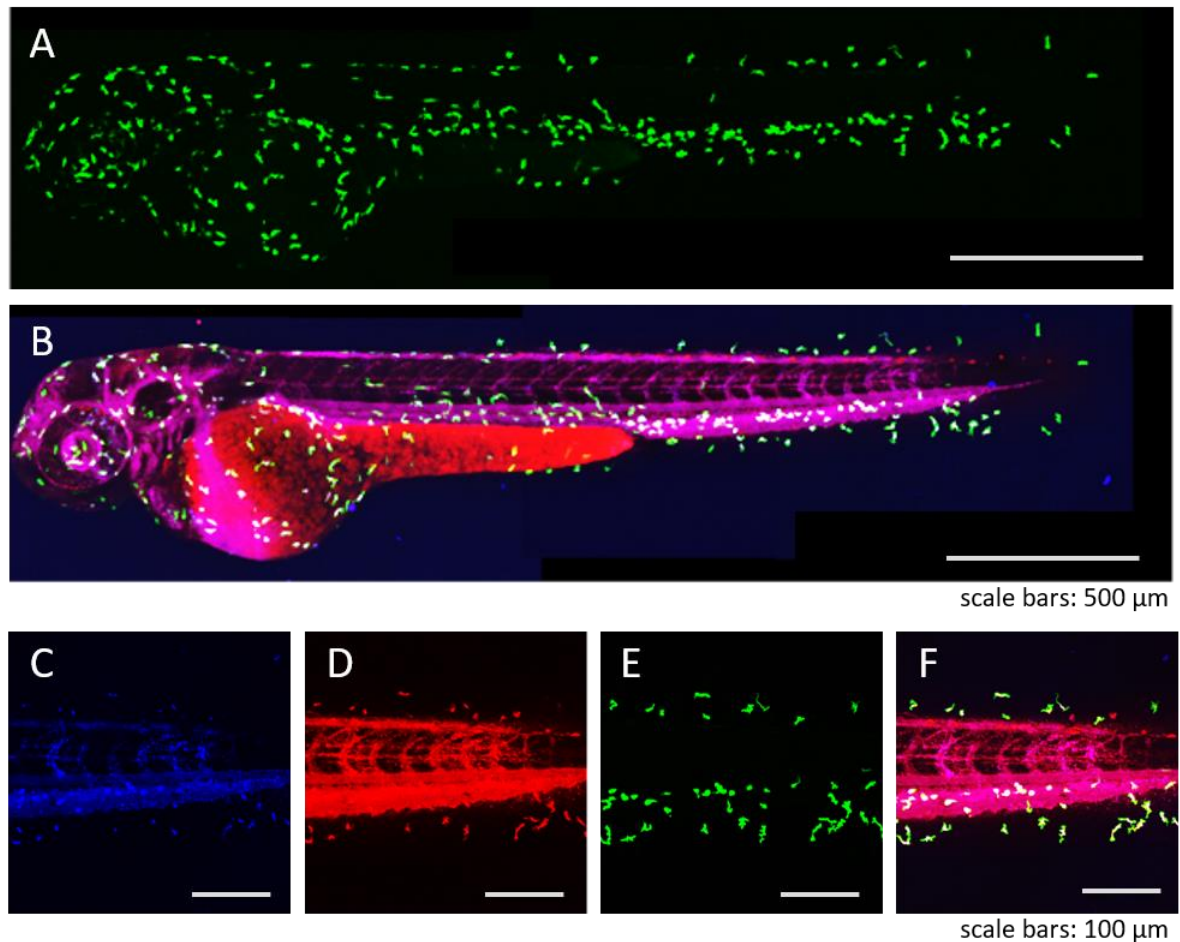
FIGURE 23: CLSM IMAGES OF TRANSGENIC ZEBRAFISH EMBRYO (ZFE) INCUBATED WITH LIPOSOMES FOR 24 HOURS. LIPOSOMES ARE DEPICTED IN BLUE (DID), LIPOSOMAL CARGO IN RED (SRB) AND MACROPHAGES IN GREEN (GFP). **(A)** WHOLE ZFE WITH MACROPHAGES EXPRESSING GREEN FLUORESCENT PROTEIN. **(B)** MERGED IMAGE OF THE WHOLE ZFE WITH CIRCULATING LIPOSOMES. THE BOTTOM FOUR IMAGES SHOW THE TAIL REGION OF THE ZFE WITH **(C)** LIPOSOMES ONLY, **(D)** CARGO ONLY, **(E)** MACROPHAGES ONLY AND **(F)** MERGED CHANNELS. CONTRAST AND BRIGHTNESS WERE ENHANCED EQUALLY ACROSS ALL PICTURES BY 40% FOR BETTER VISUALIZATION.

Second, the effect of the amount of surface polymer on liposome circulation and biodistribution was addressed by injection of liposomes containing 2 or 10 mol-% PEG or *hb*PG in sizes from small to large with SRb as cargo into transgenic ZFEs that express GFP in their vasculature (kdrl:EGFPs843).[385] This time, the tail region was magnified to better visualize differences in circulation and macrophage uptake 24 hours post injection (Figure 24 A).

A

B
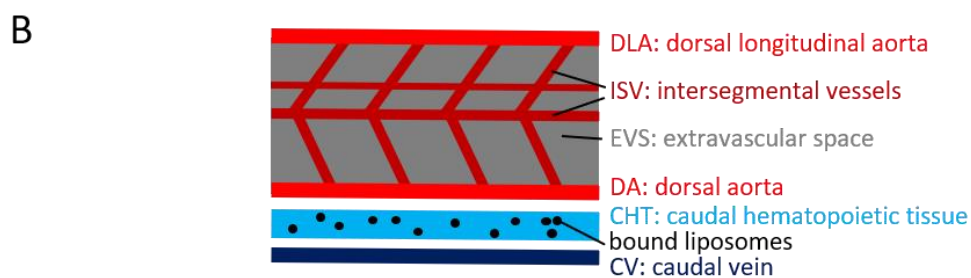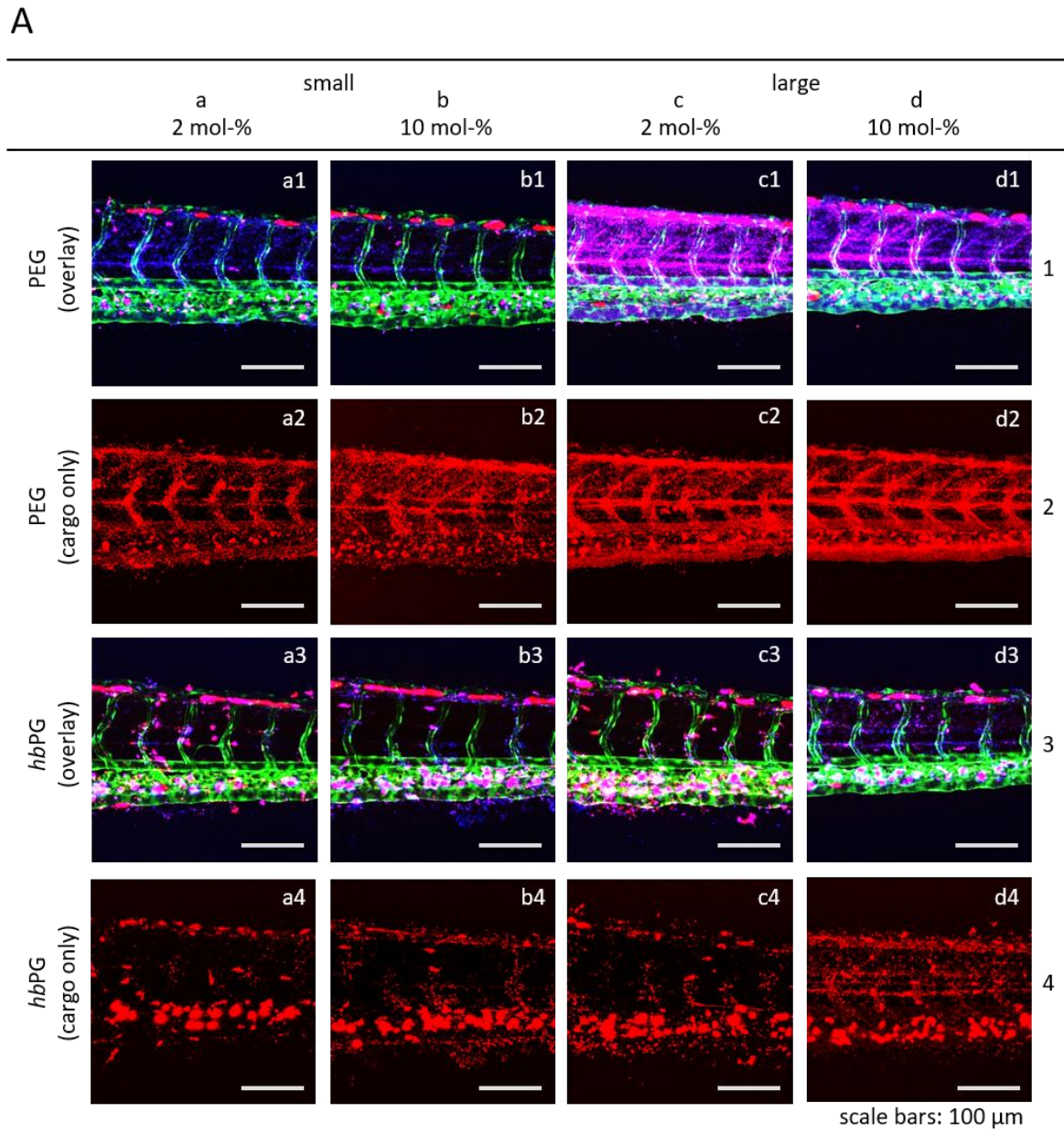
FIGURE 24: (A) CLSM IMAGES OF TAIL REGIONS OF TRANSGENIC ZEBRAFISH EMBYROS 24 HOURS POST INJECTION EITHER OF PEGYLATED LIPOSOMES (ROWS 1 & 2) OR HBPG LIPOSOMES (ROWS 3 & 4). LIPOSOMAL CARGO SRB IS DEPICTED IN RED (ROWS 2 & 4), AND MERGED IMAGES IN ROWS 1 AND 3 DEPICT ADDITIONALLY THE VASCULATURE IN GREEN (GFP), AND THE MEMBRANE LABELED LIPOSOMES IN BLUE (DID). COLUMNS a AND b DEPICT RESULTS WITH LIPOSOMES CONTAINING 2 OR 10 MOL-% OF SMALL POLYMERS, RESPECTIVELY. COLUMNS c AND d DEPICT RESULTS WITH LIPOSOMES CONTAINING 2 OR 10 MOL-% OF LARGE POLYMERS, RESPECTIVELY. CONTRAST AND BRIGHTNESS WERE ENHANCED EQUALLY ACROSS ALL PICTURES BY 40% FOR BETTER VISUALIZATION. **(B)** SCHEME OF THE TAIL REGION WITH TISSUE AND VESSEL TYPES.

Increasing the amount of small PEG on the liposomal surface from 2 to 10 mol-% (Figure 24 A, a2, b2) resulted in a more evenly distributed fluorescence pattern within the extracellular space. This suggests a qualitative increase in liposome circulation, since long circulating liposomes generally show a stronger extravasation, with differences overall best visible for the cargo only images (Figure 24 A, rows 2 and 4). For liposomes containing large PEG, there were only minor changes visible when increasing the amount of polymer, and fluorescence patterns were comparable to liposomes containing 10 mol-% small PEG (Figure 24 A, b2, c2 and d2). Images c1 and d1 suggested however that a considerable number of liposomes (pink) was extravasated and did therefore not colocalize with the green vasculature. Similar trends that increased amounts/sizes of polymer lead to a better circulation were also visible for *hb*PG bearing liposomes, whereas in sharp contrast to PEGylated liposomes, all of them were mainly located inside the caudal hematopoietic tissue (CHT, Figure 24 B), and only liposomes containing 10 mol-% *hb*PG-L showed an increased extravasation (Figure 24 d4). The CHT was reported to be functionally homologous to liver sinusoidal endothelial cells and Kupffer cells of the mammalian liver and therefore comprises the reticuloendothelial system in ZFE, which could be one explanation of the observed patterns for *hb*PG liposomes.[279] For small *hb*PG, increasing the polymer amount led to a qualitative increase in circulation visible by an increase in diffuse fluorescence along the vasculature (Figure 24 A, a4 and b4). Liposomes with 2 mol-% large *hb*PG showed a qualitatively better circulation when compared to small *hb*PG (Figure 24 A, a4 and c4), and increasing the amount presumably led to an increased circulation and extravasation regarding the fluorescence patterns (Figure 24 A, c4 and d4). When comparing PEG to *hb*PG liposomes in the respective amounts and sizes, the latter showed a highly dotted distribution pattern in all cases with clusters mainly located within the CHT, which can likely be attributed to an increased uptake by macrophages as discussed previously.

In order to semi-quantify the circulation, CHT binding/uptake and extravasation, images depicting cargo only were analyzed and cropped according to Sieber *et al.,* with a detailed description provided in the methods section.[280] Absolute fluorescence intensities in the respective compartments are illustrated in Figure 25 A, relative fluorescence distribution between compartments is shown in Figure 25 B.
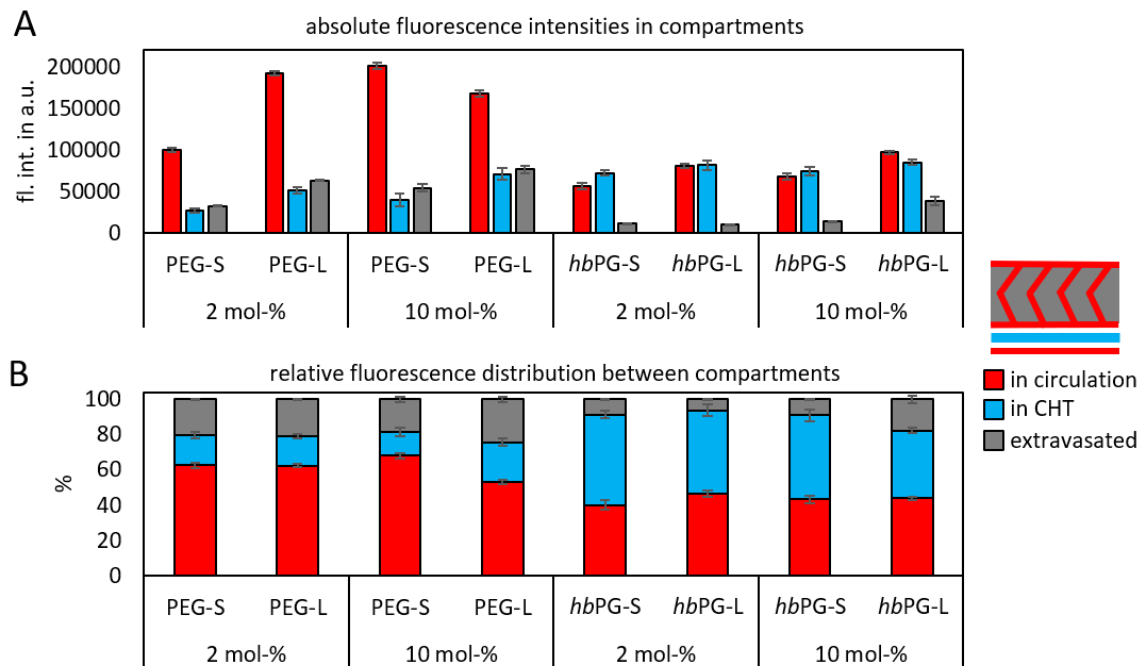
FIGURE 25: (A) ABSOLUTE FLUORESCENCE INTENSITY VALUES OF LIPOSOMAL CARGO SULFORHODAMINE B (SRB) IN ZEBRAFISH EMBRYO TAIL REGION AFTER 24 HOURS INCUBATION WITH LIPOSOMES CONTAINING SMALL OR LARGE PEG/HBPG IN AMOUNTS OF 2 AND 10 MOL-% IN CIRCULATION (RED), CHT (BLUE) AND EXTRAVASCULAR SPACE (GREY). **(B)** RELATIVE FLUORESCENCE DISTRIBUTION OF LIPOSOMAL CARGO SRB BETWEEN COMPARTMENTS IN PERCENTAGE. ERROR BARS INDICATE THREE TECHNICAL REPLICATES.

Absolute fluorescence intensities depicted in Figure 25 A indicate that PEGylated liposomes showed an overall higher total fluorescence intensity when compared to *hb*PG liposomes, which could derive from the different distribution patterns. The overall fluorescence intensity for *hb*PG liposomes with a dotted/clustered distribution pattern is likely underrepresented when compared to evenly distributed, long circulating PEGylated liposomes. The latter showed considerably higher fluorescence intensities in circulation and extravascular space, whereas *hb*PG liposomes were almost evenly distributed between circulation and CHT. This suggests that *hb*PG is less efficient in prolonging circulation when compared to PEG, probably due to an increased macrophage uptake. This phenomenon can also be observed for the relative distribution of liposomes between compartments (Figure 25 B). Differences in liposome distribution within same polymer types are only observable for 10 mol-% *hb*PG-L, which showed a 3-4 times higher extravasation compared to other *hb*PG containing liposomes.

To briefly conclude this section, *hb*PG liposomes showed dotted distribution patterns throughout all permutations, indicating an increased uptake by macrophages mainly of the CHT. They were

therefore not able to prolong liposome circulation as good as PEG. For both PEG and *hb*PG, increasing the size and amount of the surface polymer led to a qualitative increase in circulation and extravasation.

3.2   SCREENING FOR LIPID COMPOSITIONS AT THE EDGE OF STABILITY

ABSTRACT

To identify liposomes at the edge of stability, capable of releasing encapsulated cargo upon slight changes of pH or temperature, various stabilizing and modifying lipids were chosen and combined to form liposomes *via* dual centrifugation. A total of 168 formulations were screened for their membrane stability in the first section by measurement of the emission shift of the membrane-incorporated solvatochromic fluorescent probe laurdan. The edge of stability could be identified for 6 defined lipid combinations, which were optimized in the second section by variation of their lipid ratio to yield efficient model cargo release upon pH decrease and elevated temperature. Besides high cargo release determined *via* size-exclusion chromatography (SEC), insufficient cargo retention upon storage required a liposome refinement step using pH-sensitive cholesteryl-hemisuccinate (CHEMS). Three formulations were finally classified as candidates for efficient cargo release and retention *via* SEC and dynamic light scattering (DLS). In the third section, cell experiments with human macrophages and melanoma cells confirmed increased capability of fast intracellular doxorubicin release for candidate liposomes compared to conventional liposomes using flow cytometry, confocal microscopy and ImageStream®. In the fourth section, treatment of salmonella infected zebrafish embryos with antibiotic loaded candidate liposomes led to an increased zebrafish survival compared to conventional liposomes. Application of pH-sensitive PEG to candidate liposomes in section five resulted in an increased cargo release when compared to conventional PEG or *hb*PG, which could be an important advancement for further development.
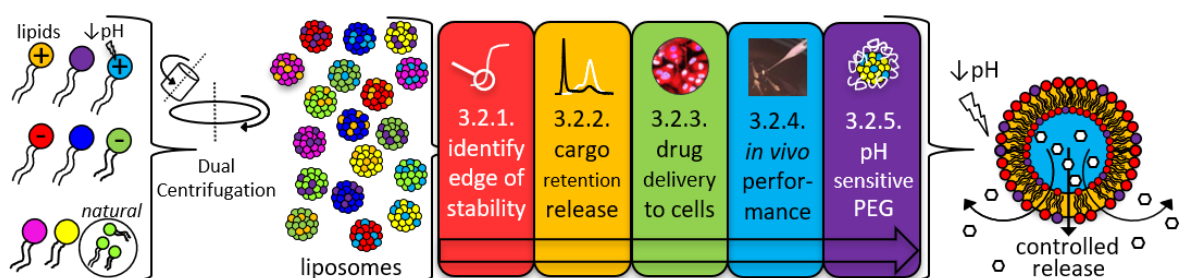
FIGURE 26: SECTION OVERVIEW INCLUDING THE SYSTEMATIC SCREENING APPROACH TO IDENTIFY LIPOSOMES AT THE EDGE OF STABILITY, CAPABLE OF RELEASING ENCAPSULATED CARGO.

INTRODUCTION

Extracellular stability and intracellular lability are contradictory requirements for nanoparticles in drug delivery. It is well known in the literature that encapsulated drugs are not bioavailable until they are released from the liposome. [82][83][173] Therefore, liposomes should grant sufficient cargo retention during storage and transit to the target site and prevent premature cargo release, while at the target tissue, the cargo should be delivered in an adequate concentration within an appropriate time period at a sufficient rate.[388] There are many molecular and biophysical concepts and compounds described in literature to address liposome stability and cargo release, as for example by the use of temperature- or pH-sensitive lipids, synthetic lipids and amphiphiles, amongst others.[10][82]–[89] Since liposomes with comparable physicochemical properties as liposomes used in this approach were reported to be primarily taken up by the endocytic pathway, experiments of this section aimed to achieve rather simple liposomes which trigger cargo release upon body temperature and decreased pH as present in late endosomes/lysosomes and pathologic tissues such as tumors or metastases.[379][395] To cover a high variety for screening, lipids with different fatty acid chain lengths, saturation, phase transition temperatures and headgroup charges were chosen for liposome formulation (table 5). As in the first section 3.1, the conventional non-shielded liposome (CL) served as control and consisted of EPC and cholesterol (55:45 mol-%, same lipid composition as clinically relevant liposome Myocet®). Dual centrifugation was used for liposome formulation, as it is suitable for screening purposes by combining high sample numbers and fast turnaround times with low material needs (2-5 mg total lipid) and high encapsulation efficiencies of around 50% for small hydrophilic molecules like sulforhodamine b (SRb) or doxorubicin (DXR) (Figure 27).[33][121][122] The latter were mainly chosen due to their comparable molecular weight and simple readout using fluorescence, with SRb as non-toxic model cargo for *in vitro* screening purposes, and toxic DXR as drug for cell experiments. It must be noted that the cargo itself can have a huge impact on liposomal parameters like size, stability, cell uptake and cargo release, which is the main reason why the abovementioned comparable model cargos were most reasonable and in line with the typical approach for liposome optimization in literature, which is often cargo based.[290] DXR, a chemotherapy medication used to treat cancer for more than 30 years, accumulates within the cell nucleus after release from liposomes, where it is proposed to intercalate into DNA to form DNA adducts and to inhibit topoisomerase II, finally resulting in apoptotic cell death.[397] Its accumulation inside the nucleus, its fluorescence and the possibility to counterstain the cell nuclei, for example with Hoechst 33258, render DXR a suitable molecule for a comfortable readout of liposomal drug release in cell experiments. To ensure that all cargo is within the liposomes before incubation *in vitro* at lower pH and elevated temperature,

with cells or *in vivo* with zebrafish embryos for cargo release studies, a method for semi-automated

SEC by HPLC was developed amenable to screening in order to handle the huge number of samples.

TABLE 5: LIPIDS USED FOR LIPOSOME FORMULATION. STABILIZING LIPIDS (TOP) WERE MIXED WITH EACH OF THE MODIFYING LIPIDS (BOTTOM). DEPICTED ARE FATTY ACID CHAIN LENGTHS (NUMBER OF CARBON ATOMS:NUMBER OF DOUBLE BONDS), PHASE TRANSITION TEMPERATURES (TM), NETTO LIPID CHARGES AT PH 7.4 (PH 5.5) AND STRUCTURES OF EACH LIPID. FOR LIPID ABBREVIATIONS, SEE SECTION 5.1 MATERIALS.

	lipid	fatty acid chain length	Tm in °C	netto lipid charge pH 7.4 (pH 5.5)	structure
stabilizing lipid 1	DMPC	14:0	24	0	
	DPPC	16:0	41	0	
	DPPG	16:0	41	-1	
	DOPC	18:1	-17	0	
	DOPG	18:1	-18	-1	
	EPC (SOPC)	var.	var. (6)	0	(typical)
modifying lipid 2	DOPE	18:1	-16	0	
	DODAP	18:1	-	0 (+1)	
	DOTAP	18:1	0	+1	
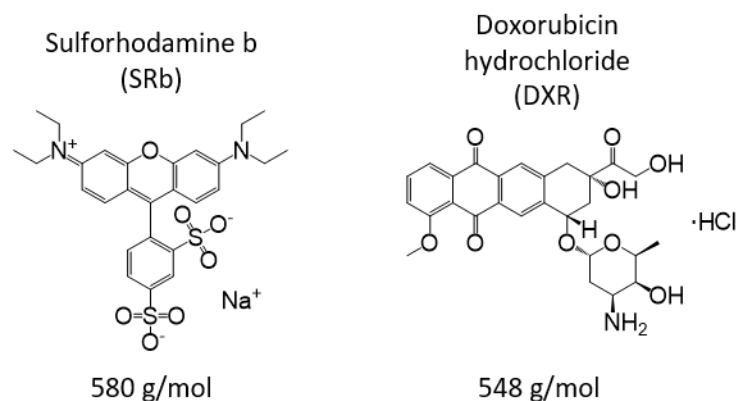
FIGURE 27: CHEMICAL STRUCUTRES OF SULFORHODAMINE B (SRB) AND DOXORUBICIN HYDROCHLORIDE (DXR) AS MODEL CARGOS WITH COMPARABLE MOLECULAR WEIGHTS FOR SCREENING AND CELL EXPERIMENTS, RESPECTIVELY.

3.2.1 MEMBRANE STABILITY

Prior encapsulating and releasing a model cargo from liposomes, it was necessary to identify the edge of liposomal membrane stability, so that small changes of pH and/or temperature would already start to destabilize the liposome for subsequent cargo release. The membrane acts as a natural barrier for encapsulated hydrophilic cargo, depending on the cargo itself and the membrane lipid order, whereas the latter depends on the lipid components and their phase transition temperatures (Tm).[398]–[401] In order to potentially identify regions of liposomal membrane stability and instability faster and to keep the number of variables as low as possible, liposomes were initially kept simple by combining two lipids as components. Therefore, membrane stability was manipulated first by mixing stabilizing lipids of group 1 with every modifying lipid from group 2 (table 5) with increasing mole percentages. Starting from 100 mol-% lipid 1, 10 mol-% were stepwise substituted by lipid 2 up to 90 mol-%. For lipid combinations L1-18, this resulted in 10 different ratios for each combination and a total number of 168 liposome samples (table 6). Modifying lipids depicted identical fatty acid chains lengths and Tms (table 5), so that their effect on membrane stability could mainly be attributed to their charge and miscibility with each stabilizing lipid of group 1. Incorporation of cholesterol into the liposomal membrane was intentionally omitted, since it can have a membrane rigidizing effect and therefore reduces the cargo release, which would obliterate the edge of stability.[402][403]

TABLE 6: CONVENTIONAL LIPOSOME (CL) AND LIPID COMBINATIONS L1-18 PREPARED FOR THE EVALUATION OF MEMBRANE STABILITY *VIA* THE LAURDAN ASSAY. STARTING FROM 100 MOL-% LIPID 1, 10 MOL-% WERE STEPWISE SUBSTITUTED BY LIPID 2 UP TO 90 MOL-%.

lipid combination (L)	stabilizing lipid 1	modifying lipid 2	lipid combination (L)	stabilizing lipid 1	modifying lipid 2
conventional (CL)	EPC	CHOL	L10	DOPC	DOPE
L1	DMPC	DOPE	L11	DOPC	DOTAP
L2	DMPC	DOTAP	L12	DOPC	DODAP
L3	DMPC	DODAP	L13	DOPG	DOPE
L4	DPPC	DOPE	L14	DOPG	DOTAP
L5	DPPC	DOTAP	L15	DOPG	DODAP
L6	DPPC	DODAP	L16	EPC	DOPE
L7	DPPG	DOPE	L17	EPC	DOTAP
L8	DPPG	DOTAP	L18	EPC	DODAP
L9	DPPG	DODAP			

The fluorescent lipophilic dye laurdan (6-dodecanoyl-2-dimethylaminonaphthalene) was additionally membrane incorporated (0.1 mol-%) during liposome preparation since it indicates membrane phase changes and destabilization by a fluorescence emission shift (Figure 28).[404][328] Membrane phase changes can occur, if the measurement temperature exceeds or falls below the specific Tm of the respective lipid forming the liposome. The Tm depends on the lipids' fatty acid chain length, saturation and headgroup.[31] In the usual case of liposomes consisting of more than one lipid, phases can be co-existing and depend on the lipid composition, ratio, lipid hydration and cholesterol content of the membrane.[108] The occurring fluorescence emission shift upon membrane phase change or destabilization is caused by an increased laurdan dipole moment upon excitation at 350 nm, which leads to a re-arrangement of surrounding dipoles like water molecules. Since the required energy for that re-arrangement increases with higher intimate water molecule concentration, laurdan fluorescence emission shifts to higher wavelengths from 440 to 490 nm upon change from gel to liquid disordered membrane phase and upon destabilization.[405] Membranes in rigid gel phase are less fluid than membranes in liquid phase, and are therefore less permeable to small molecules, retaining encapsulated cargo more effectively.[109] The changes in laurdan fluorescence emission maximum and therefore the membrane stability or phase can be described by the laurdan generalized polarization value LGP,

which can be calculated according to formula 13, with *I* as emission intensities at the respective wavelengths.[106][108][109]

$$LGP = \frac{(I_{440} - I_{490})}{(I_{440} + I_{490})} \tag{13}$$

The Tm of DPPC and DPPG as stabilizing lipid 1 is 41 °C and was therefore higher than the ambient temperature of 25 °C (table 6, L4-L9), which is why these lipids were likely in rigid gel phase and the *LGP* decreased upon liposomal destabilization caused by an increase at 490 nm fluorescence emission. All other lipids with a Tm lower than 25 °C were in liquid crystalline phase with more water molecules already within the intimate surrounding of laurdan, which resulted in moderate and high decreases of laurdan emission at 440 nm and 490 nm upon destabilization, respectively, resulting in an overall increase of *LGP*.
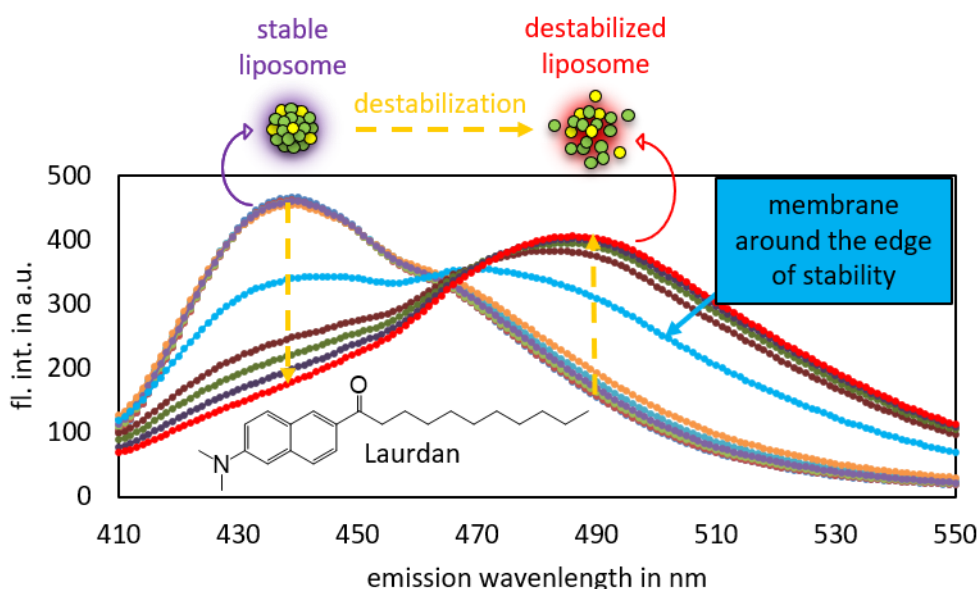
FIGURE 28: LAURDAN STRUCTURE AND FLUORESCENCE EMISSION SHIFT FROM 440 TO 490 NM UPON LIPOSOMAL MEMBRANE DESTABILIZATION OR PHASE CHANGE FROM RIGID GEL TO LIQUID DISORDERED. VALUES OBTAINED FOR A MEMBRANE AROUND THE EDGE OF STABILITY ARE INDICATED IN LIGHT BLUE. EXCITATION WAVELENGTH WAS 350 NM.

To monitor regions of membrane stability and instability, obtained *LGP* values at pH 7.4 were blotted against increasing mol-% of modifying lipid 2 (Figure 29 A). Besides linear *LGP* increase, decrease or consistency, six out of the 18 liposome samples showed a sigmoidal *LGP* shape, namely L2, L4, L6, L11, L14 and L15 (Figure 29 B). Liposome samples L4 and L9 had a negative slope in contrast to the other samples, since their stabilizing lipid 1 had a Tm above the ambient

temperature, as mentioned earlier. Of note, liposomes containing EPC did not lead to a sigmoidal curvature of LGP in any combination with modifying lipids, probably due to its heterogeneity.[108][109]
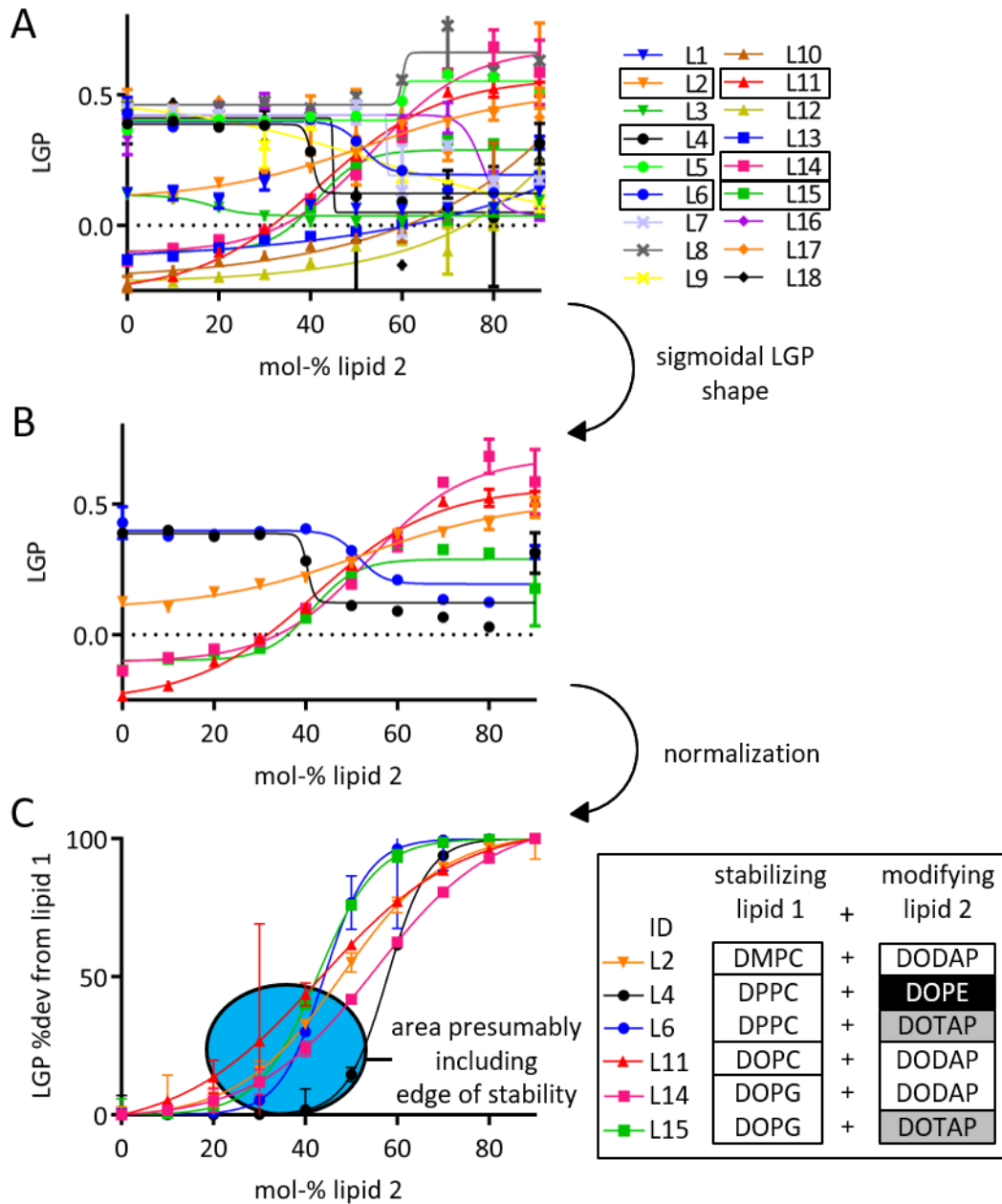
FIGURE 29: LAURDAN GENERALIZED POLARIZATION VALUES (LGP) OF LIPOSOMES CONTAINING 0.1 MOL-% LAURDAN, PLOTTED AGAINST INCREASING MOL-% OF MODIFYING LIPID 2 OF **(A)** ALL TESTED LIPID COMBINATIONS AND **(B)** LIPID COMBINATIONS WITH A SIGMOIDAL LGP CURVATURE. **(C)** NORMALIZED LGP VALUES AS ABSOLUTE DEVIATION FROM THE STARTING LIPOSOME CONTAINING 100 MOL-% LIPID 1 IN PERCENTAGE PLOTTED AGAINST INCREASING MOL-% OF MODIFYING LIPID 2. NORMALIZATION ENABLED THE VISUALIZATION OF THE AREA IN WHICH THE EDGE OF LIPOSOMAL MEMBRANE STABILITY WAS EXPECTED, INDICATED BY THE BLUE CIRCLE. LIPID COMBINATIONS ARE DEPICTED IN THE LEGEND.

For the conventional liposome CL, no changes in laurdan polarization could be observed with increasing cholesterol content (Sup Figure 5). The obtained graphs were normalized for better visualization to uncover the area of beginning liposomal membrane destabilization using a sigmoidal fit. Instead of the *LGP* values, the percentage of deviation from the *LGP* value of corresponding starting liposome with 100 mol-% lipid 1 was plotted against increasing mol-% of lipid 2, with 100 mol-% lipid 1 corresponding to 0% deviation, and 10 mol-% lipid 1 with 90 mol-% of lipid 2 corresponding to 100% deviation (Figure 29 C).

Differences in normalized *LGP* deviation curve shapes observable in Figure 29 C derive from the lipids themselves, depending on their saturation, acyl chain length, miscibility, charge and combination, as explained in the following way. Regarding liposomes L2, L11 and L14 with pH-sensitive DODAP as modifying lipid, their curvatures are quite similar, despite different stabilizing lipids. While DMPC in L2 is saturated, stabilizing lipids DOPC and DOPG in L11 and L14 are unsaturated, respectively. Additionally, the acyl chain length in DMPC is shorter than in DOPC and DOPG, with the latter bearing a negative charge in contrast to the other two neutral lipids. Besides these differences for the stabilizing lipids, the *LGP* deviation curvatures of the mentioned lipid combinations are similar, which suggests that the modifying lipids, as DODAP in this case, have more influence on their respective *LGP* deviation curve shape than the saturation, charge or acyl chain length of the respective stabilizing lipids. Other indications for this suggestion are samples L6 and L15, both with positively charged DOTAP as modifying lipid. Besides differences in saturation, charge and acyl chain length of their stabilizing lipids DPPC and DOPG, respectively, their curvatures look nearly identical. They can be clearly distinguished from L2, L11 and L14, since they have a much steeper slope and are shifted to lower mole percentages. L4 has a comparable curve shape as L6 and L15, although it is shifted to higher mole percentages of lipid 2. This is presumably caused by the modifying lipid DOPE in L4 compared to DOTAP in L6, since both consist of DPPC as stabilizing lipid. The saturation and acyl chain lengths of DOPE and DOTAP are identical, therefore this shift can probably be explained by their charge, which is neutral for DOPE and positive for DOTAP, as well as their miscibility with stabilizing lipid DPPC. Overall, it seems that the modifying positively charged lipid DOTAP in L6 and L15 leads to a slight curve shift to lower mole percentages of lipid 2 when compared to liposomes containing neutral modifying lipids. When comparing L14 and L15, which only differ in their modifying lipids with DODAP and DOTAP, respectively, this shift is also observable. That suggests that positively charged DOTAP destabilizes liposomes at even lower mol-% than neutral modifying lipids. However, *LGP* deviation starts to

increase exponentially for all tested lipid combinations around 40 mol-% of modifying lipid, which is why the edge of stability was expected around or prior this point (Figure 29 C, blue circle).

To briefly conclude, the area of beginning liposome membrane destabilization could be identified for 6 lipid compositions using the fluorescent probe laurdan, with the edge of membrane stability presumably lying within. The point of destabilization seemed to be mainly influenced by the properties of the modifying lipids rather than of the stabilizing lipids. In the next step, the edge of stability was seeked within the area of liposomes containing 20-40 mol-% modifying lipid, by evaluation of liposomal physicochemical parameters and cargo retention as well as release at lower pH and elevated temperature.

3.2.2 CARGO RELEASE AND RETENTION

TEM pictures shown in this section were recorded by Dr. Ingo Lieberwirth from the research group of Prof. Dr. Landfester (Max Planck Institute for Polymer Research, Ackermannweg 10, 5518 Mainz, Germany).

In order to identify the lipid ratio as close to the edge of liposomal membrane stability as possible within the given 10 mol-% steps, the six lipid combinations identified using the laurdan assay in section 3.2.1 were prepared again *via* dual centrifugation, starting within the abovementioned area of destabilization corresponding to 20 — 40 mol-% of modifying lipid 2. This time, the previously presented hydrophilic model cargo sulforhodamine b (SRb) was encapsulated (Figure 27). SRb was chosen because its absorption at 550 nm is independent from the pH value of the buffered medium, preventing falsification when comparing data obtained at pH 7.4 for cargo retention and at pH 5.5 for cargo release.[407] Additionally, it was expected that its comparable molecular weight to doxorubicin (DXR) (Figure 27) as mentioned earlier would lead to less alteration of liposomal physicochemical properties when liposomes are prepared with DXR as cargo for subsequent cell experiments. It was expected that liposomes at the edge of stability would display typical encapsulation efficiencies around 50%, retain cargo upon short-term storage for 1 week at pH 7.4 and 5 °C, while showing a fast cargo release within 4 hours under lysosomal conditions at 37 °C and pH 5.5.[379][111][112] Destabilized liposomes would show a decreased encapsulation efficiency and less effective cargo retention upon storage, if any, while liposomes too stable would show less effective cargo release. Also, liposomal physicochemical parameters like diameter and PDI were investigated to potentially see a beginning destabilization by a significant parameter change.

For cargo release and retention studies, freshly prepared liposomes with 20 – 40 mol-% modifying lipid 2 and SRb as cargo were first subjected to SEC to remove non-encapsulated cargo and to determine the encapsulation efficiency as described in the methods section. One aliquot of the purified liposomes was then incubated at 37 °C with a citric acid phosphate buffer resulting in a pH of 5.5 for 4 hours and subjected to SEC again to determine cargo release. Another aliquot was kept at 5 °C for 1 week and subsequently purified again to determine cargo retention upon storage. A small column filled with Sephacryl S-500 HR suitable for relatively high pressure as present in HPLC was self-packed for size exclusion and connected to an HPLC system. Using the latter with included autosampler and automated fraction collector enabled determination of encapsulation efficiency, cargo release and retention in a high throughput format. Two elution profile examples after SEC with the liposomal (L) fraction at 0.7-1.5 min, corresponding to encapsulated SRb measured *via* absorption at 550 nm, and the free cargo fraction (FC) between minutes 2 and 5, corresponding to unbound SRb, are shown in Figure 30 A, either after short incubation under lysosomal conditions (release conditions) or after 1 week storage (retention conditions).

Results for cargo release and retention of the corresponding lipid combinations can be seen in Figure 30 B. Liposomes were considered at the edge of stability (blue frames), if they showed a minimum release of 80% and additionally a maximum cargo retention within the corresponding composition. For combinations L11, L14 and L15, whose stabilizing lipid fatty acid chain was unsaturated disteaoryl, the edge of stability could be clearly identified, indicated by a drop of cargo release or retention prior or past 30 mol-% of modifying lipid 2, respectively. Similar yet less distinct results could be obtained for L2, with the edge of stability again at 30 mol-% type 2 lipid content. The difference to the first three lipid combinations could derive from the fact that L2 contained saturated DMPC as stabilizing lipid, resulting in lower release and higher retention even at 40 mol-% of modifying lipid.

FIGURE 30: (A) EXAMPLE OF AN ELUTION PROFILE OBTAINED AFTER SIZE EXCLUSION CHROMATOGRAPHY *VIA* HPLC OF A LIPOSOME WITH ENCAPSULATED SRB AFTER STORAGE FOR 1 WEEK AT PH 7.4 AND 5 °C (RETENTION CONDITIONS) OR AFTER INCUBATION AT PH 5.5 AND 37 °C FOR 4 HOURS (RELEASE CONDITIONS). (B) CARGO RELEASE AND RETENTION IN PERCENT, DEPENDING ON THE MOLE PERCENTAGE OF MODIFYING LIPID 2 FOR THE SIX LIPID COMBINATIONS L2, L4, L6, L11, L14 AND L15. LIPOSOMES THAT SHOWED A RELEASE OF ≥ 80% AFTER INCUBATION AT PH 5.5 AND 37 °C FOR 4 HOURS AND IN ADDITION A MAXIMUM CARGO RETENTION WITHIN THE CORRESPONDING COMPOSITION WERE CONSIDERED AT THE EDGE OF STABILITY (BLUE).

For lipid combinations L4 and L6, the edge of stability could not be identified within the investigated range of 20 – 40 mol-% modifying lipid. In the case of L6, consisting of neutral DPPC and positively charged DOTAP, liposomes with 20 mol-% DOTAP seemed to be more stable due to less cargo release and higher retention, hence the range for cargo release and retention evaluation was extended down to 0 mol-%. A comparable pattern to previously mentioned samples L2, L11, L14 and L15 was then detected between 0 and 20 mol-% for L6, with 10 mol-% DOTAP fulfilling the set criteria of at least 80% release with highest possible retention. This confirmed the previous suggestion based on the laurdan assay, that DOTAP as positively charged modifying lipid seemed to destabilize the liposomes already at lower mol-%. In contrast to L6, the point of destabilization for DOTAP containing L15 was reached around 30 mol-%. One explanation for this interesting fact could be that the negatively charged DOPG and the positively charged DOTAP developed an ionic interaction to a certain extent, which could have had a stabilizing effect on the liposomal membrane. For lipid combination L4, the set parameters for the edge of stability could not be reached within the 10 mol-% steps from 0 to 70, although it most likely lied around 60 mol-% and could have possibly been identified if smaller mol-% steps were used. This also suggests that a suitable binary lipid composition is not *per se* reflected by a sigmoidal *LGP* curve.

Encapsulation efficiencies around the identified edge of stability of the respective lipid combinations were also evaluated and are shown in Figure 31 A. For L11, L14 and L15, the encapsulation efficiencies dropped by at least 20% after the edge, suggesting that these liposomes were already heavily destabilized right after preparation. For L2 and L6, the drop of encapsulation efficiency was less distinct, which was in line with obtained release and retention values, suggesting a less sharpened area of liposome destabilization. Physicochemical characterization after the first purification step by SEC revealed a similar trend (Figure 31 B). While for L11, L14 and L15 in addition to L6, a strong destabilization was proposed due to a significant increase in liposome diameter and PDI measured by DLS, there were hardly any changes visible for L2 beyond the edge, besides small changes in PDI, although release and retention values indicated beginning destabilization.
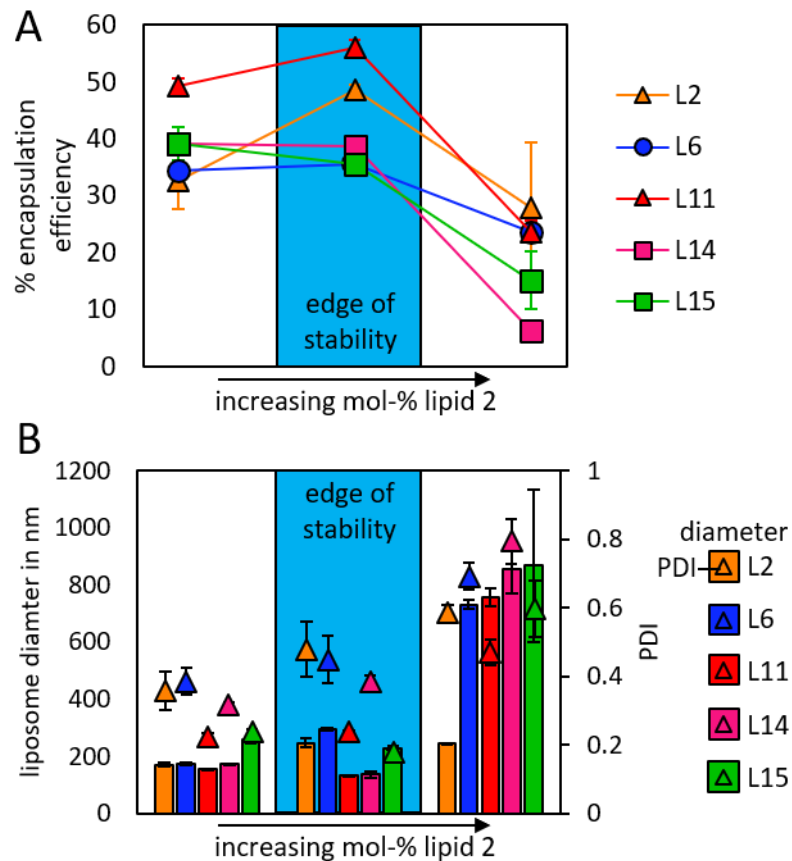
FIGURE 31: (A) ENCAPSULATION EFFICIENCIES OF SULFORHODAMINE B PRIOR, AT AND PAST THE EDGE OF STABILITY FOR LIPOSOME SAMPLES L2, L6, L11, L14 AND L15. A DROP OF UP TOP 20% PAST THE EDGE OF STABILITY INDICATED BEGINNING DESTABILIZATION. **(B)** LIPOSOME DIAMETER AND PDI MEASURED *VIA* DLS PRIOR, AT AND PAST THE EDGE OF STABILITY. AN INCREASE OF DIAMETER AND PDI INDICATED BEGINNING DESTABILIZATION. ERROR BARS INDICATE STANDARD DEVIATION FROM THREE INDIVIDUAL LIPOSOME PREPARATIONS.

However, the average cargo retention of around 43% upon storage was considered insufficient for identified liposomes, which is why a refinement step was necessary to ideally increase liposomal cargo retention to at least 90%. Standard procedures to increase cargo retention mostly involve incorporation of cholesterol (CHOL), which is thought to locate between phospholipids and act as molecular plug that hinders encapsulated hydrophilic cargo from escaping.[410] As it was feared that CHOL could decrease wanted cargo release to an insufficient level, the pH sensitive cholesterol derivative cholesteryl-hemisuccinate (CHEMS) was membrane incorporated in small amounts of 5 and 10 mol-%, to not dominate previously evaluated characteristics, and the effect on release and retention was investigated.[331] The negatively charged CHEMS gets protonated at pH 5.5 on the hemisuccinate, potentially initiating membrane destabilization and cargo release at acidic pH, while stabilizing the membrane at physiological pH for potentially increased cargo retention.[393][411] To assess cargo retention prior cellular uptake, which was wanted to be as

high as possible as the retention upon storage, liposomes were additionally incubated at pH 7.4 and 37 °C for 4 hours. Results of candidate liposomes and conventional liposome CL are shown in Figure 32, along with the new set parameters of at least 90% cargo retention upon storage (dark red bars) and prior cellular uptake (red bars) as well as at least 50% cargo release (black bars).
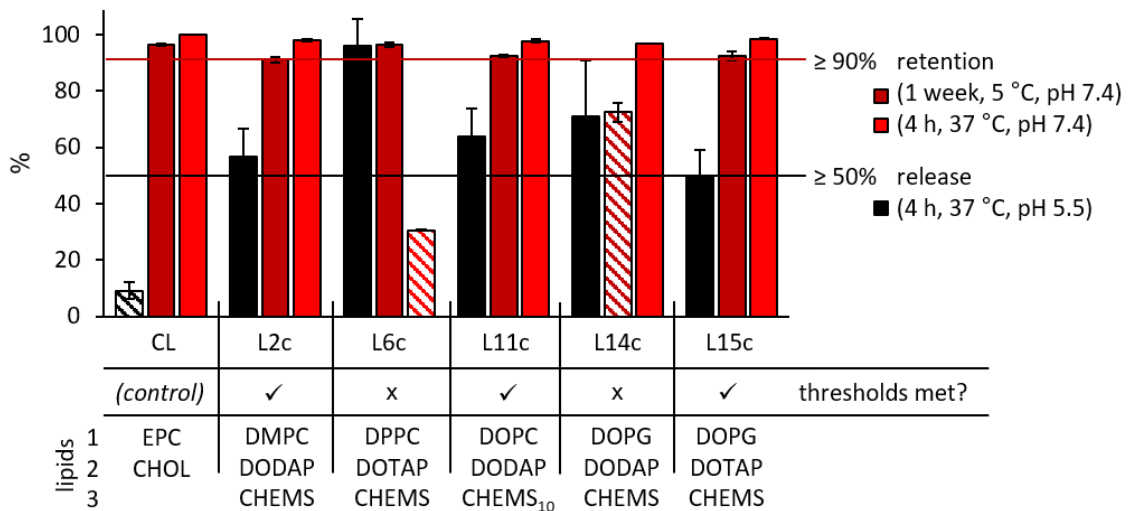
FIGURE 32: CARGO RELEASE AND RETENTION AFTER CHEMS REFINEMENT. PARAMETERS THAT DID NOT MEET THE SET THRESHOLDS OF AT LEAST 90% RETENTION (RED LINE) AND 50% RELEASE (BLACK LINE) ARE INDICATED BY DASHED BARS. REFINED CANDIDATE LIPOSOMES WERE LABELED L2C, L6C, L14C AND L15C AND INCLUDED 5 MOL-% CHEMS, WHILE L11C INCLUDED 10 MOL-% CHEMS. ERROR BARS INDICATE THREE INDIVIDUAL LIPOSOME PREPARATIONS.

For candidates L2c, L6c, L14c and L15c, refined with CHEMS indicated by the small c, best results were obtained with 5 mol-% CHEMS, whereas for candidate L11c, 10 mol-% CHEMS led to best results. L6c was the only candidate containing DPPC as stabilizing lipid with a phase transition temperature of 41 °C around body temperature, which led to insufficient cargo retention after incubation for 4 hours at 37 °C and pH 7.4, probably caused by a beginning membrane phase transition. So L6c not only showed pH-, but also temperature-triggered release, which could be advantageous for other applications, but was not pursued any further in subsequent experiments. Of note, the cargo release decreased for nearly all candidates upon refinement with CHEMS, since the overall stability of the liposomal membrane was enhanced. However, increasing cargo retention to above 90% was considered more important than keeping the release at above 80%, which is why the cargo release threshold was decreased to at least 50%. Candidate L14c did not show sufficient cargo retention above 90% upon storage although it doubled upon refinement with CHEMS from 37% (Figure 30 B) to 76%. If 10 mol-% CHEMS were incorporated, cargo retention did

not change strongly, whereas the cargo release dropped to below the desired 50%, which is why this candidate was also not pursued in further studies. As comparison, the conventional liposome with 45 mol-% CHOL showed only minor cargo release but high retention upon storage as well as at elevated temperature. These CLs were therefore considered as highly stable and served as negative control in further experiments. The three remaining candidates L2c, L11c and L15c successfully met the set retention and release thresholds and were considered as highly potent pH sensitive liposomes at the edge of stability, with the final compositions given in table 7Table 7.

TABLE 7: RESULTING LIPID COMPOSITIONS AND RATIOS OF FINAL CANDIDATE LIPOSOMES L2C, L11C AND L15C AFTER REFINEMENT WITH HELPER LIPID CHEMS.

candidate liposome	stabilizing lipid 1	modifying lipid 2	helper lipid 3	mol-% lipid 1:2:3
L2c	DMPC	DODAP	CHEMS	66.5:28.5:5
L11c	DOPC	DODAP	CHEMS	63:27:10
L15c	DOPG	DOTAP	CHEMS	66.5:28.5:5

The fluorescent dye calcein (CAL) was also encapsulated into the refined liposomes, and encapsulation efficiency, release and retention was determined the same way as for SRb *via* SEC at 490 nm absorption. Results in Figure 33 suggested that obtained values were not exclusive for SRb, but also potentially transferable to other small molecules.
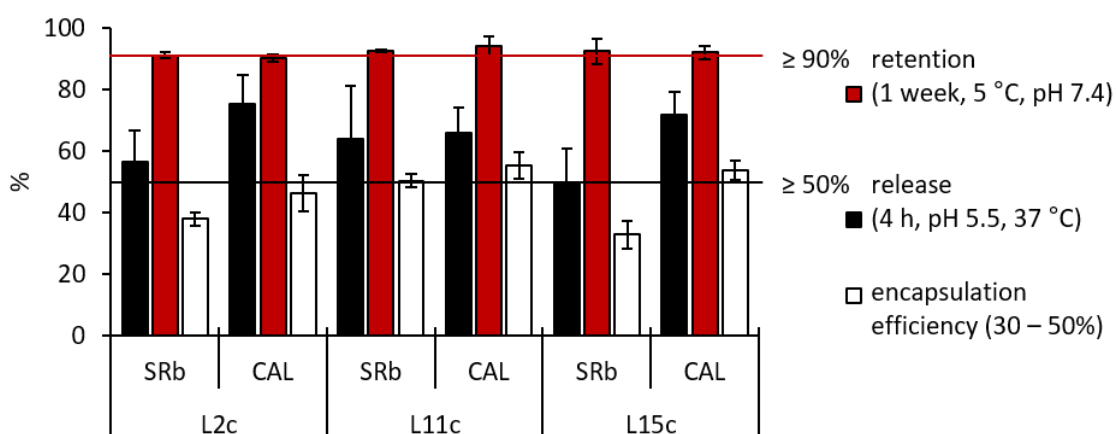
FIGURE 33: COMPARISON OF SULFORHODAMINE B (SRB) AND CALCEIN (CAL) AS CARGO FOR LEAD CANDIDATES L2C, L11C AND L15C AFTER REFINEMENT WITH CHEMS. OBTAINED DATA SUGGESTED POTENTIAL TRANSFERABILITY FROM SRB RESULTS TO OTHER SMALL MOLECULES. ERROR BARS INDICATE THREE INDIVIDUAL LIPOSOME PREPARATIONS.

When CHOL instead of CHEMS was used for refinement, obtained values for cargo retention were comparable, but cargo release was decreased, supporting the use of CHEMS over CHOL for refinement (Figure 34).
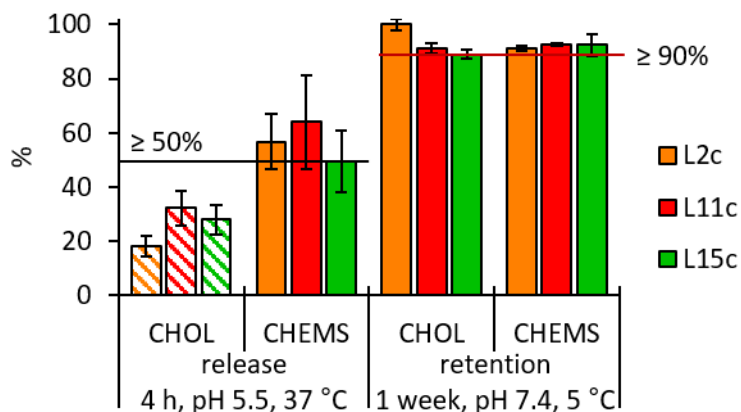
FIGURE 34: COMPARISON OF CHOLESTEROL (CHOL) AND CHOLESTERYL HEMISUCCINATE (CHEMS) USED IN THE RESPECTIVE MOLE PERCENTAGE FOR REFINEMENT OF LEAD CANDIDATES L2C, L11C AND L15C. REFINEMENT WITH CHOL LED TO INSUFFICIENT CARGO RELEASE BELOW THE SET THRESHOLD OF 50%, WHILE CARGO RETENTION WAS COMPARABLE TO RESULTS OBTAINED WITH CHEMS. ERROR BARS INDICATE THREE INDIVIDUAL LIPOSOME PREPARATIONS.

Physicochemical characterization *via* dynamic light scattering of remaining lead candidates L2c, L11c and L15c, either having 20 mM SRb or 90 mM DXR encapsulated, revealed comparable diameters between 150 and 250 nm and PDIs below 0.3 (Figure 35), which would render these candidates suitable for clinical application in accordance to literature.[83][412]–[414] Since two cargos with comparable molecular weights were chosen, besides differences in concentration, their influence on the liposomal physicochemical parameters was minimized. DXR concentration was selected to be as high as possible for subsequent cell experiments due to further dilution by cellular medium (Dulbecco's modified Eagle's medium, DMEM), whereas SRb concentration was chosen to be as low as possible but still above the limit of quantification for screening experiments. Zeta potentials were thoroughly negative except for L11c, which showed a neutral zeta potential around 0 mV. This could be of advantage for subsequent cellular release studies, since the effect of the zeta potential on uptake and release could be reviewed.
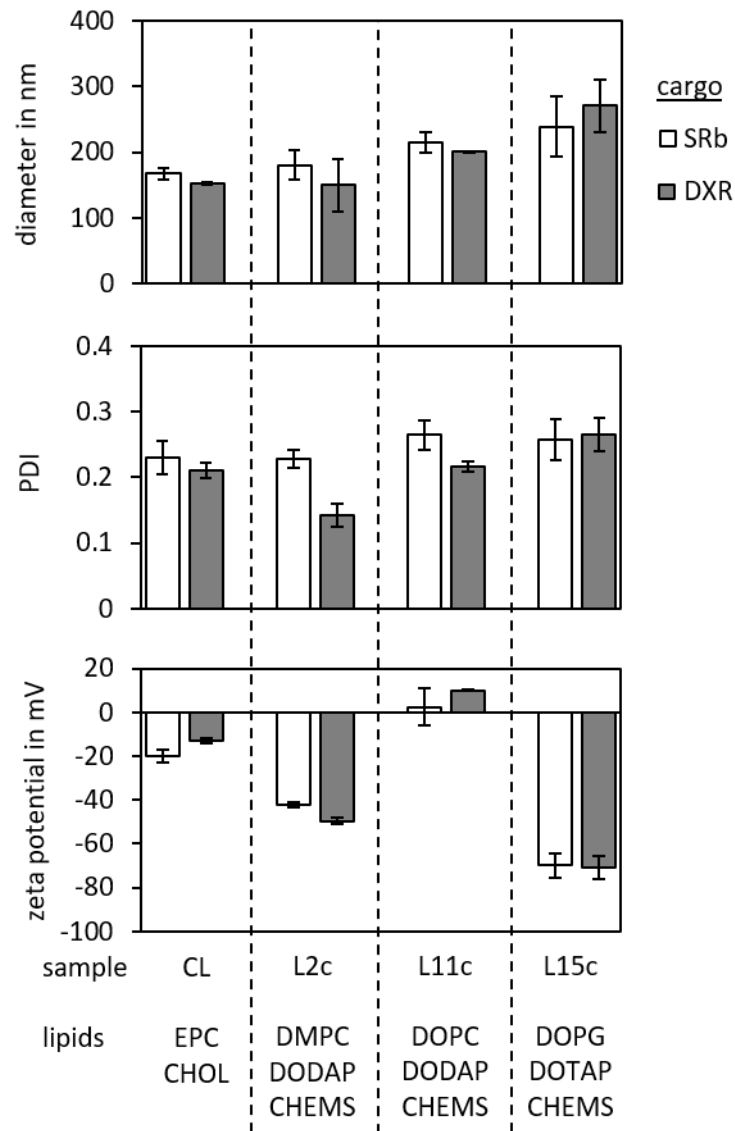
FIGURE 35: PHYSICOCHEMICAL PARAMETERS OF CANDIDATE LIPOSOMES L2C, L11C AND L15C AND CONVENTIONAL LIPOSOME (CL) ASSESSED BY DYNAMIC LIGHT SCATTERING. LIPOSOMES WERE EITHER PREPARED WITH 20 mM SRB OR 90 mM DXR AS CARGO. ERROR BARS INDICATE THREE INDIVIDUAL LIPOSOME PREPARATIONS.

Upon long-term storage of the liposome stocks at 5 °C for 4 months (Figure 36), no significant change of liposomal diameters, zeta potentials and PDIs were visible for candidates L11c and L15c, indicating that the refinement with abovementioned small amounts of CHEMS led to a stabilized membrane for at least the investigated time period. Candidate L2c showed a higher PDI and an increase in zeta potential after 4 months, indicating some sort of destabilization, possibly caused by a slow protonation of DODAP and/or CHEMS.
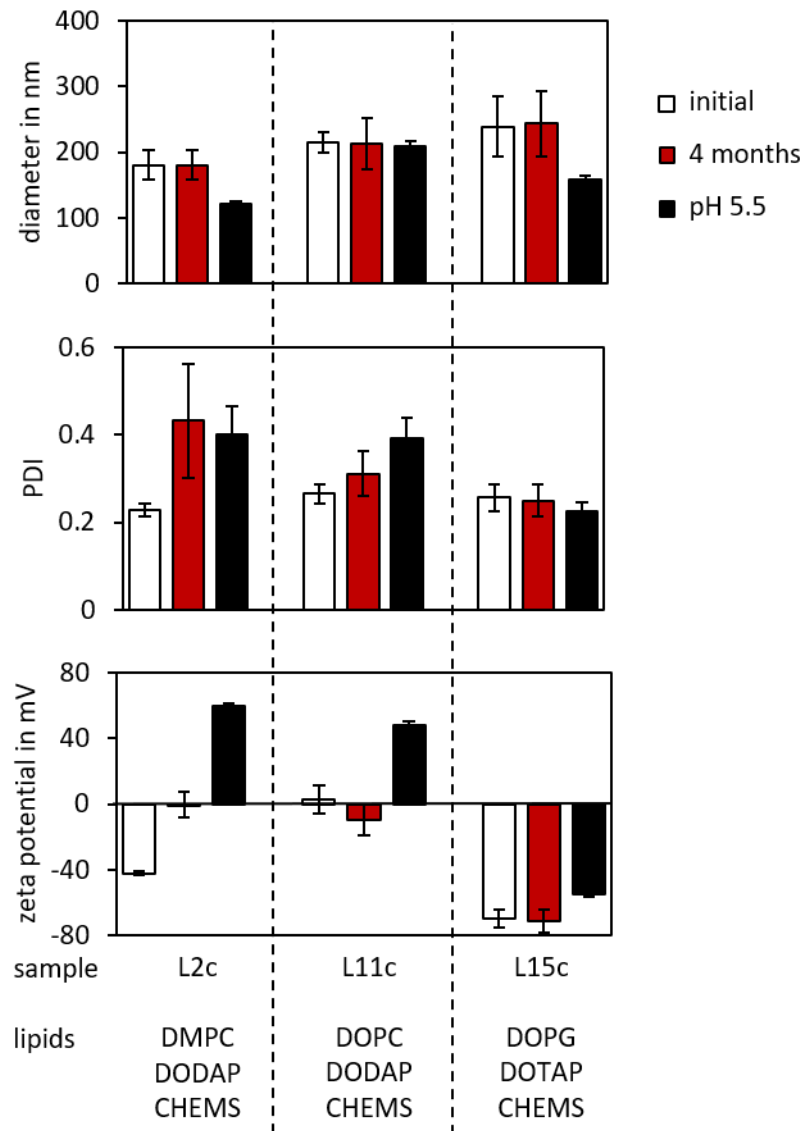
FIGURE 36: COMPARISON OF PHYSICOCHEMICAL PARAMETERS FOR CANDIDATE LIPOSOMES L2C, L11C AND L15C INITIALLY AFTER PREPARATION, AFTER STORAGE FOR 4 MONTHS AT PH 7.4 AND 5 °C, AND AFTER INCUBATION AT PH 5.5 AND 37 °C FOR 4 HOURS. ERROR BARS INDICATE THREE INDIVIDUAL LIPOSOME PREPARATIONS.

Surprisingly, after incubation under release conditions, a decrease in liposome diameter was observable for candidates L2c and L15c, while the diameter of L11c remained constant (Figure 36). This suggests that the cargo release occurred primarily due to an increased membrane permeability rather than liposome aggregation, which would have resulted in an increase in liposomal diameter. Inclusion of 0.1 mol-% of fluorescent lipophilic dye Nile Red into final candidate liposomes and subsequent incubation at pH 5.5 for 4 hours at 37 °C did not result in precipitation of Nile Red, also indicating that liposomal membranes were still intact. Zeta potentials increased for all candidates upon acidification, as expected, since all contained pH sensitive CHEMS. The strongest increase was visible for L2c from -42 to +59 mV, probably caused

by an additional protonation of pH sensitive DODAP. The stronger increase in zeta potential in comparison to also DODAP containing L11c, which consisted of DOPC as stabilizing lipid, could be caused by the fact that the shorter fatty acid chain length of DMPC in L2c probably rendered DODAP more accessible to protonation. The zeta potential of L15c increased only slightly and remained overall negative, since it did not contain lipids amenable to protonation except for CHEMS. The marginal PDI increase after acidification could be a hint that at least some of the liposomes were deformed either by an increase or decrease in size or shape. This could however not be confirmed by cryo- transmission electron microscopy (TEM) measurements conducted for L15c, since liposomes prior and after acidification looked comparable (Figure 37 A). In addition to DLS analysis, TEM pictures were recorded for all candidate liposomes to prove the formation of vesicles (Figure 37 B).

To conclude this part, it was possible to identify lipid ratios at the edge of stability for lipid combinations that showed a sigmoidal LGP curve using model cargo SRb, a semi-automated purification by SEC *via* HPLC and dynamic light scattering. While the ratio for L2, L11, L14 and L15 lied within the expected 20 and 40 mol-% range based on the previously conducted laurdan assay, lipid ratios for L4 and L6 were out of range, suggesting that a suitable binary lipid composition is not *per se* reflected by a sigmoidal LGP curvature. Refinement with small amounts of CHEMS had a significant impact on storage stability, with superior release profiles compared to CHOL. The thresholds of at least 50% cargo release and a minimum retention of 90% were finally met by lipid combinations L2c, L11c and L15c, while conventional liposomes showed only minor cargo release around 10%. The setup for release and retention determination could be transferred to model cargo calcein, and comparable values as obtained for SRb were achieved. This indicated that candidate liposomes could be suitable to retain and release other small molecules in a comparable manner to SRb. DLS and TEM results suggested that the observed cargo release occurred due to changes in membrane permeability rather than liposome aggregation. Final candidates L2c, L11c and L15c achieved pharmaceutical quality with diameters around 200 nm and PDIs below 0.3 [83] and were for the most part stable upon long-term storage. Encapsulation of DXR instead of SRb did not lead to a significant change of physicochemical parameters, an important pre-requisite for subsequent cell experiments.

A   pH 7.4   pH 5.5

B   CL   L2c

     L11c   L15c

                     scale bars: 100 nm
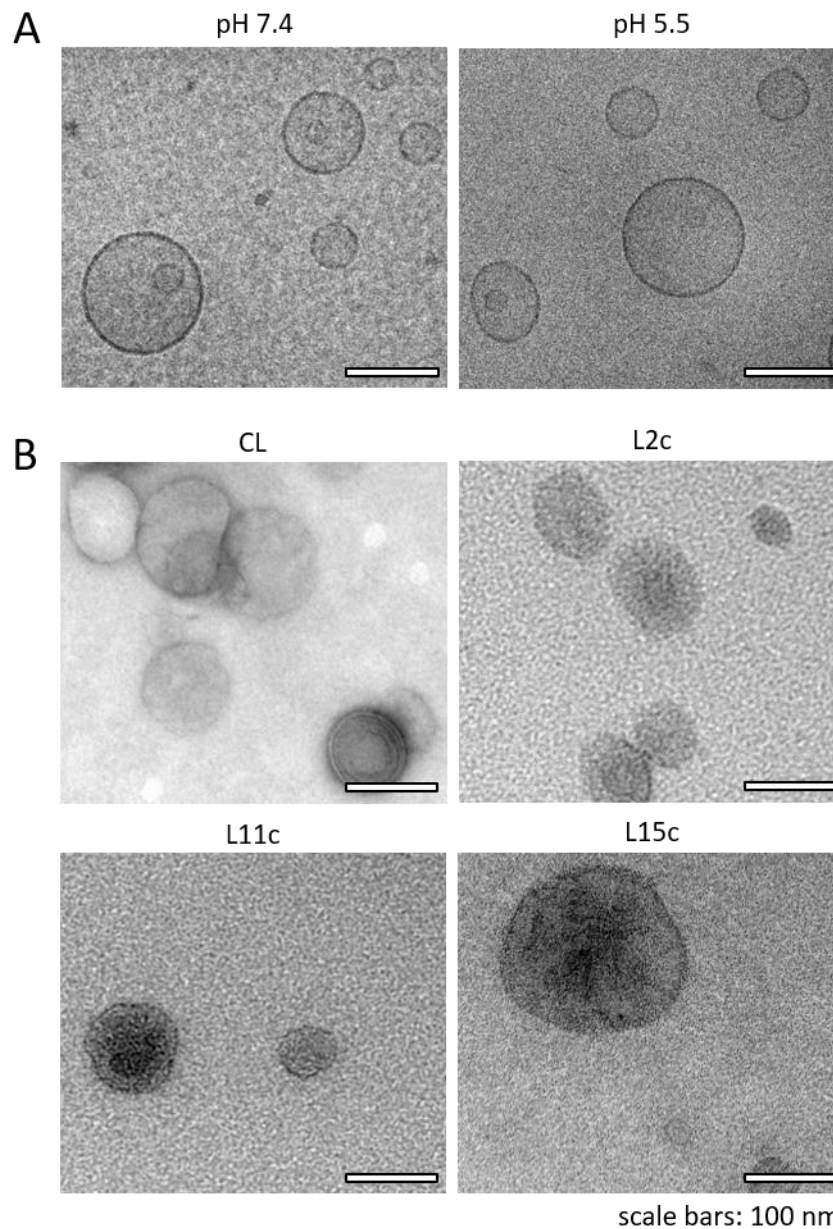
FIGURE 37: (A) CRYO-TRANSMISSION ELECTRON MICROSCOPY (TEM) IMAGES OF L15C AFTER INCUBATION FOR 4 HOURS AT PH 7.4 (LEFT) AND PH 5.5 (RIGHT). COMPARABLE DIAMETERS AND SHAPES INDICATED NO AGGREGATION UPON ACIDIFICATION. **(B)** TEM IMAGES AFTER TREHALOSE / URANYLACETATE STAINING OF CONVENTIONAL LIPOSOMES (CL) AND CANDIDATE LIPOSOMES L2C, L11C AND L15C SHOW VESICULAR STRUCTURES WITH SIZES IN THE RANGE OF OBSTAINED DLS DATA.

3.2.3 INTRACELLULAR DRUG DELIVERY

In this section, findings obtained in a collaboration with the research group of Prof. Dr. Tüttenberg (Department of Dermatology, University Medical Center of the Johannes Gutenberg-University Mainz, Langenbeckstrasse 1, 55131 Mainz, Germany) and Prof. Dr. Mailänder (Max Planck Institute for Polymer Research, Ackermannweg 10, 55128 Mainz, Germany) are illustrated. Cell experiments were performed by Jonathan Schupp, Ambis ImageStream® was performed by Adelina Haller.

The cargo release behavior of the three final candidate liposomes L2c, L11c and L15c as well as of the conventional liposome CL with a composition corresponding to that of clinically relevant Myocet® was assessed *in vitro* using monocyte derived macrophages and human melanoma cells (UKRV-Mel-15a). DXR as cytostatic drug with comparable size to SRb was used as model drug and yielded liposomes with similar physicochemical parameters (Figure 35) as previously evaluated. Its translocation to the nucleus after liposomal release and endosomal escape additionally to its fluorescence renders it a suitable model drug for a comfortable cargo release validation, enabling the discrimination between total DXR within the cell (and liposomes) and released DXR. Macrophages as the innate immune systems' major scavenger cells were chosen as a sort of positive control to investigate phagocytosis of the liposomes and subsequent intracellular DXR release. In addition, macrophages are an attractive target for manipulation by liposomes since they are involved in e.g. inflammation and immune response (M1 phenotype) or wound healing, tissue repair and tumor promotion (M2 phenotype).[415]–[417] UKRV-Mel-15a was chosen as model human melanoma cell line deriving from cutaneous melanoma metastasis [418][419], which could be a primary target for the candidate liposomes in the future, and which enabled analysis of uptake and release in comparison to macrophages.

TOXICITY

In order to evaluate whether the liposomal lipid material is toxic itself, cells incubated with empty liposomes were analyzed after 24 and 72 hours by flow cytometry using a Resazurin-based cell viability assay. In addition, liposomes loaded with DXR were also subjected to the assay, to potentially see a decrease in cell viability, which could be a first hint for a successful DXR release. Free DXR in a concentration of 1 µM served as positive toxic control, which depicted the minimum achievable concentration for all liposome samples despite differences in encapsulation efficiencies. Conventional liposomes (CLs) served as negative control as they were already shown to be non-toxic.[420][421] Results depicted in Figure 38 B indicate that the lipid material of the candidate liposomes was only slightly toxic even after 72 hours in macrophages and melanoma cells. When compared to empty CLs, empty candidate liposomes showed slightly higher toxicity

after 24 hours in melanoma cells and macrophages (Figure 38 A), although the overall toxicity after 72 hours was equalized. When DXR was encapsulated into liposomes to yield an overall stock concentration of 1 µM DXR, the Resazurin assay revealed that candidate liposomes indeed showed toxicity comparable to 1 µM free DXR after 24 and 72 hours, indicating fast and efficient cargo release, whereas CLs showed a comparable toxicity to their empty counterpart at both time points, indicating insufficient cargo release. The higher toxicity of candidate liposomes over 1 µM free DXR after 24 hours in melanoma cells or after 72 hours in macrophages was attributed to likely derive from the additional, albeit low, intrinsic toxicity of the lipid material itself. The cell viability assay therefore gave a first hint for a different cargo release pace and amount *in vitro* when comparing candidate liposomes to CLs. Also, the low toxicity of candidate liposomes similar to CLs would render them suitable for *in vivo* experiments.
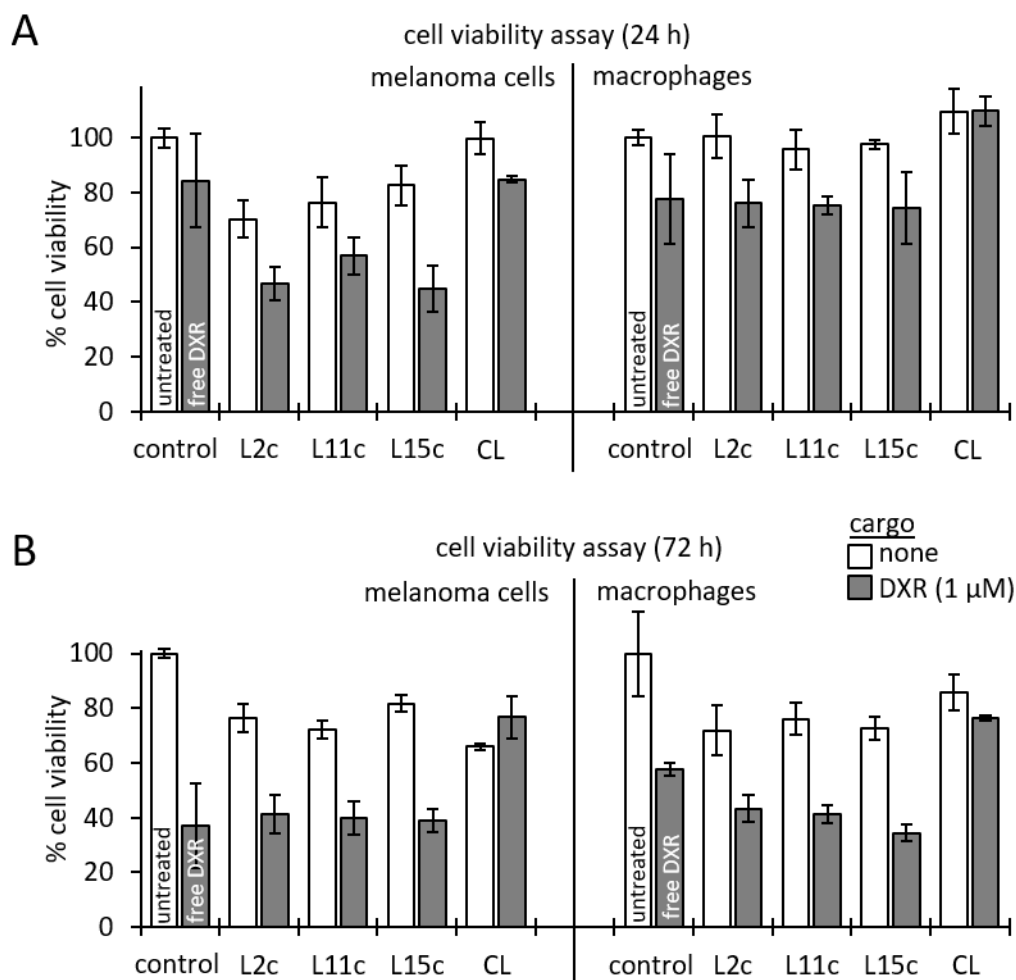
FIGURE 38: RESAZURIN-ASSAY TO DETERMINE CELL VIABILITY OF HUMAN MELANOMA CELLS AND MACROPHAGES ASSESSED BY FLOW CYTOMETRY AFTER **(A)** 24 HOURS AND **(B)** 72 HOURS. CANDIDATE LIPOSOMES L2C, L11C, L15C WERE TESTED AMONG WITH THE CONVENTIONAL LIPOSOME CL EITHER EMPTY (WHITE BARS) OR LOADED WITH DXR (GREY BARS) TO YIELD A TOTAL CONCENTRATION OF 1 µM UPON CELL INCUBATION. UNTREATED CELLS SERVED AS NEGATIVE AND 1 µM FREE DXR AS POSITIVE CONTROL. RESULTS WERE NORMALIZED TO UNTREATED CELLS. ERROR BARS INDICATE THREE INDIVIDUAL ASSAYS.

CELL UPTAKE AND CARGO RELEASE ASSESSED BY FLOW CYTOMETRY

In addition to the observed toxicity *via* the Resazurin assay, the overall DXR fluorescence signal inside the cells was monitored after incubation on melanoma cells and macrophages for 0.5 and 4 hours using flow cytometry. Since the DXR concentration within the liposomes was 50 mg/mL (90 mM), DXR fluorescence was heavily quenched, leading to a very limited fluorescence for intact liposomes.[422] Upon DXR release to the cytosol however, this fluorescence signal would be de-quenched due to dilution, and the emitting fluorescence signal increase was assessed by flow cytometry. After localization to the nucleus and intercalation into DNA, the DXR fluorescence gets also heavily quenched, which is why it was supposed that cytosolic DXR mainly contributed to the obtained signals (Figure 39).[423][424]
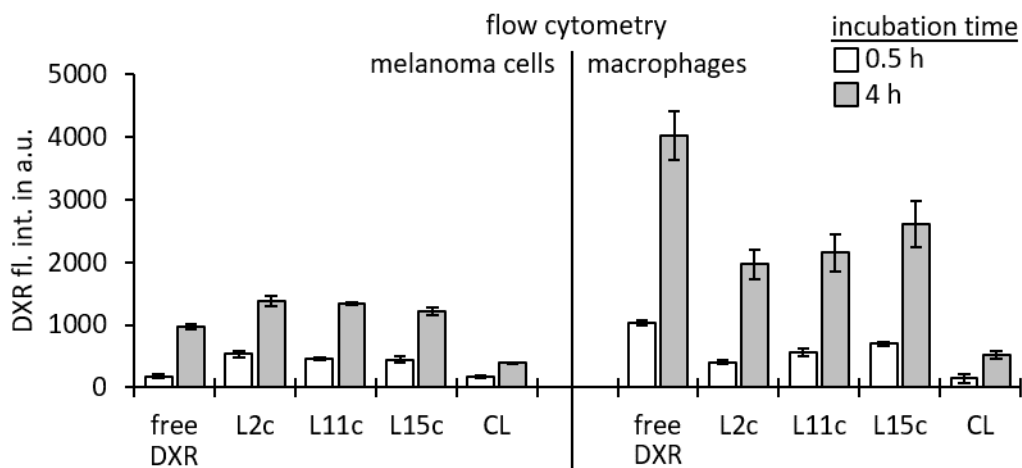
FIGURE 39: DETERMINATION OF DXR FLUORESCENCE INSIDE THE WHOLE CELL BY FLOW CYTOMETRY AFTER 0.5 H (WHITE BARS) AND 4 H (GREY BARS). HUMAN MELANOMA CELLS (UKRV-MEL-15A, LEFT) AND HUMAN MACROPHAGES (RIGHT) WERE INCUBATED WITH FREE DXR IN A CONCENTRATION OF 1 µM OR THE THREE CANDIDATE LIPOSOMES L2C, L11C AND L15C IN ADDITION TO THE CONVENTIONAL LIPOSOME (CL) ALL CONTAINING DXR EQUAL TO 1 µM. ERROR BARS INDICATE STANDARD DEVIATION FROM THEE INDIVIDUAL CELL EXPERIMENTS.

As clearly visible in Figure 39, obtained DXR fluorescence signals are higher in macrophages (right) than in melanoma cells (left), indicating an increased capability of macrophages to take up DXR and liposomes. For the melanoma cells, signals of candidate liposomes L2c, L11c, L15c and free DXR were comparable after 4 hours, whereas the signal of the CLs was about three times lower. This suggests that most of the DXR was still quenched and encapsulated in CLs, whereas DXR of the candidate liposomes was released and unquenched, as their signals were comparable to the signal obtained from cells treated with free DXR. A similar pattern can be observed for

macrophages, whereas here, albeit at least three times as high as for CLs, the DXR fluorescence signals obtained from cells treated with candidate liposomes did not reach the level of free DXR. Both cell types display a signal increase between 0.5 and 4 hours, which most likely represents accumulation of liposomal or free DXR inside the cells or DXR release from intracellular liposomes. To ensure that obtained signals arose from DXR release, microscopy experiments were performed.

CARGO RELEASE ASSESSED BY MICROSCOPY

After DXR is released from liposomes and after endosomal escape, it diffuses to the nucleus.[397] Due to quenching effects that occur upon subsequent DNA intercalation, this fraction was underrepresented in flow cytometry measurements of the whole cell, which is why it was specifically assessed now by confocal microscopy. Measuring the DXR fluorescence inside the nucleus in one z-plane of the cell enabled discrimination of intracellularly released DXR inside the nucleus and free or liposomal DXR inside the cytoplasm or organelles surrounding the nucleus at different z-values. Counterstaining the nucleus with Hoechst 33258 allowed for its easy identification, while an overlay of DXR and Hoechst fluorescence channels enabled evaluation of co-localization and therefore quantification of DXR inside the nuclei. Membrane labeling was omitted to minimize fluorescence crosstalk. Microscopy results shown in Figure 40 confirmed flow cytometry results, again with higher DXR fluorescence signals for macrophages (right). While DXR fluorescence intensities inside nuclei was quite low for CLs after 0.5 and 4 hours, indicating ineffective cargo release, it was at least three times higher for pH-sensitive candidate liposomes at both time points, also reaching the level of free DXR, which indicated sufficient cargo release. All candidate liposomes seemed to be equally potent of releasing DXR, since there was no significant difference observable between them at any time point. Previously obtained flow cytometry results also showed comparable performances.

Upon labeling of cell plasma membranes and liposomes with the membrane carbocyanine dyes DiO and DiD (see section 5.1 Materials), respectively, it was observed that most liposomes were taken up rather than adhering to the outside of the cells (Sup Figure 6), supporting the hypothesis that liposomes were mainly taken up to macrophages and melanoma cells by endocytosis rather than membrane fusion.

FIGURE 40: DETERMINATION OF DXR FLUORESCENCE INSIDE THE CELL NUCLEI BY CONFOCAL MICROSCOPY AFTER 0.5 H (WHITE BARS) AND 4 H (GREY BARS). HUMAN MELANOMA CELLS (UKRV-MEL-15A, LEFT) AND HUMAN MACROPHAGES (RIGHT) WERE INCUBATED WITH FREE DXR IN A CONCENTRATION OF 1 μM OR THE THREE CANDIDATE LIPOSOMES L2C, L11C AND L15C IN ADDITION TO THE CONVENTIONAL LIPOSOME (CL) ALL CONTAINING DXR EQUAL TO 1 μM. ERROR BARS INDICATE STANDARD DEVIATION FROM THEE INDIVIDUAL CELL EXPERIMENTS.
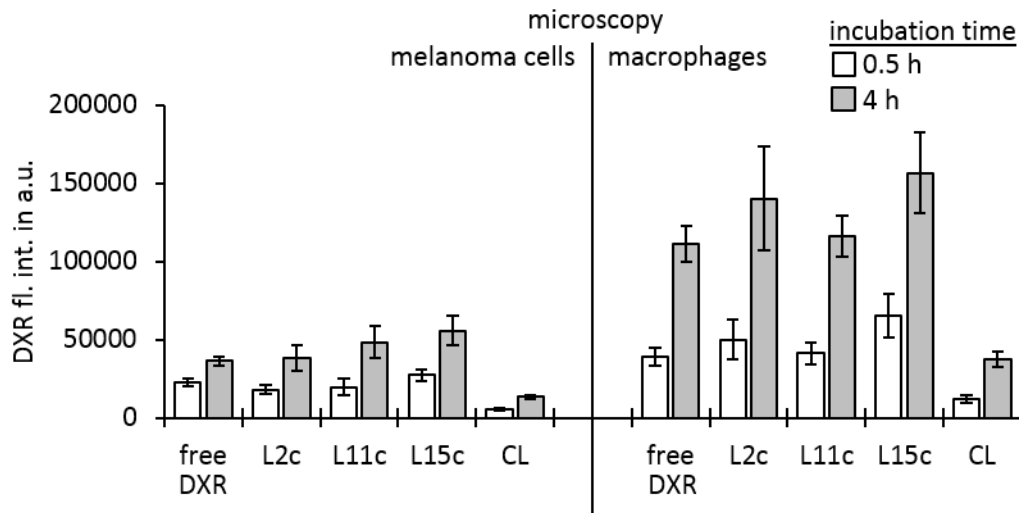
Interestingly, there was an extensive lateral diffusion of liposomal membrane dye DiD within the cellular plasma membrane observable for lead candidate liposomes L2c, L11c and L15c (Figure 41, rows 3-5) after 24 hours, although transfer of such lipophilic probes between intact membranes was reported to be negligible.[425] This suggests that membranes of pH-sensitive candidates decomposed or became more permeable inside the cell within the observed 24 h time span, releasing DiD and in consequence presumably also encapsulated DXR. This effect was more prominent in macrophages (Figure 41, D) than in melanoma cells (Figure 41, B), indicating a variable rate of liposome decomposition depending on the cell type, which could be one explanation for the observed DXR fluorescence differences between macrophages and melanoma cells obtained from microscopy and flow cytometry. Although little is known about the intracellular processing of foreign materials like liposomes by macrophages [426], stated differences would be reasonable, since macrophages as scavenger cells are majorly responsible for digestion of foreign and apoptotic material as well as cellular debris and are therefore suggested to be more effective in decomposition of pH-sensitive liposomes. Conventional liposomes did not show this diffusion pattern (Figure 41, row 6), neither in macrophages nor in melanoma cells, indicating that these liposomes and their membranes remained intact or impermeable in both cell types within the 24 hour time span, which would explain the observed insufficient cargo release.
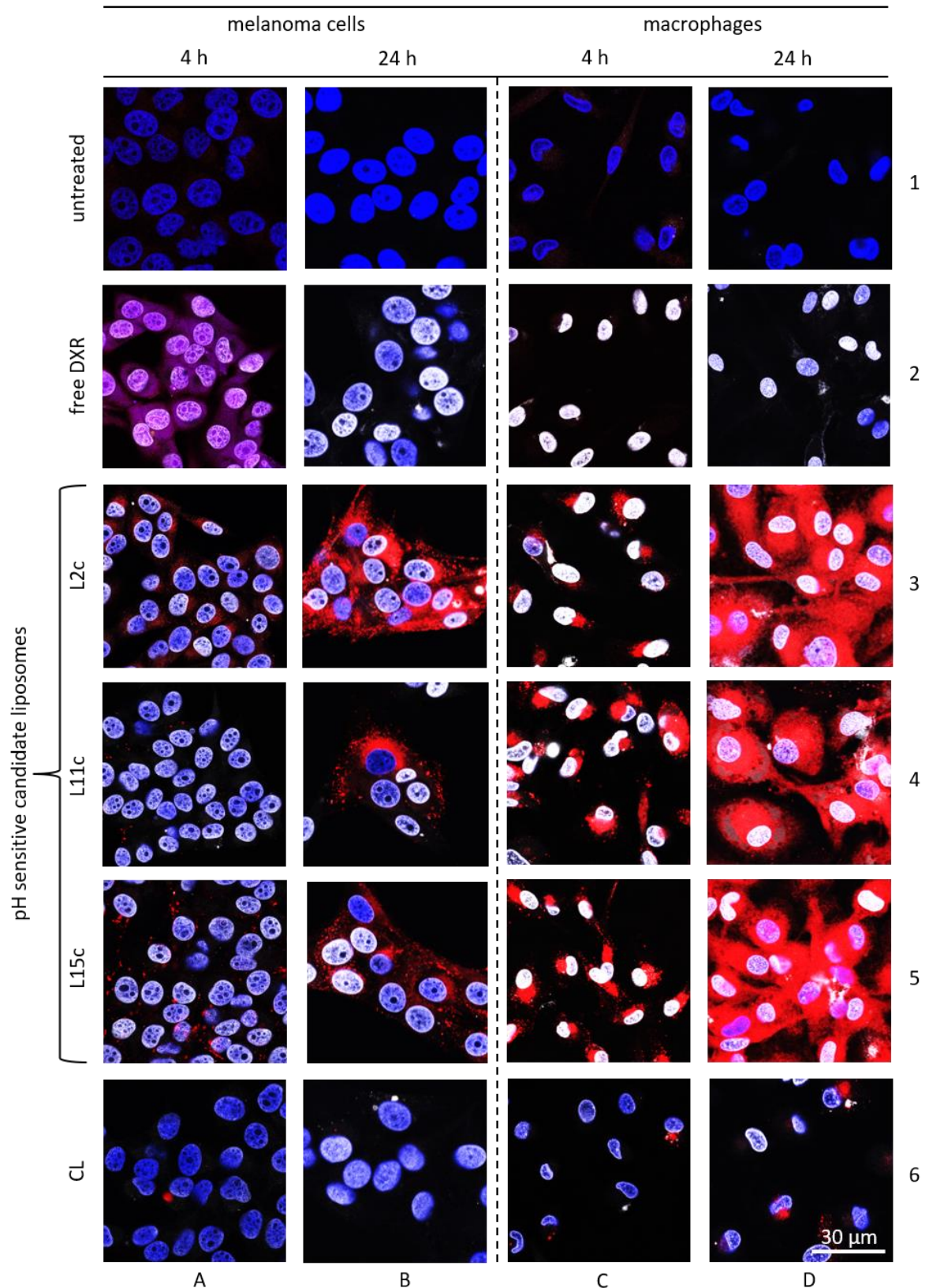
FIGURE 41: CONFOCAL LASER MICROSCOPY IMAGES OF HUMAN MELANOMA CELLS (LEFT, COLUMNS A AND B) AND MACROPHAGES (RIGHT, COLUMNS C AND D) 4 AND 24 HOURS AFTER INCUBATION WITH FREE DXR (ROW 2), DXR LOADED PH SENSITIVE CANDIDATE LIPOSOMES (ROWS 3-5) AND CONVENTIONAL LIPOSOMES CL (ROW 6). CELL NUCLEI ARE DEPICTED IN BLUE (HOECHST 33258), DXR FLUORESCENCE IN WHITE AND LIPOSOMAL MEMBRANE LABEL DID IN RED.   CONTRAST AND BRIGHTNESS WERE ENHANCED EQUALLY ACROSS ALL PICTURES BY 40% FOR BETTER VISUALIZATION.

IMAGESTREAM®

As additional method to confirm results obtained from flow cytometry and microscopy, all samples were subjected to the rather new ImageStream® system.[427] It is an advanced flow cytometer able to acquire both, high quality fluorescence images as in microscopy and integrated fluorescence signals as in flow cytometry. With this system, it was possible to analyze the DXR fluorescence within the whole cell, as well as the DXR fluorescence that co-localized with the stained nuclei. An example of the received images is shown in Figure 42 for L15c after 4 hours incubation with human macrophages. Besides analysis of the whole cell fluorescence as shown in column A row 2, a mask for the cell nuclei as visible in column E row 2 applied to the DXR fluorescence channel in column D row 2 allowed quantification of DXR-nucleus co-localization.
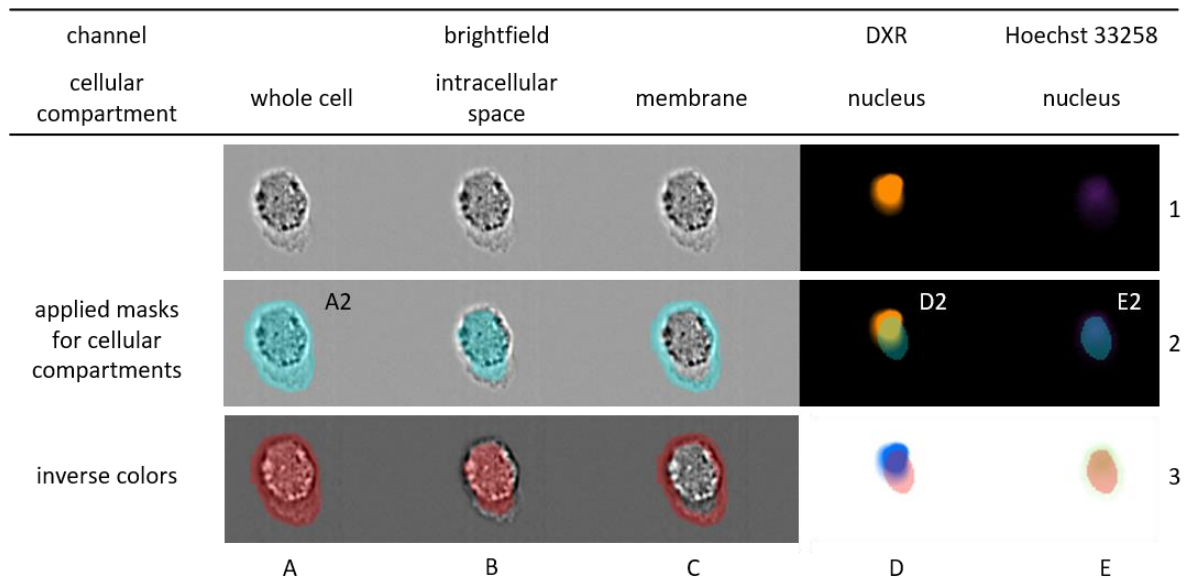
FIGURE 42: IMAGESTREAM® RESULTS FOR L15C AFTER 4 HOURS INCUBATION WITH HUMAN MACROPHAGES. APPLICATION OF MASKS ENABLED QUANTIFICATION OF DXR FLUORESCENCE WITHIN SPECIFIC CELLULAR COMPARTMENTS. CELL NUCLEI WERE STAINED WITH HOECHST 33258 (COLUMN E, PURPLE) AND ALLOWED TO APPLY A NUCLEUS MASK (COLUMN E, ROW 2) TO DXR FLUORESCENCE (YELLOW, COLUMN D, ROW 2) IN ORDER TO QUANTIFY CO-LOCALIZATION WITH THE STAINED NUCLEI. INVERTED COLOR PICTURES ARE PROVIDED IN ROW 3 FOR BETTER VISUALIZATION.

Figure 43 A and B depict the obtained results after quantification of DXR fluorescence inside the whole cell or cell nuclei, respectively.
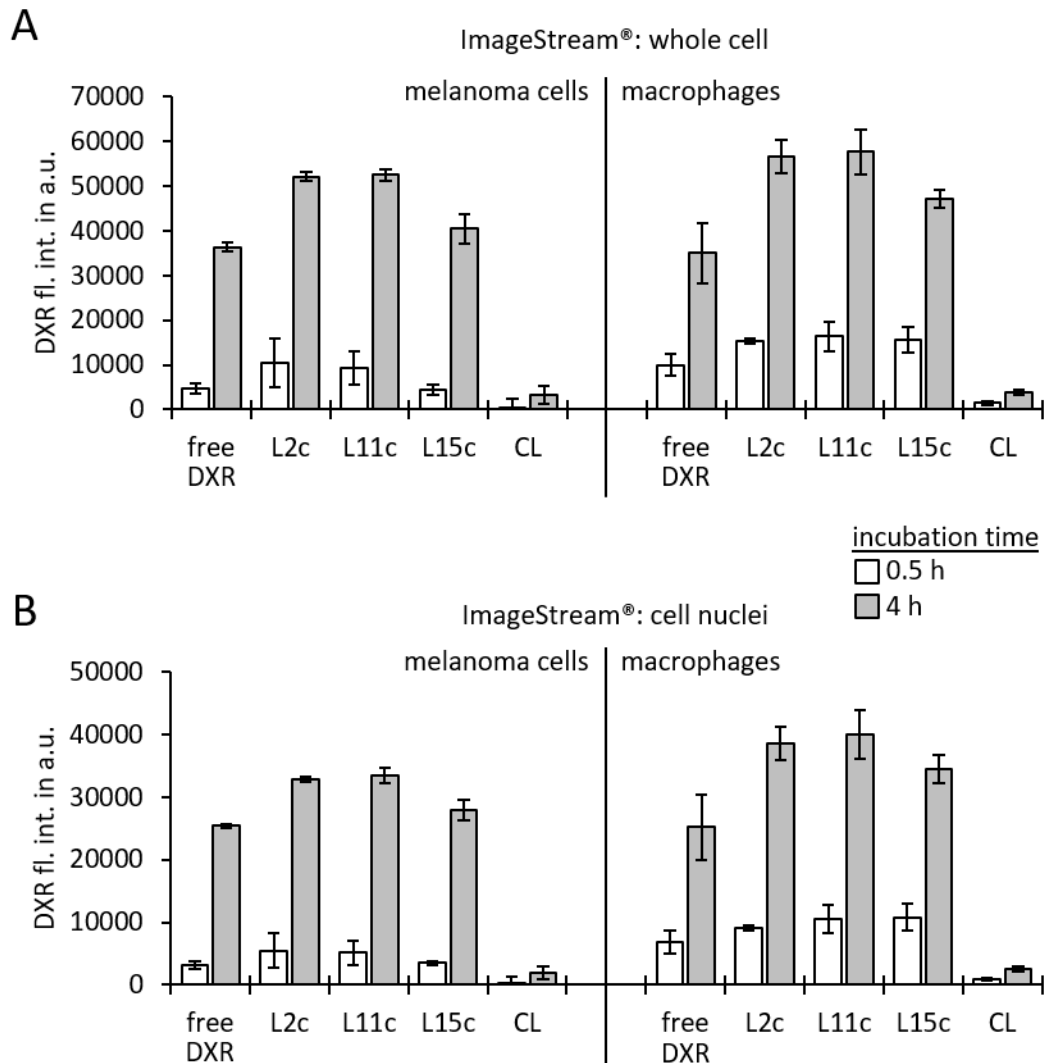
FIGURE 43: DETERMINATION OF DXR FLUORESCENCE INSIDE **(A)** THE WHOLE CELL AND **(B)** CELL NUCLEI BY IMAGESTREAM® AFTER 0.5 H (WHITE BARS) AND 4 H (GREY BARS). HUMAN MELANOMA CELLS (UKRV-MEL-15A, LEFT) AND HUMAN MACROPHAGES (RIGHT) WERE INCUBATED WITH FREE DXR IN A CONCENTRATION OF 1 µM OR THE THREE CANDIDATE LIPOSOMES L2C, L11C AND L15C IN ADDITION TO THE CONVENTIONAL LIPOSOME (CL) ALL CONTAINING DXR EQUAL TO 1 µM. ERROR BARS INDICATE STANDARD DEVIATION FROM THEE INDIVIDUAL CELL EXPERIMENTS.

Trends already observed in results from flow cytometry and microscopy could be confirmed by ImageStream®. While candidate pH-sensitive liposomes L2c, L11c and L15c showed DXR fluorescence levels around or even above free DXR after 0.5 and 4 hours for melanoma cells and macrophages within the whole cell and cell nuclei, the conventional liposomes CL showed very diminished levels of fluorescence in any case, indicating that these liposomes were not capable of effectively releasing DXR (Figure 43). A direct comparison of DXR released from conventional liposomes and DXR released from candidate liposomes revealed a 10-fold increased DXR release capability for pH-sensitive candidate liposomes, which was even higher than the 3-fold increase

obtained from flow cytometry and microscopy. This is especially evident when results from flow cytometry, microscopy and ImageStream® after 4 hours incubation are normalized to the same scale, with free DXR referring to 100% release (Figure 44). In addition to the differences for the conventional liposomes CL, which showed a higher release capability in flow cytometry and microscopy when compared to ImageStream®, flow cytometry results of candidate liposomes for macrophages (Figure 44 A, right) showed a decreased level of fluorescence when normalized to free DXR compared to ImageStream® results. The comparable results from the whole cell and nuclei only measurements could be explained by a fast diffusion of released DXR to the nuclei within the observed time span of 4 hours. Notably, in contrast to microscopy and flow cytometry results, there were only little differences of the absolute DXR fluorescence between melanoma cells and macrophages visible in ImageStream®.
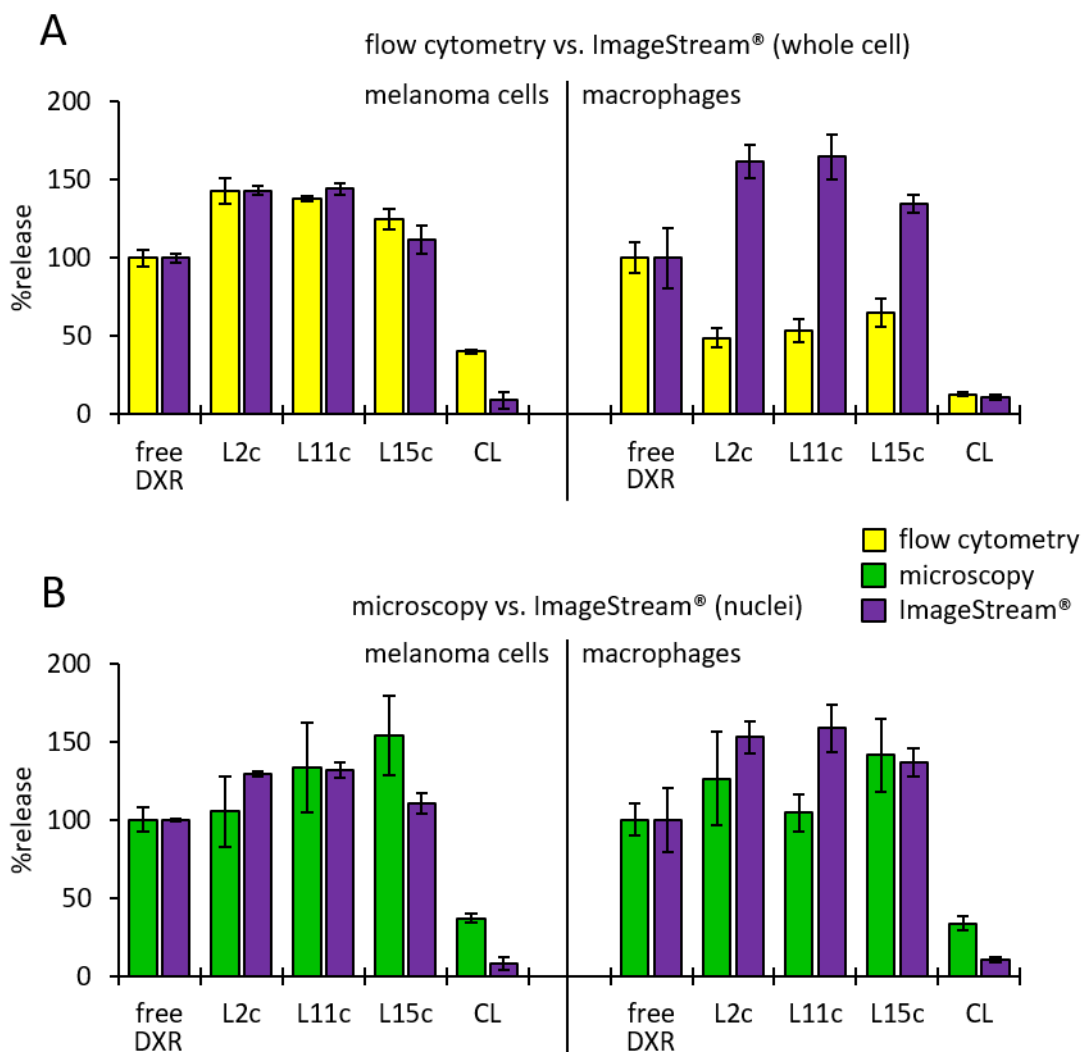
FIGURE 44: (A) RELATIVE DXR FLUORESCENCE WITHIN THE WHOLE CELL ANALYZED BY FLOW CYTOMETRY (YELLOW BARS) OR IMAGESTREAM® (PURPLE BARS) NORMALIZED TO FREE DXR REFERRING TO 100% RELEASE. **(B)** RELATIVE DXR FLUORESCENCE WITHIN CELL NUCLEI ANALYZED BY MICROSCOPY (GREEN BARS) OR IMAGESTREAM® (PURPLE BARS) NORMALIZED TO FREE DXR REFERRING TO 100% RELEASE. ERROR BARS INDICATE RESULTS FROM THREE INDIVIDUAL CELL EXPERIMENTS.

To briefly conclude, cell experiments revealed the low toxicity of candidate pH-sensitive liposomes, rendering them suitable for *in vivo* applications, and most importantly their up to 10-fold increased DXR release capability in comparison to conventional liposomes, monitored *via* flow cytometry, microscopy and ImageStream® for human melanoma cells and macrophages after 0.5 and 4 hours.

3.2.4 *IN VIVO* PERFORMANCE

In this section, recent findings obtained in a collaboration with the research group of Prof. Dr. Huwyler (Pharmaceutical Technology Uni Basel, Klingelbergstrasse 50, 4056 Basel, Switzerland) are briefly illustrated. Zebrafish experiments were performed by Dr. Sandro Sieber and Jonas Buck.

In order to verify previous findings and evaluate their relevance under *in vivo* conditions, the three pH-sensitive candidate liposomes L2c, L11c and L15c were tested in zebrafish embryo (ZFE) model. As already discussed in section 3.1.3, ZFEs are increasingly and successfully used to assess the performance of nanomedicines.[267] Especially regarding liposome biodistribution [73][79] and uptake into macrophages [284], the ZFEs have shown their validity as a predictive animal model system. To this end, the selected candidate liposomes and the conventional liposomes (CL) were loaded with the antibiotic compound ceftriaxone (Figure 45) and injected into salmonella infected ZFEs. The liposomal ceftriaxone content was determined *via* absorption measurements at 254 nm. Over time, salmonella accumulated predominately in zebrafish macrophages, as already demonstrated by Torraca *et al*. [428]. Importantly, all injected liposomes (empty and loaded) were also sequestered to a certain extent by macrophages independent of their lipid composition (Sup Figure 7), identified by using the transgenic zebrafish cell line expressing green fluorescent protein (GFP) in their macrophages (see section 3.1.3, p. 65). This finding is consistent with a previous study, where the uptake of non-pegylated liposomes by zebrafish macrophages had been demonstrated.[284] During intracellular trafficking, nanoparticle containing macrophage compartments are acidified [429], which should trigger the pH-sensitive candidates to release their encapsulated cargo.

Ceftriaxone

662 g/mol
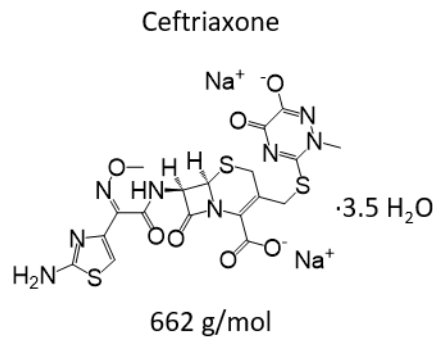
FIGURE 45: CHEMICAL STRUCTURE OF CEFTRIAXONE DISODIUM SALT HEMI(HEPTAHYDRATE).

In a next step, treated ZFEs were analyzed regarding their overall survival rate (Figure 46). Whereas only 20% of untreated salmonella infected ZFEs (Sa+Dulbecco's phosphate buffered saline (DPBS) control) survived after 24 hours post injection, ceftriaxone loaded lead candidate liposomes (L2c CEF, L11c CEF, L15c CEF) considerably increased the survival rate up to 90%. The ceftriaxone loaded conventional formulation (CL CEF) had a considerably lower effect on ZFE survival when compared to the lead candidates, indicating insufficient release of its antibiotic cargo. Of note, empty liposomes had no beneficial effect regarding survival. Conclusively, the sustainable release from lead candidates was able to keep the salmonella burden at a non-lethal level but was not able to completely eradicate the infection. In contrast, the slow releasing control formulation CL was not able to keep the salmonella burden below a critical level, resulting in ZFE death.
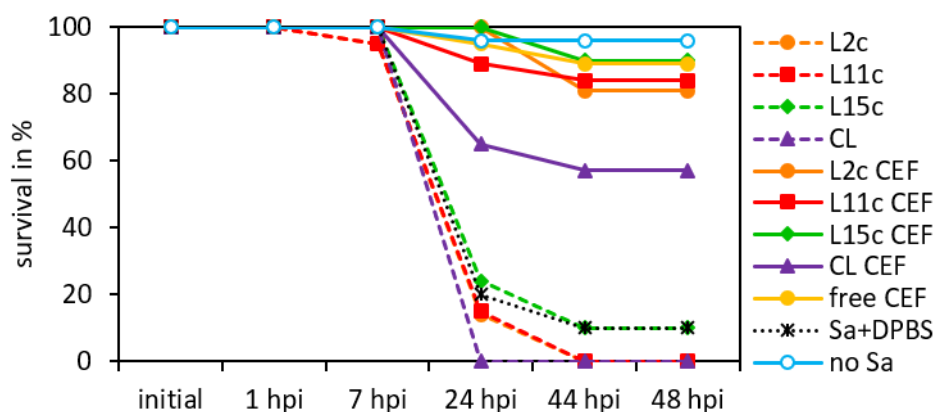
FIGURE 46: SURVIVAL OF SALMONELLA INFECTED ZEBRAFISH EMBRYOS (ZFE) AT DIFFERENT HOURS POST INJECTION (HPI) OF LIPOSOMES AND CONTROLS. ZFE WERE INFECTED WITH 300 COLONY FORMING UNITS OF SALMONELLA (SA) AND TREATED WITH FREE CEFTRIAXONE (CEF) AS POSITIVE CONTROL, EMPTY LIPOSOMES (L2C, L11C, L15C, CL), CEFTRIAXONE LOADED LIPOSOMES (L2C CEF, L11C CEF, L15C CEF, CL CEF) OR DPBS AS NEGATIVE CONTROL IN ADDITION TO UNTREATED ZFE (NO SA). ZEBRAFISH WERE KEPT AT 35 °C AND SURVIVAL WAS ASSESSED BASED ON HEARTBEAT AT INDICATED TIMEPOINTS. EACH TREATMENT GROUP CONSISTED OF AT LEAST 19 INDIVIDUAL ZFE.
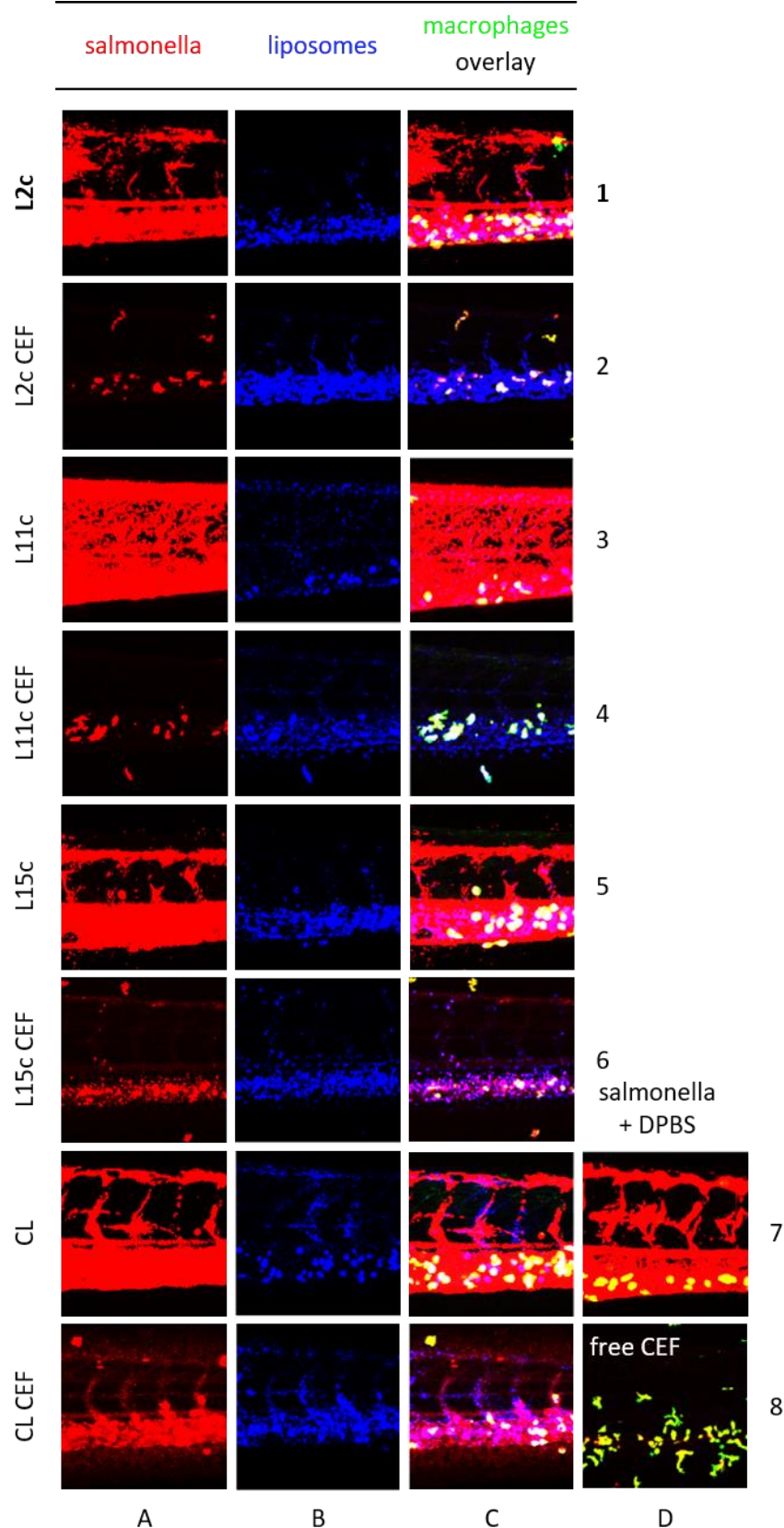
FIGURE 47: CONFOCAL LASER MICROSCOPY IMAGES OF THE TAIL REGION OF ZFE 24 HOURS POST INJECTION OF EMPTY AND CEFTRIAXONE LOADED (CEF) CANDIDATE LIPOSOMES L2C, L11C AND L15C IN ADDITION TO CONVETNIONAL LIPOSOMES (CL), ALL DEPICTED IN BLUE. FREE CEF AND DPBS SERVED AS POSITIVE AND NEGATIVE CONTROL, RESPECTIVELY. SALMONELLA ARE DEPICTED IN RED, MACROPHAGES IN GREEN. CONTRAST AND BRIGHTNESS WERE ENHANCED EQUALLY ACROSS ALL PICTURES BY 40% FOR BETTER VISUALIZATION.

In case of the free ceftriaxone (Figure 47, column D row 7), confocal images revealed a low remaining burden of salmonella 24-hours post injection. On the other hand, a higher salmonella burden was observed when ZFEs were treated with the ceftriaxone loaded lead candidates L2c CEF, L11c CEF and L15c CEF (Figure 47, column A, rows 2, 4 and 6). Nevertheless, no considerably different effect regarding the overall survival on ZFEs was observed (Figure 46). This could be explained by the sustained release properties of the liposome formulations, which should mainly release their cargo intracellularly. The once administered free ceftriaxone dose was enough to eradicate almost all circulating bacteria from ZFE already 7 hours post injection. This prevented a further progression of the infection which resulted in the high ZFE survival. The same total dose of ceftriaxone was administered in case of the liposome treatments. In contrast to free ceftriaxone, the sustainable released amount of liposome formulated ceftriaxone was only able to keep the salmonella burden at a non-lethal level but was not able to completely eradicate all of them in circulation. Of note, ceftriaxone is sensitive to hydrolysis at its β-lactam structure and was encapsulated into liposomes at least 6 hours prior injection. During this time, some of the ceftriaxone could undergo hydrolysis and become ineffective, although this amount is reported to be in the single digit percentage range.[430] The administered free ceftriaxone was freshly prepared prior injection into ZFE and should therefore not undergo hydrolysis. Importantly, the conventional liposomes failed to release a sufficient amount of ceftriaxone resulting in a decreased ZFE survival.

To conclude, salmonella infected ZFE treated with conventional ceftriaxone loaded liposomes showed a considerably lower survival rate when compared to the ceftriaxone loaded pH-sensitive lead candidates, which were able to increase the ZFE survival to the level of free ceftriaxone. A beneficial effect could possibly be achieved by treating the salmonella infection with free and liposomal ceftriaxone, to eradicate both, salmonella in circulation and in macrophages, respectively.

3.2.5 pH-SENSITIVE PEG

Lukas Gleue contributed to liposome preparation and release/retention assays during his master thesis. All polymeric amphiphiles were synthesized by ███████████████████████████████ and ███████████████ from the research group of Prof. Dr. Frey (Johannes Gutenberg-University, Duesbergweg 10-14, Mainz, Germany).

Final pH-sensitive candidate liposomes lack shielding by polymers like PEG or *hb*PG as introduced in chapter 3.1. However, the advantages of steric shielding can include enhanced stability, longer circulation times, less tendency for aggregation, lower protein adsorption, alternated recognition by macrophages, potential size control and modification with targeting moieties.[12] To investigate the effect of such modifications on cargo release, pH-sensitive candidate liposomes L2c, L11c and L15c were prepared with 5 mol-% of amphiphilic polymers with comparable molecular weights, as *hb*PG-S and PEG-S already introduced in section 3.1. In addition, candidate liposomes were also prepared with 5 mol-% of novel amphiphilic PEGs that include ketal or vinyl-ether (VE) moieties synthesized by the Frey group [8][39][432][199], providing pH-sensitive shielding that could have an advantageous effect on cargo release capability (table 8).

TABLE 8: HYPERBRANCHED POLYGLYCEROL (HBPG), POLY-(ETHYLENE GLYCOL) (PEG), AND PH-SENSITIVE KETAL- AND VINYLETHER-PEG BASED LIPIDS SYNTHESIZED BY THE FREY GROUP. MOLECULAR WEIGHTS (MW) AND MOLECULAR WEIGHT DISTRIBUTION (Đ) ARE INDICATED. VALUES WERE OBTAINED FROM [39][141].

amphiphilic polymer	polymer MW in g/mol [a]	Đ [b]	amphiphilic polymer formula and acid cleavage reaction
*hb*PG	3084	1.20	
PEG	3191	1.09	
ketal-PEG	3590	1.08	
vinylether (VE)-PEG	3290	1.23	
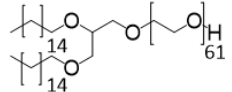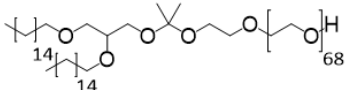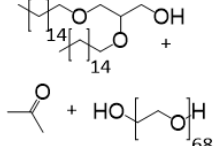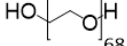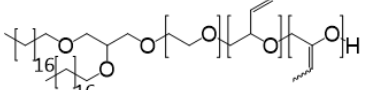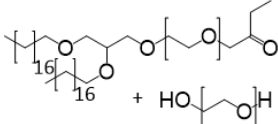
[a]determined using ^{1}H-NMR spectroscopy
[b]determined by SEC

The previously established protocol for cargo release was used, with sulforhodamine b (SRb) as model cargo and liposome incubation at pH 5.5 for 4 hours and 37 °C to mimic lysosomal conditions. Physicochemical properties of the liposomes containing the different amphiphilic polymer modifications measured by DLS are shown in sup table 2, with the tendency of smaller sizes and PDIs for shielded liposomes, and comparable encapsulation efficiencies for all samples.
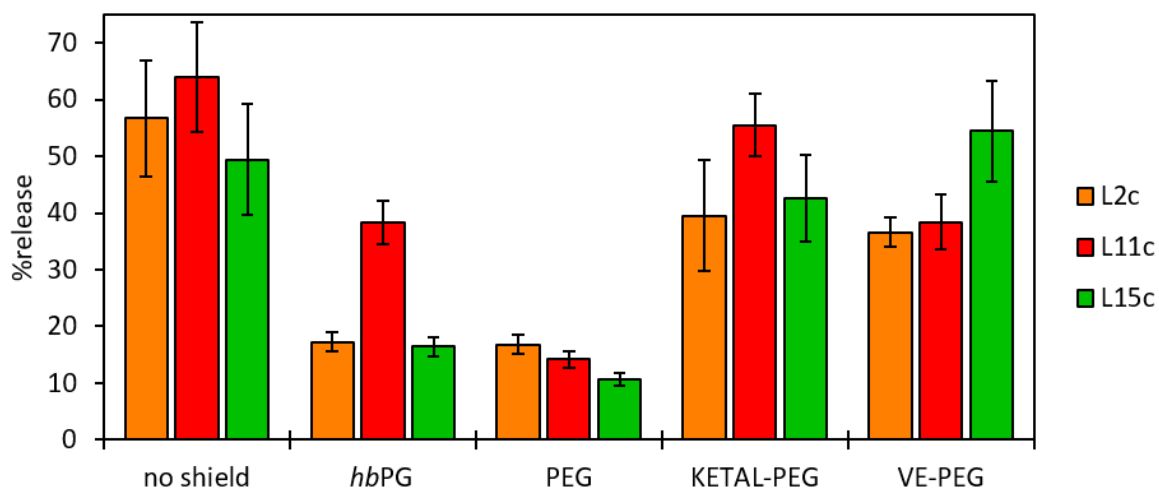
FIGURE 48: SULFORHODAMINE B RELEASE IN PERCENT FROM UNMODIFIED (NO SHIELD) LIPOSOMES AND LIPOSOMES CONTAINING 5 MOL-% HBPG, PEG, KETAL-PEG OR VINYL-ETHER (VE)-PEG. RESULTS FOR PH-SENSITIVE CANDIDATE LIPOSOMES L2C, L11C AND L15C IN ADDITION TO CONVENTIONAL LIPOSOMES (CL) ARE DEPICTED. ERROR BARS INDICATE STANDARD DEVIATION FROM THREE INDIVIDUAL LIPOSOME PREPARATIONS.

Results obtained from cargo release experiments shown in Figure 48 revealed that shielding with non pH-sensitive PEG and *hb*PG reduced cargo release strongly, presumably caused membrane stabilization, as expected. Only for candidate L11c containing 5 mol-% *hb*PG, the cargo release was not reduced considerably. Strikingly however, 5 mol-% of ketal-PEG and VE-PEG restored cargo release capability almost to the level of the non-shielded liposomes. This indicates that the properties of liposomal membranes containing amphiphilic ketal- and VE-PEG were restored at pH 5.5 within 4 hours for the most part, presumably due to cleaving off PEG at ketal/VE sites and therefore reducing membrane stabilization effects. Cleavage kinetics previously conducted by Worm *et al.* [354] and Fritz *et al.* [77] suggest that almost 100% of ketal-PEG is cleaved after 4 hours incubation at pH 5.4, supporting aforementioned assumption. Cleavage kinetics for VE-PEG however showed half-lifes of around 112 hours as measured by Danner *et al.* [199], but surprisingly led to comparable release capability after formulation within liposomes.

To further evaluate the performance of pH-sensitive candidate liposomes shielded with pH-cleavable ketal- or vinylether PEG in comparison to conventional liposomes shielded with PEG, they were loaded with DXR to yield a total concentration of 1 μM and incubated for 0.5 and 4 hours with human macrophages or melanoma cells (UKRV-Mel-15a) and subsequently analyzed by flow cytometry. Preliminary results shown in Figure 49 indicated that pH-sensitive liposomes shielded with ketal- and vinylether PEG showed an average six times higher cargo release capability over conventional PEGylated liposomes.
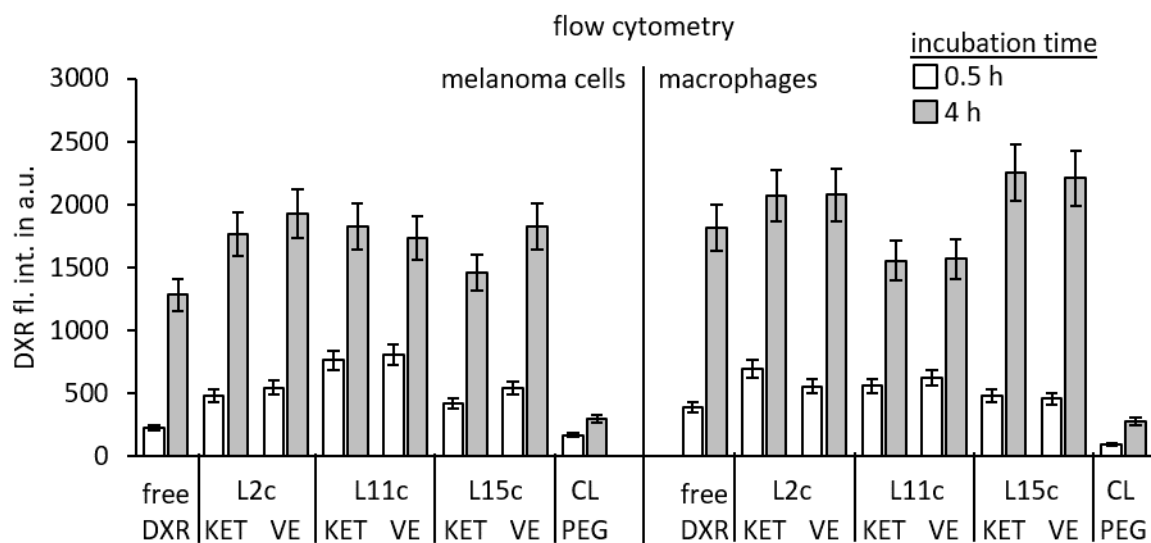
FIGURE 49: DETERMINATION OF DXR FLUORESCENCE INSIDE THE WHOLE CELL BY FLOW CYTOMETRY AFTER 0.5 H (WHITE BARS) AND 4 H (GREY BARS). HUMAN MELANOMA CELLS (UKRV-MEL-15A, LEFT) AND HUMAN MACROPHAGES (RIGHT) WERE INCUBATED WITH FREE DXR IN A CONCENTRATION OF 1 μM OR THE THREE CANDIDATE LIPOSOMES L2C, L11C AND L15C EITHER SHIELDED WITH 5 MOL-% KETAL-PEG (KET) OR VINYLETHER-PEG (VE) IN ADDITION TO THE CONVENTIONAL LIPOSOME SHIELDED WITH 5 MOL-% CONVENTIONAL PEG (CL PEG) ALL CONTAINING DXR EQUAL TO 1 μM.

To briefly conclude, shielding of pH-sensitive liposomes with ketal- or VE-PEG could be a powerful tool for future development, e.g. to potentially increase their storage stability or to achieve active targeting by modification of the polymers with targeting moieties, for instance by click chemistry, while maintaining cargo release efficiency at a high level.

4. Conclusion and outlook

Hyperbranched polyglycerol shielded liposomes: Control of physical behavior and biological performance

Physicochemical parameters

The effect of *hb*PG- and PEG-based lipids on liposomal physicochemical parameters was investigated by dynamic light scattering and nanoparticle tracking analysis and revealed that increased amounts and sizes of *hb*PG and PEG up to 8 mol-% resulted in a relative diameter decrease of corresponding liposomes up to 50%. The main explanation of the observed phenomenon was suggested to be the induced steric repulsion upon increasing amounts and sizes of polymers, which also depended on the polymers' structural conformation and hydrodynamic volume.[60][73][74] Theory based calculations indicated however only a minor increase in liposomal surface area upon formation of smaller liposomes, albeit four times more liposomes could be formed with a constant lipid amount out of a liposome double the size, a calculation that was partly backed by liposome concentration measurements using NTA. Although observed non-linearity in liposomal diameter decrease can be explained for PEG with the established mushroom-brush transition theory [346], no such theory is reported for *hb*PG, since the architecture of those polymers is far more complex. Based on several simplifications, assumed rather compact structures of *hb*PG were in line with ^{1}HNMR measurements [354] and, also based on DLS results, it was tentatively suggested that *hb*PG polymers larger than 5000 g/mol begin to sterically hinder another even earlier than PEG chains with comparable molecular weights, leading to a stronger decrease in liposomal diameter at lower mole percentages. Interestingly, *hb*PG liposomes were overall better reproducible than PEG liposomes although the molecular weight distribution of the *hb*PG polymer was higher. This could probably be explained by a higher sample viscosity of PEGylated liposomes that resulted in a worse mixing during dual centrifugation. Incorporation of *hb*PG with around 3000 g/mol did not lead to an alteration of the liposomal diameter when compared with PEG in the same size, indicated by DLS and NTA results, suggesting that the lateral repulsion of small *hb*PGs potentially promoting a higher curvature of the liposomal surface occurs above 8 mol-%, which could be a subject for further investigation. It became clear however, that micelles were formed upon liposome preparation with more than 8 mol-% of large polymers as indicated by DLS measurements, suggesting a completely saturated liposomal surface. Recorded TEM images confirmed the formation of unilamellar liposomes in close range of sizes obtained from DLS. Of note, the formation of more and smaller liposomes led to an absolute decrease in

encapsulation efficiency of hydrophilic model cargo SRb up to 50% according to the respective liposome size. All in all, modification of liposomes with 6—8 mol-% of *hb*PG or PEG based lipids with a molecular weight above 5000 g/mol led to the formation of small liposomes in pharmaceutical quality. Therefore, *hb*PG and PEG modification of liposomes, tunable in terms of polymer size and amount, could be a powerful tool to enhance liposomal passive targeting and tumor penetration ability while potentially providing enhanced stealth properties due to an increased steric shielding of the liposomal surface.[117] Since the stealth effect of *hb*PG in comparison to PEG is not sufficiently addressable by physicochemical characterization alone, it was further investigated in the subsequent sections.

Protein corona & macrophage uptake

Conventional, *hb*PG or PEG modified liposomes were analyzed in terms of their protein corona composition by LC-MS after incubation with human plasma and subsequent purification by asymmetric flow field flow fractionation or centrifugation. Additionally, cellular uptake by murine macrophages of mentioned liposomes was investigated before or after incubation with 5 and 100% human plasma using flow cytometry and confocal microscopy. Although differences within the hard corona assessed by centrifugation were observed for liposomes containing *hb*PG, the macrophage uptake was strongly altered independently of the corona. While the uptake of PEGylated liposomes was decreased as expected and reported in literature [368], the uptake of *hb*PG containing liposomes was surprisingly enhanced. This outcome was contra-intuitive in many respects, since it was expected that *hb*PG as comparable hydrophilic barrier to PEG would also induce a stealth effect which would consequently result in a decreased recognition by macrophages. Sizes obtained from DLS revealed that liposomes with PEG of a molecular weight around 3000 g/mol were 1.5 times smaller than liposomes containing *hb*PG with a comparable molecular weight, which is in line with findings described in section 3.1.1 and is reported to not alter the uptake by macrophages strongly.[375] Overall, the low protein adsorption on surface modified liposomes led to the formation of a protein corona with a specific composition, which however seemed to not correlate with recognition and uptake by macrophages as indicated by flow cytometry results. In contrast to that, the surface modification itself had a huge impact on the latter, since *hb*PG liposomes showed an enhanced uptake to macrophages contradictory to PEG liposomes, suggesting that *hb*PG represents no classical stealth barrier as PEG. These outcomes lead to several conclusions. First of all, the use of body-similar nanovesicles like liposomes for drug delivery is supported by their overall low protein adsorption, since disease-specific protein corona effects and patient variations are potentially decreased.[23][97][98] Furthermore, the biological

identity of liposomes can be altered strongly by surface modifications, as shown here for *hb*PG. The latter can lead to a particularly interesting approach of 'targeting' liposomes to monocytes and macrophages, which play a distinct role in inflammatory and infectious diseases like human immunodeficiency virus (HIV) and tuberculosis in addition to asthma, atherosclerosis, leishmaniasis and other macrophage-resident microorganisms and parasites, as well as cancer.[221][433]–[436] It could be possible to reduce an inflammatory response of the body by administering *hb*PG liposomes with encapsulated anti-inflammatory drugs or cell killing drugs like Clodronate to deplete monocytes or macrophages.[332][437] In regard to cancer therapy, which often suffers due to biological heterogeneity in metastatic tumors, *hb*PG liposomes loaded with immunomodulators like Interferon gamma [438] could target and activate macrophages present within tumor tissue to bestow tumor suppressive properties and circumvent the aforementioned heterogeneity.[439] Therefore, targeting these types of cells can be of scientific and therapeutic importance. The uptake of respectively labeled *hb*PG liposomes (e.g. loaded with a contrast agent like ^{99m}Tc [440]) by macrophages could also pe useful for diagnostic purposes, e.g. to asses clearance and phagocytic activity, or to localize tumors due to changes in macrophage presence and distribution.[441] In future studies, investigations using *hb*PG liposomes in comparison to liposomes containing linear PG, with a tailored degree of methylated hydroxylgroups as recently reported by Schubert *et al.* from the group of Prof. Frey [442], could yield additional information on the effect of branching and hydroxylgroups on macrophage recognition and uptake. The impact of the '*hb*PG-macrophage' phenomenon remains to be investigated *in vivo* for potential pharmacological effects and limitations.

Biodistribution & blood circulation

Biodistribution and blood circulation of conventional, PEGylated and *hb*PG bearing liposomes was analyzed qualitatively and semi-quantitatively in zebrafish embryos by confocal microscopy and subsequent image analysis to investigate the effect of the respective surface modification with different molecular weights and amounts. Findings regarding conventional liposomes were in line with the literature and suggested fast clearance and low circulation half-lifes due to binding to the vasculature and uptake by macrophages.[12][16] For the surface modified liposomes, results indicated that an increased amount and size of surface modification led to a qualitatively better circulation, which can however be partly attributed to the resulting smaller liposomal diameter. PEG liposomes circulated better than *hb*PG liposomes, that showed a high uptake by macrophages, which was identified by liposome-macrophage co-localization using a transgenic zebrafish cell line expressing GFP in its macrophages. Biodistribution studies 24 hours post injection revealed that in

contrast to PEGylated liposomes, distinct amounts of *hb*PG liposomes ended up within the caudal hematopoietic tissue, a tissue which represents the reticuloendothelial system of zebrafish embryos, further supporting the previously observed increased uptake of *hb*PG liposomes by macrophages. Additionally, more PEGylated liposomes were still in circulation and a higher amount was extravasated in comparison to *hb*PG liposomes. Only liposomes with high amounts of large *hb*PG showed a relatively high extravasation close to the level of PEGylated liposomes. These results indicate that *hb*PG is less efficient than PEG in prolonging liposomal circulation, mostly due to a higher uptake by macrophages. While this outcome represents a major drawback for using *hb*PG liposomes as drug delivery vehicles to target cells other than phagocytic cells, it provides the unique opportunity of passively targeting cells of the reticuloendothelial system to potentially enhance its homeostatic function against cancer cells, parasites and other microorganisms.[433] Monocytes and macrophages as peripheral blood cells can infiltrate all normal tissue, which could make active targeting of *hb*PG liposomes obsolete, since they could be delivered to nearly all tissues after phagocytosis, given that mentioned cells are recruited there.[329] Only future studies can determine the capability of *hb*PG liposomes to activate macrophages. There is also still a great need of appropriately designing the whole liposome not only in regard of its surface modification, but also in terms of its overall lipid composition, to potentially enhance its therapeutic efficiency. This particular task was explored in part 3.2.

Screening for lipid compositions at the edge of stability

Membrane stability

The membrane stability was investigated for 18 lipid combinations using laurdan, by mixing stabilizing lipids with modifying lipids in variegated proportions. The laurdan generalized polarization value (LGP) revealed the area of beginning liposomal destabilization for 6 lipid combinations. For the other 12 combinations, there was no sigmoidal curvature of the LGP visible. Several reasons could account for this phenomenon. First, conventional liposomes and L16-18 consisted of EPC, which is a heterogenous lipid mixture and therefore possess lipids with various phase transition temperatures, which are also altered by the variegated cholesterol or modifying lipid content. For those heterogenous lipid combinations, laurdan seemed to be inappropriate to identify a distinct area of membrane destabilization. Second, the area of membrane destabilization could be quite narrow and was potentially missed within the used 10 mol-% steps. Smaller steps

could help to identify the edge of stability for more lipid combinations. There is also the possibility that there were no stable liposomes formed at all for several lipids, or that some modifying lipids were not miscible with the respective stabilizing lipids, resulting in no change of the LGP curvature. Choosing a different lipid pattern of stabilizing and modifying lipids for mixing could however reveal more lipid combinations at the edge of stability. It remains to be investigated if other solvatochromic fluorescent membrane probes like Prodan or Nile Red amongst others could reveal additional information about membrane stability or at least confirm the results obtained with laurdan.[443] The size and shape of the 6 sigmoidal LGP curvatures that were obtained depended mainly on the nature of the respective modifying lipid, with positively charged DOTAP destabilizing liposomes at slightly lower mole percentages than neutral DOPE and DODAP. However, for those six combinations, the LGP started to alter exponentially around 40 mol-% of modifying lipid content, indicating that around this point, the liposomal membranes were destabilized.

Cargo release and retention

The edge of membrane stability for five out of the six lipid compositions that showed a sigmoidal LGP curvature could be identified *via* a cargo release and retention assay using model cargo sulforhodamine b and semi-automated size exclusion chromatography by HPLC in addition to physicochemical characterizations conducted by dynamic light scattering. For four samples, the edge of stability, first defined by a minimum cargo release of 80% together with the highest cargo retention of the respective lipid composition, lied with 30 mol-% of modifying lipid within the 20-40 mol-% range previously proposed by the laurdan assay. However, one sample was out of range with 10 mol-% of modifying lipid, which was already partially indicated by a shift of the LGP curve to lower mol-% during the laurdan assay. The edge of stability for the last sample could not be identified within the used 10 mol-% steps, suggesting that a sigmoidal LGP curvature does not necessarily yield a lipid composition at the edge of stability. Additional evaluation of cargo encapsulation efficiency and liposomal physicochemical parameters supported the proposed edge of stability. Liposome modification with small amounts of CHEMS increased mandatory cargo retention to above 90% upon storage for three samples, while, in contrast to cholesterol, maintaining pH dependent cargo release above 50%. In comparison to the three final candidate liposomes, conventional liposomes showed a cargo release of only around 10% with comparable cargo retention, indicating that new candidate liposomes might have an enhanced capability of intracellularly releasing higher amounts of encapsulated drugs. Also, one lipid composition that could potentially be pursued in the future was identified as temperature-sensitive, a feature that might be of advantage for temperature-triggered cargo release.[390] Altogether, it can be said

that the developed method for determination of cargo encapsulation, release and retention *via* SEC by HPLC is suitable for high throughput and enabled the identification of the edge of stability for three liposomes, with the previously conducted laurdan assay as a first hint to narrow down the area of interest and therefore decrease the amount of necessary samples. Nonetheless, dynamic light scattering is also mandatory for stability measurements and to ensure pharmaceutical quality of resulting liposomes. As commendable notion, the proposed screening for cargo release and retention is only achievable after liposomal preparation by dual centrifugation or comparable methods which allow simultaneous preparation of a huge number of samples while most importantly providing high encapsulation efficiencies for hydrophilic cargo, an important pre-requisite to reliably quantify cargo release after the first purification step, which is not trivial due to high dilution. Of note, preliminary results indicated that the stability of the three identified liposomes in serum might be hampered, which would lead to a destabilization of the liposomes before they reach their designated target. Therefore, it would be of advantage to include stability measurements and cargo release and retention assays in human serum during the workflow in the future, since the serum proteins can alter liposomal membrane stability, as for example by exchange of phospholipids between liposomes and lipoproteins, and therefore also cargo release and retention properties.[329][444]

Intracellular drug delivery

First, a Resazurin assay revealed low toxicity of empty candidate liposomes L2c, L11c and L15c comparable to self-prepared conventional liposomes with a lipid composition of liposomes that are used in the clinic (Myocet®) after 72 hours for macrophages and melanoma cells. This suggests that candidate liposomes are suitable for application *in vivo*. Upon encapsulation of DXR, candidate liposomes showed toxicity comparable to free DXR after 24 and 72 hours, a first indication for increased capability of releasing cargo in comparison to CLs. However, there is still a need to find a lipid composition that shows even lower toxicity, to potentially decrease unwanted side effects. In addition, the overall DXR fluorescence after incubation of macrophages and melanoma cells with DXR loaded purified candidate liposomes and CLs for 0.5 and 4 hours was measured by flow cytometry. Low overall fluorescence signals for CLs indicated insufficient DXR release and were probably caused by quenching effects of DXR at high concentrations as present inside liposomes. In comparison to CLs, candidate liposomes showed three times higher fluorescence signals for macrophages and melanoma cells, even reaching the level of free DXR for the latter, indicating cargo release due to dequenching of the DXR fluorescence signal. Subsequent microscopy experiments enabled the quantification of released DXR present within cell nuclei by

counterstaining with Hoechst 33258. Results after 0.5 and 4 hours incubation indicated that candidate liposomes were around three times more effective in cargo release compared to CLs, even reaching the level of free DXR in melanoma cells and macrophages. Additionally, the observed extensive lateral diffusion of liposomal membrane dye DiD within the cellular plasma membrane after 24 hours indicated that lipid membranes of candidate liposomes became decomposed or permeable, an effect not visible for CLs. Results obtained from ImageStream® suggested an up to 10 times higher release capability of candidate liposomes in comparison to CLs after 0.5 and 4 hours incubation with melanoma cells and macrophages, although in contrast to microscopy and flow cytometry results, there was no difference in fluorescence intensities observable between the two cell types. To identify whether DXR was released by membrane disruption or diffusion, encapsulation of the pH-sensitive fluorophore 8-hydroxypyrene-1,3,6-trisulfonic acid (HPTS) [330] (Figure 50 A) into candidate liposomes could be a helpful tool. HPTS is membrane impermeable, so a HPTS release out of liposomes would suggest liposomal membrane disruption, while HPTS retention would indicate that DXR is rather released by diffusion due to an increased liposomal membrane permeability.[173][174] HPTS release and retention could be assessed by its strong pH-dependent fluorescence at 450 nm excitation wavelength, which would cause the fluorescence emission to decrease upon HPTS release in a cellular compartment with lower pH, as present in late endosomes and lysosomes.[446] A potential DXR release by diffusion was supported by steady physicochemical parameters of candidate liposomes prior and after incubation under release conditions during screening (see Figure 36, section 3.2.2). There is also a need to prove that liposomal cargo is retained within pH-sensitive candidate liposomes upon pH increase within late endosomes and/or lysosomes. This could be obtained by co-incubation of cells with (RS)-7-Chlor-4-(4-diethylamino-1-methylbutylamino)-chinolin (Chloroquine, Figure 50 B), a membrane permeable weak base usually used to treat malaria and rheumatic diseases that accumulates within acidic cellular compartments and consumes hydrogen ions due to its protonation, while potentially also inhibiting proteolytic enzymes, leading to an increase of pH.[447] However, it has to be taken into account that Chloroquine has been shown to inhibit pinocytosis [448], increases lysosomal membrane stability *in vitro* [449] while also leading to a swelling of lysosomes at high concentrations, which can decrease lysosomal mechanical stability [450]. Alternatively, ammonium chloride or Monensin [451] (Figure 50 C), a polyether antibiotic, could be used for intracellular alkalization or to collapse proton gradients. Ammonium chloride as lysosomotropic amine [447] and Monensin as proton ionophore both raise the pH of acidic intracellular organelles, and consequently the release from candidate liposomes should decrease. Of note, proton gradients and therefore the pH is quickly re-established upon removal of

ammonium chloride or Monensin, which could potentially enable the monitoring of release kinetics.
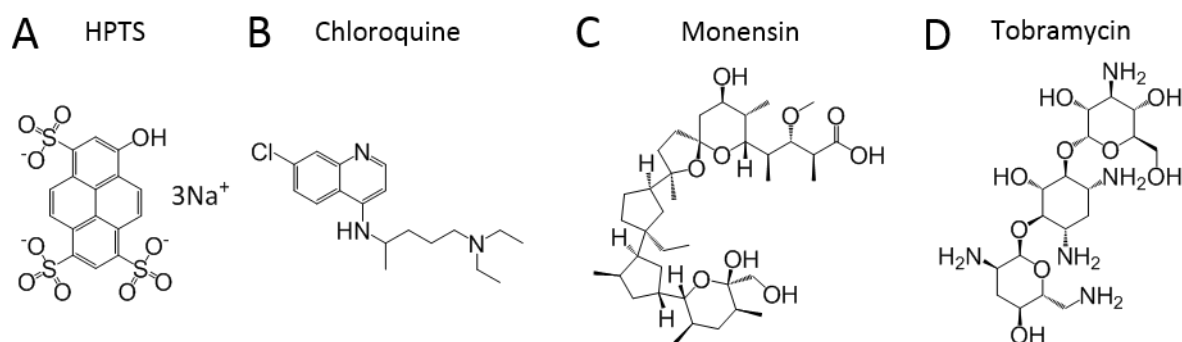
FIGURE 50: CHEMICAL STRUCUTRES OF (**A**) HPTS (8-HYDROXYPYRENE-1,3,6-TRISULFONIC ACID) (**B**) CHLOROQUINE ((*RS*)-7-CHLOR-4-(4-DIETHYLAMINO-1-METHYLBUTYLAMINO)-CHINOLIN), (**C**) MONENSIN AND (**D**) TOBRAMYCIN.

In vivo performance

Candidate pH-sensitive liposomes L2c, L11c and L15c in addition to conventional liposomes either empty or loaded with antibiotic ceftriaxone were injected into salmonella infected zebrafish embryos. The survival rate was monitored up to 48 hours post injection and revealed an increased ZFE survival for CEF loaded pH-sensitive candidate liposomes at the level of free CEF, while conventional liposomes showed a considerably lower survival rate. This suggests an increased cargo release capability of candidate liposomes over conventional liposomes, although they were not able to completely eradicate the infection. However, it remains unclear if the candidate liposomes released their cargo inside the blood stream, probably caused by liposomal membrane destabilization in the presence of serum proteins, or intracellularly. As mentioned earlier, this problem could be addressed already during screening by incubation of candidate liposomes with serum and subsequent quantification of cargo release and characterization of liposomal physicochemical parameters. Preliminary results for L15c suggested that around 20% of the cargo might already be released upon incubation with serum proteins, indicating that observed effects on survival might be caused by a combination of CEF release from the liposomes inside the bloodstream and intracellularly. Also, the aforementioned co-administration of compounds like Chloroquine could yield additional information. Empty candidate and conventional liposomes had no effect on the ZFE survival, indicating that candidate liposomes are as suitable for *in vivo* application as tested conventional liposomes, albeit differences in lipid composition. However, CEF might not be the optimal choice for treatment, since it is labile to hydrolysis and would therefore

require the use of freshly prepared and purified liposomes, a pre-requisite which is not always manageable. Therefore, other more storage stable antibiotics which can diffuse through a liposomal membrane upon its acidification are needed, with the additional requirement for simple quantification of encapsulation. Preliminary results encapsulating the more stable antibiotic aminoglycoside Tobramycin (Figure 50 D), quantified after modification with fluorescamine according to Tekkeli *et al.* [452], suggested however that it is less membrane permeable than ceftriaxone or probably remains trapped within endosomes/lysosomes and therefore the treatment of salmonella infected ZFEs was less successful than with free Tobramycin. Also, it has still to be evaluated if a combination of liposomal and free antibiotics can be of advantage.

pH-sensitive PEG

Cargo release properties of pH-sensitive candidate liposomes L2c, L11c and L15c modified with 5 mol-% PEG, *hb*PG and pH-sensitive ketal- and vinylether-PEG were evaluated by SEC and flow cytometry. SEC results revealed that conventional PEG and *hb*PG reduced liposomal cargo release most likely due to stabilization effects, whereas ketal- and vinylether-PEG shielded liposomes showed cargo release capabilities almost at the level of their unshielded counterparts. Flow cytometry results indicated that pH-sensitive candidate liposomes containing 5 mol-% of ketal- or vinylether-PEG were in average six times more effective in releasing encapsulated cargo as conventional PEGylated liposomes. Albeit differences in cleavage kinetics of the sole polymers, ketal- and vinylether-PEG led to comparable cargo release when formulated within liposomes, probably due to negatively charged lipid phosphates in close proximity to cleavage sites which might accelerate hydrolysis, an effect already observed for vinylether-PEG in literature.[453] However, cleavage kinetics for vinylether-PEG after formulation within candidate liposomes have still to be determined, as for example by click modification of respective modified PEG with fluorophores as conducted by Fritz *et al.* for ketal-PEG.[77] In conclusion, the synergy of shielding pH-sensitive liposomes with pH-sensitive PEG could be a powerful tool for further development, since it was shown that the pH-dependent cargo release could be maintained at a high level, while the PEG shield can potentially increase liposomal stability within the blood stream and upon storage and offers the possibility of active targeting. Besides presented pH-sensitive PEGs, other PEG modifications including pH-sensitive hydrazones [183][455] or (di)orthoesters [196], [197], [456] could also be tested in combination with candidate liposomes in the future. Of note, it remains unclear to what extent the cleaved PEG moieties can cause side effects, and that the size of the cleaved parts can be tuned by the relative amount of PEG incorporated 3,4-Epoxy-1-butene during synthesis to potentially reduce any unwanted issues.[354] All in all, pH-sensitive PEG has

the potential to avoid certain drawbacks associated with classical PEG, as reduced intracellular cargo release or decreased cellular uptake in tumor microenvironment.[457] However, only future *in vivo* experiments can demonstrate the potential and limitations of pH-sensitive shielding in combination with pH-sensitive candidate liposomes.

5. MATERIALS AND METHODS

5.1 MATERIALS

CARGO

Calcein	Merck KGaA (Germany)
Ceftriaxone	Merck KGaA
Doxorubicin (DXR)	Merck KGaA
Sulforhodamine b (SRb)	Merck KGaA
Tobramycin	Merck KGaA

BUFFERS & CHEMICALS

Accutase™ (StemPro, cell dissociation reagent)	Thermo-Fisher Scientific
Ammonium bicarbonate solution	Waters, USA
Biocoll	Merck KGaA
Chloroform	Merck KGaA (Sigma-Aldrich)
Dimethylsulfoxid (DMSO)	Carl Roth GmbH (Karlsruhe, Germany)
Dithiothreitol (DTT)	Merck KGaA (Sigma-Aldrich)
DMEM (Dulbeccos Modified Eagle Medium)	Gibco, USA
Dulbacco's Buffered Saline (DPBS)	Thermo-Fisher Scientific (Waltham, MA, USA)
Ethanol 99.5%	Carl Roth GmbH
Fetal bovine serum	Invitrogen, Germany
Fetal calf serum	Thermo-Fisher Scientific
Formic acetonitrile	Biosolve, Netherlands
Formic acid	Thermo-Fisher Scientific
Formic water	Biosolve, Netherlands
Glu-Fibrinopeptide	Merck KGaA (Sigma-Aldrich)
GlutaMAX™	Thermo-Fisher Scientific

Glutamin	Invitrogen
Hellmanex®	Hellma (Müllheim, Germany)
Hydrochloric acid (HCl)	VWR (Darmstadt, Germany) and Merck KGaA (Sigma-Aldrich)
Iodoacetamide	Merck KGaA (Sigma-Aldrich)
Leucine enkephalin	Merck KGaA (Sigma-Aldrich)
Methanol	Carl Roth GmbH
Milli-Q water	Merck Millipore
Nitrilgloves	Carl Roth GmbH
Paraformaldehyde	Carl Roth GmbH
PBS 10x pH 6.8	1.4 M NaCl, 80.6 mM Na_2HPO_4, 27 mM KCl, 15 mM KH_2PO_4 in H_2O
PBS pH 7.4	140 mM NaCl, 8.06 mM Na_2HPO_4 2.7 mM KCl, 1.5 mM KH_2PO_4 in H_2O (dilution of PBS 10x)
Penicillin	Invitrogen
Potassium Chloride (KCl)	Merck KGaA
Potassium dihydrogen phosphate (KH_2PO_4)	Carl Roth GmbH
Primocin™	InvivoGen
Release buffer pH 5.5	0.1 M Na_2HPO_4, 0.05 M citric acid, 7 mM KCl, 0.34 M NaCl in H_2O
Resazurin sodium salt	Merck KGaA
RPMI-1640 medium	Thermo-Fisher Scientific
Sephacryl S500-HR	GE Healthcare Life-Sciences
Sodium Chloride (NaCl)	Carl Roth GmbH
Streptomycin	Invitrogen
Trehalose	Thermo-Fisher Scientific
Trisodium phosphate (Na_3HPO_4)	Carl Roth GmbH
Triton-X 100 ™	Carl Roth GmbH
Trypsin	Gibco, Germany

Trypsin-EDTA	Thermo-Fisher Scientific
Uranyl acetate	Thermo-Fisher Scientific

DISPOSABLES AND GLASSWARE

8 well μ-slides	Ibidi
86-well PP plates, black	Greiner
96-well optical bottom plates, black	Greiner (Frickenhausen, Germany)
Disposable plastic macro cuvettes	Sarstedt
Filter top vacuum bottles, PES, pore: 0.2 μm, 500 mL	Sarsted
Folded capillary zeta cell	Malvern Panalytical
HPLC glass vials 1.5 mL	Thermo-Fisher Scientific
PCR vials for dual centrifugation, 200 μL	Biozym
Pipet tips, with filter, sterile RNase/DNase free	Starlab group
Reaction tube, 1.5 mL and 2.0 mL	Carl Roth GmbH
Screw cap vials, 0.65 mL and 2.0 mL	Carl Roth GmbH
Screw cap vials for dual centrifugation	Hettich GmbH, Germany
Serological pipett 10 mL / 25 mL	Sarstedt
SiLiBeads® ZY ceramic beads, 0.3 – 0.4 mm	Sigmund Lindner (Warmensteinach, Germany)
Suprasil® quartz glass cuvette, 1 cm	Hellma
Syringe filter units, cellulose, pore: 0.2 μm	Carl Roth GmbH

DYES

DAPI	Thermo-Fisher Scientific
DiD (1,1'-Dioctadecyl-3,3,3',3'-Tetramethylindo-dicarbocyanine, 4-Chlorobenzenesulfonate Salt)	Thermo-Fisher Scientific
DiO (3,3'-Dioctadecyloxacarbocyanine Perchlorate)	Thermo-Fisher Scientific
eFluor™	Thermo-Fisher Scientific
Hoechst 33285	PromoCell

Laurdan (1,1'-dioctadecyl-3,3,3',3'-tetramethylindo-
dicarbocyanine)   Thermo-Fisher Scientific

LIPIDS

Cholesterol   Carl Roth GmbH

EPC (egg phosphatidyl choline)   Lipoid

Following lipids were all acquired from Merck (former Sigma-Aldrich)

CHEMS (cholesterolhemisuccinate)

DMPC (1,2-dimyristoyl-sn-glycero-3-phosphocholine)

DODAP (1,2-dioleoyl-3-dimethylammonium-propane)

DOPC (1,2-dioleoyl-sn-glycero-3-phosphocholine)

DOPE (1,2-dioleoyl-sn-glycero-3-phosphoethanolamine

DOPG (1,2-dioleoyl-sn-glycero-3-phospho-rac-(1-gylcerol) sodium salt)

DOTAP (N-[1-(2,3-Dioleoyloxy)propyl]-N,N,N-trimethylammonium chloride)

DPPC (1,2-dipalmitoyl-sn-glycero-3-phosphocholine)

DPPG (1,2-dipalmitoyl-sn-glycero-3-phospho-(1'-rac-glycerol) sodium salt)

POLYMERIC AMPHIPHILES

All polymeric amphiphiles were synthesized as indicated by ████████████████

██████ and ███████████████ from the research group of Prof. Dr. Frey (Johannes Gutenberg-University, Duesbergweg 10-14, Mainz, Germany).

AD185 (Bisoctadecylglycerol-PEG-EPB (4.5 mol-% vinylether))   VE-PEG

MW94 (Bishexadecylglycerol-linPEG$_{61}$-OH)   PEG-S

MW170 (Bishexadecylglycerol-linPEG$_{113}$-OH)   PEG-M

MW191 (Bishexadecylglycerol-linPEG$_{160}$-OH)   PEG-L

MW201 (Bishexadecylglycerol-Ketal-linPEG$_{68}$-Alkin)   KETAL-PEG

UK338 (Bishexadecylglycerol-*hb*PG$_{35}$-OH)   *hb*PG-S

UK364 (Bishexadecylglycerol-*hb*PG$_{30}$-OH)   *hb*PG-S2

UK367 (Bishexadecylglycerol-hbPG$_{106}$-OH) hbPG-L

UK368 (Bishexadecylglycerol-hbPG$_{67}$-OH) hbPG-M

5.2 METHODS

LIPOSOME PREPARATION AND PROCESSING

LIPOSOME FORMULATION BY DUAL CENTRIFUGATION

First, the dissolved lipid components were combined in the respective mole percentage within a PCR tube and then pre-ried in a SpeedVac® vacuum centrifuge overnight. Afterwards, the pre-dried lipids were thoroughly dried for at least 3 hours using an Alpha 2-4 LD (Christ) lyophilization unit and then stored at -20 °C until usage. For dual centrifugation, 5 mmol of the dried lipids were incubated with 9.3 µL of hydrophilic cargo containing buffer for 10 min and then 350 mg ceramic beads (SiLiBeads®) were added. The stated buffer volume and beads weight scale linearly with the lipid amount. After dual centrifugation for 20 min at 2500 RPM and 25 °C using a Zentrimix 380R (Hettich GmbH, Germany), the resulting phospholipid gel was suspended in 77.2 µL DPBS and submitted to DC again for 2x2 min. Resulting liposome dispension was kept at 5 °C until usage.

LIPOSOME PURIFICATION

Preparative size exclusion chromatography was performed *via* an Agilent 1100 System (Agilent, Germany) to remove non-encapsulated cargo and free lipids from the nanocarrier solution. The liposome dispension was transferred from the PCR tubes to 1.5 mL HPLC glass vials with a 100 µL pipette with respective tip, which omits uptake of the small ceramic beads. The residue within the PCR tube was washed with 40 µL of DPBS to not lose any lipid material. Up to 100 µL of the liposome dispension as obtained after dual centrifugation and washing was injected into the HPLC system running with DPBS at a flowrate of 1 mL/min. A BioRad UNO Q1 column (BioRad, Munich, Germany) filled with 2 mL of slurry Sephacryl S500-HR thoroughly cleaned with DPBS was used for separation. A multiwavelength detector (G1365A Agilent 1100 Series, Germany) was used for detection of the absorption of cargos and labels like ceftriaxon at 254 nm, laurdan at 380 nm, calcein and DXR at 490 nm, DiI, SRb at 550 nm or DiD at 640 nm. An automated fraction collector collected the resulting purified liposome solution with a volume of 600 µL. The encapsulation efficiency was calculated by dividing the absorbance within the liposomal faction (L) by the total absorbance according to formula 14.

$$%EE=\frac{absorption\ L}{total\ absorption}\times100\%$$ (14)

The cargo release or retention was accordingly calculated as 100% minus the encapsulation efficiency (formula 15).

$$%release=100\%-\ %EE$$ (15)

LAURDAN ASSAY

A mixture of 2 mmol of total lipids containing 0.1 mol-% Laurdan was used for Laurdan screening experiments. 10 µL of obtained liposome stock dispersions were diluted with 50 µL DPBS 1x in a black 96-well polypropylene optical bottom plate (Greiner) and subjected to a M200 Pro multiplate reader (Tecan). The sample was excited at 350 nm and fluorescence emission intensities were obtained at 440 (I_{440}) and 490 nm (I_{490}). For calculation of the Laurdan generalized polarization value (LGP), formula 16 was used.

$$LGP=\frac{(I_{440}-I_{490})}{(I_{440}+I_{490})}$$ (16)

Values for LGP were plotted against the mole percentage of modifying lipid 2 using GraphPad Prism 7 (San Diego, USA). A sigmoidal 4PL fit with least squares method (formula 17) was applied.

$$y=bottom\ value+\frac{(top\ value-bottom\ value)}{(1+10^{((logEC50-x)*HillSlope)})}$$ (17)

The same formula was applied when LGP values were normalized to percentage of deviation from lipid 1, with the LGP value of lipid 1 set to 0% deviation, and the LGP value of liposomes containing 10 mol-% lipid 1 and 90 mol-% of lipid 2 to 100% deviation.

PROTEIN CORONA

In order to obtain liposome-protein complexes, liposomes were incubated in PBS containing 5 vol-% human blood plasma for 1 h at 37 °C under constant agitation. A Pierce 660 nm Protein Assay (Thermo-Fisher Scientific, Germany) was used for protein quantification according to the manufacturer's instruction.

ASYMMETRIC FLOW FIELD FLOW FRACTIONATION

For AF4, the postnova AF2000 system equipped with a TIP- and focus-pump, a fraction collector, an auto-samples, a degasser and a smart stream splitter was used. A regenerated cellulose membrane with a molecular cut-off of 10 kD, a 500 µm spacer and a stainless steel frit were equipped to the separation channel. A 1260 Infinity fluorescence detector (Agilent Technologies, USA) at 549 nm excitation and 565 nm emission and a UV detector (SPD-20A, Postnova, Germany) were used, and data was evaluated with the AF2000Control 2.0.8.0 (Postnova, Germany). Splitting of the channel flow resulted in a detector flow of 0.2 mL/min for the separation of 50 µL sample. For 7.2 min, the initial crossflow using PBS as carrier liquid was held at 1 mL/min, while it was exponentially decreased over 20 min afterwards to achieve a crossflow of 0.05 mL/min, which was kept for 7 min. Subsequently, the cross flow was exponentially lowered to 0 mL/min for elution of remaining components. Liposome containing fractions were collected by an automated fraction collector, dried using a SpeedVac® concentrator (Savant DNA120, Thermo-Fisher Scientific, USA) and resuspended in 350 µL PBS.

CENTRIFUGATION

50 µL of the liposome sample were subjected to centrifugation (Sigma 3-30k, Germany) at 20 000 g and 4 °C for 1 h to remove unbound proteins. The liposome pellet containing adsorbed proteins was resuspended in 1 mL PBS and washed three times by centrifugation as stated above. Finally, the liposomes were resuspended in 200 µL PBS, dried with a SpeedVac® and resuspended again to be comparable to the AF4 procedure.

ANALYTICS

DYNAMIC LIGHT SCATTERING

The size, polydispersity (PDI) and zeta-potential (ζ-potential) of 20 µL purified liposome samples were determined in a disposable folded capillary cell at 25 °C using a Malvern Zetasizer Nano series (UK). Liposome samples were diluted in 1 mL of freshly filtered 1 mM potassium chloride for analysis. The water viscosity was set to 0.8872 cP, with a refractive index of 1.33 (1.59 for liposomes) and a scattering angle of 173°.

IMAGE ANALYSIS

Images were analyzed using Fiji application. The integrated area density of the whole zebrafish embryo image or of the tail image was subtracted by the background, which was manually selected three times. Results shown were background corrected. Tail images were analyzed and cropped according to Sieber *et al.*[280] In detail, compartments A, B, C and E were individually selected for each image, and the mean fluorescence in each compartment was measured (Figure 51). Compartments A refer to liposomes in circulation, B refer to background fluorescence, C to liposomes in CHT (caudal hematopoietic tissue) and E to extravasated liposomes outside vasculature.

scale bars: 100 µm
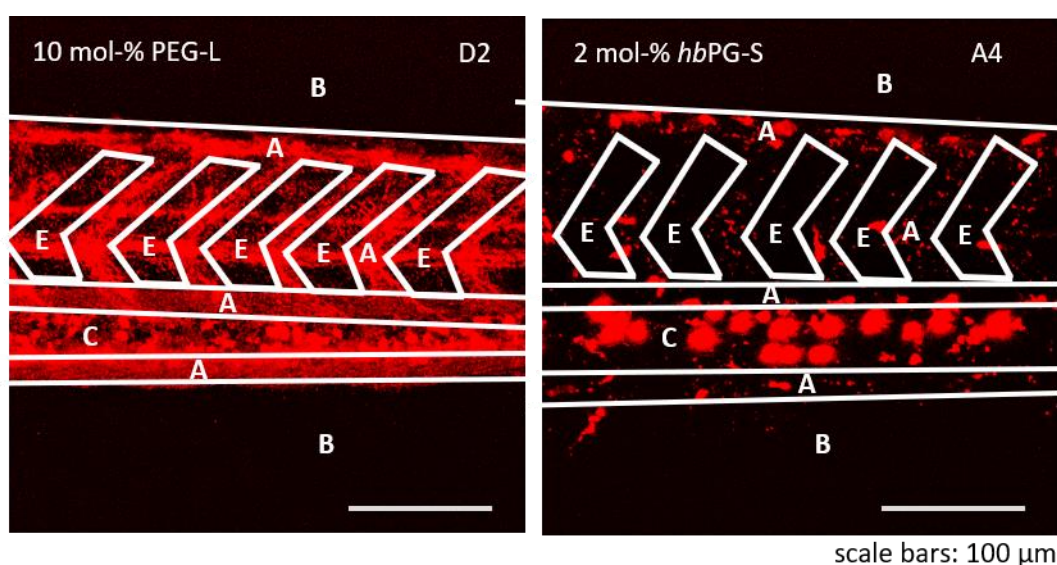
FIGURE 51: ZEBRAFISH EMBRYO TAIL IMAGES RECORDED BY CLSM AFTER 24 H INCUBATION WITH LIPOSOMES (RED) CONTAINING 10 MOL-% PEG-L (LEFT) OR 2 MOL-% HBPG-S (RIGHT). COMPARTMENTS A (LIPOSOMES IN CIRCULATION), B (BACKGROUND), C (LIPOSOMES IN CAUDAL HEMATOPOIETIC TISSUE) AND E (EXTRAVASATED LIPOSOMES) WERE INDICIDUALLY SELECTED FOR EACH IMAGE AND FLUORESCENCE INTENSITIES WERE QUANTIFIED USING APPLICATION FIJI.

LIQUID CHROMATOGRAPHY – MASS SPECTROMETRY (LC-MS) FOR PROTEIN ANALYSIS

Proteins were first precipitated using a Proteo Extract protein precipitation kit (Merck KgaA, Germany) and then resuspended with 0.1% RapiGest SF (50 mM ammonium bicarbonate solution, Waters, USA) and incubated for 15 min at 80 °C, as already described in [360][372][373]. 15 mM Iodoacetamide and 5 mM DTT (both Merck KGaA) were added to the protein solution for 1 h and 45 min at 56 °C, respectively. Protein digestion was performed using trypsin in a 1:50 ratio to proteins and stopped on the next day using 2 µL HCl (Merck KGaA). For absolute quantification, resulting peptide samples were diluted with 0.1% formic acid and 50 fmol/µL Hi3 e.coli standard (Waters, USA). For proteomics, the Synapt G2 Si mass spectrometer was coupled to NanoACQUITY

with an analytical reversed-phase C18 column (1.7 µm, 75 µm x 150 mm, Waters, USA) and a nanoACQUITY C18 trap column (5 µm, 180 µm x 20 mm, Waters, USA). The mobile phase at a flow rate of 0.3 µL/min consisted of water (A) and acetonitrile (B) each containing 0.1 vol-% formic acid. A constant gradient starting from 98% A and 2% B and ending at 60% A and 40% B was applied. As reference, Glu-Fibrinopeptide and Leucine Enkephaline (both Merck KGaA) were infused at a flow rate of 0.5 µL/min. A NanoLockSpray in positive ion mode was used for electrospray ionization, and data-independent acquisition (MSe) experiments were carried out. The Protenesis QI software enabled identification of proteins and peptides, which were searched against a human reviewed database from Uniprot, spiked with the sequence of Hi3 e.coli standard and porcine trypsin, resulting in final protein amounts.[458] Relative protein amounts derive from the total amount of identified proteins.

NANOPARTICLE TRACKING ANALYSIS

A Malvern NanoSight LM10 (Malvern Panalytical, Kassel, Germany) with a sCMOS camera and a 532 nm laser was used for nanoparticle tracking analysis of purified liposome samples. Typically, 100 µL of the sample prepared for dynamic light scattering analysis was further diluted in PBS by the factor of 10. The sample was subjected to the analysis chamber *via* a 1 mL syringe. Instrument settings were adjusted as follows: camera level: 12, gain: 300, measurements per sample: 3, duration: 60 seconds, temperature: 25 °C.

TRANMISSION ELECTRON MICROSCOPY

Corresponding liposome samples with a volume of 2 µL were placed and embedded in 1 wt-% trehalose with 4 wt-% uranyl acetate on a lacey grid. A FEI Tecnai F20 transmission electron microscope was used for measurement at a working voltage of 200 kV. The electron micrographs were taken by an Ultrascan 1000 (Gatan) charged-coupled device (CCD) camera, while the Digital Mictrograph software (Gatan) collected the images.

For cyro-TEM, 5 µL of a liposome sample was vitrified with a Vitrobot™ (FEI) plunging device. The sample was applied to a holey carbon coated TEM grid and immediately plunged into liquid ethane. For the measurement using the FEI Tecnai F20 TEM, cryogenic conditions were ensured using a Gatan 926 cryo TEM holder. Imaging was again performed at an acceleration voltage of 200 kV and resulting micrographs were captured by the Ultrascan 1000 (Gatan) CCD camera.

***In vitro* AND *IN VIVO* EXPERIMENTS**

HUMAN MACROPHAGE CULTURE

Buffy coats obtained from healthy volunteers with approval by the local ethical committee (Landesaerztekammer Rhineland-Palatinate) enabled the isolation of human peripheral blood mononuclear cells (PBMCs) *via* Biocoll (Merck KgAA Germany) density gradient centrifugation. Monocytes were extracted by plastic adherence. Cells were harvested using Accutase™ (Thermo-Fisher Scientific) after cell growth for six days in RPMI-1640 (Merck KGaA Germany) supplemented with 1 vol-% human plasma, Primocin™ (InvivoGen), 50 ng/mL human M-CSF (Immunotools) and GlutaMAX™ (Thermo-Fisher Scientific).

MELANOMA CELL LINE UKRV-MEL-15a

UKRV-Mel-15a cell line deriving human melanoma cells were grown in RPMI-1640 medium supplemented with 10 vol-% fetal calf serum (FCS, Thermo Fisher Scientific), GlutaMAX™ (Thermo-Fisher Scientific) and Primocin™ (InvivoGen). Cells were harvested using a Trypsin-EDTA solution (Thermo-Fisher Scientific).

RAW264.7 CELLS

Cells were obtained from ATCC® TIB-71™ (UK), cultured in DMEM supplemented with 10 vol-% fetal bovine serum (FBS), 100 mg/mL streptomycin, 100 U/mL penicillin and 2 mM glutamine. Cells were seeded out in 24-well plates with 100 000 cells per well in culture medium after having reached 80% confluency. The medium was exchanged to serum-free DMEM after 24 hours, and liposomes were added to achieve final concentrations of 7.5 µg/mL. Flow cytometry analysis was performed using a Attune NxT flow cytometer (Thermo-Fisher, USA) at stated time points after detachment of cells using 2.5 vol-% trypsin (Gibco, Germany).

HUMAN BLOOD PLASMA

Ten healthy donors provided human blood plasma according to standard guidelines at the transfusion center of the university clinic Mainz, Germany. The plasma was pooled and stored at -20 °C until usage. Directly before usage, the plasma was centrifuged (Sigma 3-30K, Germany) at 20 000 g and 4 °C for 1 h in order to remove debris.

FLOW CYTOMETRY

Human melanoma cells (UKRV-Mel-15a) and human macrophages were seeded in 24-well plates containing 1 mL culture medium and $5 \cdot 10^4$ cells or $2.5 \cdot 10^5$ cells per well, respectively. Cells were harvested after incubation with the liposome samples at stated time points using Accutase™, while dead cells were excluded using fixable viability dye eFluor™ 780 (Thermo-Fisher Scientific). Cells were fixed by incubation for 30 min with DPBS containing 4 vol-% paraformaldehyde. A LSRII cytometer (BD Biosciences, USA) and Cytobank were used for flow cytometry and data analysis, respectively.[459]

CELL VIABILITY ASSAY (RESAZURIN)

Human melanoma cells (UKRV-Mel-15a) and human macrophages were seeded in 96-well plates containing 0.2 mL culture medium and $1 \cdot 10^4$ cells or $5 \cdot 10^4$ cells per well, respectively. After incubation with liposome samples for 24 or 72 hours, Resazurin sodium salt dissolved in DPBS was added to achieve a final concentration of 6 μg/mL. After incubation for 1 hour at 37 °C, a Sense Beta Plus Microplate Reader (Hidex) was used for fluorescence measurements at 544 nm excitation and 590 nm emission wavelengths.

CONFOCAL MICROSCOPY

For cargo release experiments, human melanoma cells (UKRV-Mel-15a) and human macrophages were seeded in 8-well μ-slides (Ibidi, Germany) containing 0.3 mL culture medium and $1.5 \cdot 10^4$ cells or $7.5 \cdot 10^4$ cells per well, respectively. After incubation with liposome samples, cells were washed and fixed by 30 min incubation with DPBS containing 4 vol-% paraformaldehyde. Cell nuclei were stained using 10 μM Hoechst 33258 dissolved in DPBS, and cell membranes were stained using the green-fluorescent cytoplasmic membrane staining kit (PromoCell). A Leica TCS SP8 confocal microscope acquired the images, which were analyzed using the Fiji application.[460]

For protein corona experiments, murine macrophages (RAW264.7) were seeded in 8-well μ-slides (Ibidi, Germany) containing 0.3 mL culture medium and $5 \cdot 10^4$ cells per well. Prior incubation with liposomes for 2 or 24 h, cells were washed with PBS and kept in DMEM without serum for 2 hours. After stated time points, cells were washed and fixed by 15 min incubation with PBS containing 4 vol-% Roti-Histofix (Carl Roth GmbH, Germany). Cell membranes were stained using CellMask™ Deep red (Thermo-Fisher Scientific) diluted 1:5000 in PBS. A Leica TCS SP5 II confocal microscope with a HC PL APO CS 63x/1.4 oil objective in a serial scan mode acquired the images, which were captured using the LAS AF 3000 software. Cell membranes were pseudo-colored in red and liposomes were pseudo-colored in green.

LIPOSOME CARGO QUANITIFCATION

In order to quantify liposomal DXR content by absorption and external calibration, a part of the liposome dispersions was transferred to a 96-well plate and cracked by adding PBS containing 5 vol-% of Triton-X100 ™ (Carl Roth GmbH). DXR absorbance was then measured at 488 nm using a Sense Beta Plus Microplate Reader (Hidex).

ZEBRAFISH

Normal and transgenic zebrafish embryos (ZFE) expressing a green fluorescent protein in their macrophages (*Tg(mpeg1:Gal4;UAS:KAEDE)*) or vasculature (*kdrl:EGFPs843*) were raised at 28 °C in zebrafish culture media and treated with 1-phenyl-2-thiourea (PTU) to avoid pigment cell formation as already described previously.[461] All zebrafish experiments were performed in accordance with Swiss animal welfare regulations. At 2 days post fertilization (dpf), ZFE were anesthetized using tricaine and immobilized in agarose (0.3% w/v). Via the duct of Cuvier, immobilized ZFE (approx. 20 ZFE per treatment) were intravenously injected directly into blood circulation with 1 nL of respective liposomes for biodistribution and blood circulation studies or 300 colony forming units (CFU) of mCherry expressing salmonella (SDB15) for survival studies. Salmonella infected ZFE were kept at 35 °C for 15 min in order to allow salmonella distribution throughout the whole ZFE. Afterwards, 3 nL of ceftriaxone loaded liposomes, empty liposomes, free ceftriaxone, or DPBS as a negative control were injected *via* the same route. ceftriaxone loaded liposomes and free Ceftriaxone were injected at concentrations of 200 µg/mL ceftriaxone. Infected and successfully injected ZFE were removed from agarose and kept at 35 °C in zebrafish culture media. After indicated time points, ZFE survival was determined based on the presence of heartbeat. In addition, confocal images were taken in order to analyze biodistribution of liposomes and salmonella. All microinjections were performed using a micromanipulator (Wagner Instrumentenbau KG, Schöffengrund, Germany), a pneumatic Pico Pump PV830 (WPI, Sarasota, Florida), and a Leica S8APO microscope (Leica, Wetzlar, Germany). Confocal images were taken using a Leica SP5-II-Matrix point scanning confocal microscope equipped with a 40x HCXPlanApo (NA 1.10) objective.

REFERENCES

[1]   L. Sercombe, T. Veerati, F. Moheimani, S. Y. Wu, A. K. Sood, and S. Hua, "Advances and challenges of liposome assisted drug delivery," *Front. Pharmacol.*, vol. 6, no. DEC, pp. 1–13, 2015.

[2]   R. M. Mozafari, "LIPOSOMES: AN OVERVIEW OF MANUFACTURING TECHNIQUES," *Cell. Mol. Biol. Lett.*, vol. 10, pp. 711–719, 2005.

[3]   E. H. L. Martínez-balbuena and I. Santamaría-holek, "Thermodynamics and dynamics of the formation of spherical lipid vesicles," pp. 297–308, 2009.

[4]   C. Tanford, "The hydrophobic effect and the organization of living matter," *Science (80-.).*, vol. 200, no. 4345, pp. 1012–1018, 1978.

[5]   D. Chandler, "Interfaces and the driving force of hydrophobic assembly," *Nature*, vol. 437, pp. 640–647, 2005.

[6]   A. S. Ulrich, "Biophysical aspects of using liposomes as delivery vehicles," *Biosci. Rep.*, vol. 22, no. 2, pp. 129–150, 2002.

[7]   N. Monteiro, A. Martins, R. L. Reis, and N. M. Neves, "Liposomes in tissue engineering and regenerative medicine," *MicroRNA Regen. Med.*, pp. 1159–1200, 2014.

[8]   B. Sen Ding, T. Dziubla, V. V. Shuvaev, S. Muro, and V. R. Muzykantov, "Advanced drug delivery systems that target the vascular endothelium," *Mol. Interv.*, vol. 6, no. 2, pp. 98–112, 2006.

[9]   S. Hua and S. Y. Wu, "The use of lipid-based nanocarriers for targeted pain therapies," *Front. Pharmacol.*, vol. 4 NOV, no. November, pp. 1–7, 2013.

[10]   A. Jain and S. K. Jain, "Stimuli-responsive Smart Liposomes in Cancer Targeting," *Curr. Drug Targets*, vol. 19, no. 3, pp. 259–270, 2018.

[11]   V. Deepthi and A. Kavitha, "Liposomal drug delivery systems - A review," *Int. J. Pharm. Sci. Rev. Res.*, vol. 23, no. 1, pp. 295–301, 2013.

[12]   Maria Laura Immordino, Franco Dosio, and Luigi Cattel, "Stealth liposomes: review of the basic science, rationale, and clinical applications, existing and potential," *Int. J. Nanomedicine*, vol. 1, no. 3, pp. 297–315, 2006.

[13]   A. D. Bangham and R. W. Horne, "Negative staining of phospholipids and their structural modification by surface-active agents as observed in the electron microscope," *J. Mol. Biol.*, vol. 8, no. 5, pp. 660–668, 1964.

[14]   A. D. Bangham, M. M. Standish, and J. C. Watkins, "Diffusion of Univalent Ions across the Lamellae of Swollen Phospholipids," *J. Mol. Biol.*, vol. 13, no. 1, pp. 238–252, IN26-IN27, 1965.

[15]   G. Bozzuto and A. Molinari, "Liposomes as nanomedical devices," *Int. J. Nanomedicine*, vol. 10, pp. 975–999, 2015.

[16]   D. C. Drummond, O. Meyer, K. Hong, D. B. Kirpotin, and D. Papahadjopoulos, "Optimizing liposomes for delivery of chemotherapeutic agents to solid tumors.," *Pharmacol. Rev.*, vol. 51, no. 4, pp. 691–743, 1999.

[17]   V. P. Torchilin, F. Zhou, and L. Huang, "pH-Sensitive Liposomes," *J. Liposome Res.*, vol. 2104, no. 3(2), pp. 201–255, 1993.

[18]   V. P. Torchilin, "Immunoliposomes and PEGylated Immunoliposomes: Possible use for Targeted Delivery of Imaging Agents." Immunomethods, pp. 244–258, 1994.

[19]   H. Faneca *et al.*, "Cationic liposomes for gene delivery," *Expert Opin. Drug Deliv.*, vol. 2, no. 2, pp. 237–254, 2005.

[20]   A. Samad, Y. Sultana, and M. Aqil, "Liposomal Drug Delivery Systems: An Update Review," *Curr. Drug Deliv.*, vol. 4, pp. 297–305, 2007.

[21]   U. Bulbake, S. Doppalapudi, N. Kommineni, and W. Khan, "Liposomal Formulations in Clinical Use : An Updated Review," *Pharmaceutics*, vol. 9, no. 12, pp. 1–33, 2017.

[22]   C. Zheng, C. Ma, E. Bai, K. Yang, and R. Xu, "Transferrin and cell-penetrating peptide dual-functioned liposome for targeted drug delivery to glioma," *Int. J. Clin. Exp. Med.*, vol. 8, no. 2, pp. 1658–1668, 2015.

[23]   N. Duzgunes, C. T. de Ilarduya, S. Simoes, R. I. Zhdanov, and K. K. and M. C. P. de Lima, "Cationic Liposomes for Gene Delivery: Novel Cationic Lipids and Enhancement by Proteins and Peptides," *Current Medicinal Chemistry*, vol. 10, no. 14. pp. 1213–1220, 2003.

[24]   D. Papahadjopoulos, "Phospholipid model membranes," *Biochim. Biophys. Acta*, vol. 135, pp. 639–652, 1967.

[25]   J. N. Israelachvili, S. Marcelja, and R. G. Horn, "Physical principles of membrane organization," *Q. Rev. Biophys.*, vol. 13, pp. 121–200, 1980.

[26]   R. N. A. H. Lewis and R. N. McElhaney, "Membrane lipid phase transitions and phase organization studied by Fourier transform infrared spectroscopy," *Biochim. Biophys. Acta - Biomembr.*, vol. 1828, no. 10, pp. 2347–2358, 2013.

[27]   T. P. Begley, R. Koynova, and B. Tenchov, "Lipids: Phase Transitions," *Wiley Encycl. Chem. Biol.*, 2008.

[28]   J. F. Nagle, "Lipid Bilayer Phase Transition," *Ann. Rev. Phys. Chem*, vol. 31, pp. 157–195, 1980.

[29]   O. G. Mouritsen and K. Jørgensen, "Dynamical order and disorder in lipid bilayers," *Chem. Phys. Lipids*, vol. 73, no. 1–2, pp. 3–25, 1994.

[30]   S. Raffy and J. Teissié, "Control of lipid membrane stability by cholesterol content," *Biophys. J.*, vol. 76, no. 4, pp. 2072–2080, 1999.

[31]   G. M'Baye, Y. Mély, G. Duportail, and A. S. Klymchenko, "Liquid ordered and gel phases of lipid bilayers: Fluorescent probes reveal close fluidity but different hydration," *Biophys. J.*, vol. 95, no. 3, pp. 1217–1225, 2008.

[32]   L. P. Tseng, H. J. Liang, T. W. Chung, Y. Y. Huang, and D. Z. Liu, "Liposomes incorporated with cholesterol for drug release triggered by magnetic field," *J. Med. Biol. Eng.*, vol. 27, no. 1, pp. 29–34, 2007.

[33]   T. J. McIntosh, "The effect of cholesterol on the structure of phosphatidylcholine bilayers," *BBA - Biomembr.*, vol. 513, no. 1, pp. 43–58, 1978.

[34]   K. Simons and E. Ikonen, "Functional rafts in cell membranes," *Nature*, vol. 387, no. 6633, pp. 569–572, 1997.

[35]   S. Krasnici *et al.*, "Effect of the surface charge of liposomes on their uptake by angiogenic tumor vessels," *Int. J. Cancer*, vol. 105, no. 4, pp. 561–567, 2003.

[36]   S. Tristram-Nagle and J. F. Nagle, "Lipid bilayers: Thermodynamics, structure, fluctuations, and interactions," *Chem. Phys. Lipids*, vol. 127, no. 1, pp. 3–14, 2004.

[37]   D. J. Mitchell and B. W. Ninham, "Micelles, vesicles and microemulsions," *J. Chem. Soc. Faraday Trans. 2 Mol. Chem. Phys.*, vol. 77, no. 4, pp. 601–629, 1981.

[38]   L. Rilfors and G. Lindblom, "Regulation of lipid composition in biological membranes - Biophysical studies of lipids and lipid synthesizing enzymes," *Colloids Surfaces B Biointerfaces*, vol. 26, no. 1–2, pp. 112–124, 2002.

[39]   R. Koynova and R. C. MacDonald, "Natural lipid extracts and biomembrane-mimicking lipid compositions are disposed to form nonlamellar phases, and they release DNA from lipoplexes most efficiently,"

Biochim. Biophys. Acta - Biomembr., vol. 1768, no. 10, pp. 2373–2382, 2007.

[40]   T. Parasassi, G. De Stasio, G. Ravagnan, R. M. Rusch, and E. Gratton, "Quantitation of lipid phases in phospholipid vesicles by the generalized polarization of Laurdan fluorescence," *Biophys. J.*, 1991.

[41]   T. Parasassi, G. De Stasio, A. d'Ubaldo, and E. Gratton, "Phase fluctuation in phospholipid membranes revealed by Laurdan fluorescence," *Biophys. J.*, vol. 57, no. 6, pp. 1179–1186, 1990.

[42]   B. M. Harrison, D. Tomlinson, and S. Stewart, "Liposomal-Entrapped Doxorubicin : An Active Agent in AIDS-Related Kaposi ' s Sarcoma," vol. 13, no. 4, pp. 914–920, 2019.

[43]   U. Pick, "Liposomes with a large trapping capacity prepared by freezing and thawing of sonicated phospholipid mixtures," *Arch. Biochem. Biophys.*, vol. 212, no. 1, pp. 186–194, 1981.

[44]   C. H. Huang, "Studies on Phosphatidylcholine Vesicles. Formation and Physical Characteristics," *Biochemistry*, vol. 8, no. 1, pp. 344–352, 1969.

[45]   F. Olson, C. A. Hunt, F. C. Szoka, W. J. Vail, and D. Papahadjopoulos, "Preparation of liposomes by defined size distribution by extrusion through polycarbonate membranes," *Biochim. Biophys. Acta*, vol. 557, pp. 9–23, 1979.

[46]   N. Sharma and S. Verma, "Current and future prospective of liposomes as drug delivery vehicles for the effective treatment of cancer," *Int. J. Green Pharm.*, vol. 11, no. 3, pp. S377–S384, 2017.

[47]   V. Nele, M. N. Holme, U. Kauscher, M. R. Thomas, J. J. Doutch, and M. M. Stevens, "Effect of Formulation Method, Lipid Composition, and PEGylation on Vesicle Lamellarity: A Small-Angle Neutron Scattering Study," *Langmuir*, vol. 35, no. 18, pp. 6064–6074, 2019.

[48]   E. Mayhew, R. Lazo, W. J. Vail, J. King, and A. M. Green, "Characterization of liposomes prepared using a microemulsifier," *BBA - Biomembr.*, vol. 775, no. 2, pp. 169–174, 1984.

[49]   M. Brandl, M. Drechsler, D. Bachmann, C. Tardi, M. Schmidtgen, and K. H. Bauer, "Preparation and characterization of semi-solid phospholipid dispersions and dilutions thereof," *Int. J. Pharm.*, vol. 170, no. 2, pp. 187–199, 1998.

[50]   M. Brandl, D. Bachmann, M. Drechsler, and K. H. Bauer, "Liposome preparation by a new high pressure homogenizer gaulin micron lab 40," *Drug Dev. Ind. Pharm.*, vol. 16, no. 14, pp. 2167–2191, 1990.

[51]   R. Barnadas-Rodríguez and M. Sabés, "Factors involved in the production of liposomes with a high-pressure homogenizer," *Int. J. Pharm.*, vol. 213, no. 1–2, pp. 175–186, 2001.

[52]   S. Vemuri and C. T. Rhodes, "Preparation and characterization of liposomes as therapeutic delivery systems: a review," *Pharm. Acta Helv.*, vol. 70, no. 2, pp. 95–111, 1995.

[53]   R. Cortesi, E. Esposito, S. Gambarin, P. Telloli, E. Menegatti, and C. Nastruzzi, "Preparation of liposomes by reverse-phase evaporation using alternative organic solvents," *J. Microencapsul.*, vol. 16, no. 2, pp. 251–256, 1999.

[54]   A. Wagner *et al.*, "GMP production of liposomes - A new industrial approach," *J. Liposome Res.*, vol. 16, no. 3, pp. 311–319, 2006.

[55]   A. Wagner, K. Vorauer-Uhl, G. Kreismayr, and H. Katinger, "The crossflow injection technique: An improvement of the ethanol injection method," *J. Liposome Res.*, vol. 12, no. 3, pp. 259–270, 2002.

[56]   A. Wagner, K. Vorauer-Uhl, and H. Katinger, "Liposomes produced in a pilot scale: Production, purification and efficiency aspects," *Eur. J. Pharm. Biopharm.*, vol. 54, no. 2, pp. 213–219, 2002.

[57]   F. Szoka and D. Papahadjopoulos, "Procedure for preparation of liposomes with large internal aqueous space and high capture by reverse-phase evaporation," *Proc. Natl. Acad. Sci. U. S. A.*, vol. 75, no. 9, pp. 4194–4198, 1978.

[58]   P. W. Holloway, "A simple procedure for removal of triton X-100 from protein samples," *Anal. Biochem.*, vol. 53, no. 1, pp. 304–308, 1973.

[59]   M. H. W. Milsmann, R. A. Schwendener, and H. G. Weder, "The preparation of large single bilayer liposomes by a fast and controlled dialysis," *BBA - Biomembr.*, vol. 512, no. 1, pp. 147–155, 1978.

[60]   J. Brunner, P. Skrabal, and H. Hausser, "Single bilayer vesicles prepared without sonication physico-chemical properties," *BBA - Biomembr.*, vol. 455, no. 2, pp. 322–331, 1976.

[61]   J.-L. Rigaud, D. Levy, G. Mosser, and O. Lambert, "Detergent removal by non-polar polystyrene beads," *Eur. Biophys. J.*, vol. 27, no. 4, pp. 305–319, 1998.

[62]   T. D. Madden *et al.*, "The accumulation of drugs within large unilamellar vesicles exhibiting a proton gradient: a survey," *Chem. Phys. Lipids*, vol. 53, no. 1, pp. 37–46, 1990.

[63]   A. Vigevani and M. J. Williamson, "Doxorubicin," *Anal. Profiles Drug Subst.*, vol. 9, pp. 246–274, 1980.

[64]   U. Massing, S. Cicko, and V. Ziroli, "Dual asymmetric centrifugation (DAC)-A new technique for liposome preparation," *J. Control. Release*, vol. 125, no. 1, pp. 16–24, 2008.

[65]   U. Massing, S. G. Ingebrigtsen, N. Škalko-basnet, and A. M. Holsæter, "Dual Centrifugation - A Novel ' in-vial ' Liposome Processing Technique," *Intech*, pp. 3–28, 2017.

[66]   M. Brandl, "Vesicular phospholipid gels," in *Liposomes: Methods and Protocols, Volume 1: Pharmaceutical Nanocarriers*, V. Weissig, Ed. New York, 2010, pp. 205–212.

[67]   M. Hirsch, V. Ziroli, M. Helm, and U. Massing, "Preparation of small amounts of sterile siRNA-liposomes with high entrapping efficiency by dual asymmetric centrifugation (DAC)," *J. Control. Release*, vol. 135, no. 1, pp. 80–88, 2009.

[68]   J. Parmentier *et al.*, "Improved Oral Bioavailability of Human Growth Hormone by a Combination of Liposomes Containing Bio-Enhancers and Tetraether Lipids and Omeprazole," *J. Pharm. Sci.*, vol. 103, no. 12, pp. 3985–3993, 2014.

[69]   H. Pohlit, I. Bellinghausen, M. Schömer, B. Heydenreich, J. Saloga, and H. Frey, "Biodegradable pH-Sensitive Poly(ethylene glycol) Nanocarriers for Allergen Encapsulation and Controlled Release," *Biomacromolecules*, vol. 16, no. 10, pp. 3103–3111, 2015.

[70]   A. Raynor *et al.*, "Saturated and mono-unsaturated lysophosphatidylcholine metabolism in tumour cells: A potential therapeutic target for preventing metastases," *Lipids Health Dis.*, vol. 14, no. 1, pp. 1–15, 2015.

[71]   J. E. Adrian, A. Wolf, A. Steinbach, J. Rössler, and R. Süss, "Targeted delivery to neuroblastoma of novel siRNA-anti-GD2-liposomes prepared by dual asymmetric centrifugation and sterol-based post-insertion Method," *Pharm. Res.*, vol. 28, no. 9, pp. 2261–2272, 2011.

[72]   S. Meier *et al.*, "Immuno-magnetoliposomes targeting activated platelets as a potentially human-compatible MRI contrast agent for targeting atherothrombosis," *Biomaterials*, vol. 53, pp. 137–148, 2015.

[73]   S. G. Ingebrigtsen, N. Škalko-Basnet, and A. M. Holsæter, "Development and optimization of a new processing approach for manufacturing topical liposomes-in-hydrogel drug formulations by dual asymmetric centrifugation," *Drug Dev. Ind. Pharm.*, vol. 42, no. 9, pp. 1375–1383, 2016.

[74]   S. G. Ingebrigtsen, N. Škalko-Basnet, C. de Albuquerque Cavalcanti Jacobsen, and A. M. Holsæter, "Successful co-encapsulation of benzoyl peroxide and chloramphenicol in liposomes by a novel manufacturing method - dual asymmetric centrifugation," *Eur. J. Pharm. Sci.*, vol. 97, pp. 192–199, 2017.

[75]   R. Tremmel *et al.*, "Delivery of Copper-chelating Trientine (TETA) to the central nervous system by surface modified liposomes," *Int. J. Pharm.*, vol. 512, no. 1, pp. 87–95, 2016.

[76]   S. F. Pantze, J. Parmentier, G. Hofhaus, and G. Fricker, "Matrix liposomes: A solid liposomal formulation for oral administration," *Eur. J. Lipid Sci. Technol.*, vol. 116, no. 9, pp. 1145–1154, 2014.

[77]   T. Fritz, "Multifunctional liposomes: Microscale formulation, modification and in vitro interaction," *PhD Thesis*, 2016.

[78]   B. Weber *et al.*, "PeptoSomes for Vaccination: Combining Antigen and Adjuvant in Polypept(o)ide-Based Polymersomes," *Macromol. Biosci.*, vol. 17, no. 10, pp. 1–6, 2017.

[79]   M. Scherer *et al.*, "Pentafluorophenyl Ester-based Polymersomes as Nanosized Drug-Delivery Vehicles," *Macromol. Rapid Commun.*, vol. 37, no. 1, pp. 60–66, 2016.

[80]   D. Baczynska, K. Widerak, M. Ugorski, and M. Langner, "Surface charge and the association of liposomes with colon carcinoma cells," *Zeitschrift für Naturforsch. - Sect. C J. Biosci.*, vol. 56, no. 9–10, pp. 872–877, 2001.

[81]   M. Winterhalter and D. D. Lasic, "Liposome stability and formation: Experimental parameters and theories on the size distribution," *Chem. Phys. Lipids*, vol. 64, no. 1–3, pp. 35–43, 1993.

[82]   P. Blasi, S. Giovagnoli, A. Schoubben, M. Ricci, and C. Rossi, "Solid lipid nanoparticles for targeted brain drug delivery," *Adv. Drug Deliv. Rev.*, vol. 59, no. 6, pp. 454–477, 2007.

[83]   M. Danaei *et al.*, "Impact of Particle Size and Polydispersity Index on the Clinical Applications of Lipidic Nanocarrier Systems," *Pharmaceutics*, vol. 10, no. 57, pp. 1–17, 2018.

[84]   F. C. Szoka, D. Milholland, and M. Barza, "Effect of lipid composition and liposome size on toxicity and in vitro fungicidal activity of liposome-intercalated amphotericin B," *Antimicrob. Agents Chemother.*, vol. 31, no. 3, pp. 421–429, 1987.

[85]   L. A. S. Bahari and H. Hamishehkar, "The impact of variables on particle size of solid lipid nanoparticles and nanostructured lipid carriers; A comparative literature review," *Adv. Pharm. Bull.*, vol. 6, no. 2, pp. 143–151, 2016.

[86]   R. Pecora, "Dynamic Light Scattering Measurement of Nanometer Particles in Liquids," *J. Nanoparticle Res.*, vol. 2, pp. 123–131, 2000.

[87]   M. Instruments, "Inform White Paper: Dynamic Light Scattering, Common terms defined.," *Malvern Guid.*, pp. 1–6, 2011.

[88]   S. U. Egelhaaf, E. Wehrli, M. Müller, M. Adrian, and P. Schurtenberger, "Determination of the size distribution of lecithin liposomes: A comparative study using freeze fracture, cryoelectron microscopy and dynamic light scattering," *J. Microsc.*, vol. 184, no. 3, pp. 214–228, 1996.

[89]   V. Filipe, A. Hawe, and W. Jiskoot, "Critical evaluation of nanoparticle tracking analysis (NTA) by NanoSight for the measurement of nanoparticles and protein aggregates," *Pharm. Res.*, vol. 27, no. 5, pp. 796–810, 2010.

[90]   J. A. Gallego-Urrea, J. Tuoriniemi, and M. Hassellöv, "Applications of particle-tracking analysis to the determination of size distributions and concentrations of nanoparticles in environmental, biological and food samples," *TrAC - Trends Anal. Chem.*, vol. 30, no. 3, pp. 473–483, 2011.

[91]   B. Carr and M. Wright, "NanoParticle Tracking Analysis," *NanoSight Ltd*, vol. 44, no. 0, pp. 1–193, 2010.

[92]   H. Zhang and D. Lyden, "Asymmetric-flow field-flow fractionation technology for exomere and small extracellular vesicle separation and characterization," *Nat. Protoc.*, vol. 14, no. 4, pp. 1027–1053, 2019.

[93]   W. Fraunhofer and G. Winter, "The use of asymmetrical flow field-flow fractionation in pharmaceutics and biopharmaceutics," *Eur. J. Pharm. Biopharm.*, vol. 58, no. 2, pp. 369–383, 2004.

[94]   H. K. Shon, S. H. Kim, L. Erdei, and S. Vigneswaran, "Analytical methods of size distribution for organic matter in water and wastewater," *Korean J. Chem. Eng.*, vol. 23, no. 4, pp. 581–591, 2006.

[95]   M. N. Myers, "Overview of Field-Flow Fractionation," *J Micro Sep*, vol. 9, pp. 151–162, 1997.

[96]   R. F. Domingos *et al.*, "Characterizing manufactured nanoparticles in the environment: Multimethod determination of particle sizes," *Environ. Sci. Technol.*, vol. 43, no. 19, pp. 7277–7284, 2009.

[97]   J. A. Zasadzinski, L. E. Scriven, and H. T. Davis, "Liposome Structure and Defects.," *Philos. Mag. A Phys. Condens. Matter, Struct. Defects Mech. Prop.*, vol. 51, no. 2, pp. 287–302, 1985.

[98]   J. Robin Harris, W. Gebauer, and J. Markl, "Keyhole limpet haemocyanin: negative staining in the presence of trehalose," *Micron*, vol. 26, no. 1, pp. 25–33, 1995.

[99]   M. Nakakoshi, H. Nishioka, and E. Katayama, "New versatile staining reagents for biological transmission electron microscopy that substitute for uranyl acetate," *J. Electron Microsc. (Tokyo).*, vol. 60, no. 6, pp. 401–407, 2011.

[100]   S. De Carlo and J. R. Harris, "Negative staining and cryo-negative staining of macromolecules and viruses for TEM," *Micron*, vol. 42, no. 2, pp. 117–131, 2011.

[101]   J. Dubochet *et al.*, "Cryo-electron microscopy of vitrified specimens," *Q. Rev. Biophys.*, vol. 21, no. 2, pp. 129–228, 1988.

[102]   M. Almgren, K. Edwards, and G. Karlsson, "Cryo transmission electron microscopy of liposomes and related structures," *Colloids Surfaces A Physicochem. Eng. Asp.*, vol. 174, no. 1–2, pp. 3–21, 2000.

[103]   Y. Talmon, "Transmission electron microscopy of complex fluids: The state of the art," *Ber. Bunsenges. Phys. Chem*, vol. 100, no. 3, pp. 364–372, 1996.

[104]   S. Bhattacharjee, "DLS and zeta potential - What they are and what they are not?," *J. Control. Release*, vol. 235, pp. 337–351, 2016.

[105]   F. J. Montes Ruiz-Cabello, G. Trefalt, P. Maroni, and M. Borkovec, "Electric double-layer potentials and surface regulation properties measured by colloidal-probe atomic force microscopy," *Phys. Rev. E*, vol. 90, no. 1, pp. 1–10, 2014.

[106]   F. J. Vidal-Iglesias, J. Solla-Gullón, A. Rodes, E. Herrero, and A. Aldaz, "Understanding the Nernst equation and other electrochemical concepts: An easy experimental approach for students," *J. Chem. Educ.*, vol. 89, no. 7, pp. 936–939, 2012.

[107]   P. Panwar, B. Pandey, P. C. Lakhera, and K. P. Singh, "Study of Albendazole-Encapsulated Nanosize Liposomes," *Int. J. Nanomedicine*, vol. 5, pp. 101–108, 2010.

[108]   G. Taylor, "Drug entrapment and release from multilamelar RPE liposomes," *Int. J. Pharm.*, vol. 58, pp. 49–55, 1990.

[109]   S. Y. Hwang, H. K. Kim, J. Choo, G. H. Seong, T. B. D. Hien, and E. K. Lee, "Effects of operating parameters on the efficiency of liposomal encapsulation of enzymes," *Colloids Surfaces B Biointerfaces*, vol. 94, pp. 296–303, 2012.

[110]   J. A. Allen Zhang and J. Pawelchak, "Effect of pH, ionic strength and oxygen burden on the chemical stability of EPC/cholesterol liposomes under accelerated conditions. Part 1: Lipid hydrolysis," *Eur. J. Pharm. Biopharm.*, vol. 50, no. 3, pp. 357–364, 2000.

[111]   P. Milla, F. Dosio, and L. Cattel, "PEGylation of Proteins and Liposomes: a Powerful and Flexible Strategy to Improve the Drug Delivery," *Curr. Drug Metab.*, vol. 13, no. 1, pp. 105–119, 2011.

[112]   G. L. Scherphof, J. Dijkstra, H. H. Spanjer, J. T. P. Derksen, and F. H. Roerdink, "Uptake and Intracellular Processing of Targeted and Nontargeted Liposomes by Rat Kupffer Cells In Vivo and In Vitro," *Ann. N. Y. Acad. Sci.*, vol. 446, no. 1, pp. 368–384, 1985.

[113]   X. Yan, G. L. Scherphof, and J. A. A. M. Kamps, "Liposome opsonization," *J. Liposome Res.*, vol. 15, no. 1–2, pp. 109–139, 2005.

[114] A. Chonn, S. C. Semple, and P. R. Cullis, "β2-Glycoprotein i is a major protein associated with very rapidly cleared liposomes in vivo, suggesting a significant role in the immune clearance of 'non-self' particles," *J. Biol. Chem.*, vol. 270, no. 43, pp. 25845–25849, 1995.

[115] H. Harashima, K. Sakata, K. Funato, and H. Kiwada, "Enhanced Hepatic Uptake of Liposomes Through Complement Activation Depending on the Size of Liposomes," *Pharmaceutical Research: An Official Journal of the American Association of Pharmaceutical Scientists*, vol. 11, no. 3. pp. 402–406, 1994.

[116] T. Ishida, H. Harashima, and H. Kiwada, "Liposome clearance," *Biosci. Rep.*, vol. 22, no. 2, pp. 197–224, 2002.

[117] D. D. Lasic and D. Needham, "The 'Stealth' Liposome: A Prototypical Biomaterial," *Chem. Rev.*, vol. 95, no. 8, pp. 2601–2628, 1995.

[118] R. Zeisig, K. Shimada, S. Hirota, and D. Arndt, "Effect of sterical stabilization on macrophage uptake in vitro and on thickness of the fixed aqueous layer of liposomes made from alkylphosphocholines," *Biochim. Biophys. Acta - Biomembr.*, vol. 1285, no. 2, pp. 237–245, 1996.

[119] T. M. Allen and A. Chonn, "Large unilamellar liposomes with low uptake into the reticuloendothelial system," *FEBS Lett.*, vol. 223, no. 1, pp. 42–46, 1987.

[120] D. D. Lasic, F. J. Martin, A. Gabizon, S. K. Huang, and D. Papahadjopoulos, "Sterically stabilized liposomes: a hypothesis on the molecular origin of the extended circulation times," *BBA - Biomembr.*, vol. 1070, no. 1, pp. 187–192, 1991.

[121] M. C. Woodle, M. S. Newman, and J. A. Cohen, "Sterically stabilized liposomes: Physical and biological properties," *J. Drug Target.*, vol. 2, no. 5, pp. 397–403, 1994.

[122] O. K. Nag and V. Awasthi, "Surface engineering of liposomes for stealth behavior," *Pharmaceutics*, vol. 5, no. 4, pp. 542–569, 2013.

[123] E. Nogueira *et al.*, "Liposome and protein based stealth nanoparticles," *Faraday Discuss.*, vol. 166, pp. 417–429, 2013.

[124] D. Liu, A. Mori, and L. Huang, "Role of liposome size and RES blockade in controlling biodistribution and tumor uptake of GM1-containing liposomes," *BBA - Biomembr.*, vol. 1104, no. 1, pp. 95–101, 1992.

[125] H. Yamauchi *et al.*, "Effects of sialic acid derivative on long circulation time and tumor concentration of liposomes," *Int. J. Pharm.*, vol. 113, no. 2, pp. 141–148, 1995.

[126] M. C. Taira, N. S. Chiaramoni, K. M. Pecuch, and S. Alonso-Romanowski, "Stability of Liposomal Formulations in Physiological Conditions for Oral Drug Delivery," *Drug Deliv. J. Deliv. Target. Ther. Agents*, vol. 11, no. 2, pp. 123–128, 2004.

[127] M. Mora, M. L. Sagristá, D. Trombetta, F. P. Bonina, A. De Pasquale, and A. Saija, "Design and characterization of liposomes containing long-chain N-acylPEs for brain delivery: Penetration of liposomes incorporating GM1 into the rat brain," *Pharm. Res.*, vol. 19, no. 10, pp. 1430–1438, 2002.

[128] G. Powell, *Handbook of water-soluble gums and resins*. New York: MCGraw-Hill, 1980.

[129] C. Dingels, M. Schömer, and H. Frey, "Die vielen Gesichter des Poly(ethylenglykol)s: Von der Kosmetik zum Ionenleiter," *Chemie Unserer Zeit*, vol. 45, no. 5, pp. 338–349, 2011.

[130] S. Dreborg and E. B. Akerblom, "Immunotherapy with monomethoxypolyethylene glycol modified allergens," *Crit. Rev. Ther. Drug Carrier Syst.*, vol. 6, no. 4, p. 315—365, 1990.

[131] T. Yamaoka, Y. Tabata, and Y. Ikada, "Distribution and tissue uptake of poly(ethylene glycol) with different molecular weights after intravenous administration to mice," *J. Pharm. Sci.*, vol. 83, no. 4, pp. 601–606, 1994.

[132] T. M. Allen, C. Hansen, F. Martin, C. Redemann, and A. Yau-Young, "Liposomes containing synthetic lipid

derivatives of poly(ethylene glycol) show prolonged circulation half-lives in vivo," *BBA - Biomembr.*, vol. 1066, no. 1, pp. 29–36, 1991.

[133] C. Allen *et al.*, "Controlling the physical behavior and biological performance of liposome formulations through use of surface grafted poly(ethylene glycol)," *Biosci. Rep.*, vol. 22, no. 2, pp. 225–250, 2002.

[134] P. Caliceti and F. M. Veronese, "Pharmacokinetic and biodistribution properties of poly(ethylene glycol)-protein conjugates," *Adv. Drug Deliv. Rev.*, vol. 55, no. 10, pp. 1261–1277, 2003.

[135] G. Blume and G. Cevc, "Liposomes for the sustained drug release in vivo," *BBA - Biomembr.*, vol. 1029, no. 1, pp. 91–97, 1990.

[136] M. Vert and D. Domurado, "Poly(ethylene glycol): Protein-repulsive or albumin-compatible?," *J. Biomater. Sci. Polym. Ed.*, vol. 11, no. 12, pp. 1307–1317, 2000.

[137] S. M. Moghimi, I. S. Muir, L. Illum, S. S. Davis, and V. Kolb-Bachofen, "Coating particles with a block co-polymer (poloxamine-908) suppresses opsonization but permits the activity of dysopsonins in the serum," *BBA - Mol. Cell Res.*, vol. 1179, no. 2, pp. 157–165, 1993.

[138] S. A. Johnstone, D. Masin, L. Mayer, and M. B. Bally, "Surface-associated serum proteins inhibit the uptake of phosphatidylserine and poly(ethylene glycol) liposomes by mouse macrophages," *Biochim. Biophys. Acta - Biomembr.*, vol. 1513, no. 1, pp. 25–37, 2001.

[139] D. Needham, T. J. McIntosh, and D. D. Lasic, "Repulsive interactions and mechanical stability of polymer-grafted lipid membranes," *BBA - Biomembr.*, vol. 1108, no. 1, pp. 40–48, 1992.

[140] V. P. Torchilin *et al.*, "Poly(ethylene glycol) on the liposome surface: on the mechanism of polymer-coated liposome longevity," *BBA - Biomembr.*, vol. 1195, no. 1, pp. 11–20, 1994.

[141] P. G. de Gennes, "Conformations of Polymers Attached to an Interface," *Macromolecules*, vol. 13, no. 5, pp. 1069–1075, 1980.

[142] Q. Yang, S. W. Jones, C. L. Parker, W. C. Zamboni, J. E. Bear, and S. K. Lai, "Evading immune cell uptake and clearance requires PEG grafting at densities substantially exceeding the minimum for brush conformation," *Mol. Pharm.*, vol. 11, no. 4, pp. 1250–1258, 2014.

[143] H. Lee and R. G. Larson, "Adsorption of Plasma Proteins onto PEGylated Lipid Bilayers: The Effect of PEG Size and Grafting Density," *Biomacromolecules*, vol. 17, no. 5, pp. 1757–1765, 2016.

[144] Y. Matsumura and H. Maeda, "A New Concept for Macromolecular Therapeutics in Cancer Chemotherapy: Mechanism of Tumoritropic Accumulation of Proteins and the Antitumor Agent Smancs," *Cancer Res.*, vol. 46, no. 8, pp. 6387–6392, 1986.

[145] J. Fang, H. Nakamura, and H. Maeda, "The EPR effect: Unique features of tumor blood vessels for drug delivery, factors involved, and limitations and augmentation of the effect," *Adv. Drug Deliv. Rev.*, vol. 63, no. 3, pp. 136–151, 2011.

[146] H. Maeda, "The enhanced permeability and retention (EPR) effect in tumor vasculature: The key role of tumor-selective macromolecular drug targeting," *Adv. Enzyme Regul.*, vol. 41, no. 1, pp. 189–207, 2001.

[147] V. Torchilin, "Tumor delivery of macromolecular drugs based on the EPR effect," *Adv. Drug Deliv. Rev.*, vol. 63, no. 3, pp. 131–135, 2011.

[148] H. Maeda, G. Y. Bharate, and J. Daruwalla, "Polymeric drugs for efficient tumor-targeted drug delivery based on EPR-effect," *Eur. J. Pharm. Biopharm.*, vol. 71, no. 3, pp. 409–419, 2009.

[149] A. K. Iyer, G. Khaled, J. Fang, and H. Maeda, "Exploiting the enhanced permeability and retention effect for tumor targeting," *Drug Discov. Today*, vol. 11, no. 17–18, pp. 812–818, 2006.

[150] Y. Lee and D. H. Thompson, "Stimuli-responsive liposomes for drug delivery," *Wiley Interdiscip. Rev. Nanomedicine Nanobiotechnology*, vol. 9, no. 5, pp. 1–40, 2017.

[151] F. M. Muggia, "Liposomal encapsulated anthracyclines: new therapeutic horizons.," *Curr. Oncol. Rep.*, vol. 3, no. 2, pp. 156–162, 2001.

[152] B. W. Neun, Y. Barenholz, J. Szebeni, and M. A. Dobrovolskaia, "Understanding the Role of Anti-PEG Antibodies in the Complement Activation by Doxil in Vitro," *Molecules*, vol. 23, no. 7, 2018.

[153] E. T. M. Dams *et al.*, "Accelerated blood clearance and altered biodistribution of repeated injections of sterically stabilized liposomes," *J. Pharmacol. Exp. Ther.*, vol. 292, no. 3, pp. 1071–1079, 2000.

[154] T. Ishida and H. Kiwada, "Accelerated blood clearance of pegylated liposomes after repeated injection," *Drug Deliv. Syst.*, vol. 19, no. 6, pp. 495–510, 2004.

[155] H. Hatakeyama, H. Akita, and H. Harashima, "Polyethyleneglycol : A Classical but Innovative Material The Polyethyleneglycol Dilemma : Advantage and Disadvantage of PEGylation of Liposomes for Systemic Genes and Nucleic Acids Delivery to Tumors," *Biol. Pharm. Bull.*, vol. 36, no. 6, pp. 892–899, 2013.

[156] H. Hatakeyama, H. Akita, and H. Harashima, "A multifunctional envelope type nano device (MEND) for gene delivery to tumours based on the EPR effect: A strategy for overcoming the PEG dilemma," *Adv. Drug Deliv. Rev.*, vol. 63, no. 3, pp. 152–160, 2011.

[157] M. Riaz *et al.*, "Surface Functionalization and Targeting Strategies of Liposomes in Solid Tumor Therapy: A Review," *Int. J. Mol. Sci.*, vol. 19, no. 1, p. 195, 2018.

[158] S. B. Lim, A. Banerjee, and H. Önyüksel, "Improvement of drug safety by the use of lipid-based nanocarriers," *J. Control. Release*, vol. 163, no. 1, pp. 34–45, 2012.

[159] P. S. Uster, T. M. Allen, B. E. Daniel, C. J. Mendez, M. S. Newman, and G. Z. Zhu, "Insertion of poly(ethylene glycol) derivatized phospholipid into pre-formed liposomes results in prolonged in vivo circulation time," *FEBS Lett.*, vol. 386, no. 2–3, pp. 243–246, 1996.

[160] T. M. Allen, P. Sapra, and E. Moase, "Use of the post-insertion method for the formation of ligand-coupled liposomes," *Cell. Mol. Biol. Lett.*, vol. 7, no. 3, p. 889—894, 2002.

[161] V. P. Torchilin, "Recent Approaches To Intracellular Delivery of Drugs and Dna and Organelle Targeting," *Annu. Rev. Biomed. Eng.*, vol. 8, no. 1, pp. 343–375, 2006.

[162] J. M. Saul, A. Annapragada, J. V. Natarajan, and R. V. Bellamkonda, "Controlled targeting of liposomal doxorubicin via the folate receptor in vitro," *J. Control. Release*, vol. 92, no. 1–2, pp. 49–67, 2003.

[163] T. D. Heath, D. Robertson, M. S. C. Birbeck, and A. J. S. Davies, "Covalent attachment of horseradish peroxidase to the outer surface of liposomes," *BBA - Biomembr.*, vol. 599, no. 1, pp. 42–62, 1980.

[164] T. Takizawa, K. Maruyama, and M. Iwaturu, "Stealth immunoliposome : Novel immunoliposomes modified with amphipathic polyethyleneglycols conjugated at their distal terminals to monoclonal antibodies," *Drug Deliv. Syst.*, vol. 10, no. 3, pp. 167–173, 1995.

[165] H. C. Kolb, M. G. Finn, and K. B. Sharpless, "Click Chemistry: Diverse Chemical Function from a Few Good Reactions," *Angew. Chemie - Int. Ed.*, vol. 40, no. 11, pp. 2004–2021, 2001.

[166] V. V. Rostovtsev, L. G. Green, V. V. Fokin, and K. B. Sharpless, "A stepwise huisgen cycloaddition process: Copper(I)-catalyzed regioselective 'ligation' of azides and terminal alkynes," *Angew. Chemie - Int. Ed.*, vol. 41, no. 14, pp. 2596–2599, 2002.

[167] T. Fritz *et al.*, "Orthogonal Click Conjugation to the Liposomal Surface Reveals the Stability of the Lipid Anchorage as Crucial for Targeting," *Chem. Eur. J.*, vol. 22, no. 33, pp. 1–6, 2016.

[168] Y. D. P. Limasale, A. Tezcaner, C. Özen, D. Keskin, and S. Banerjee, "Epidermal growth factor receptor-targeted immunoliposomes for delivery of celecoxib to cancer cells," *Int. J. Pharm.*, vol. 479, no. 2, pp. 364–373, 2015.

[169] C. Mamot *et al.*, "Epidermal growth factor receptor-targeted immunoliposomes significantly enhance the

efficacy of multiple anticancer drugs in vivo," *Cancer Res.*, vol. 65, no. 24, pp. 11631–11638, 2005.

[170] Y. K. Lee *et al.*, "Inhibition of pulmonary cancer progression by epidermal growth factor receptor-targeted transfection with Bcl-2 and survivin siRNAs," *Cancer Gene Ther.*, vol. 22, no. 7, pp. 335–343, 2015.

[171] P. S. Low, W. A. Henne, and D. D. Doorneweerd, "Discovery and development of folic-acid-based receptor targeting for imaging and therapy of cancer and inflammatory diseases," *Acc. Chem. Res.*, vol. 41, no. 1, pp. 120–129, 2008.

[172] X. M. Li, L. Y. Ding, Y. Xu, Y. Wang, and Q. N. Ping, "Targeted delivery of doxorubicin using stealth liposomes modified with transferrin," *Int. J. Pharm.*, vol. 373, no. 1–2, pp. 116–123, 2009.

[173] T. M. Allen and P. R. Cullis, "Liposomal drug delivery systems: From concept to clinical applications," *Adv. Drug Deliv. Rev.*, vol. 65, no. 1, pp. 36–48, 2013.

[174] M. Kapoor, S. L. Lee, and K. M. Tyner, "Liposomal Drug Product Development and Quality : Current US Experience and Perspective," *AAPS J.*, no. 6, 2017.

[175] K. Knop, R. Hoogenboom, D. Fischer, and U. S. Schubert, "Poly(ethylene glycol) in drug delivery: Pros and cons as well as potential alternatives," *Angew. Chemie - Int. Ed.*, vol. 49, no. 36, pp. 6288–6308, 2010.

[176] V. P. Torchilin, M. I. Shtilman, V. S. Trubetskoy, K. Whiteman, and A. M. Milstein, "Amphiphilic vinyl polymers effectively prolong liposome circulation time in vivo," *BBA - Biomembr.*, vol. 1195, no. 1, pp. 181–184, 1994.

[177] V. P. Torchilin, V. S. Trubetskoy, K. R. Whiteman, P. Caliceti, P. Ferruti, and F. M. Veronese, "New Synthetic Amphiphilic Polymers for Steric Protection of Liposomes in Vivo," *J. Pharm. Sci.*, vol. 84, no. 9, p. 139, 1995.

[178] V. P. Torchilin *et al.*, "Amphiphilic poly-N-vinylpyrrolidones: synthesis, properties and liposome surface modi"cation," *Biomaterials*, vol. 22, no. 22, pp. 3035–3044, 2001.

[179] H. Takeuchi, H. Kojima, H. Yamamoto, and Y. Kawashima, "Evaluation of circulation profiles of liposomes coated with hydrophilic polymers having different molecular weights in rats," *J. Control. Release*, vol. 75, no. 1–2, pp. 83–91, 2001.

[180] M. C. Woodle, C. M. Engbers, and S. Zalipsky, "New Amphipatic Polymer—Lipid Conjugates Forming Long-Circulating Reticuloendothelial System-Evading Liposomes," *Bioconjug. Chem.*, vol. 5, no. 6, pp. 493–496, 1994.

[181] K. Maruyama, S. Okuizumi, O. Ishida, H. Yamauchi, H. Kikuchi, and M. Iwatsuru, "Phosphatidyl polyglycerols prolong liposome circulation in vivo," *Int. J. Pharm.*, vol. 111, no. 1, pp. 103–107, 1994.

[182] K. R. Whiteman, V. Subr, K. Ulbrich, and V. P. Torchilin, "Poly(HPMA)-coated liposomes demonstrate prolonged circulation in mice," *J. Liposome Res.*, vol. 11, no. 2–3, pp. 153–164, 2001.

[183] D. Wilms, S. E. Stiriba, and H. Frey, "Hyperbranched polyglycerols: From the controlled synthesis of biocompatible polyether polyols to multipurpose applications," *Acc. Chem. Res.*, vol. 43, no. 1, pp. 129–141, 2010.

[184] A. M. Hofmann, F. Wurm, E. Huhn, T. Nawroth, P. Langguth, and H. Frey, "Hyperbranched polyglycerol-based lipids via oxyanionic polymerization: Toward multifunctional stealth liposomes," *Biomacromolecules*, vol. 11, no. 3, pp. 568–574, 2010.

[185] K. Mohr *et al.*, "Evaluation of Multifunctional Liposomes in Human Blood Serum by Light Scattering," *Langmuir*, 2014.

[186] K. Wagener *et al.*, "Comparison of Linear and Hyperbranched Polyether Lipids for Liposome Shielding by 18F-Radiolabeling and Positron Emission Tomography," *Biomacromolecules*, vol. 19, no. 7, pp. 2506–2516, 2018.

[187]   A. S. Abu Lila, K. Nawata, T. Shimizu, T. Ishida, and H. Kiwada, "Use of polyglycerol (PG), instead of polyethylene glycol (PEG), prevents induction of the accelerated blood clearance phenomenon against long-circulating liposomes upon repeated administration.," *Int. J. Pharm.*, vol. 456, no. 1, pp. 235–242, 2013.

[188]   J. B. Massey, "Effect of cholesteryl hemisuccinate on the interfacial properties of phosphatidylcholine bilayers," *Biochim. Biophys. Acta - Biomembr.*, vol. 1415, no. 1, pp. 193–204, 1998.

[189]   M. B. Yatvin, W. Kreutz, B. Horwitz, and M. Shinitzky, "Induced drug release from lipid vesicles in serum by pH-change," *Biophys. Struct. Mech.*, vol. 6, no. 3, pp. 233–234, 1980.

[190]   D. Dumas, S. Muller, F. Gouin, F. Baros, M. L. Viriot, and J. F. Stoltz, "Membrane fluidity and oxygen diffusion in cholesterol-enriched erythrocyte membrane," *Arch. Biochem. Biophys.*, vol. 341, no. 1, pp. 34–39, 1997.

[191]   M. Z. Lai, N. Diizgune, and F. C. Szoka, "Effects of Replacement of the Hydroxyl Group of Cholesterol and Tocopherol on the Thermotropic Behavior of Phospholipid Membranes," *Biochemistry*, vol. 24, no. 7, pp. 1646–1653, 1985.

[192]   J. J. Sudimack, W. Guo, W. Tjarks, and R. J. Lee, "A novel pH-sensitive liposome formulation containing oleyl alcohol," *Biochim. Biophys. Acta*, vol. 1564, pp. 31–37, 2002.

[193]   D. C. F. Soares, M. C. De Oliveira, A. L. B. De Barros, V. N. Cardoso, and G. A. Ramaldes, "Liposomes radiolabeled with 159Gd: In vitro antitumoral activity, biodistribution study and scintigraphic image in Ehrlich tumor bearing mice," *Eur. J. Pharm. Sci.*, vol. 43, no. 4, pp. 290–296, 2011.

[194]   E. Fleige, M. A. Quadir, and R. Haag, "Stimuli-responsive polymeric nanocarriers for the controlled transport of active compounds: Concepts and applications," *Adv. Drug Deliv. Rev.*, vol. 64, no. 9, pp. 866–884, 2012.

[195]   P. L. Yeagle, *The Membranes of Cells*, Third Edit. 2016.

[196]   C. Masson *et al.*, "pH-Sensitive PEG lipids containing orthoester linkers: New potential tools for nonviral gene delivery," *J. Control. Release*, vol. 99, no. 3, pp. 423–434, 2004.

[197]   W. Li, Z. Huang, J. A. MacKay, S. Grube, and F. C. Szoka, "Low-pH-sensitive poly(ethylene glycol) (PEG)-stabilized plasmid nanolipoparticles: Effects of PEG chain length, lipid composition and assembly conditions on gene delivery," *J. Gene Med.*, vol. 7, no. 1, pp. 67–79, 2005.

[198]   S. S. Müller, T. Fritz, M. Gimnich, M. Worm, M. Helm, and H. Frey, "Biodegradable hyperbranched polyether-lipids with in-chain pH-sensitive linkages," *Polym. Chem.*, vol. 7, no. 40, pp. 6257–6268, 2016.

[199]   A.-K. Danner, "Multifunctional Amphiphilic Polyethers : From Polyether Lipids to Tapered Structures," *PhD Thesis*, p. 111, 2018.

[200]   J. Shin, P. Shum, and D. H. Thompson, "Acid-triggered release via dePEGylation of DOPE liposomes containing acid-labile vinyl ether PEG-lipids," *J. Control. Release*, vol. 91, no. 1–2, pp. 187–200, 2003.

[201]   D. C. Drummond, C. O. Noble, M. E. Hayes, J. W. Park, and D. B. Kirpotin, "Pharmacokinetics and in vivo drug release rates in liposomal nanocarrier development," *J. Pharm. Sci.*, vol. 97, no. 11, pp. 4696–4740, 2008.

[202]   A. Partanen *et al.*, "Mild hyperthermia with magnetic resonance-guided high-intensity focused ultrasound for applications in drug delivery," *Int. J. Hyperth.*, vol. 28, no. 4, pp. 320–336, 2012.

[203]   M. S. Kim *et al.*, "Temperature-triggered tumor-specific delivery of anticancer agents by cRGD-conjugated thermosensitive liposomes," *Colloids Surfaces B Biointerfaces*, vol. 116, pp. 17–25, 2014.

[204]   S. Ibsen, M. Benchimol, D. Simberg, and S. Esener, "Ultrasound mediated localized drug delivery," *Adv. Exp. Med. Biol.*, vol. 733, p. 145—153, 2012.

[205] S. Sirsi and M. Borden, "Microbubble Compositions, Properties and Biomedical Applications," *Bubble Sci Eng Technol.*, vol. 1, no. 1–2, pp. 3–17, 2009.

[206] S. E. Ahmed, A. M. Martins, and G. A. Husseini, "The use of ultrasound to release chemotherapeutic drugs from micelles and liposomes," *J. Drug Target.*, vol. 23, no. 1, pp. 16–42, 2015.

[207] C. Y. Lin, M. Javadi, D. M. Belnap, J. R. Barrow, and W. G. Pitt, "Ultrasound sensitive eLiposomes containing doxorubicin for drug targeting therapy," *Nanomedicine Nanotechnology, Biol. Med.*, vol. 10, no. 1, pp. 67–76, 2014.

[208] H. Fu *et al.*, "Tumor-targeted paclitaxel delivery and enhanced penetration using TAT-decorated liposomes comprising redox-responsive poly(ethylene glycol)," *J. Pharm. Sci.*, vol. 104, no. 3, pp. 1160–1173, 2015.

[209] D. S. Conceição, D. P. Ferreira, and L. F. Vieira Ferreira, "Photochemistry and cytotoxicity evaluation of heptamethinecyanine near infrared (NIR) dyes," *Int. J. Mol. Sci.*, vol. 14, no. 9, pp. 18557–18571, 2013.

[210] S. J. Leung and M. Romanowski, "Light-activated content release from liposomes," *Theranostics*, vol. 2, no. 10, pp. 1020–1036, 2012.

[211] T. Sun, Y. S. Zhang, B. Pang, D. C. Hyun, M. Yang, and Y. Xia, "Engineered nanoparticles for drug delivery in cancer therapy," *Angew. Chemie - Int. Ed.*, vol. 53, no. 46, pp. 12320–12364, 2014.

[212] A. Singh, E. M. Wong, and J. M. Schnur, "Toward the rational control of nanoscale structures using chiral self-assembly: Diacetylenic phosphocholines," *Langmuir*, vol. 19, no. 5, pp. 1888–1898, 2003.

[213] F. Braunschweig and H. Bässler, "Photopolymerization of diacetylenes under hydrostatic pressure," *Chem. Phys.*, vol. 93, no. 2, pp. 307–318, 1985.

[214] A. Yavlovich, A. Singh, S. Tarasov, J. Capala, R. Blumenthal, and A. Puri, "Design of liposomes containing photopolymerizable phospholipids for triggered release of contents," *J. Therm. Anal. Calorim.*, vol. 98, no. 1, pp. 97–104, 2009.

[215] N. Brasseur, R. Ouellet, C. La Madeleine, and J. Van Lier, "Water soluble aluminium phthalocyanine-polymer conjugates for PDT: Photodynamic activities and pharmacokinetics in tumour bearing mice," *Br. J. Cancer*, vol. 80, no. 10, pp. 1533–1541, 1999.

[216] J. Morgan, A. J. Macrobert, A. G. Gray, and E. R. Huehns, "Use of photosensitive, antibody directed liposomes to destroy target populations of cells in bone marrow: A potential purging method for autologous bone marrow transplantation," *Br. J. Cancer*, vol. 65, no. 1, pp. 58–64, 1992.

[217] Y. Wan, J. Han, G. Fan, Z. Zhang, T. Gong, and X. Sun, "Enzyme-responsive liposomes modified adenoviral vectors for enhanced tumor cell transduction and reduced immunogenicity," *Biomaterials*, vol. 34, no. 12, pp. 3020–3030, 2013.

[218] L. Zhu, P. Kate, and V. P. Torchilin, "Matrix metalloprotease 2-responsive multifunctional liposomal nanocarrier for enhanced tumor targeting," *ACS Nano*, vol. 6, no. 4, pp. 3491–3498, 2012.

[219] C. Yan *et al.*, "Anti-αvβ3 antibody guided three-step pretargeting approach using magnetoliposomes for molecular magnetic resonance imaging of breast cancer angiogenesis," *Int. J. Nanomedicine*, vol. 8, pp. 245–255, 2013.

[220] M. V. Barbosa *et al.*, "Experimental design of a liposomal lipid system: A potential strategy for paclitaxel-based breast cancer treatment," *Colloids Surfaces B Biointerfaces*, vol. 136, pp. 553–561, 2015.

[221] C. Kelly, C. Jefferies, and S.-A. Cryan, "Targeted Liposomal Drug Delivery to Monocytes and Macrophages," *J. Drug Deliv.*, vol. 2011, pp. 1–11, 2011.

[222] C. Varol, S. Yona, and S. Jung, "Origins and tissue-context-dependent fates of blood monocytes," *Immunol. Cell Biol.*, vol. 87, no. 1, pp. 30–38, 2009.

[223] C. S. Robbins and F. K. Swirski, "The multiple roles of monocyte subsets in steady state and inflammation," *Cell. Mol. Life Sci.*, vol. 67, no. 16, pp. 2685–2693, 2010.

[224] S. B. Coffelt, R. Hughes, and C. E. Lewis, "Tumor-associated macrophages: Effectors of angiogenesis and tumor progression," *Biochim. Biophys. Acta - Rev. Cancer*, vol. 1796, no. 1, pp. 11–18, 2009.

[225] D. Christensen, E. M. Agger, L. V. Andreasen, D. Kirby, P. Andersen, and Y. Perrie, "Liposome-based cationic adjuvant formulations (CAF): Past, present, and future," *J. Liposome Res.*, vol. 19, no. 1, pp. 2–11, 2009.

[226] J. O. Rädler, I. Koltover, T. Salditt, and C. R. Safinya, "A model for the local arrangement of cationic liposome/DNA complexesÐsuch complexes may be of great importance in the future for gene therapy," *Science (80-.).*, vol. 275, pp. 810–814, 1997.

[227] B. Becker, R. H. Furneaux, F. Reck, and O. a. Zubkov, "A simple synthesis of 8- (methoxycarbonyl) octyl and derivatives and their use in the preparation of neoglycoconjugates," *Carbohydr. Res.*, vol. 315, pp. 148–158, 1999.

[228] W. Wijagkanalan, S. Kawakami, M. Takenaga, R. Igarashi, F. Yamashita, and M. Hashida, "Efficient targeting to alveolar macrophages by intratracheal administration of mannosylated liposomes in rats," *J. Control. Release*, vol. 125, no. 2, pp. 121–130, 2008.

[229] Y. Kuramoto, S. Kawakami, S. Zhou, H. Kyouichi, F. Fumiyoshi, and Y. Mitsuru, "Use of mannosylated cationic liposomes/ immunostimulatory CpG DNA complex for effective inhibition of peritoneal dissemination in mice," *J. Gene Med.*, vol. 10, no. 6, pp. 610–618, 2008.

[230] H. Takagi *et al.*, "Cooperation of specific ICAM-3 grabbing nonintegrin-related 1 (SIGNR1) and complement receptor type 3 (CR3) in the uptake of oligomannose-coated liposomes by macrophages," *Glycobiology*, vol. 19, no. 3, pp. 258–266, 2009.

[231] S. Kramer, J. Langhanki, M. Krumb, T. Opatz, M. Bros, and R. Zentel, "HPMA-Based Nanocarriers for Effective Immune System Stimulation," *Macromol. Biosci.*, vol. 19, no. 6, pp. 1–10, 2019.

[232] H. Epstein-Barash *et al.*, "Physicochemical parameters affecting liposomal bisphosphonates bioactivity for restenosis therapy: Internalization, cell inhibition, activation of cytokines and complement, and mechanism of cell death," *J. Control. Release*, vol. 146, no. 2, pp. 182–195, 2010.

[233] S. Takano, Y. Aramaki, and S. Tsuchiya, "Physicochemical properties of liposomes affecting apoptosis induced by cationic liposomes in macrophages," *Pharm. Res.*, vol. 20, no. 7, pp. 962–968, 2003.

[234] S. Chono, T. Tanino, T. Seki, and K. Morimoto, "Uptake characteristics of liposomes by rat alveolar macrophages: influence of particle size and surface mannose modification," *J. Pharm. Pharmacol.*, vol. 59, no. 1, pp. 75–80, 2007.

[235] F. Ahsan, I. P. Rivas, M. A. Khan, and A. I. Torres Suárez, "Targeting to macrophages: Role of physicochemical properties of particulate carriers - Liposomes and microspheres - On the phagocytosis by macrophages," *J. Control. Release*, vol. 79, no. 1–3, pp. 29–40, 2002.

[236] C. Foged, C. Arigita, A. Sundblad, W. Jiskoot, G. Storm, and S. Frokjaer, "Interaction of dendritic cells with antigen-containing liposomes: Effect of bilayer composition," *Vaccine*, vol. 22, no. 15–16, pp. 1903–1913, 2004.

[237] G. L. Scherphof and J. A. A. M. Kamps, "Receptor versus non-receptor mediated clearance of liposomes," *Adv. Drug Deliv. Rev.*, vol. 32, no. 1–2, pp. 81–97, 1998.

[238] J. A. Kanis, E. V. McCloskey, and M. N. C. Beneton, "Clodronate and osteoporosis," *Maturitas*, vol. 23, pp. S81–S86, 1996.

[239] K. Hiraoka *et al.*, "Inhibition of bone and muscle metastases of lung cancer cells by a decrease in the number of monocytes/macrophages," *Cancer Sci.*, vol. 99, no. 8, pp. 1595–1602, 2008.

[240] P. J. Richards, B. D. Williams, and A. S. Williams, "Suppression of chronic streptococcal cell wall-induced arthritis in Lewis rats by liposomal clodronate," *Rheumatology*, vol. 40, no. 9, pp. 978–987, 2001.

[241] S. Chono, Y. Tauchi, Y. Deguchi, and K. Morimoto, "Efficient drug delivery to atherosclerotic lesions and the antiatherosclerotic effect by dexamethasone incorporated into liposomes in atherogenic mice," *J. Drug Target.*, vol. 13, no. 4, pp. 267–276, 2005.

[242] S. Chono, Y. Tauchi, and K. Morimoto, "Pharmacokinetic analysis of the uptake of liposomes by macrophages and foam cells in vitro and their distribution to atherosclerotic lesions in mice.," *Drug Metab. Pharmacokinet.*, vol. 21, no. 1, pp. 37–44, 2006.

[243] K. C. Briley-Saebo *et al.*, "Magnetic resonance imaging of vulnerable atherosclerotic plaques: Current imaging strategies and molecular imaging probes," *J. Magn. Reson. Imaging*, vol. 26, no. 3, pp. 460–479, 2007.

[244] A. Maiseyeu *et al.*, "Gadolinium-containing phosphatidylserine liposomes for molecular imaging of atherosclerosis," *J. Lipid Res.*, vol. 50, no. 11, pp. 2157–2163, 2009.

[245] C. J. Bailey, "Metformin: historical overview," *Diabetologia*, vol. 60, no. 9, pp. 1566–1576, 2017.

[246] L. Ding *et al.*, "Metformin prevents cancer metastasis by inhibiting M2-like polarization of tumor associated macrophages," *Oncotarget*, vol. 6, no. 34, pp. 36441–36455, 2015.

[247] C. F. Chiang *et al.*, "Metformin-treated cancer cells modulate macrophage polarization through AMPK-NF-κB signaling," *Oncotarget*, vol. 8, no. 13, pp. 20706–20718, 2017.

[248] J. Pieters and J. Gatfield, "Hijacking the host: Survival of pathogenic mycobacteria inside macrophages," *Trends Microbiol.*, vol. 10, no. 3, pp. 142–146, 2002.

[249] E. Cassol, M. Alfano, P. Biswas, and G. Poli, "Monocyte-derived macrophages and myeloid cell lines as targets of HIV-1 replication and persistence," *J. Leukoc. Biol.*, vol. 80, no. 5, pp. 1018–1030, 2006.

[250] D. A. C. Stapels *et al.*, "Salmonella persisters undermine host immune defenses during antibiotic treatment," *Science (80-.).*, vol. 362, no. 6419, pp. 1156–1160, 2018.

[251] S. P. M. Drescher, S. W. Gallo, P. M. A. Ferreira, C. A. S. Ferreira, and S. D. de Oliveira, "Salmonella enterica persister cells form unstable small colony variants after in vitro exposure to ciprofloxacin," *Sci. Rep.*, vol. 9, no. 1, pp. 1–11, 2019.

[252] C. A. Carter and L. S. Ehrlich, "Cell Biology of HIV-1 Infection of Macrophages," *Annu. Rev. Microbiol.*, vol. 62, no. 1, pp. 425–443, 2008.

[253] S. Gunaseelan, K. Gunaseelan, M. Deshmukh, X. Zhang, and P. J. Sinko, "Surface modifications of nanocarriers for effective intracellular delivery of anti-HIV drugs," *Adv. Drug Deliv. Rev.*, vol. 62, no. 4–5, pp. 518–531, 2010.

[254] E. Ojewole, I. Mackraj, P. Naidoo, and T. Govender, "Exploring the use of novel drug delivery systems for antiretroviral drugs," *Eur. J. Pharm. Biopharm.*, vol. 70, no. 3, pp. 697–710, 2008.

[255] J. Bestman-Smith, P. Gourde, A. Désormeaux, M. J. Tremblay, and M. G. Bergeron, "Sterically stabilized liposomes bearing anti-HLA-DR antibodies for targeting the primary cellular reservoirs of HIV-1," *Biochim. Biophys. Acta- Biomembr.*, vol. 1468, no. 1–2, pp. 161–174, 2000.

[256] A. K. Agrawal and C. M. Gupta, "Tuftsin-bearing liposomes in treatment of macrophage-based infections," *Adv. Drug Deliv. Rev.*, vol. 41, no. 2, pp. 135–146, 2000.

[257] M. Garg, A. Asthana, H. B. Agashe, G. P. Agrawal, and N. K. Jain, "Stavudine-loaded mannosylated liposomes: in-vitro anti-HIV-I activity, tissue distribution and pharmacokinetics," *J. Pharm. Pharmacol.*, vol. 58, no. 5, pp. 605–616, 2006.

[258] Z. M. Saiyed, N. H. Gandhi, and M. P. N. Nair, "Magnetic nanoformulation of azidothymidine 5'-

triphosphate for targeted delivery across the blood-brain barrier," *Int. J. Nanomedicine*, vol. 5, no. 1, pp. 157–166, 2010.

[259] S. Mitragotri *et al.*, "Drug Delivery Research for the Future: Expanding the Nano Horizons and Beyond," *J. Control. Release*, vol. 246, pp. 183–184, 2017.

[260] G. J. Lieschke and P. D. Currie, "Animal models of human disease: Zebrafish swim into view," *Nat. Rev. Genet.*, vol. 8, no. 5, pp. 353–367, 2007.

[261] J. Szebeni *et al.*, "Animal models of complement-mediated hypersensitivity reactions to liposomes and other lipid-based nanoparticles," *J. Liposome Res.*, vol. 17, no. 2, pp. 107–117, 2007.

[262] S. L. Craig and V. B. Jensen, *Animal models in cancer nanotechnology*. Elsevier Inc., 2016.

[263] G. Streisinger, C. Walker, N. Dower, D. Knauber, and F. Singer, "Production of clones of homozygous diploid zebra fish (Brachydanio rerio)," *Nature*, vol. 291, no. May, pp. 293–296, 1981.

[264] W. Driever *et al.*, "A genetic screen for mutations affecting embryogenesis in zebrafish," *Development*, vol. 123, pp. 37–46, 1996.

[265] P. Haffter *et al.*, "The identification of genes with unique and essential functions in the development of the zebrafish, Danio rerio," *Development*, vol. 123, pp. 1–36, 1996.

[266] A. Amsterdam *et al.*, "A large-scale insertional mutagenesis screen in zebrafish," *Genes Dev.*, vol. 13, no. 20, pp. 2713–2724, 1999.

[267] S. Sieber *et al.*, "Zebrafish as a preclinical in vivo screening model for nanomedicines," *Adv. Drug Deliv. Rev.*, pp. 1–52, 2019.

[268] S. Chang *et al.*, "Identification of small molecules rescuing fragile X syndrome phenotypes in Drosophila," *Nat. Chem. Biol.*, vol. 4, no. 4, pp. 256–263, 2008.

[269] W. B. Barbazuk *et al.*, "The syntenic relationship of the zebrafish and human genomes," *Genome Res.*, vol. 10, no. 9, pp. 1351–1358, 2000.

[270] T. X. Liu *et al.*, "Evolutionary conservation of zebrafish linkage group 14 with frequently deleted regions of human chromosome 5 in myeloid malignancies," *Proc. Natl. Acad. Sci. U. S. A.*, vol. 99, no. 9, pp. 6136–6141, 2002.

[271] K. Howe *et al.*, "The zebrafish reference genome sequence and its relationship to the human genome," *Nature*, vol. 496, no. 7446, pp. 498–503, 2013.

[272] C. Delvecchio, J. Tiefenbach, and H. M. Krause, "The Zebrafish: A Powerful Platform for In Vivo, HTS Drug Discovery," *Assay Drug Dev. Technol.*, vol. 9, no. 4, pp. 354–361, 2011.

[273] H. P. Spaink *et al.*, "Robotic injection of zebrafish embryos for high-throughput screening in disease models," *Methods*, vol. 62, no. 3, pp. 246–254, 2013.

[274] R. Macarron, "Critical review of the role of HTS in drug discovery," *Drug Discov. Today*, vol. 11, no. 7–8, pp. 277–279, 2006.

[275] T. C. Tran *et al.*, "Automated, quantitative screening assay for antiangiogenic compounds using transgenic zebrafish," *Cancer Res.*, vol. 67, no. 23, pp. 11386–11392, 2007.

[276] M. Kasahara, T. Suzuki, and L. Du Pasquier, "On the origins of the adaptive immune system: Novel insights from invertebrates and cold-blooded vertebrates," *Trends Immunol.*, vol. 25, no. 2, pp. 105–111, 2004.

[277] S. H. Lam, H. L. Chua, Z. Gong, T. J. Lam, and Y. M. Sin, "Development and maturation of the immune system in zebrafish, Danio rerio: A gene expression profiling, in situ hybridization and immunological study," *Dev. Comp. Immunol.*, vol. 28, no. 1, pp. 9–28, 2004.

[278] G. N. Wheeler and A. W. Brändli, "Simple vertebrate models for chemical genetics and drug discovery

screens: Lessons from zebrafish and Xenopus," *Dev. Dyn.*, vol. 238, no. 6, pp. 1287–1308, 2009.

[279] F. Campbell, F. L. Bos, S. Sieber, G. Arias-alpizar, A. Kros, and J. Bussmann, "Directing Nanoparticle Biodistribution through Evasion and Exploitation of Stab2-Dependent Nanoparticle Uptake," *ACS Nano*, vol. 12, pp. 2138–2150, 2018.

[280] S. Sieber, P. Grossen, P. Detampel, S. Siegfried, D. Witzigmann, and J. Huwyler, "Zebrafish as an early stage screening tool to study the systemic circulation of nanoparticulate drug delivery systems in vivo," *J. Control. Release*, vol. 264, no. August, pp. 180–191, 2017.

[281] L. Evensen *et al.*, "Zebrafish as a model system for characterization of nanoparticles against cancer," *Nanoscale*, vol. 8, no. 2, pp. 862–877, 2016.

[282] P. Herbomel, B. Thisse, and C. Thisse, "Ontogeny and behaviour of early macrophages in the zebrafish embryo," *Development*, vol. 126, no. 17, pp. 3735–3745, 1999.

[283] M. Nguyen-Chi *et al.*, "Identification of polarized macrophage subsets in zebrafish," *Elife*, vol. 4, no. JULY 2015, pp. 1–14, 2015.

[284] S. Sieber *et al.*, "Zebrafish as a predictive screening model to assess macrophage clearance of liposomes in vivo," *Nanomedicine Nanotechnology, Biol. Med.*, vol. 17, no. 2019, pp. 82–93, 2019.

[285] J. A. L. Flynn, "Lessons from experimental Mycobacterium tuberculosis infections," *Microbes Infect.*, vol. 8, no. 4, pp. 1179–1188, 2006.

[286] D. M. Tobin and L. Ramakrishnan, "Comparative pathogenesis of Mycobacterium marinum and Mycobacterium tuberculosis," *Cell. Microbiol.*, vol. 10, no. 5, pp. 1027–1039, 2008.

[287] F. Fenaroli *et al.*, "Nanoparticles as drug delivery system against tuberculosis in zebrafish embryos: Direct visualization and treatment," *ACS Nano*, vol. 8, no. 7, pp. 7014–7026, 2014.

[288] A. S. Narang, R. K. Chang, and M. A. Hussain, "Pharmaceutical development and regulatory considerations for nanoparticles and nanoparticulate drug delivery systems," *J. Pharm. Sci.*, vol. 102, no. 11, pp. 3867–3882, 2013.

[289] S. Jessop, "HIV-Associated Kaposi's Sarcoma," *Dermatol Clin*, vol. 24, pp. 509–520, 2006.

[290] Y. C. Barenholz, "Doxil ® — The first FDA-approved nano-drug : Lessons learned," *J. Control. Release*, vol. 160, no. 2, pp. 117–134, 2012.

[291] A. Gabizon *et al.*, "Prolonged Circulation Time and Enhanced Accumulation in Malignant Exudates of Doxorubicin Encapsulated in Polyethylene-glycol Coated Liposomes," *Cancer Res.*, vol. 54, no. 4, pp. 987–992, 1994.

[292] G. Batist, "Cardiac safety of liposomal anthracyclines," *Cardiovasc. Toxicol.*, vol. 7, no. 2, pp. 72–74, 2007.

[293] J. A. Sparano and E. P. Winer, "Liposomal anthracyclines for breast cancer," *Semin. Oncol.*, vol. 28, no. 4 SUPPL. 12, pp. 32–40, 2001.

[294] J. W. Cowens *et al.*, "Initial Clinical (Phase I) Trial of TLC D-99 (Doxorubicin Encapsulated in Liposomes)," *Cancer Res.*, vol. 53, no. 12, pp. 2796–2802, 1993.

[295] L. Harris *et al.*, "Liposome-encapsulated doxorubicin compared with conventional doxorubicin in a randomized multicenter trial as first-line therapy of metastatic breast carcinoma," *Cancer*, vol. 94, no. 1, pp. 25–36, 2002.

[296] J. P. Adler-moore and R. T. Proffitt, "Development, characterization, efficacy and mode of action of Ambisome, a unilamellar liposomal formulation of Amphotericin B," *J. Liposome Res.*, vol. 3, no. 3, pp. 429–450, 1993.

[297] T. J. Walsh *et al.*, "Safety, tolerance, and pharmacokinetics of a small unilamellar liposomal formulation

of amphotericin B (AmBisome) in neutropenic patients," *Antimicrob. Agents Chemother.*, vol. 42, no. 9, pp. 2391–2398, 1998.

[298] G. Boswell, D. Buell, and B. I., "AmBisome (Liposomal Amphotericin B): A Comparative Review," *J. Clin. Pharmacol.*, vol. 38, no. 7, pp. 583–592, 1998.

[299] N. M. Bressler, "Photodynamic Therapy of Subfoveal Choroidal Neovascularization in Age-related Macular Degeneration With Verteporfin," *Arch Ophthalmol*, vol. 117, pp. 1329–1345, 1999.

[300] R. Glück and I. C. Metcalfe, "New technology platforms in the development of vaccines for the future," *Vaccine*, vol. 20, no. SUPPL. 5, pp. 10–16, 2002.

[301] R. Glück, R. Mischler, B. Finkel, J. U. Que, S. J. Cryz Jr, and B. Scarpa, "Immunogenicity of new virosome influenza vaccine in elderly people," *Lancet*, vol. 344, no. 8916, pp. 160–163, Jul. 1994.

[302] Z. Li *et al.*, "Characterization of nebulized liposomal amikacin (Arikace^{TM}) as a function of droplet size," *J. Aerosol Med. Pulm. Drug Deliv.*, vol. 21, no. 3, pp. 245–253, 2008.

[303] S. Zahid and I. Brownell, "Repairing DNA damage in xeroderma pigmentosum: T4N5 lotion and gene therapy," *J. Drugs Dermatol.*, vol. 7, no. 4, p. 405—408, Apr. 2008.

[304] J. Chen *et al.*, "Thermosensitive liposomes with higher phase transition temperature for targeted drug delivery to tumor," *Int. J. Pharm.*, vol. 475, no. 1, pp. 408–415, 2014.

[305] G. P. Stathopoulos and T. Boulikas, "Lipoplatin Formulation Review Article," *J. Drug Deliv.*, vol. 2012, pp. 1–10, 2012.

[306] M. E. Eichhorn *et al.*, "Vascular targeting by EndoTAGTM-1 enhances therapeutic efficacy of conventional chemotherapy in lung and pancreatic cancer," *Int. J. Cancer*, vol. 126, no. 5, pp. 1235–1245, 2010.

[307] X. Zhang, J. Qi, Y. Lu, W. He, X. Li, and W. Wu, "Biotinylated liposomes as potential carriers for the oral delivery of insulin," *Nanomedicine Nanotechnology, Biol. Med.*, vol. 10, no. 1, pp. 167–176, 2014.

[308] J. Marques *et al.*, "Application of heparin as a dual agent with antimalarial and liposome targeting activities toward Plasmodium-infected red blood cells," *Nanomedicine Nanotechnology, Biol. Med.*, vol. 10, no. 8, pp. 1719–1728, 2014.

[309] W. Rojanarat, T. Nakpheng, E. Thawithong, N. Yanyium, and T. Srichana, "Inhaled pyrazinamide proliposome for targeting alveolar macrophages," *Drug Deliv.*, vol. 19, no. 7, pp. 334–345, 2012.

[310] W. Rojanarat, T. Nakpheng, E. Thawithong, N. Yanyium, and T. Srichana, "Levofloxacin-Proliposomes: Opportunities for Use in Lung Tuberculosis," *Pharmaceutics*, vol. 4, no. 3, pp. 385–412, 2012.

[311] B. S. Pattni, V. V. Chupin, and V. P. Torchilin, "New Developments in Liposomal Drug Delivery," *Chem. Rev.*, vol. 115, no. 19, pp. 10938–10966, 2015.

[312] G. Pasut and F. M. Veronese, "Pasut, G. & Veronese, F. M. Polymer-drug conjugation, recent achievements and general strategies. Prog. Polym. Sci. 32, 933-961," *Prog. Polym. Sci.*, vol. 32, pp. 933–961, Aug. 2007.

[313] C. Dingels and H. Frey, "From Biocompatible to Biodegradable: Poly(Ethylene Glycol)s with Predetermined Breaking Points BT - Hierarchical Macromolecular Structures: 60 Years after the Staudinger Nobel Prize II," V. Percec, Ed. Cham: Springer International Publishing, 2013, pp. 167–190.

[314] A. L. Klibanov, K. Maruyama, V. P. Torchilin, and L. Huang, "Amphipathic polyethyleneglycols effectively prolong the circulation time of liposomes," *FEBS Lett.*, vol. 268, no. 1, pp. 235–237, 1990.

[315] P. Mishra, B. Nayak, and R. K. Dey, "PEGylation in anti-cancer therapy: An overview," *Asian J. Pharm. Sci.*, vol. 11, no. 3, pp. 337–348, 2016.

[316] S. Mishra, P. Webster, and M. E. Davis, "PEGylation significantly affects cellular uptake and intracellular

trafficking of non-viral gene delivery particles," *Eur. J. Cell Biol.*, vol. 83, no. 3, pp. 97–111, 2004.

[317] K. Remaut, B. Lucas, K. Braeckmans, J. Demeester, and S. C. De Smedt, "Pegylation of liposomes favours the endosomal degradation of the delivered phosphodiester oligonucleotides," *J. Control. Release*, vol. 117, no. 2, pp. 256–266, 2007.

[318] T. Suzuki *et al.*, "Accelerated blood clearance of PEGylated liposomes containing doxorubicin upon repeated administration to dogs," *Int. J. Pharm.*, vol. 436, no. 1–2, pp. 636–643, 2012.

[319] M. Mohamed *et al.*, "PEGylated liposomes: immunological responses," *Sci. Technol. Adv. Mater.*, vol. 20, no. 1, pp. 710–724, 2019.

[320] B. I. Voit and A. Lederer, "Hyperbranched and Highly Branched Polymer Architectures—Synthetic Strategies and Major Characterization Aspects," *Chem. Rev.*, vol. 109, no. 11, pp. 5924–5973, 2009.

[321] Y. Zheng, S. Li, Z. Weng, and C. Gao, "Hyperbranched polymers: advances from synthesis to applications," *Chem. Soc. Rev.*, vol. 44, no. 12, pp. 4091–4130, 2015.

[322] T. Fritz *et al.*, "Click modification of multifunctional liposomes bearing hyperbranched polyether chains," *Biomacromolecules*, vol. 15, no. 7, pp. 2440–2448, 2014.

[323] S. Palchetti *et al.*, "Protein corona fingerprints of liposomes: New opportunities for targeted drug delivery and early detection in pancreatic cancer," *Pharmaceutics*, vol. 11, no. 1, 2019.

[324] A. Bigdeli *et al.*, "Exploring Cellular Interactions of Liposomes Using Protein Corona Fingerprints and Physicochemical Properties," *ACS Nano*, vol. 10, no. 3, pp. 3723–3737, 2016.

[325] C. Corbo, R. Molinaro, M. Tabatabaei, O. C. Farokhzad, and M. Mahmoudi, "Personalized protein corona on nanoparticles and its clinical implications," *Biomater. Sci.*, vol. 5, no. 3, pp. 378–387, 2017.

[326] M. Bros *et al.*, "The protein corona as a confounding variable of nanoparticle-mediated targeted vaccine delivery," *Front. Immunol.*, vol. 9, no. AUG, pp. 1–10, 2018.

[327] J. Simon *et al.*, "Exploiting the biomolecular corona: Pre-coating of nanoparticles enables controlled cellular interactions," *Nanoscale*, vol. 10, no. 22, pp. 10731–10739, 2018.

[328] F. M. Harris, K. B. Best, and J. D. Bell, "Use of laurdan fluorescence intensity and polarization to distinguish between changes in membrane fluidity and phospholipid order," *Biochim Biophys Acta.*, vol. 1565, pp. 123–128, 2002.

[329] A. J. Schroit, J. Madsen, and R. Nayar, "Liposome-cell interactions: In vitro discrimination of uptake mechanism and in vivo targeting strategies to mononuclear phagocytes," *Chem. Phys. Lipids*, vol. 40, no. 2–4, pp. 373–393, 1986.

[330] C. J. Chu, J. Dijkstra, M. Z. Lai, K. Hong, and F. C. Szoka, "Efficiency of Cytoplasmic Delivery by pH-Sensitive Liposomes to Cells in Culture," *Pharmaceutical Research: An Official Journal of the American Association of Pharmaceutical Scientists*, vol. 7, no. 8. pp. 824–834, 1990.

[331] T. Ishida and M. J. Kirchmeier, "Targeted delivery and triggered release of liposomal doxorubicin enhances cytotoxicity against human B lymphoma cells," *Biochim. Biophys. Acta*, vol. 1515, pp. 144–158, 2001.

[332] F. Piaggio *et al.*, "A novel liposomal Clodronate depletes tumor-associated macrophages in primary and metastatic melanoma : Anti-angiogenic and anti-tumor effects," *J. Control. Release*, vol. 223, pp. 165–177, 2016.

[333] S. Lee, S. Kivimäe, A. Dolor, and F. C. Szoka, "Macrophage-based cell therapies: The long and winding road," *J. Control. Release*, vol. 240, pp. 527–540, 2016.

[334] A. T. Reibel *et al.*, "Fate of Linear and Branched Polyether-Lipids in Vivo in Comparison to Their Liposomal Formulations by 18F-Radiolabeling and Positron Emission Tomography," *Biomacromolecules*, vol. 16, no.

3, pp. 842–851, 2015.

[335] L. Nobs, F. Buchegger, R. Gurny, and E. Allémann, "Current methods for attaching targeting ligands to liposomes and nanoparticles," *J. Pharm. Sci.*, vol. 93, no. 8, pp. 1980–1992, 2004.

[336] C.-H. Chen, D.-Z. Liu, H.-W. Fang, H.-J. Liang, T.-S. Yang, and S.-Y. Lin, "Evaluation of Multi-Target and Single-Target Liposomal Drugs for the Treatment of Gastric Cancer," *Biosci. Biotechnol. Biochem.*, vol. 72, no. 6, pp. 1586–1594, 2008.

[337] M. Kun *et al.*, "Development of a successive targeting liposome with multi-ligand for efficient targeting gene delivery," *J. Gene Med.*, vol. 13, no. 6, pp. 290–301, 2011.

[338] S. S. Rane and P. Choi, "Polydispersity Index: How Accurately Does It Measure the Breadth of the Molecular Weight Distribution?," *Chem. Mater.*, vol. 17, no. 4, pp. 926–926, 2005.

[339] J. W. Gooch, "Encyclopedic Dictionary of Polymers," *Springer*, p. 556, 2011.

[340] P. P. Deshpande, S. Biswas, and V. P. Torchilin, "Current trends in the use of liposomes for tumor targeting," *Nanomedicine*, vol. 8, no. 9, pp. 1509–1528, 2013.

[341] R. R. Sawant and V. P. Torchilin, "Challenges in Development of Targeted Liposomal Therapeutics," *AAPS J.*, vol. 14, no. 2, pp. 303–315, 2012.

[342] V. P. Torchilin, "Passive and Active Drug Targeting: Drug Delivery to Tumors as an Example," in *Drug Delivery*, M. Schäfer-Korting, Ed. Berlin, Heidelberg: Springer Berlin Heidelberg, 2010, pp. 3–53.

[343] T. Lammers, F. Kiessling, W. E. Hennink, and G. Storm, "Drug targeting to tumors: Principles, pitfalls and (pre-) clinical progress," *J. Control. Release*, vol. 161, no. 2, pp. 175–187, 2012.

[344] J. Kuntsche, J. C. Horst, and H. Bunjes, "Cryogenic transmission electron microscopy (cryo-TEM) for studying the morphology of colloidal drug delivery systems," *Int. J. Pharm.*, vol. 417, no. 1–2, pp. 120–137, 2011.

[345] O. Garbuzenko, Y. Barenholz, and A. Priev, "Effect of grafted PEG on liposome size and on compressibility and packing of lipid bilayer," *Chem. Phys. Lipids*, vol. 135, no. 2, pp. 117–129, 2005.

[346] P. G. de Gennes, "Polymers at an interface; a simplified view," *Adv. Colloid Interface Sci.*, vol. 27, no. 3–4, pp. 189–209, 1987.

[347] O. Tirosh, Y. Barenholz, J. Katzhendler, and A. Priev, "Hydration of polyethylene glycol-grafted liposomes," *Biophys. J.*, vol. 74, no. 3, pp. 1371–1379, 1998.

[348] A. K. Kenworthy, K. Hristova, D. Needham, and T. J. McIntosh, "Range and magnitude of the steric pressure between bilayers containing phospholipids with covalently attached poly(ethylene glycol)," *Biophys. J.*, vol. 68, no. 5, pp. 1921–1936, 1995.

[349] W. R. Perkins, S. R. Minchey, P. L. Ahl, and A. S. Janoff, "The determination of liposome captured volume," *Chem. Phys. Lipids*, vol. 64, no. 1–3, pp. 197–217, 1993.

[350] F. Oesterhelt, M. Rief, and H. E. Gaub, "Single molecule force spectroscopy by AFM indicates helical structure of poly(ethylene-glycol) in water," *New J. Phys.*, vol. 1, no. 6, pp. 1–11, 1999.

[351] M. Zhengyu *et al.*, "Tcr triggering by pMHC ligands tethered on surfaces via poly(ethylene glycol) depends on polymer length," *PLoS One*, vol. 9, no. 11, pp. 1–10, 2014.

[352] H. I. Labouta *et al.*, "Surface-grafted polyethylene glycol conformation impacts the transport of PEG-functionalized liposomes through a tumour extracellular matrix model," *RSC Adv.*, vol. 8, no. 14, pp. 7697–7708, 2018.

[353] M. L. Alessi, A. I. Norman, S. E. Knowlton, D. L. Ho, and S. C. Greer, "Helical and Coil Conformations of Poly(ethylene glycol) in Isobutyric Acid and Water," *Macromolecules*, no. 38, pp. 9333–9340, 2005.

[354] M. Worm, "pH-cleavable and hyperbranched polyether architectures: from novel synthesis strategies to applications in nanotechnology and biomedicine," *Ph.D. thesis*, p. 185, 2016.

[355] J. Bandup, E. H. Immergut, and E. A. Grulke, "Polymer Handbook," *Wiley*, vol. 4, 1999.

[356] M. R. Kasaai, "Intrinsic viscosity-molecular weight relationship and hydrodynamic volume for pullulan," *J. Appl. Polym. Sci.*, vol. 100, no. 6, pp. 4325–4332, 2006.

[357] Tieke, *Makromolekulare Chemie*, vol. 3. 2014.

[358] G. Boehmke and R. Heusch, "Über die Hydratisierung von Polyglykoläthern," *Fette, Seifen, Anstrichm.*, vol. 62, no. 2, pp. 87–91, 1960.

[359] R. Nikam, X. Xu, and J. Dzubiella, "Charge and hydration structure of dendritic polyelectrolytes : molecular simulations of polyglycerol sulphate," *Soft Matter*, vol. 14, no. 4300, pp. 62–67, 2018.

[360] C. Weber *et al.*, "Functionalization of liposomes with hydrophilic polymers results in macrophage uptake independent of the protein corona," *Biomacromolecules*, 2019.

[361] G. Caracciolo, "Liposome-protein corona in a physiological environment: Challenges and opportunities for targeted delivery of nanomedicines," *Nanomedicine Nanotechnology, Biol. Med.*, vol. 11, no. 3, pp. 543–557, 2015.

[362] C. D. Walkey and W. C. W. Chan, "Understanding and controlling the interaction of nanomaterials with proteins in a physiological environment," *Chem. Soc. Rev.*, vol. 41, no. 7, pp. 2780–2799, 2012.

[363] B. Kharazian, N. L. Hadipour, and M. R. Ejtehadi, "Understanding the nanoparticle-protein corona complexes using computational and experimental methods," *Int. J. Biochem. Cell Biol.*, vol. 75, pp. 162–174, 2016.

[364] M. P. Monopoli, C. Åberg, A. Salvati, and K. A. Dawson, "Biomolecular coronas provide the biological identity of nanosized materials," *Nat. Nanotechnol.*, vol. 7, no. 12, pp. 779–786, 2012.

[365] R. M. Pearson, V. V. Juettner, and S. Hong, "Biomolecular corona on nanoparticles: a survey of recent literature and its implications in targeted drug delivery," *Front. Chem.*, vol. 2, no. November, pp. 1–7, 2014.

[366] D. Walczyk, F. Bombelli, M. Monopoli, I. Lynch, and K. Dawson, "What the Cell 'Sees' in Bionanoscience," *J. Am. Chem. Soc.*, vol. 132, no. 16, pp. 5761–5768, 2010.

[367] V. Cauda, C. Argyo, and T. Bein, "Impact of different PEGylation patterns on the long-term bio-stability of colloidal mesoporous silica nanoparticles," *J. Mater. Chem.*, vol. 20, no. 39, pp. 8693–8699, 2010.

[368] R. Gref, M. Lu, P. Sud, and E. Pharmaceutiques, "'Stealth' corona-core nanoparticles surface modified by polyethylene glycol (PEG): influences of the corona (PEG chain length and surface density) and of the core composition on phagocytic uptake and plasma protein adsorption," *Colloids Surfaces B Biointerfaces*, vol. 18, pp. 301–313, 2000.

[369] G. Caracciolo *et al.*, "The liposome-protein corona in mice and humans and its implications for in vivo delivery," *J. Mater. Chem. B*, vol. 2, no. 42, pp. 7419–7428, 2014.

[370] D. Pozzi *et al.*, "Effect of polyethyleneglycol (PEG) chain length on the bio-nano- interactions between PEGylated lipid nanoparticles and biological fluids: From nanostructure to uptake in cancer cells," *Nanoscale*, vol. 6, no. 5, pp. 2782–2792, 2014.

[371] S. Winzen *et al.*, "Complementary analysis of the hard and soft protein corona: Sample preparation critically effects corona composition," *Nanoscale*, vol. 7, no. 7, pp. 2992–3001, 2015.

[372] S. Schöttler *et al.*, "Protein adsorption is required for stealth effect of poly(ethylene glycol)- and poly(phosphoester)-coated nanocarriers," *Nat. Nanotechnol.*, vol. 11, no. 4, pp. 372–377, 2016.

[373]   D. Hofmann *et al.*, "Mass spectrometry and imaging analysis of nanoparticle-containing vesicles provide a mechanistic insight into cellular trafficking," *ACS Nano*, vol. 8, no. 10, pp. 10077–10088, 2014.

[374]   C. Weber, J. Simon, V. Mailänder, S. Morsbach, and K. Landfester, "Preservation of the soft protein corona in distinct flow allows identification of weakly bound proteins," *Acta Biomater.*, vol. 76, pp. 217–224, 2018.

[375]   J. S. Lee, S. Y. Hwang, and E. K. Lee, "Imaging-based analysis of liposome internalization to macrophage cells: Effects of liposome size and surface modification with PEG moiety," *Colloids Surfaces B Biointerfaces*, vol. 136, pp. 786–790, 2015.

[376]   I. J. Fidler, A. Raz, W. E. Fogler, R. Kirsh, P. Bugelski, and G. Poste, "Design of liposomes to improve delivery of macrophage-augmenting agents to alveolar macrophages.," *Cancer Res.*, vol. 40, no. 12, pp. 4460–6, 1980.

[377]   R. J. Allen, B. Mathew, and K. G. Rice, "PEG-Peptide Inhibition of Scavenger Receptor Uptake of Nanoparticles by the Liver," *Mol. Pharm.*, vol. 15, no. 9, pp. 3881–3891, 2018.

[378]   N. J. Baumhover *et al.*, "Structure-Activity Relationship of PEGylated Polylysine Peptides as Scavenger Receptor Inhibitors for Non-Viral Gene Delivery," *Mol. Pharm.*, vol. 12, no. 12, pp. 4321–4328, 2015.

[379]   R. M. Straubinger and K. Hong, "Endocytosis of Liposomes and Intracellular Fate of Encapsulated Molecules : Encounter with a Low pH Compartment after Internalization in Coated Vesicles," *Cell*, vol. 32, pp. 1069–1079, 1983.

[380]   F. K. Swirski *et al.*, "Identification of Splenic Reservoir," *Sci. Rep.*, vol. 325, no. July, pp. 612–617, 2009.

[381]   J. Yang, L. Zhang, Y. Caijia, X.-F. Yang, and H. Wang, "Monocyte and macrophage differentiation: circulation inflammatory monocyte as biomarker for inflammatory diseases," *Biomark. Res.*, vol. 2, no. 1, 2014.

[382]   M. J. Hajipour, S. Laurent, A. Aghaie, F. Rezaee, and M. Mahmoudi, "Personalized protein coronas: A 'key' factor at the nanobiointerface," *Biomater. Sci.*, vol. 2, no. 9, pp. 1210–1221, 2014.

[383]   V. Colapicchioni *et al.*, "Personalized liposome-protein corona in the blood of breast, gastric and pancreatic cancer patients," *Int. J. Biochem. Cell Biol.*, vol. 75, pp. 180–187, 2016.

[384]   X. Y. Jiang, C. D. Sarsons, M. J. Gomez-Garcia, D. T. Cramb, K. D. Rinker, and S. J. Childs, "Quantum dot interactions and flow effects in angiogenic zebrafish (Danio rerio) vessels and human endothelial cells," *Nanomedicine Nanotechnology, Biol. Med.*, vol. 13, no. 3, pp. 999–1010, 2017.

[385]   S.-W. Jin, D. Beis, T. Mitchell, J.-N. Chen, and D. Y. R. Stainier, "Cellular and molecular analyses of vascular tube and lumen formation in zebrafish," *Development*, vol. 132, no. 23, pp. 5199–5209, 2005.

[386]   G. J. R. Charrois and T. M. Allen, "Drug release rate influences the pharmacokinetics, biodistribution, therapeutic activity, and toxicity of pegylated liposomal doxorubicin formulations in murine breast cancer," *Biochim. Biophys. Acta - Biomembr.*, vol. 1663, no. 1–2, pp. 167–177, 2004.

[387]   N. L. Boman, L. D. Mayer, and P. R. Cullis, "Optimization of the retention properties of vincristine in liposomal systems," *BBA - Biomembr.*, vol. 1152, no. 2, pp. 253–258, 1993.

[388]   K. M. Laginha, S. Verwoert, G. J. R. Charrois, and T. M. Allen, "Determination of doxorubicin levels in whole tumor and tumor nuclei in murine breast cancer tumors," *Clin. Cancer Res.*, vol. 11, no. 19 I, pp. 6944–6949, 2005.

[389]   C. L. Walsh, V. J. Venditto, P. H. Kierstead, F. C. Szoka, and A. G. Kohli, "Designer lipids for drug delivery: From heads to tails," *J. Control. Release*, vol. 190, pp. 274–287, 2014.

[390]   B. Kneidl, M. Peller, G. Winter, L. H. Lindner, and M. Hossann, "Thermosensitive liposomal drug delivery systems: state of the art review," *Int. J. Nanomedicine*, vol. 9, pp. 4387–4398, 2014.

[391]   M. Dellian *et al.*, "Novel Temperature-Sensitive Liposomes with Prolonged Circulation Time," *Clin. Cancer Res.*, vol. 10, no. 6, pp. 2168–2178, 2005.

[392]   D. Needham, G. Anyarambhatla, G. Kong, and M. W. Dewhirst, "A new temperature-sensitive liposome for use with mild hyperthermia: Characterization and testing in a human tumor xenograft model," *Cancer Res.*, vol. 60, no. 5, pp. 1197–1201, 2000.

[393]   S. R. Paliwal, R. Paliwal, and S. P. Vyas, "A review of mechanistic insight and application of pH-sensitive liposomes in drug delivery," *Drug Deliv.*, vol. 22, no. 3, pp. 231–242, 2015.

[394]   H. Karanth and R. S. R. Murthy, "pH-Sensitive liposomes-principle and application in cancer therapy," *J. Pharm. Pharmacol.*, vol. 59, no. 4, pp. 469–483, 2007.

[395]   M. B. Yatvin, W. Kreutz, B. A. Horwitz, and M. Shinitzky, "pH-sensitive liposomes: possible clinical implications," *Science (80-.).*, vol. 210, no. 4475, pp. 1253–1255, 1980.

[396]   M. Hagedorn, A. Bögershausen, M. Rischer, R. Schubert, and U. Massing, "Dual centrifugation – A new technique for nanomilling of poorly soluble drugs and formulation screening by an DoE-approach," *Int. J. Pharm.*, vol. 530, no. 1–2, pp. 79–88, 2017.

[397]   D. A. Gewirtz, "A critical evaluation of the mechanisms of action proposed for the antitumor effects of the anthracycline antibiotics adriamycin and daunorubicin," *Biochem. Pharmacol.*, vol. 57, no. 7, pp. 727–741, 1999.

[398]   S. Judith and G. Gregory, "Is half-life of circulating liposomes determined by changes in their permeability?," *FEBS Lett.*, vol. 145, no. 1, pp. 109–114, 2018.

[399]   T. M. Allen and L. G. Cleland, "Serum-induced leakage of liposome contents," vol. 597, pp. 418–426, 1980.

[400]   P. J. Quinn and C. Wolf, "The liquid-ordered phase in membranes," *Biochim. Biophys. Acta - Biomembr.*, vol. 1788, no. 1, pp. 33–46, 2009.

[401]   D. Stamp and R. L. Juliano, "Factors affecting the encapsulation of drugs within liposomes," *Can. J. Physiol. Pharmacol.*, vol. 57, no. 5, pp. 535–539, 2011.

[402]   P. R. Cullis, "Lateral diffusion rates of phosphatidylcholine in vesicle membranes: effects of cholesterol and hydrocarbon phase transitions," *FEBS Lett.*, vol. 70, no. 1, pp. 223–228, 1976.

[403]   A. S. Abu Lila and T. Ishida, "Liposomal Delivery Systems: Design Optimization and Current Applications," *Biol. Pharm. Bull. Pharm. Bull.*, vol. 40, no. 1, pp. 1–10, 2016.

[404]   M. J. Sheffield, B. L. Baker, D. Li, N. L. Owen, M. L. Baker, and J. D. Bell, "Enhancement of Agkistrodon piscivorus Venom Phospholipase A2 Activity toward Phosphatidylcholine Vesicles by Lysolecithin and Palmitic Acid: Studies with Fluorescent Probes of Membrane Structure," *Biochemistry*, vol. 34, no. 24, pp. 7796–806, 1995.

[405]   R. Hennig *et al.*, "IM30 triggers membrane fusion in cyanobacteria and chloroplasts," *Nat. Commun.*, vol. 6, no. 1, 2015.

[406]   E. Evans and D. Needham, "Physical properties of surfactant bilayer membranes: Thermal transitions, elasticity, rigidity, cohesion, and colloidal interactions," *J. Phys. Chem.*, vol. 91, no. 16, pp. 4219–4228, 1987.

[407]   F. V. V. O. N. Steyern, J. Josefsson, and S. Tagerud, "Rhodamine B , a Fluorescent Probe for Acidic Organelles in Denervated Skeletal Muscle," *J Histochem Cytochem.*, vol. 44, no. 3, pp. 267–274, 1996.

[408]   S. Ohkuma and B. Poole, "Fluorescence probe measurement of the intralysosomal pH in living cells and the perturbation of pH by various agents," *Proc Natl Acad Sci USA.*, vol. 75, no. 7, pp. 3327–31, 1978.

[409]   N. Duzgunes and S. Nir, "Mechanisms and kinetics of liposome–cell interactions," *Adv Drug Deliv Rev.*, vol. 40, no. 1–2, pp. 3–18, 1999.

[410]   M. Willis and E. Forssen, "Ligand-targeted liposomes.," *Adv. Drug Deliv. Rev.*, vol. 29, no. 3, pp. 249–271, 1998.

[411]   T. Ta and T. M. Porter, "Thermosensitive liposomes for localized delivery and triggered release of chemotherapy," *J. Control. Release*, vol. 169, no. 1–2, pp. 112–125, 2013.

[412]   M. Badran, "Formulation and in vitro evaluation of flufenamic acid loaded deformable liposomes for improved skin delivery," *Dig. J. Nanomater. Biostructures*, vol. 9, no. 1, pp. 83–91, 2014.

[413]   A. C. D. Putri, R. Dwiastuti, Marchaban, and A. K. Nugroho, "Optimization of mixing temperature and sonication duration in liposome preparation," *J. Farm. SAINS DAN KOMUNITAS*, vol. 14, no. 2, pp. 79–85, 2017.

[414]   M. Chen, X. Liu, and A. Fahr, "Skin penetration and deposition of carboxyfluorescein and temoporfin from different lipid vesicular systems: In vitro study with finite and infinite dosage application," *Int. J. Pharm.*, vol. 408, no. 1–2, pp. 223–234, 2011.

[415]   C. D. Mills, K. Kincaid, J. M. Alt, M. J. Heilman, and A. M. Hill, "M-1/M-2 Macrophages and the Th1/Th2 Paradigm," *J. Immunol.*, vol. 164, no. 12, pp. 6166–6173, 2000.

[416]   F. O. Martinez and S. Gordon, "The M1 and M2 paradigm of macrophage activation: Time for reassessment," *F1000Prime Rep.*, vol. 6, no. March, pp. 1–13, 2014.

[417]   A. Mantovani, A. Sica, S. Sozzani, P. Allavena, A. Vecchi, and M. Locati, "The chemokine system in diverse forms of macrophage activation and polarization," *Trends Immunol.*, vol. 25, no. 12, pp. 677–686, 2004.

[418]   Y. Sun, P. Möller, C. Berking, E. M. Schlüpen, M. Volkenandt, and D. Schadendorf, "In vivo selective expansion of a tumour-specific cytotoxic T-cell clone derived from peripheral blood of a melanoma patient after vaccination with gene-modified autologous tumour cells," *Immunology*, vol. 98, no. 4, pp. 535–540, 1999.

[419]   P. Möller *et al.*, "Vaccination with IL-7 gene-modified autologous melanoma cells can enhance the anti-melanoma lytic activity in peripheral blood of patients with a good clinical performance status: A clinical phase I study," *Br. J. Cancer*, vol. 77, no. 11, pp. 1907–1916, 1998.

[420]   S. Ferreira, E. A. Leite, and M. C. Oliveira, "Liposomes as Carriers of Anticancer Drugs," *Intech*, pp. 85–124, 2013.

[421]   P. M. Kanter, G. A. Bullard, F. G. Pilkiewicz, L. D. Mayer, P. R. Cullis, and Z. P. Pavelic, "Preclinical toxicology study of liposome encapsulated doxorubicin (TLC D-99): comparison with doxorubicin and empty liposomes in mice and dogs," *In Vivo*, vol. 7, no. 1, p. 85—95, 1993.

[422]   N. Sadat, H. Motlagh, P. Parvin, F. Ghasemi, and F. Atyabi, "Fluorescence properties of several chemotherapy drugs : doxorubicin , paclitaxel and bleomycin," *Biomed. Opt. Express*, vol. 7, no. 6, pp. 2400–2406, 2016.

[423]   R. Hajian, N. Shams, and M. Mohagheghian, "Study on the interaction between doxorubicin and deoxyribonucleic acid with the use of methylene blue as a probe," *J. Braz. Chem. Soc.*, vol. 20, no. 8, pp. 1399–1405, 2009.

[424]   B. Gnapareddy *et al.*, "Chemical and Physical Characteristics of Doxorubicin Hydrochloride Drug-Doped Salmon DNA Thin Films," *Sci. Rep.*, vol. 5, no. March, pp. 1–9, 2015.

[425]   D. E. Wolf, "Determination of the Sidedness of Carbocyanine Dye Labeling of Membranes," *Biochemistry*, vol. 24, no. 3, pp. 582–586, 1985.

[426]   C. Odaka and T. Mizuochi, "Role of macrophage lysosomal enzymes in the degradation of nucleosomes of apoptotic cells.," *J. Immunol.*, vol. 163, no. 10, pp. 5346–52, 1999.

[427]   E. K. Zuba-Surma, M. Kucia, A. Abdel-Latif, J. W. Lillard, and M. Z. Ratajczak, "The ImageStream system: A key step to a new era in imaging," *Folia Histochem. Cytobiol.*, vol. 45, no. 4, pp. 279–290, 2007.

[428]   V. Torraca, S. Masud, H. P. Spaink, and A. H. Meijer, "Macrophage-pathogen interactions in infectious diseases : new therapeutic insights from the zebrafish host model," *Dis. Model. Mech.*, vol. 7, pp. 785–797, 2014.

[429]   H. Hillaireau, "Investigating Interactions Between Nanoparticles and Cells: Internalization and Intracellular Trafficking," in *Polymer Nanoparticles for Nanomedicines*, C. Vauthier and G. Ponchel, Eds. Cham: Springer International Publishing, 2016, pp. 291–323.

[430]   M. De Diego, G. Godoy, and S. Mennickent, "Chemical stability of ceftriaxone by a validated stability-indicating liquid chromatographic method," *J. Chil. Chem. Soc.*, vol. 55, no. 3, pp. 335–337, 2010.

[431]   M. Worm, D. Leibig, C. Dingels, and H. Frey, "Cleavable Polyethylene Glycol: 3,4-Epoxy-1-butene as a Comonomer to Establish Degradability at Physiologically Relevant pH," *ACS Macro Lett.*, vol. 5, no. 12, pp. 1357–1363, 2016.

[432]   C. Dingels, S. S. Müller, T. Steinbach, C. Tonhauser, and H. Frey, "Universal concept for the implementation of a single cleavable unit at tunable position in functional poly(ethylene glycol)s," *Biomacromolecules*, vol. 14, no. 2, pp. 448–459, 2013.

[433]   W. C. Koff and I. J. Fidler, "The potential use of liposome-mediated antiviral therapy," *Antiviral Res.*, vol. 5, no. 3, pp. 179–190, 1985.

[434]   I. Eue, "Growth inhibition of human mammary carcinoma by liposomal hexadecylphosphocholine: Participation of activated macrophages in the antitumor mechanism," *Int. J. Cancer*, vol. 92, no. 3, pp. 426–433, 2001.

[435]   S. Chono, T. Tanino, T. Seki, and K. Morimoto, "Efficient drug targeting to rat alveolar macrophages by pulmonary administration of ciprofloxacin incorporated into mannosylated liposomes for treatment of respiratory intracellular parasitic infections," *J. Control. Release*, vol. 127, no. 1, pp. 50–58, 2008.

[436]   L. Kole, L. Das, and P. K. Das, "Synergistic Effect of Interferon-γ and Mannosylated Liposome-Incorporated Doxorubicin in the Therapy of Experimental Visceral Leishmaniasis," *J. Infect. Dis.*, vol. 180, no. 3, pp. 811–820, 1999.

[437]   B. Axelsson, "Liposomes as carriers for anti-inflammatory agents," *Adv. Drug Deliv. Rev.*, vol. 3, no. 3, pp. 391–404, 1989.

[438]   R. Nayar and I. J. Fidler, "The systemic activation of macrophages by liposomes containing immunomodulators," *Springer Semin. Immunopathol.*, vol. 8, no. 4, pp. 413–428, 1985.

[439]   J. J. Killion and I. J. Fidler, "Therapy of cancer metastasis by tumoricidal activation of tissue macrophages using liposome-encapsulated immunomodulators," *Pharmacol. Ther.*, vol. 78, no. 3, pp. 141–154, 1998.

[440]   S. E. Seltzer, "The role of liposomes in diagnostic imaging," *Radiology*, vol. 171, no. 1, pp. 19–21, 1989.

[441]   S. M. Moghimi, A. C. Hunter, and J. C. Murray, "Long-Circulating and Target-Specific Nanoparticles : Theory to Practice," *Pharmacol. Rev.*, vol. 53, no. 2, pp. 283–318, 2001.

[442]   C. Schubert *et al.*, "Synthesis of linear polyglycerols with tailored degree of methylation by copolymerization and the effect on thermorheological behavior," *Polymer (Guildf).*, vol. 121, pp. 328–339, 2017.

[443]   A. S. Klymchenko, "Solvatochromic and Fluorogenic Dyes as Environment-Sensitive Probes: Design and Biological Applications," *Acc. Chem. Res.*, vol. 50, no. 2, pp. 366–375, 2017.

[444]   T. M. Allen, "A study of phospholipid interactions between high-density lipoproteins and small unilamellar vesicles," *BBA - Biomembr.*, vol. 640, no. 2, pp. 385–397, 1981.

[445]   T. Ishida, Y. Okada, T. Kobayashi, and H. Kiwada, "Development of pH-sensitive liposomes that efficiently retain encapsulated doxorubicin (DXR) in blood," *Int. J. Pharm.*, vol. 309, no. 1–2, pp. 94–100, 2006.

[446] R. M. Straubinger, D. Papahadjopoulos, K. Hong, R. M. Straubinger, D. Papahadjopoulos, and K. Hong, "Endocytosis and Intracellular Fate of Liposomes Using Pyranine as a Probe," *Biochemistry*, vol. 29, no. 20, pp. 4929–4939, 1990.

[447] C. De Duve, T. De Barsy, B. Poole, A. Trouet, P. Tulkens, and F. Van Hoof, "Lysosomotropic agents," *Biochem. Pharmacol.*, vol. 23, pp. 2495–2531, 1974.

[448] M. E. Fedorko, J. G. Hirsch, and Z. A. Cohn, "Autophagic vacuoles produced in vitro. I. Studies on cultured macrophages exposed to chloroquine.," *J. Cell Biol.*, vol. 38, no. 2, pp. 377–391, 1968.

[449] G. Weissmann, "Lysosomes," *N. Engl. J. Med.*, vol. 273, no. 20, pp. 1084–1090, Nov. 1965.

[450] J. P. Filkins, "Comparison of in vivo and in vitro effects of chloroquine on hepatic lysosomes," *Biochem. Pharmacol.*, vol. 18, no. 11, pp. 2655–2660, 1969.

[451] A. M. Tartakoff, "Perturbation of vesicular traffic with the carboxylic ionophore monensin," *Cell*, vol. 32, no. 4, pp. 1026–1028, 1983.

[452] S. E. K. Tekkeli, A. Önal, and A. O. Sağirli, "Spectrofluorimetric determination of tobramycin in human serum and pharmaceutical preparations by derivatization with fluorescamine," *Luminescence*, vol. 29, no. 1, pp. 87–91, 2014.

[453] H. K. Kim, J. Van Den Bossche, S. H. Hyun, and D. H. Thompson, "Acid-triggered release via dePEGylation of fusogenic liposomes mediated by heterobifunctional phenyl-substituted vinyl ethers with tunable pH-sensitivity," *Bioconjug. Chem.*, vol. 23, no. 10, pp. 2071–2077, 2012.

[454] D. Chen *et al.*, "Effects of a novel pH-sensitive liposome with cleavable esterase-catalyzed and pH-responsive double smart mPEG lipid derivative on ABC phenomenon.," *Int. J. Nanomedicine*, vol. 6, pp. 2053–2061, 2011.

[455] D. Chen, X. Jiang, Y. Huang, C. Zhang, and Q. Ping, "Ph-sensitive mPEG-Hz-cholesterol conjugates as a liposome delivery system," *J. Bioact. Compat. Polym.*, vol. 25, no. 5, pp. 527–542, 2010.

[456] X. Guo and F. C. Szoka, "Steric stabilization of fusogenic liposomes by a low-pH sensitive PEG - Diortho ester - Lipid conjugate," *Bioconjug. Chem.*, vol. 12, no. 2, pp. 291–300, 2001.

[457] L. Kong, F. Campbell, and A. Kros, "DePEGylation strategies to increase cancer nanomedicine efficacy," *Nanoscale Horizons*, vol. 4, no. 2, pp. 378–387, 2019.

[458] J. C. Silva, M. V. Gorenstein, G. Z. Li, J. P. C. Vissers, and S. J. Geromanos, "Absolute quantification of proteins by LCMSE: A virtue of parallel MS acquisition," *Mol. Cell. Proteomics*, vol. 5, no. 1, pp. 144–156, 2006.

[459] N. Kotecha, P. O. Krutzik, and J. M. Irish, "Web-Based Analysis and Publication of Flow Cytometry Experiments," *Curr. Protoc. Cytom.*, vol. 53, no. 1, p. 10.17.1-10.17.24, Jul. 2010.

[460] J. Schindelin *et al.*, "Fiji: An open-source platform for biological-image analysis," *Nat. Methods*, vol. 9, no. 7, pp. 676–682, 2012.

[461] S. Sieber, S. Siegrist, S. Schwarz, F. Porta, S. H. Schenk, and J. Huwyler, "Immobilization of Enzymes on PLGA Sub-Micrometer Particles by Crosslinked Layer-by-Layer Deposition," *Macromol. Biosci.*, vol. 17, no. 8, pp. 1–10, 2017.

ABBREVIATIONS

ABC	Accelerated blood clearance
AF4	asymmetric flow field flow fractionation
AROP	Anionic ring-opening polymerization
BBB	Blood-brain-barrier
CAL	Calcein
CCD	Charged-coupled device
CEF	Ceftriaxone
CHEMS	Cholesterolhemisuccinat
CHOL	Cholesterol
CL	Conventional liposome
CLSM	Confocal laser scanning microscopy
CPP	Cell penetrating peptide
CuAAC	Copper catalyzed azide-alkyne cycloaddition
$DC_{8,9}PC$	1,2-bis(tricosa-10,12-diynoyl)-sn-glycero-3-phosphocholine
DLS	Dynamic light scattering
DMEM	Dulbecco's modified Eagle's medium
DMPC	1,2-dimyristoyl-sn-glycero-3-phosphocholine
DNA	Desoxyribonucleic acid
DOPC	1,2-diolyeol-sn-glyocero-3-phosphatidylcholine
DOPE	1,2-dioleoyl-*sn*-glycero-3-phospho-ethanolamine
DOPG	1,2-dioleoyl-sn-glycero-3-phospho-rac-(1-gylcerol) sodium salt
DOTAP	1,2-dioleoyl-3-trimethylammonium-propane
DPPC	1,2-dipalmitoyl-sn-glycero-3-phosphatidylcholine
DPPE	1,2-dipalmitoyl-sn-glycero-3-phosphoethanolamine
DPPG	1,2-dipalmitoyl-sn-glycero-3-phosphatidylglycerol
DSPE	1,2-disteaoryl-sn-glycero-3-phospho-ethanolamine
DSPG	1,2-disteaoryl-sn-glycero-3-phosphatidylglycerol
DTT	Dithiothreitol
DXR	Doxorubicin
EE	Encapsulation efficiency
EGFT	endothelial growth factor receptors

EPC	Egg phosphatidylcholine
ESI	Electrospray ionization
FBS	Fetal bovine serum
FCS	Fetal calf serum
FR	Folate receptor
GFP	Green fluorescent protein
GUV	Giant unilamellar vesicles
H_{II}	Inverted hexagonal phase
hbPG	Hyperbranched polyglycerol
HDL	High-density lipoportein
HIV	Human immunodeficiency virus
HP	Human plasma
HPTS	8-hydroxypyrene-1,3,6-trisulfonic acid
Hpf	Hours post fertilization
Hpi	Hours post injection
HSPC	hydrogenated soy phosphatidylcholine
HTS	High throughput screening
IEDDA	Inverse electron demand Diels-Alder cycloaddition
L_{alpha}	Liquid disordered phase
Laurdan	6-dodecanoyl-2-dimethylaminonaphthalene
L_{beta}	Gel phase
LC-MS	Liquid chromatography/mass spectrometry
LDL	Low-density lipoprotein
LGP	Laurdan generalized polarization
Lo	Liquid ordered phase
MLV	Multilamellar vesicles
MMP	Matrix metalloproteinase
mPEG	Methoxypoly-(ethylene) glycol
MR	Mannose receptor
MVV	Multivesicular vesicles
OLV	Oligolamellar vesicles
PAMPS	Pathogen-associated molecular patterns
PDI	Polydispersity index

|	
PE	Phosphatidylethanolamine
PEG	Poly-(ethylene) glycol
PG	Phosphatidylglycerol
PS	Phosphatidylserine
RES	Reticuloendothelial system
RNA	Ribonucleic acid
ROS	Reactive oxygen species
SEC	Size exclusion chromatography
siRNA	Small interfering RNA
SOPC	1-steoryl-2-oleoyl-sn-glycero-3-phosphocholine
SPC	Soy phosphatidylcholine
SR	Scavenger receptor
SrB	Sulforhodamine B
SUV	Small unilamellar vesicles
T	Temperature
TAMS	Tumor associated macrophages
TEM	Transmission electron microscopy
TfR	Transferrin receptors
TL	Thermosensitive liposome
TLR	Toll-like receptor
Tm	Phase transition temperature
UK	United Kingdom
UV	Ultra violet
ZFE	Zebrafish embryo

LIST OF PUBLICATIONS

2019   *Biomacromolecules*, DOI: 10.1021/acs.biomac.9b00539

Weber C., <u>Voigt M.</u>, *et al.*; Functionalization of liposomes with hydrophilic polymers results in biological identity independent from the protein corona.

2019   *Pharm. Nanotechnology*, DOI:10.1007/978-1-4939-9516-5_16

<u>Voigt M.</u>, Fritz T., Frey H., Helm M.; Surface modification of nanoparticles and nanovesicles *via* click chemistry.

2016   *Chemistry – A Eur. J. Comm.*, DOI:0.1002/chem.201602758

Fritz T., <u>Voigt M.</u>, *et al.*; Orthogonal click conjugation to the liposomal surface reveals the stability of the lipid anchorage as crucial for targeting.

2016   *Int. J. Environ. Sci.*, 2016, DOI:10.1016/j.jes.2016.08.009

Aborode F., Raab A., <u>Voigt M.</u>, Malta Costa L., Krupp E., Feldmann J.; The importance of glutathione and phytochelatins on the selenite and arsenate detoxification in *Arabidopsis Thaliana*.

SUPPLEMENT

|		Size (d.nm):	% Intensity:	St Dev (d.nm):
Z-Average (d.nm): 97,51	Peak 1:	106,0	95,1	37,09
Pdl: 0,321	Peak 2:	26,35	4,9	5,651
Intercept: 0,954	Peak 3:	0,000	0,0	0,000
Result quality : Good				
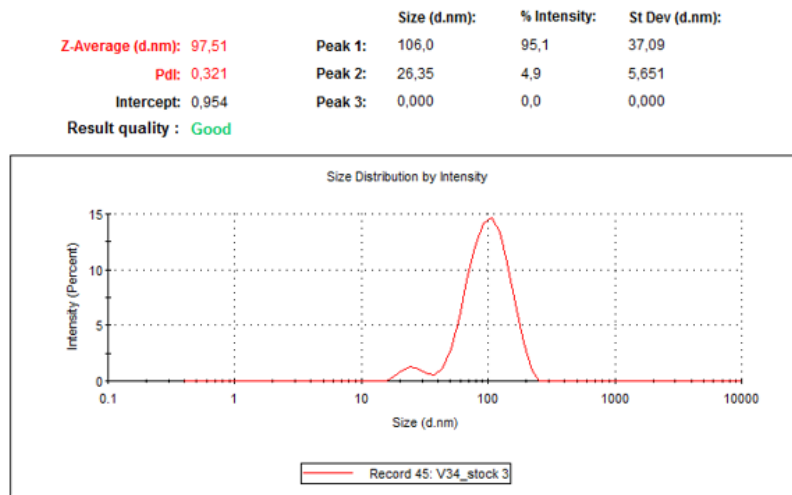
SUP FIGURE 1: DLS RESULTS FROM A LIPOSOME WTH 30 MOL-% LARGE HBPG SHOW A SECONDS SPECIES AT AROUND 25 NM, INDICATING THE FORMATION OF MICELLES.
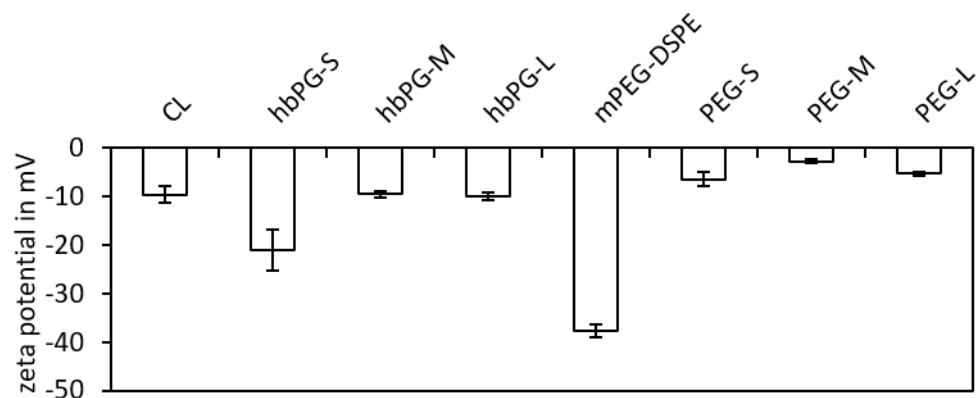
SUP FIGURE 2: ZETA POTENTIALS OF CONVENTIONAL NON-SHIELDED LIPOSOME (CL), AND LIPOSOMES BEARING SMALL (S), MEDIUM (M) OR LARGE (L) HBPG OR PEG. ERROR BARS INDICATE THREE INDIVIDUAL LIPOSOME PREPARATIONS.
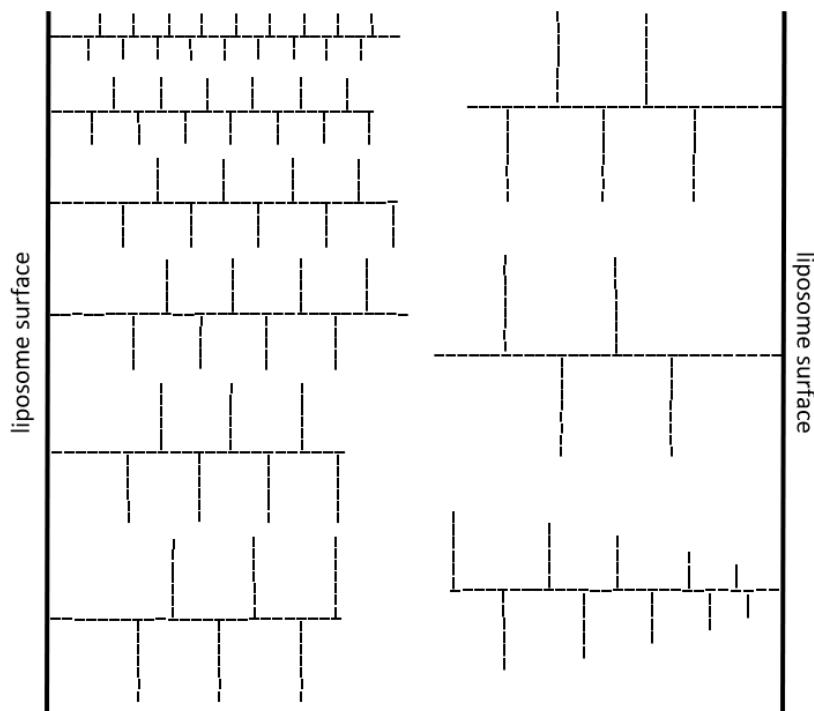
**SUP FIGURE 3:** POSSIBLE STRUCTURES AS BASIS FOR MATHEMATICAL CALCULATIONS FOR HBPG-M (67 MONOMERS).
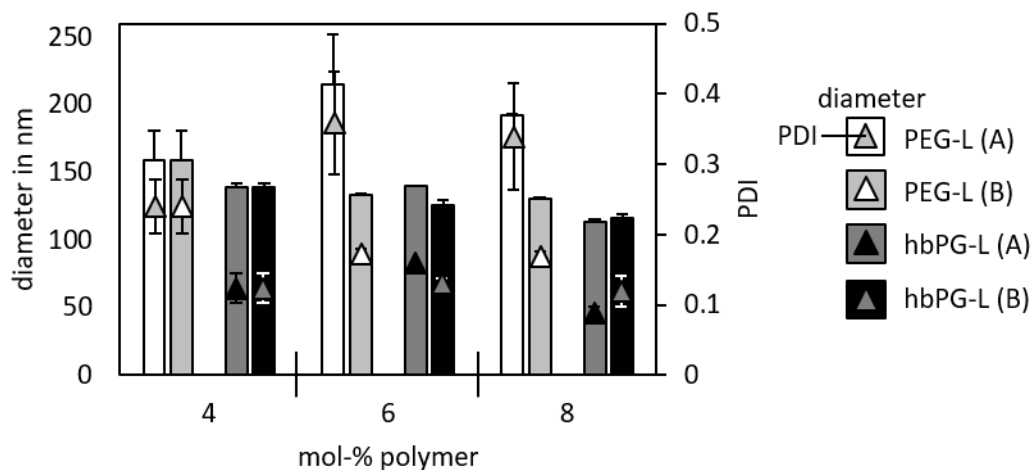

SUP FIGURE 4: DIAMETER AND PDI OF LIPOSOMES BEARING 8 MOL-% PEG-L OR HBPG-L, FORMULATED WITH **(A)** LIPID:AQUEOUS BUFFER RATIO OF 0.13 **(B)** LIPID:AQUEOUS BUFFER RATIO OF 0.06. INCREASING THE BUFFER AMOUNT LED TO A DECREASE IN DIAMETER AND PDI FOR PEGYLATED LIPOSOMES, WHEREAS HBPG LIPOSOMES REMAINED CONSTANT.

SUP TABLE 1: PHYSICOCHEMCIAL PARAMETERS OF LIPOSOME SAMPLES USED IN BIODISTRIBUTION AND BLOOD CIRCULATION STUDIES IN CHAPTER 3.1.3.

sample	polymer in mol-%	d_H in nm	PDI	zeta potential in mV	sample	polymer in mol-%	d_H in nm	PDI	zeta potential in mV
PEG-S 3191 g/mol	2	180±2	0.12±0.02	-29±1	hbPG-S 3084 g/mol	2	238±3	0.34±0.02	-34±1
	5	144±1	0.12±0.02	-35±1		5	210±3	0.22±0.03	-22±1
	10	113±2	0.25±0.01	-32±1		10	148±2	0.23±0.02	-23±1
PEG-M 5470 g/mol	2	141±1	0.12±0.01	-7±1	hbPG-M 5420 g/mol	2	293±1	0.31±0.01	-27±1
	5	125±1	0.22±0.2	-6±1		5	184±2	0.29±0.01	-22±1
	10	113±2	0.16±0.02	-10±1		10	133±2	0.23±0.01	-29±1
PEG-L 7560 g/mol	2	136±1	0.17±0.01	-9±1	hbPG-L 8270 g/mol	2	151±1	0.19±0.01	-24±1
	5	123±1	0.17±0.01	-10±1		5	141±1	0.21±0.01	-23±1
	10	140±1	0.12±0.02	-10±1		10	108±2	0.30±0.02	-19±1
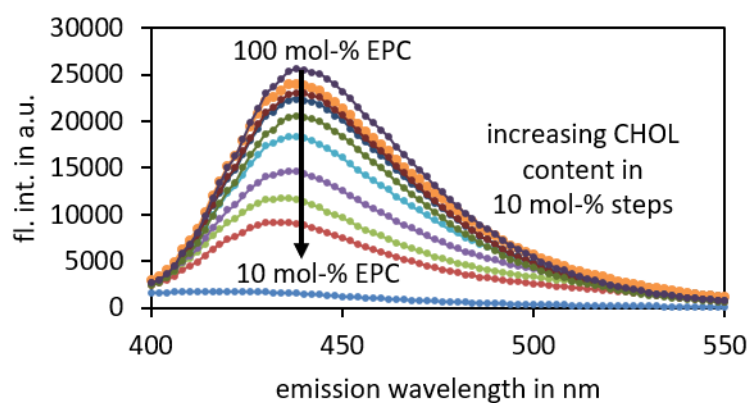
SUP FIGURE 5: LAURDAN FLUORESCENCE EMISSION OF CONVENTIONAL LIPOSOME, STARTING FROM 100 MOL-% EPC, STEPWISE SUBSTITUTED BY 10 MOL-% CHOLESTEROL (CHOL) UP TO 90 MOL-%. NO FLUORESCENCE SHIFT FROM 440 TO 490 NM WAS OBSERVABLE. EXCITATION WAVELENGTH WAS 350 NM.
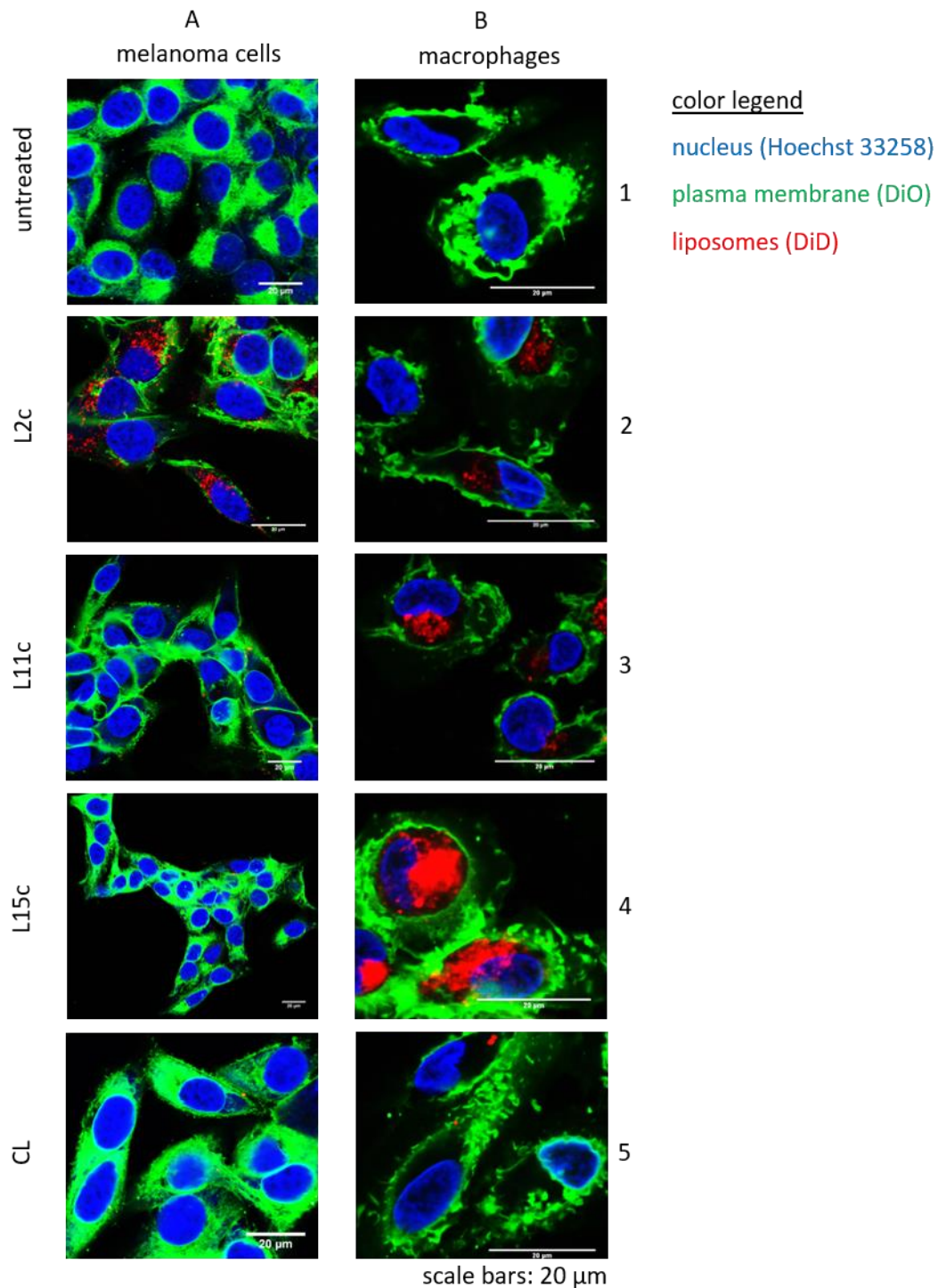
SUP FIGURE 6: CONFOCAL LASER MICROSCOPY IMAGES OF MELANOMA CELLS (COLUMN A) AND MACROPHAGES (COLUMN B) 4 HOURS AFTER INCUBATION WITH CANDIDATE LIPOSOMES L2C, L11C AND L15C IN ADDITION TO CONVENTIONAL LIPOSOME CL AND UNTREATED CELLS. PLASMA MEMBRANES WERE STAINED WITH 3,3'-DIOCTADECYLOXACARBOCYANINE PERCHLORATE (DIO, GREEN), CELL NUCLEI WITH HOECHST 33258 (BLUE) AND LIPOSOMES WITH 1,1'-DIOCTADECYL-3,3,3',3'-TETRAMETHYLINDODICARBOCYANINE 4-CHLOROBENZENESULFONATE SALT (DID, RED).
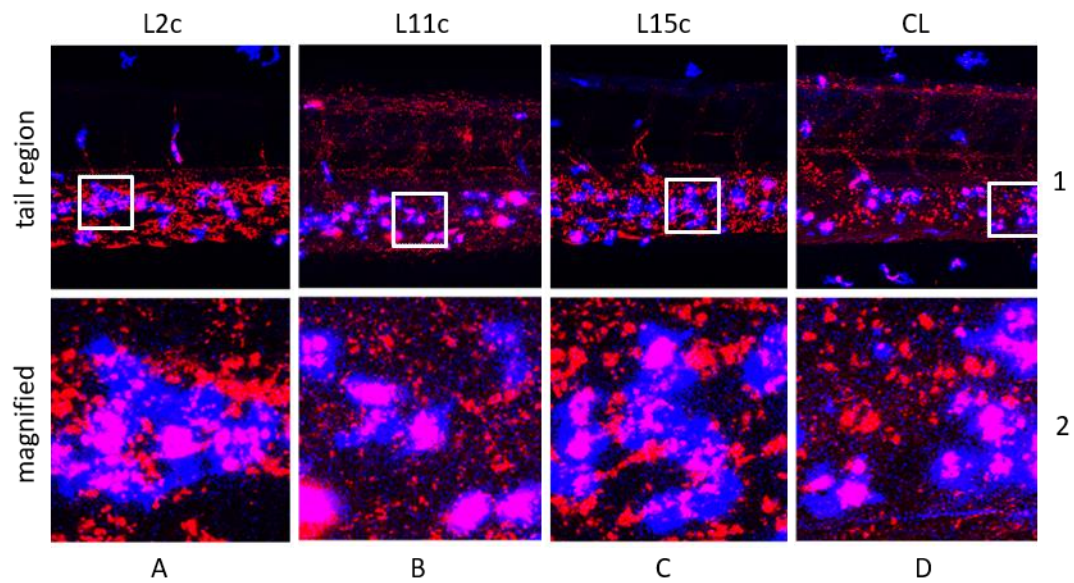
SUP FIGURE 7: CONFOCAL LASER MISCROSCOPY IMAGES OF ZFE EMBRYOS EXPRESSING A GREEN FLUORESCENT PROTEIN IN THEIR MACROPHAGES (BLUE) 7 HOURS POST INJECTION OF PH-SENSITIVE CANDIDATE LIPOSOMES L2C, L11C AND L15C AND CONVENTIONAL LIPOSOMES CL. LIPOSOMES WERE DID LABELED AND ARE DEPICTED IN RED. ALL LIPOSOMES WERE SEQUESTERED TO A CERTAIN EXTENT BY MACROPHAGES, WHICH IS ESPECIALLY EVIDENT IN THE MAGNIFIED IMAGES (BOTTOM).

SUP TABLE 2: PHYSICOCHEMICAL PARAMETERS OF FINAL CANDIDATE LIPOSOMES EITHER WITHOUT OR WITH 5 MOL-% OF POLYMER MEASURED BY DLS. ERRORS INDICATE STANDARD DEVIATION FROM THREE TECHNICAL REPLICATES, EXCEPT FOR THE UNSHIELDED LIPOSOMES (THREE INDIVIDUAL PREPARATIONS).

sample	polymer 5 mol-%	d_H in nm	PDI	zeta potential in mV	%EE (SRb)
L2c	-	178±6	0.31±0.04	-40±1	38±2
	*hb*PG	219±5	0.26±0.03	-17±1	33±5
	PEG	126±1	0.38±0.05	-1±1	30±3
	ketal-PEG	103±1	0.32±0.01	-1±1	47±14
	VE-PEG	185±3	0.40±0.02	1±1	32±13
L11c	-	204±13	0.28±0.06	-1±2	50±2
	*hb*PG	124±2	0.35±0.02	0±1	41±2
	PEG	183±2	0.34±0.04	-3±1	44±1
	ketal-PEG	136±1	0.16±0.02	-5±1	42±8
	VE-PEG	117±1	0.18±0.01	-5±1	42±6
L15c	-	243±49	0.25±0.04	-71±7	33±5
	*hb*PG	190±5	0.43±0.07	-23±2	38±1
	PEG	161±4	0.29±0.01	-9±1	32±3
	ketal-PEG	178±3	0.16±0.01	-66±1	37±10
	VE-PEG	139±1	0.17±0.01	-42±7	42±7

CURRICULUM VITAE

Matthias Voigt

Anschrift: ███████████

███████

Nationalität: █████

Geburtsdatum: ████████

Geburtsort: ███

Ausbildung

██

███████████████████████████████████

███

██████████████████████

██████████████████████

███████████████████████████████████████

██

████████████████████████████████

██

████████████████████████████████████

████████████████████████████████████

██

███████████████████████

_____   _____
Ort, Datum   **Matthias Voigt**